Performance comparison of LP vs. MP mercury vapour lamps

Degradation of organic micropollutants via UV/H_2O_2

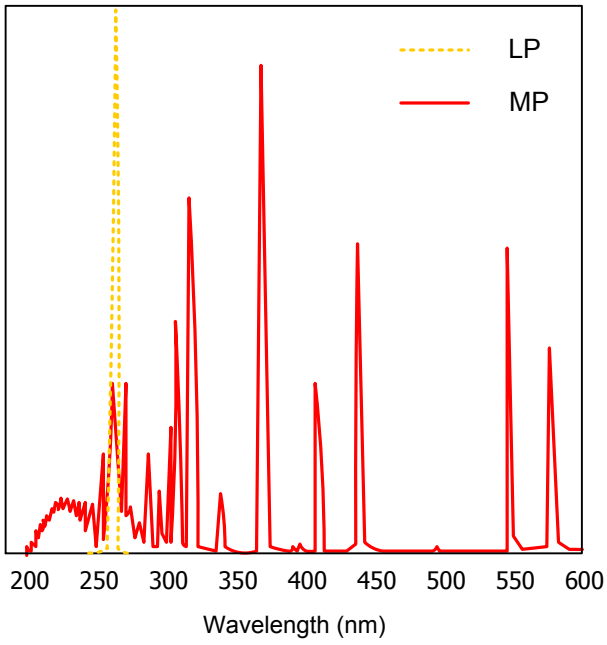

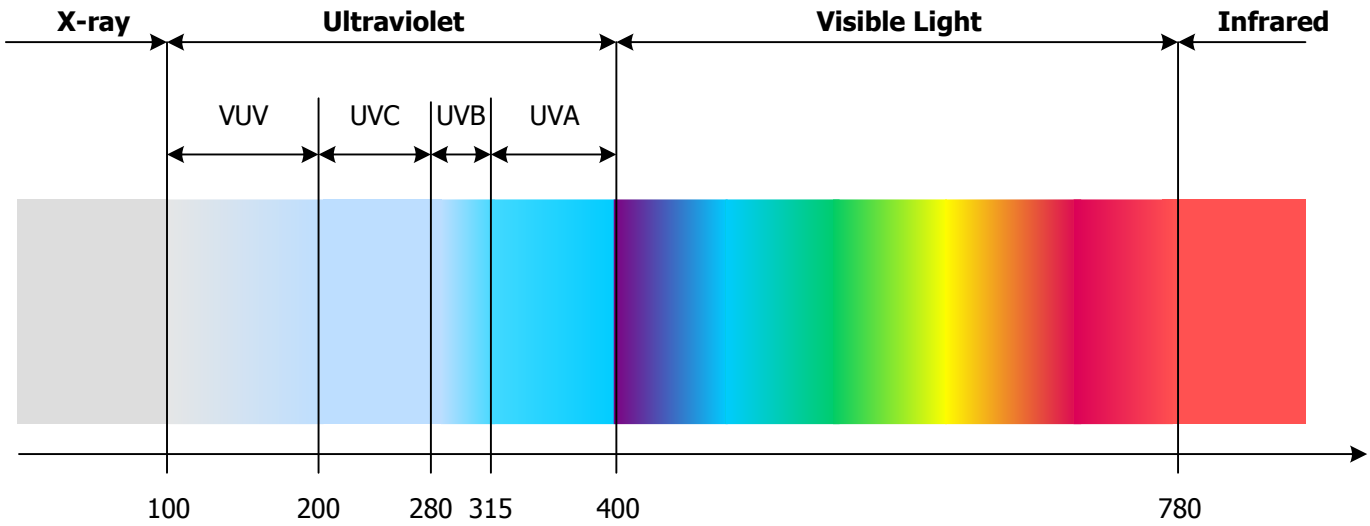

Josanne Derks

January 2010

dunea DUIN & WATER

TU Delft

Delft University of Technology

Degradation of organic micropollutants by advanced oxidation through UV/H_2O_2

Performance comparison of MP vs. LP lamps

Johanna Georgina Derks

For the degree of:
Master of Science in Civil Engineering

Date of submission:
January 21st, 2010

Date of defense:
January 29th, 2010

Committee:

Prof.ir. J.C. van Dijk	Delft University of Technology Sanitary Engineering Section
Dr.ir. J.Q.J.C. Verberk	Delft University of Technology Sanitary Engineering Section
Ir. K. Lekkerkerker-Teunissen	Delft University of Technology Sanitary Engineering Section Dunea Duin en Water
Prof.dr.ir. T.N. Olsthoorn	Delft University of Technology Section of Water Resources

Sanitary Engineering Section, Department of Water Management
Faculty of Civil Engineering and Geosciences
Delft University of Technology, Delft

Abstract

Drinking water company *Dunea Duin en Water* produces drinking water from the Meuse River, which contains a variety of organic micropollutants (OMPs) from upstream activity. OMPs found in Dunea's source are plant protection products, pharmaceuticals, hormones and endocrine disruptors and X-ray contrast media. Continues development of measuring equipment has resulted in lower detection limits for most substances and measuring programs are expended yearly. Consequently, more substances are found in the Meuse River and other surface water bodies.

Dunea is currently performing research to extend the multiple barrier treatment with advanced oxidation processes (AOP) via UV and hydrogen peroxide. Mostly medium pressure (MP) mercury vapour ultraviolet lamps are used that emit a broad spectrum of light, coinciding with the absorbance spectrum of many substances, which results in a high photolytic capacity. Low pressure (LP) mercury vapour lamps emit ultraviolet light at just one single wavelength (254 nm). Consequently, the direct photolysis of target substances is less effective and the yield of hydroxyl radicals is lower compared to MP lamps. However, LP lamps have advantages over MP lamps such as significantly lower energy consumption and fewer by-products such as Assimilable Organic Carbon (AOC) and nitrite are formed. The objective of this research is formulated as follows:

Performance comparison of low pressure versus medium pressure mercury vapour lamps in advanced oxidation via UV/H_2O_2, by means of experimental research with a pilot-scale set-up.

In order to simulate the AOP, a pilot scale experimental set-up was built with a design flow of 5 m^3/h per reactor. Two reactors are used during the experiments: a reactor equipped with 4 medium pressure mercury vapour ultraviolet lamps (P_{total} = 4.4 kW) and a reactor equipped with two low pressure mercury vapour ultraviolet lamps (P_{total} = 1.32 kW). Atrazine, bromacil, ibuprofen and NDMA are dosed to the influent which is abstracted directly from the full-scale plant after pre-treatment by coagulation, microstraining and dual media rapid sand filtration. Hydrogen peroxide concentrations are varied (0, 5 and 10 ppm) and static mixers are installed to ensure homogenic water mixture and samples. The maximum UV dose in the MP-reactor is approximately 850 mJ/cm^2 and the maximum UV dose in the LP-reactor is approximately 1140 mJ/cm^2. The UV doses are estimates based on the information given by the suppliers which at the moment of writing have not yet been confirmed by computational fluid dynamics (CFD) modelling. Experiments have been performed between March and October 2009, using different combinations of UV and peroxide doses.

Although reduction in concentration of the model compounds - atrazine in particular - is the key performance indicator, the degradation capacity should be judged in relation to the energy consumption, the formation of undesirable by- and degradation products and the overall sensitivity towards seasonal fluctuations of the Meuse water.

The target set for atrazine degradation is 80%, which is not reached yet: the average degradation levels of atrazine achieved at maximum UV and peroxide doses using LP and MP lamps are 72% and 75% respectively. However, the average degradation levels of atrazine may not reach 80%; this level has been achieved once by both reactors. During this particular experiment, the water quality of the pre-treated Meuse water was optimal: high UV transmission (>80%), low concentrations of nitrate (8.65 mg/L NO_3^-), dissolved organic carbon (DOC, 3.36 mg/L C) and bicarbonate (137 mg/L HCO_3^-). The poorest performances occurred when the quality of the pre-treated Meuse water was poor: low UVT (74%), high concentrations of nitrate (16 mg/L NO_3^-), DOC (4 mg/L C) and bicarbonate (151 mg/L HCO_3^-).

Performance comparison of achieved degradation based on variations in UV doses is difficult. The UV dose is a reactor specific characteristic and varies due to hydraulic influences and variations in water quality. Therefore a parameter known as the electrical energy per order EEO (kWh/m^3) is used, defined as the electrical energy in kWh required for achieving 1 log degradation of a substance per unit of treated water. The EEO of the LP reactor is considerably lower than the EEO of the MP reactor. The energy requirement of the MP reactor is 2 to 5 times higher then the energy requirement of the LP reactor, depending on the dosed amount of peroxide. Determined EEO values for atrazine degradation are 0.48 kWh/m^3 (LP) and 1.45 kWh/m^3 (MP).

Assimilable Organic Carbon (AOC) is a readily available food source for microorganisms. AOC is formed as a result from direct photolysis of dissolved organic carbon (DOC) or through a reaction of DOC with hydroxyl radicals. AOC in water can result in bio-films on surfaces like pipe walls. In the Netherlands chlorination in the distribution net is not allowed which stresses the need for biologically stable water. From the results can be concluded that AOC formation is enhanced in the presence of peroxide, since more DOC can be oxidized. In general, the observed AOC formation is relatively low and similar levels for both lamps types (60-70 µg/L) are observed in the presence of 10 ppm H_2O_2. In the absence of hydrogen peroxide, AOC formation using MP lamps (50 µg/L) is twice as high as AOC formation using LP lamps (25 µg/L).

Nitrite is formed from photolysis of nitrate and has adverse effects on public health, like for instance methemoglobinemia (blue-baby syndrome) in infants younger then 6 months caused by decreased O_2 uptake of blood. Furthermore, nitrite is a radical scavenger and competes with the model compounds for availability of free hydroxyl radicals. Observed nitrite formation using LP lamps is generally well below 0.015 mg/L, regardless of the hydrogen peroxide dose and can thus be considered negligible. Nitrite concentrations observed in the MP effluent during the research were highest in the absence of hydrogen peroxide (0.61 mg/L). Dosing 5 and 10 ppm H_2O_2 yields nitrite concentrations of 0.56 and 0.48 mg/L NO_2^- respectively.

Nitrate is the water matrix parameter with the largest influence on the performance of the AOP because nitrate absorbs more UV light then other water matrix parameters, especially between 200-250 nm. Moreover, the characteristic of the UV absorbance by the influent is similar to the characteristic of the UV absorbance by nitrate. Consequently, the influence of higher nitrate concentrations on the degradation of model compounds is stronger than the influence of other parameters such as DOC. Seasonal variations of nitrate concentrations can be used to estimate the seasonal variations in performance of both reactors. Between December and March the performance will be poor because nitrate concentrations are maximal (14-17 mg/L NO_3^-), resulting in low UV transmission of the water. Nitrate concentrations decrease from 14 mg/L NO_3^- in April to a minimum of 8.9 mg/L NO_3^- in August. During the summer period the performance will be best due to a higher UV transmission. In September the concentrations of nitrate start to increase, resulting in poorer performances.

	Degradation model compounds (%)				**Energy performance**	**Formation of by-products**		
	ATZ	BRO	IBU	NDMA	EEO_{ATZ}	AOC (µg/L C)	mg/L NO_2^-	mg/L H_2O_2
LP lamps (1140 mJ/cm^2)	72	74	78	90	0.48	64 (23-106)	0.01-0.015	9.5
MP lamps (850 mJ/cm^2)	75	71	76	88	1.45	71 (51-90)	0.436-0.504	9.5

From the research can be concluded that the performance of low pressure mercury vapour lamps in terms of degradation of model compounds, energy performance and nitrite formation is superior to the performance of medium pressure mercury vapour lamps, when applied for advanced oxidation. It is suspected that the high UV doses are responsible for the fact that the amount of AOC formed in the presence of 10 ppm H_2O_2 is similar to the amount of AOC formed when medium pressure lamps are applied. Residual hydrogen peroxide levels in the effluents are also equal.

Preface

This report is the result of the research I have performed in order to obtain my MSc. Degree in Civil Engineering. I was very lucky to have the opportunity of performing the research at *Dunea Duin en Water*: the drinking water company serving the Hague area, including myself. I hope that my research provides a contribution to the knowledge and practice among the drinking water sector regarding the issue of organic micropollutants in drinking water sources.

I am grateful for the help and support I received from the employees of Dunea, without them this report would not exist. First of all I would like to thank Karin Lekkerkerker-Teunissen and Ton Knol for their trust and for allowing me to figure things out on my own. You were always willing to help performing the experiments, to answer my questions and to provide me with valuable feedback. I would also like to thank the Bergambacht-crew: the *'kippenhok'* will be a bit empty from now on! I would especially like to thank Leo because he always knew how and was always willing to help me solve problems with the pilot installation. Marie, thank you so much for taking such good care of us! Cheryl; I really enjoyed the fact that you are doing your research at Dunea as well. Thank you for the endless chats, helping me with experiments and for discussing and comparing our results.

During the research I must have called Marco Vos from *Het Waterlaboratorium* at least 3 times per week. Thank you for everything! I am very thankful to Professor van Dijk and Jasper Verberk who provided me with critical feedback and points of view that kept me sharp.

My lacrosse team-mates understood that I could not make it to practice very often because combining playing a sport in Rotterdam with performing research in Delft, Scheveningen and Bergambacht was a hassle. I thank you all for the fun I had when I actually did make it to the field – it helped me put my mind of off things!

I am however most grateful to my parents and Coen, my boyfriend. My parents have always believed in me and my capabilities. I thank you for your support, for allowing me to make the most out of my student days and for letting me make my own choices. My father and Coen always know how to motivate me and both are particularly good at putting everything into perspective! Thank you so much for everything.

Josanne Derks

Delft, January 2010

List of illustrations

List of tables

Contents

1. Introduction

1.1 Background

Organic micropollutants (OMPs) such as pesticides, pharmaceuticals and industrial chemicals have found their way into water bodies and from there into drinking water supplies (CRC, 2007). Over the years continues development of measuring equipment has resulted in lower detection limits for most substances and measuring programs are expended yearly. Consequently, more substances are detected in surface waters. OMPs are also found in the Meuse River which forms the primary source for the production of drinking water by *Dunea Duin en Water*.
Adverse effects of OMPs include among others aquatic toxicity and endocrine disruption in fish and crustaceans (Yuan et al., 2009). The potential chronic effects on public health associated with long term exposure to pharmaceutical residues through drinking water consumption are suspected to be negligible (Schriks et al., 2009): seventy years consumption of Dutch drinking water will result in a total intake of less then one pill. However, the Dutch approach is to protect sources and remove undesired compounds when necessary. Furthermore, increased awareness among the public stresses the need for extension of traditional water treatment schemes.

Figure 1.1: Media attention to the problem

Depending on the characteristics of a specific compound, application of membrane filtration, GAC/PAC, soil passage or advanced oxidation processes is effective. Unfortunately no single technology is capable of removing or converting all types of organic micropollutants, so multiple barriers are required.

1.2 Drinking water production

Dunea Duin en Water produces drinking water from the River Meuse. After coagulation, the water is abstracted, pre-treated and transported to dune areas in the province of South Holland. The water is infiltrated, recovered and receives post-treatment before it is distributed to 1.2 million customers in The Hague region. Currently, dune passage and dosing of Powdered Activated Carbon (PAC) is applied for the removal of OMPs. Unfortunately PAC was proven to be insufficiently robust for the removal of priority substances (Beerendonk et al., 2006). Dune passage does a positive contribution towards the removal of priority substances but is incapable of removing or converting all types of organic micropollutants (Segers et al., 2007). The main functions of dune passage are the provision of a barrier against micro-organisms and pathogens, levelling of peaks and provision of a reservoir (de Moel et al, 2005). Furthermore, the dune areas have a nature reserve status and it remains unsure whether the infiltration license granted by the Province of South-Holland will be prolonged.

Dunea is performing research to extend the current multiple-barrier treatment with advanced oxidation processes (AOP) via UV and hydrogen peroxide. UV light can weaken or break the double bonds of the complex molecular structures that characterize organic micropollutants, which can potentially enhance the biological degradation during dune passage (Lekkerkerker-Teunissen et al., 2009 and MWH, 2005). Furthermore, when H_2O_2 is subjected to UV radiation, hydroxyl radicals are formed that have a large oxidative capacity, capable of oxidizing several target compounds.

1.3 Research objectives

Advanced oxidation processes (AOP) have been applied successfully for disinfection and degradation of organic micropollutants during drinking water production (e.g. PWN Water Supply Company North Holland). Mostly medium pressure mercury (MP) vapour ultraviolet lamps are applied. Medium pressure UV lamps emit a broad spectrum of light (200-600 nm), coinciding with the absorbance spectrum of many substances which results in a high photolytic capacity. A drawback of MP lamps is the fact that the only a fraction of the emitted spectrum (200-300 nm) is relevant for the AOP, resulting in a low energy efficiency (IJpelaar et al., 2007-a).The fact that the polychromatic spectrum coincides with the absorbance spectrum of many substances is a drawback it self; non-targeted substances can be influenced resulting in competition for available light but also could result in the formation of unwanted by-products. Low pressure (LP) mercury vapour lamps emit ultraviolet light at just one single wavelength (254 nm). Consequently the photolytic capacity of LP lamps is lower but the energy performance is higher compared to MP lamps. The formation of unwanted by-products could be lower as well (IJpelaar et al., 2007-a). Furthermore, the yield of hydroxyl radicals is lower, which results in an overall reduced performance of the UV/H_2O_2 AOP in terms of degradation capacity. However, LP lamps have advantages over MP lamps such as significantly lower energy consumption and fewer by-products such as Assimilable Organic Carbon (AOC) and nitrite are formed. The objective of this research is formulated as follows:

Performance comparison of low pressure versus medium pressure mercury vapour lamps in advanced oxidation via UV/H_2O_2, by means of experimental research with a pilot scale set up.

The outcomes of this research should provide insight into the relevant mechanisms behind AOP via UV/H_2O_2, in particular the differences between the two lamp types. Furthermore, Dunea can use the outcomes for the design and implementation of full-scale AOP in her drinking water treatment scheme.

1.5 Research approach

The degradation of organic micropollutants by advanced oxidation through UV/H_2O_2 is assessed with a pilot-scale experimental set-up, located at Dunea's pre-treatment in Bergambacht. A reactor equipped with MP lamps and a reactor equipped with LP lams are used in parallel configuration. Both receive a feed flow abstracted directly from the full-scale plant, spiked with four model compounds: atrazine, bromacil, ibuprofen and NDMA. The quality of the Meuse water shows seasonal variations in concentrations of dissolved organic carbon (DOC), nitrogen compounds, bicarbonate and parameters such as the water temperature and UV transmission. In order to gain insight into the influence of the seasonal variations, the experiments are performed weekly, over a longer period of time. Although reduction in concentrations of model compounds is the key performance indicator, the degradation capacity should be judged in relation to the energy consumption, the formation of undesirable by and degradation products (increased toxicity for instance) and the overall sensitivity towards seasonal fluctuations. The performances of the reactors are compared based on the following aspects:

1. The degradation of the dosed model compounds at different combinations dosages of UV (mJ/cm^2) and hydrogen peroxide (ppm), calculated as a relative reduction in concentrations:
    i. ≥80% Atrazine degradation
2. The energy consumption corresponding with the degradation capacity, EEO, expressed as the total consumed energy per unit of treated water (kWh/m^3).
3. Minimal formation of by-products:
    i. The levels of formed Assimilable Organic Carbon (AOC, µg/L)
    ii. The levels of formed nitrite (µg/L)
    iii. Toxicity of the effluent
    iv. Residual hydrogen peroxide in effluent
4. Sensitivity and influence to seasonal fluctuations of the influent water.

Although very important, the toxicity of the effluent is not addressed in this research.
The performed experiments yield a large amount of data which allows for a qualitative and quantitative comparison of the performances.

1.7 Structure of report

This report starts with a description of the current situation at Dunea: the applied treatment and the identified substances that form a threat are elaborated in chapter 2. Prevention at the source is of utmost importance, that is why Dunea engaged in a project aimed at reducing the emission of pesticides from the Bommelerwaard, an agricultural area located just upstream of the intake. A description of the project, the results and the results of an investigation into the possibilities for other emission reduction measures can be found in chapter 3. The motivation for implementing AOP and the arguments for the chosen location in the pre-treatment, are elaborated in chapter 4. The theory behind the advanced oxidation processes is explained in chapter 5. A detailed description of the experimental research -the heart of this thesis- and the results can be found in chapter 6 and 7. Conclusions and recommendations resulting from the experiments are formulated in chapter 8.

2. Current situation

2.1 Production of drinking water by Dunea

2.1.1 General principles

Dunea Duin en water supplies 1.2 million customers in the western part of South-Holland with safe drinking water of high quality. As is suggested by the name, Dunea uses dune-water for the production of drinking water and has done so since 1874. The residents of The Hague consumed untreated water from canals, wells and other sources which caused major outbreaks of cholera- and typhoid epidemics, claiming thousands of lives. The solution was found in the dune area: during hundreds of years, a fresh water supply was build up from rain water passing through the soil. The water proved to be a perfect, safe and reliable source for drinking water production. Drinking water production was simple from a technology point of view: open channels were dough in the dunes where fresh water was collected. Post treatment with sand filtration was sufficient to produce safe drinking water that was transported to the city via pipelines. When the population grew significantly at the start of the twentieth century, the demand for drinking water increased as well. The amount of precipitation was insufficient to maintain the freshwater volume, which could eventually result in salination of the dune water. From 1940 Dunea started infiltrating surface water and since 1996, water abstracted from the Meuse River is used for infiltration. The treatment scheme has been extended over years, and currently Dunea applies a typical multiple-barrier treatment, consisting of an extensive infrastructure and multiple treatment steps (Lekkerkerker-Teunissen et al, 2009). Water from the river Meuse is collected in a dead end side stream (Afgedamde Maas) where coagulation, flocculation and sedimentation take place. The water is taken in, treated by microstraining and transported via pipeline to Bergambacht where dual media rapid filtration is applied. From Bergambacht the pre-treated water is transported to a dune area where open infiltration takes place. The soil passage takes on average 120 days after which the water is abstracted, post-treated and distributed (Lekkerkerker-Teunissen, 2009).

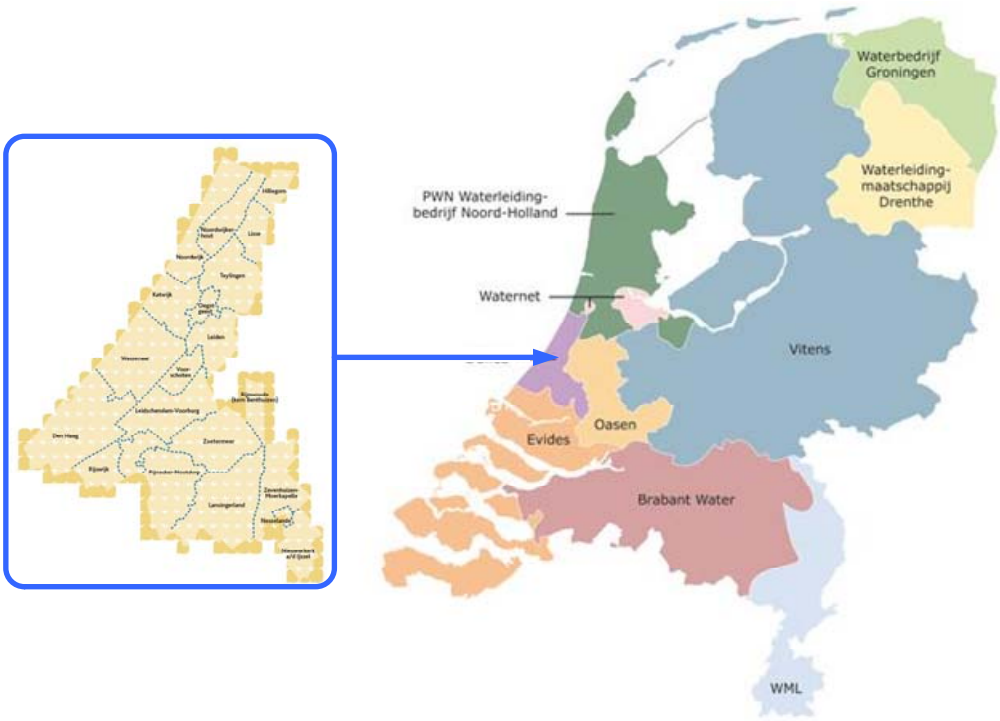

Figure 2.1: Supply area Dunea

2.1.2 Intake and pre-treatment

Dunea's intake is located in Brakel, a village in the province of North-Brabant, on the banks of a dead-end side stream of the Meuse River. Ferrous sulphate is dosed at the beginning of the side-stream resulting in coagulation, flocculation and sedimentation. Furthermore, there is a certain amount of self-cleaning during the total retention time of seven weeks. At the *Wilhelminasluis* the water is taken in and micro straining is applied during spring and summer, necessary due to the higher concentration of organic material and organisms in the water. From Brakel the water is pumped over a distance of 35 km to the pre-treatment in Bergambacht. The location of the pre-treatment has her origin in the history of Dunea: before 1975, water from the river Lek (a tributary to the river Rhine) was used. When the intake was relocated to the Afgedamde Maas, it was decided to maintain the pre-treatment in Bergambacht. Whenever a calamity occurs in the Afgedamde Maas or the transport pipeline, the Lek water can be abstracted and pre-treated on site. This configuration increased Dunea's continuity of supply. From Bergambacht the water is transported to the dune areas via two pipelines, with a length of 46 and 57 km (Lekkerkerker-Teunissen, 2009).

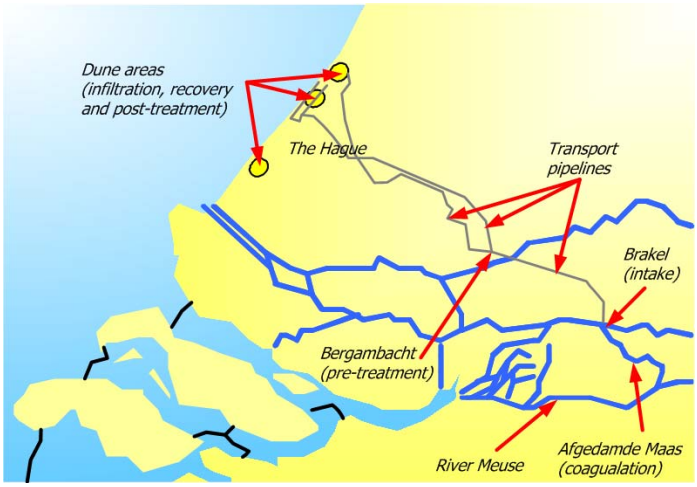

Figure 2.2: Infrastructure Dunea

2.1.3 Artificial recharge and recovery

When the water arrives in the dune areas Meijendel, Solleveld and Berkheide, the bulk volume is infiltrated via open ponds. A smaller volume is infiltrated in deeper layers after receiving extra pre-treatment. After an average retention time of 2 months, a mixture of artificial and original dune water is abstracted and receives post-treatment in Scheveningen, Katwijk or Monster (Lekkerkerker-Teunissen, 2009).

2.1.5 Post-treatment and distribution

The abstracted water receives more or less the same treatment at all three locations. In general the following treatment is applied: softening, aeration with dosing of powdered activated carbon (PAC), dual media rapid filtration followed by slow sand filtration. The water is collected in the clear water reservoirs from where it is distributed to the customers (Lekkerkerker-Teunissen, 2009).

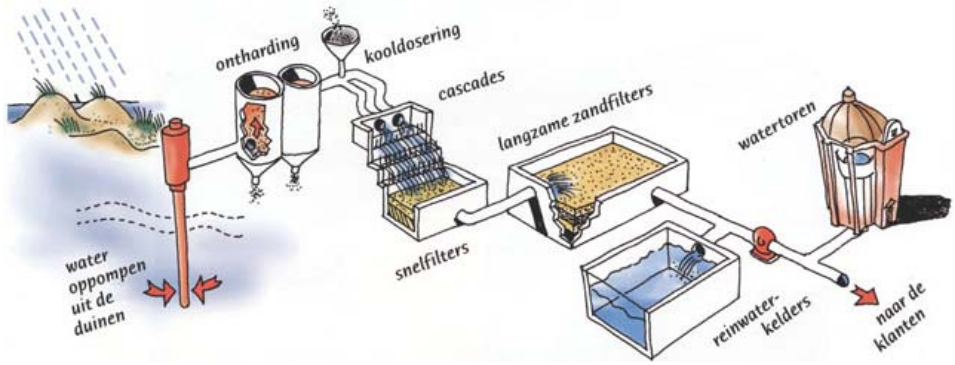

Figure 2.3: Post-treatment

2.2 Priority substances relevant to Dunea

2.2.1 Introduction

On request of and in cooperation with Dunea, *KWR Watercycle Research Institute* and *HWL* (Dutch laboratory for drinking water) made an inventory of (priority) substances which may threaten the production of drinking water, today and in the near future. The inventory is limited to chemical water quality parameters only. The most recent data is used, at the disposal of RIWA – Maas, HWL, KWR Watercycle Research Institute and RIZA. In this paragraph a summary of the identified substances is given. For further information on this specific research and the used methods, the reader is referred to Puijker et al. (2008).

2.2.2 Identified substances

A specific priority substance threatening the drinking water treatment was selected if one or more of the following characterisations apply:

A. Possible norm exceedence, found regularly in surface water
B. Found in drinking water, undesirable, found regularly in surface water or infiltrate
C. Highly polar (logKOW <3), mobile and/or persistent (poor biodegradability) difficult to remove, found regularly in surface water
D. Carcinogenic or toxicologically relevant substance found in surface water
E. Substance has high production volume and is found regularly in surface water
F. Relevant for infiltration license

Table 2.1: Inventory of threats to the treatment of Dunea

	Application	**Emission route**	**Characterisation**
	Pharmaceuticals		
Carbamazepine	Anti-eplilepticum	DW	B
Diclofenac	Analgesic	DW	B
Ibuprofen	Analgesic	DW	B
Fenazon	Analgesic	DW	B
Metoprolol	Beta blocker	DW	B
Sulfamethoxazole	Anti biotic	DW	B
Bezafibrate	Cholesterol lowering	DW	B
Acetylsalicylic acid	Analgesic (aspirin component)	DW	B
Clofibric acid	Cholesterol lowering	DW	B
	Pesticides		
2,4-D	Herbicide	AR (BW&M)	A, F
DEET	Insecticide	DW, drift (M)	A, F
Dimethenamide	Herbicide/ foliage dead plea	AR (BW&M)	A, F
Diuron	Herbicide	AR (BW&M)	A, F
Carbendazim	Fungicide	AR (BW&M)	A, F
Chloridazon	Fungicide	AR (BW&M)	A, F
Isoproturon	Herbicide	AR (M)	A, F
MCPP, MCPA	Herbicide/ growth regulator	AR (BW&M)	A, F
Nicosulfuron	Herbicide/ foliage dead plea	AR (M)	A, F
Glyphosate	Herbicide/ foliage dead plea	AR (BW&M)/ use on pavement	A, F
AMPA	Degradation product glyphosate/ zinc phosphonates cooling water	AR (BW&M)/ IW	B
	Hormones and endocrine disruptors		
17β-oestradiol	Natural hormone	DW, AR	B, C, D
Oestron	Natural hormone	DW, AR	B, C, D
17α-ethynyloestradiol	Synthetic hormone, anti conception	DW	B, C, D
Bisfenol-A	Monomer for polycarbonates and epoxy resins/ PVC Stabilizer	IW	B, C, D, E
Diethylftalaat	PVC plasticizer	IW, DW	B, C, D, E
Dibutylftalaat	PVC plasticizer	IW, DW	B, C, D, E
Diethylhexylftalaat	PVC plasticizer	IW, DW	B, C, D, E

X-ray contrast media			
Amidotrizonacid	Contrast agent	DW (hospital)	B, C
Iopamidol	Contrast agent	DW (hospital)	B, C
Iomeprol	Contrast agent	DW (hospital)	B, C
Iopromide	Contrast agent	DW (hospital)	B, C
Iohexol	Contrast agent	DW (hospital)	B, C
Additional emerging substances			
PFOS	Surfactant in fat-repelling paper, textile, fire extinguishers	IW, DW	B, C
PFOA	Surfactant in fat-repelling paper, textile, fire extinguishers	IW, DW	B, C
MTBE, ETBE	Fuel additive	IW, shipping	E
NDMA	Industrial intermediate product	IW	C, D
Diglyme	Industrial solvent	IW	D,
p,p-sulfonyldifenol	Industrial intermediate product	IW	C, E
TCEP	Reducing agent	IW	C, D,
EDTA	Chelating agent, preservative	IW, DW	E
Urotropine	Fuel additive	IW	?
Tributyl phosphate	Plasticizer, solvent, anti-foaming agent,	IW, DW	?

DW = Discharge domestic WWTP
W = Discharge industrial WWTP
AR = Agricultural runoff
BM = Bommelerwaard
M = Maas

3. Preventative measures

3.1 "Zuiver water in de Bommelerwaard"

3.1.1 Introduction

Dunea's intake point is located just downstream of an area with a cluster of agri- and horticulture that uses and consequently discharges pesticides (see figure 3.1). Together with involved stakeholders, the project *Zuiver Water in de Bommelerwaard* was started in 2002, aimed at reducing the emission of plant protection products to aquatic environment of the Bommelerwaard.
Water is released to the Afgedamde Maas from four pumping locations whenever the water level in the Bommelerwaard too high. If the Bommelerwaard requires extra water, it is taken in from the Meuse when needed. On average 40% of the total water volume in the Afgedamde Maas consists of Bommelerwaard-water, the rest originates directly from the Meuse. It therefore makes sense to aim at reducing the emissions from the Bommelerwaard with location specific preventative measures.
This paragraph describes the relevant aspects and outcomes of the initiative.

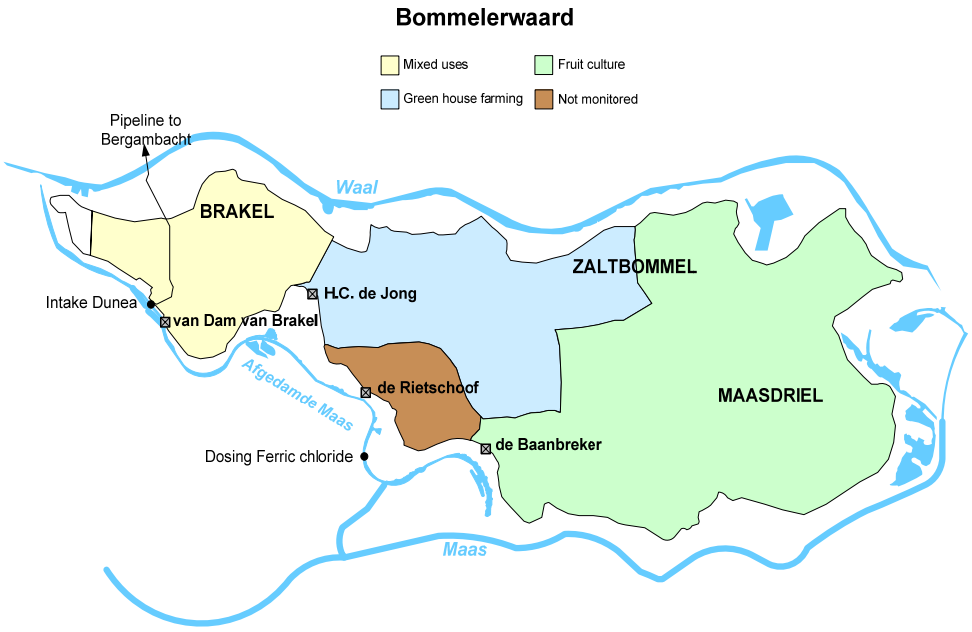

Figure 3.1: Water system "de Bommelerwaard"

3.1.2 Motivation and objectives

The project is an initiative of Dunea, water board Rivierenland (WSRL) and Rijkswaterstaat Direction South- Holland (RWS-DZH) and aims at reaching agreements with stakeholders towards reduced usage and emission of pesticides. In 2002 a 'intention agreement' has been signed by the involved actors: the province of Gelderland, the municipalities of Maasdriel and Zaltbommel, representatives of region's farmers/horticulturists (GLTO) and drinking water company Vitens. The project's main objective is to improve the surface water quality of the Afgedamde Maas, by realising an improvement in quality of the water released from the Bommelerwaard. The quality of the Bommelerwaard-water should comply with the maximum permissible risk (MTR) or with the drinking water norm when no MTR exists or when the MTR exceeds the drinking water norm (Hoekstra et al., 2002).

The multifunctional principal applies when surface water is infiltrated in the soil. It requires that the quality of the infiltrated water should pose no threat to the other functions of infiltrated soil and the quality of the groundwater. The quality of surface water used for infiltration and abstraction in the dunes does not meet the standards set by law (Infiltratiebesluit Bodembescherming or IB). As a result, the province of South-Holland has decided to allow infiltration until 2016 under a few conditions. Those conditions require Dunea to execute several projects and activities (Speets, 2005):

1. Improvement of surface water quality via preventative measures.

2. Improvement of pre-treatment.
3. Aiming at reduced agricultural run-off.
4. Mapping of the dispersion of substances that are foreign and of high concentrations of substances known to be used in the area.
5. Compensate/mitigate harm to nature/environment caused by infiltration of undesirable substances.

3.1.3 Preventative measures Bommelerwaard

Several different types of measures have been designed and put into practice. Some were sector specific; others had a more general aim. The measures are categorized as reducing the use of pesticides (1), use of alternative technologies (2) or use of alternative (more eco-friendly) pesticides (3). In table 3.1 a summary of the measures can be found. For a more detailed description the reader is referred to Speets (2005), Hoekstra et al. (2002) and Vlaar et al. (2007).

Table 3.1: Preventative measures Bommelerwaard

General		
Financial contribution to investments in emission-reduction (mainly fruit culture Advising on pesticide usage Prevention at source: reduced usage as 1st step Altering pumping regime Bommelerwaard Communication		
Fruit culture		
Category	**Measure**	**Comment**
Reduction of usage	Application of AseptaColl	Improves the effect of glyphosate and thus reduces the required dose
	Usage of models and weather station information to optimise usage fungicides in scab control	
	Smaller 'black strip' (zwarte strook)	Smaller black strips around trees require less pesticide use
	Vegetation black strip	Vegetation on black strips significantly limits pesticides use
	Manual grubbing	
	Biological control	Use of assassin-bugs
Alternative technologies	Windshields on ditch sides	
	Sprayer filler machine	Central, mobile filler for sprayers, meeting all latest requirements
	Alternative nozzles	
	Using lime against fruit tree cancer	
	Use of 'Wannerspuit'	Sprayer with emission shields
Other	Cost/Benefit analysis of emission reducing measures Informing about new policies	
Green house farming (chrysanthemum)		
Category	**Measure**	**Comment**
Reduction of usage	Increase steaming frequency	Steam used to heat the ground controls several diseases and pests
	Improved steaming efficiency	
Usage alternative substances	Use of Mycotal	A mould preparation, capable of replacing several chemical pesticides
	Use of Nemasys	An eel preparation, capable of replacing several chemical pesticides
	Biological control	One type of millipedes preys on another type of millipedes
Alternative technologies	Recirculation of irrigation water Optimising usage fertilizer by a software tool that calculates evaporation from plants	
Other	Monitoring development of reconstruction/expansion green house farming in Bommelerwaard	

3.1.4 Results

The water quality is an important indicator for the success of the project, and is monitored intensively. In the figures below trends of norm exceedence (concentrations above drinking water norm or maximum allowable risk, MTR) can be found. The interpretation is a bit problematic because the measuring package is changed every year; more compounds are included annually.
Speets (2005) has evaluated the outcomes of the project over the period 2002-2004 and concludes that the implementation of the measures was lagging behind the planning, despite the financial contribution and contribution of manpower. The results of the first couple of years of the project did not meet the expectations: the direct measurable effect in terms of a reduction in the emission of pesticides from the Bommelerwaard is very limited (see figures below).

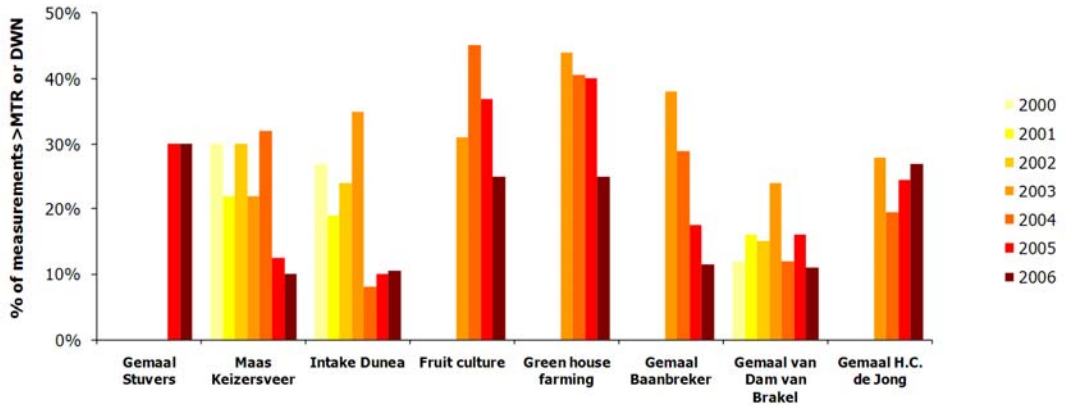

Figure 3.2: Monitoring results Bommelerwaard, location specific (adapted from Visser et al., 2007).

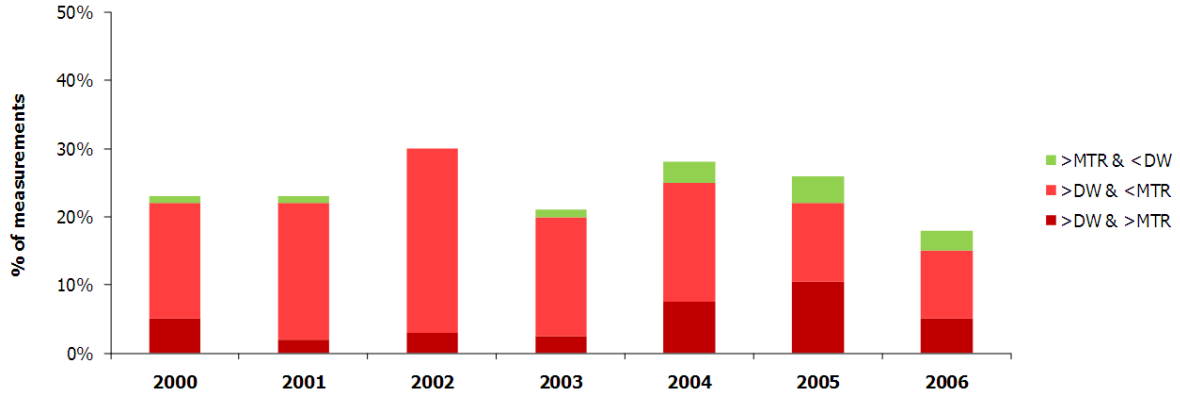

Figure 3.3: Average water quality Bommelerwaard. Amount of measurements exceeding the norms in relation to the total number of measurements. (Adapted from Visser et al., 2007)

In 2007 the results were evaluated again (Visser et al., 2007, Speets, 2007 and Vlaar et al.,2007). Overall, the water quality in the Bommelerwaard has improved since the project 'Zuiver water in de Bommelerwaard' commenced in 2002. It is difficult to state just how much of the improvement can be fully attributed to the project, since autonomous policy developments have their influence as well. Speets (2007) concludes his evaluation by stating that based on the results achieved up to 2005, it will be unlikely that the water quality goals for 2010 will be reached, even though a significant increase in water quality was observed in 2006. The exceedence of norms may have been reduced for the whole of the Bommelerwaard, however at Dunea's intake point the exceedence show increments from 2004 and onwards.

3.2 Reduced emission of pesticides, national levels

Reducing the contamination of surface waters is one of the main objectives of the European Water Framework Directive, which is implemented via national legislation of the member states. The Netherlands, Belgium, Germany and France have implemented policies and programs aiming at a reduction of pesticide use and emission to the natural environment.

The Dutch Ministry of Agriculture, Nature and Food Quality has formulated a target concerning the environment and the protection of crops: a 95% reduction of the environmental impact to surface waters in 2010 compared to 1998, in an economically sound way (maintaining the competitive position). The quality of surface waters used for the production of drinking water has improved, but the intermediate target of 50% reduction in the number of drinking water problems – exceedence of the drinking water standard at site of abstraction - has not been achieved. In 2005 a reduction of 18% has been reached. The reduction can be fully attributed to the prohibition of three types of pesticides in the Netherlands: atrazine, diuron and simazin. It is suspected that 27% of the problems concerning drinking water have an origin outside the Netherlands (MNP, 2008).

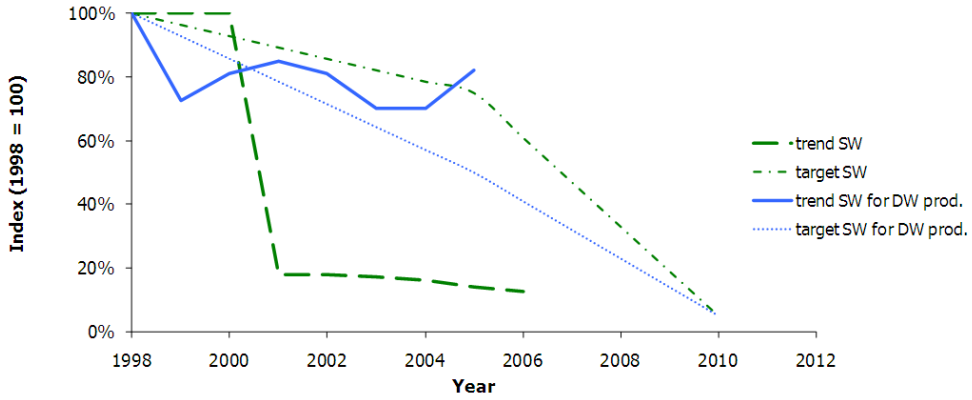

Figure 3.4: Trends and targets concerning norm-exceedence (MTR and DWN) pesticide concentrations in Dutch surface waters

From figure 3.4 can be concluded that the impact of pesticide use to the Dutch aquatic environment has been reduced. For a more detailed description of the pesticide reduction programs of EU member states and the results, the reader is referred to Derks (2010).

3.3 Reduced emission of pharmaceuticals

Pharmaceuticals are biologically active substances, designed to have an effect at relatively low concentrations. Most pharmaceuticals are highly polar –easily dissolved in water- since they are designed to spread well via the bloodstream. The problematic substances found in waters include a large number of human and veterinary pharmaceuticals, veterinary food additives and the formed metabolites (degradation products). Almost 100% of total amount of pharmaceuticals and hormones found in domestic wastewater comes from human urine, which consists of only 1% of the total wastewater volume (Scheffer, 2007). Pharmaceuticals are not adequately removed during conventional wastewater treatment. Consequently, the solution may be to implement advanced post-treatment of wastewater, or to collect and treat urine separately from other sewerage. For a description of pilot projects, the advantages and drawbacks, the reader is referred to Derks (2010).

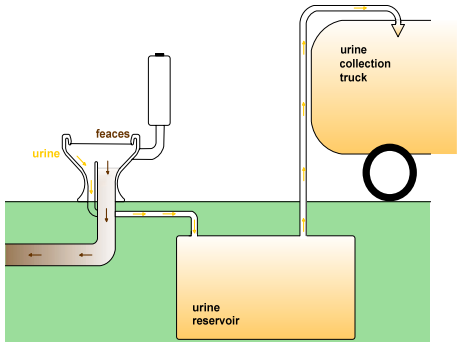

Figure 3.5: 1-Step filter for removal of nitrate, phosphate and organic micropollutants from WWTP effluent (left, van de Sandt, 2009) and principle of separate urine collection (right, Scheffer, 2007)

4. Motivation for AOP in pre-treatment

" To prevent, to remove or to convert"

4.1 Introduction

Drinking water companies that use surface water as their primary source for production of drinking water face the threats posed by OMPs. Prevention at the source is the preferred solution. Emission reduction is however very complex and where organic micropollutants are used, a portion will always find its way into the aquatic environment. Prohibition of one substance is often a short term solution, as is shown by the atrazine/glyphosate problem. Atrazine use has been prohibited in the Netherlands since 2000 but unfortunately glyphosate, an even more persistent pollutant has taken its place. The "solution" for tackling the issues of OMPs and drinking water production is two-folded:

> *Continues effort should go towards reducing the emission of organic micropollutants to the aquatic environment, combined with extended drinking water treatment capable of removing or converting OMPs.*

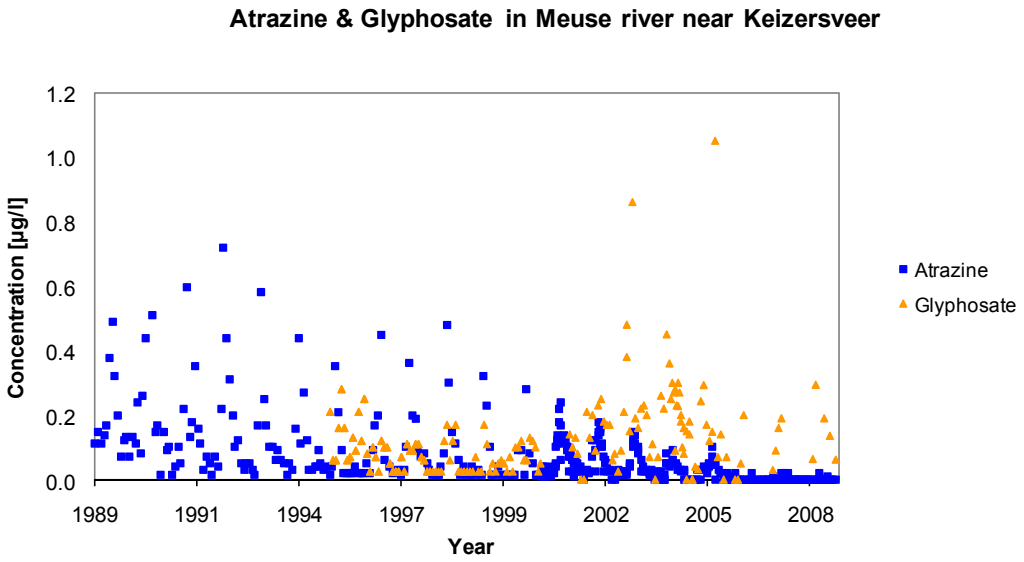

Figure 4.1 Glyphosate has gradually replaced Atrazine (adapted from Lekkerkerker-Teunissen, 2009)

The extended treatment should be robust and capable of removing future substances as well. Dunea's primary barriers against micropollutants are the dune passage followed by dosing of PAC in the post-treatment. Research has shown that dune passage has positive effect on the removal of OMPs, however, 15 substances currently present in the pre-treated Meuse water are poorly adsorbed and cannot be degraded biologically (Segers and Stuyfzand, 2007). Furthermore, PAC proved to provide an insufficient barrier against OMPs found in the Meuse water. Small, polar substances in particular are difficult to remove with the current treatment (Beerendonk et al., 2006).

4.2 Choice for AOP

Dunea's treatment philosophy is *to prevent (1), to remove (2) or to convert (3)* unwanted substances from her source water. The emission of OMPs to her source should be prevented and when that is not possible, OMPs should be removed. When removal is not possible, OMPs should be converted into less harmful substances. Three possibilities for extended treatment are viable (Lekkerkerker-Teunissen, 2009):

- Reverse osmosis (RO, to remove)
- Nano-filtration combined with granular activated carbon filtration (NF + GAC, to remove),
- Advanced oxidation (AOP, to convert).

Not just the technology itself but the relation to Dunea's existing multiple barrier treatment and the status of the dune areas (nature reserves) are important. Currently infiltration of pre-treated river water is allowed until 2016. The license will have to be renewed and it is expected that stricter criteria

regarding the concentration of OMPs will be formulated. In order words, the level of pre-treatment needs improvement.
Membrane filtration can remove most organic micropollutants, but have significant drawbacks like for instance high energy consumption and the remaining concentrate containing the OMPs. The concentrate should receive treatment or perhaps it can be transported and discharged into the ocean, not the most environmental friendly solution. The recovery of the membranes may introduce capacity problems for Dunea in the future. Furthermore, when reverse osmosis is applied the water should be remineralized before being suitable for human consumption. These drawbacks made Dunea decide to start pilot-scale AOP research and to monitor the development in the field of membrane technology (Lekkerkerker-Teunissen, 2009).

4.3 Location in pre-treatment

Besides the environmental motivation for extension of the pre-treatment, AOP in the post-treatment would introduce extra risks for the biological stability of the produced water. A drawback of advanced oxidation is the formation of extra assimilable organic carbon (AOC), a readily available food source for microorganisms. This implies a significant increase in the load of the slow sand filters - assuming their capability of removing the extra AOC - and probably increases the biological activity in the distribution network. The current AOC levels in Dunea's drinking water are very low, which should be maintained in the future (Lekkerkerker-Teunissen, 2009).

The fact that advanced oxidation and dune passage are complementary makes the combination a promising multiple barrier approach. Advanced oxidation is a short, chemical process while dune passage is characterized as a long-term biological process that levels peak concentrations (Lekkerkerker-Teunissen et al., 2009). During advanced oxidation, double bonds that characterize many OMPs are weakened or broken, resulting in smaller molecules that are more easily degraded biologically (Lekkerkerker-Teunissen et al., 2009 and MWH, 2005). When AOP is applied in the pre-treatment, AOP followed by dune passage form a multiple-barrier against OMPs. The dunes provide a first barrier against the increased AOC levels, followed by slow sand filtration.

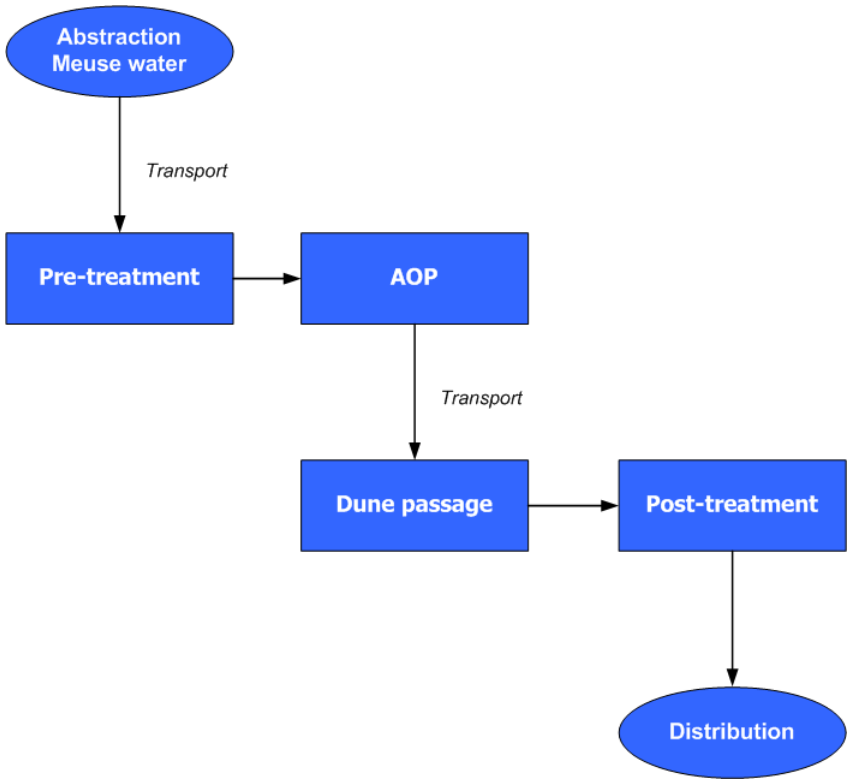

Figure 4.2: Future treatment schema Dunea

5. Theory of advanced oxidation processes

5.1 Introduction

From the late 1970s UV-radiation has been applied in the Netherlands for water disinfection since the discovery of chlorinated disinfection by-products (EPA, 2003) became a concern. In 1995, Water Company PWN started to perform research towards the application of UV-radiation in combination with hydrogen peroxide as the barrier against OMPs (IJpelaar et al., 2007) and has implemented advanced oxidation at her production site in Andijk.
Advanced oxidation processes (AOP) is a collective term for treatment methods capable of oxidizing undesirable substances by hydroxyl radicals. AOP through UV/H_2O_2 combines two mechanisms that contribute towards the degradation of undesirable substances: photolysis and oxidation. This chapter describes the relevant aspects concerning the theory of advanced oxidation.

5.2 UV radiation

5.2.1 Quantification of UV radiation

Ultraviolet is the region of the electromagnetic spectrum between x-ray and visible light, with a wavelength of 100-400 nm (EPA, 2003). The UV spectrum can be divided into four regions:

- Vacuum-UV,
- UVC,
- UVB,
- UVA,

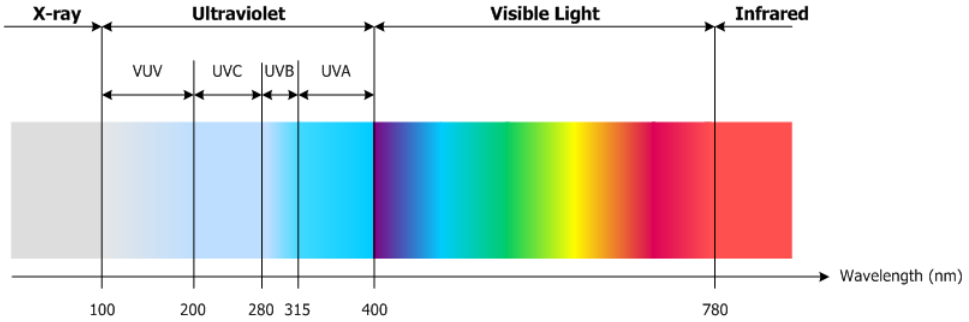

Figure 5.1: Spectrum electromagnetic radiation

The wavelength required for effective and practical disinfection, also known as germicidal wavelength is between 200 and 300 nm. UV light is generated by a applying a voltage across a gas mixture (usually mercury vapour), which results in a discharge of photons. The specific wavelengths of the emitted photons depend on both the composition of the gas and the power of the used lamp.

5.2.2 Mercury vapour lamps

The output of light is depended on the concentration of mercury atoms and thus on the mercury vapour pressure. At a low vapour pressure (near vacuum, 0.13 – 1.33 Pa) the produced light is *monochromatic,* it is emitted at a single wavelength (254 nm).
When a higher vapour pressure ($1.33 * 10^4$ – $1.33 * 10^6$ Pa) and high operating temperatures (600-900 ºC) are applied, collisions between mercury atoms occur more frequent. The produced light is *polychromatic* (spectrum between 200-800 nm) and has an overall higher intensity. Mercury vapour pressure between 1.33 and 1.33 *10 pa does not produce UV radiation efficiently (EPA, 2003).
Both low and medium pressure UV lamps are applied effectively for the disinfection of water. For oxidative purposes mainly, but not exclusively, medium pressure lamps are applied (IJpelaar et al., 2007).

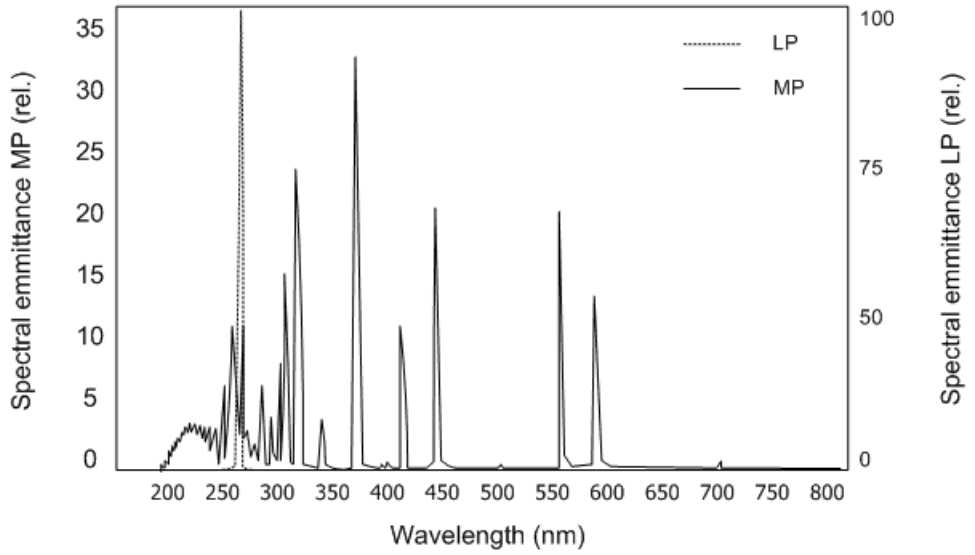

Figure 5.2: Relative spectral distributions of medium and low pressure UV lamps (adapted from Stefan, 2004)

5.2.3 Influence on propagation of light

Propagation of UV light depends on absorption, reflection, refraction and scattering, phenomena occurring as a result of interactions between the emitted light, the reactor components and the water being treated (EPA, 2003).

The transformation of light to other forms of energy when passing through a medium, a phenomena known as *absorption,* varies with the specific wavelength. The water in the reactor, but also the reactor components will absorb UV light in varying degrees, depending on the materials. When UV light is being adsorbed, it is no longer available for disinfection. Scattering, refraction and reflection merely change the direction of the UV light, thus the light is still available for disinfection.

Refraction or the change in direction of propagation when light passes from one medium to another, changes the angle of the UV light. For instance, when light passes trough the lamp sleeve and through the water, refraction will occur.

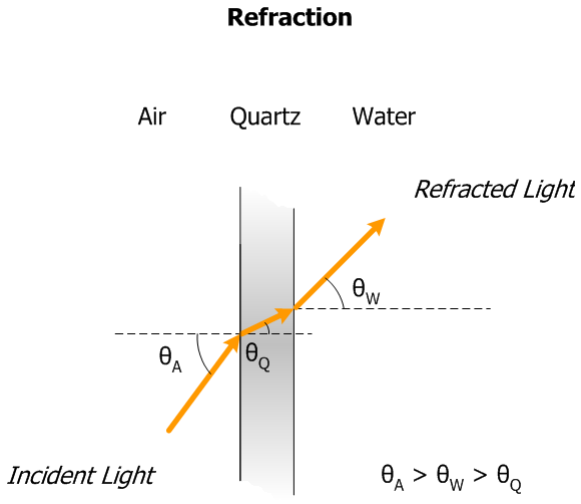

Figure 5.3: Refraction of light (adapted from EPA, 2003)

When light is deflected by a surface, its direction of light propagation is changed, a phenomena known as *reflection*. Reflection can be either specular or diffuse. Reflection of smooth polished surfaced can be qualified as specular and follows the Law of Reflection ($\theta_i = \theta_r$). When light is reflected from a rough surface, diffuse reflection occurs. The light scatters in all directions and shows little dependence with the angle of incidence. Reflection in UV reactors takes place at interfaces that

do not transmit the UV light, for instance the reactor walls, but also at transmitting interfaces like the inside of a lamp sleeve.

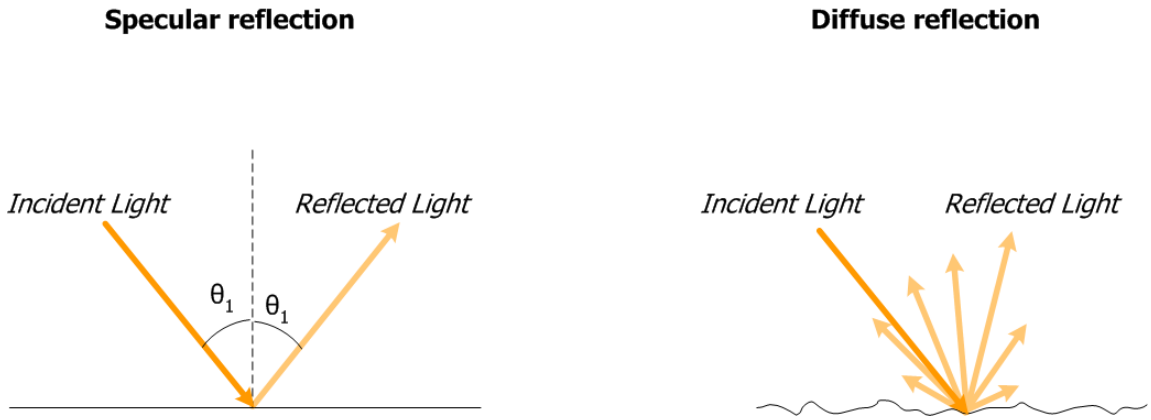

Figure 5.4: Reflection of light (adapted from EPA, 2003)

Scattering occurs due to interaction with a particle, which can change the direction of propagation in all directions. Several types of scattering can be distinguished, such as back-scattering when the light is scattered towards the incident light source but also forward scattering, which occurs mostly when the particle size is larger then the wavelength. Rayleigh scattering occurs when the particle size is smaller than the wavelength.

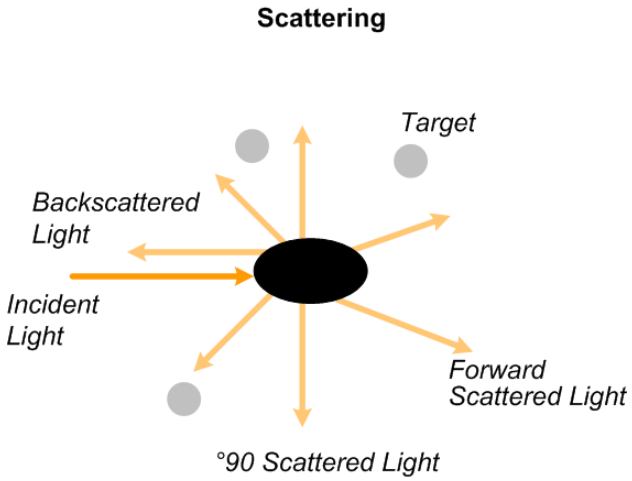

Figure 5.5: Scattering of light (adapted from EPA, 2003)

5.2.4 Application of UV

When the wavelength of emitted UV light coincides with the wavelength spectrum at which a substance adsorbs, the substance can be degraded photolytic (IJpelaar et al., 2007).
Disinfection by UV is significantly different from chemical disinfection by for instance chlorine or ozone. Chemical disinfectants destroy or damage cellular structures, can interfere with the metabolism of microorganisms and hinder its biosynthesis and growth. UV light inactivates microorganisms because it damages nucleic acids (DNA and RNA), which inhibits microbiological replication. Damage to nucleic acid will not prevent basic cell functions such as metabolism. However, the microorganism cannot reproduce and therefore cannot infect a host. In order to kill a microorganism, the required dose of UV is several orders of magnitude larger than the dose needed to prevent reproduction (EPA, 2003).

5.2.5 UV dose and microbiological response

The UV dose can be characterized as the energy per unit that is incident on a surface. It is the product of the average intensity (in all directions) and the exposure time. Several units are commonly used for UV dose: J/m^2, mJ/cm^2 and mWs/cm^2.

The response of microorganisms to exposure of UV light can be calculated by determining the concentrations of microorganisms before and after the exposure to a measured dose. Mostly the UV dose-response relationship is expressed as the proportion of microorganisms inactivated (log inactivation):

$$\log inactivation = \log \frac{N_0}{N}$$

Eq. 1

Where
N_0 = Concentration of infectious microorganisms before exposure to UV light
N = Concentration of infectious microorganisms after exposure to UV light

5.3 Theory of photolysis

Photolysis is a process in which chemical bonds of a substance are broken down by light, which results in the production of carbon dioxide and water (Tang, 2004). This photochemical reaction can be understood when the energy of those bonds is compared with the wavelength of light that corresponds with that amount of energy.

5.3.1 Energy of light

A quantum (smallest physically realizable unit) of light, called a photon possesses an amount of energy equal to E. As becomes apparent from the formula below, the energy of a photon is dependent on its wavelength; shorter wavelengths correspond to a higher amount of energy per photon.

$$E = hv = h \cdot \frac{c}{\lambda}$$

Eq. 2

Where					
h	=	*6.64*10^{-34}*	=	*Plank's constant*	*J.s*
v	=		=	*frequency*	*s^{-1}*
c	=	*3.0*10^{8}*	=	*speed of light in vacuum*	*m/s*
λ	=		=	*wavelength*	*nm*

5.3.2 Absorption of light

An essential step in initiating any photochemical reaction is the absorption of light by a molecule (Champagne et al., 2008). *The Beer-Lambert Law*, an empirical relationship between the absorption of light and the properties of the medium through which the light penetrates, describes absorption of light:

$$A = \log \frac{I_{0,\lambda}}{I_\lambda} = [\alpha_\lambda + \varepsilon_\lambda \cdot C] \cdot l$$

Eq. 3

Where		
$I_{0,\lambda}$	=	*intensity of incident light at wavelength λ*
I_λ	=	*intensity of light after passing through water solution*
ε_λ	=	*molar absorptivity/ extinction coefficient of absorbing species of interest in water*
a_λ	=	*absorption coefficient/ attenuation coefficient of the medium*
C	=	*concentration of absorbing species of interest in water*
L	=	*distance travelled by light trough water (path length)*
A	=	*absorbance*

The absorbance A for a particular substance with concentration C and path length L depends on the wavelength. The absorption spectrum or the plot of absorbance versus wavelength can be determined with a spectrophotometer. Generally, a substance will absorb light over a wide wavelength range but

may show one ore more absorption peaks. The wavelengths that correspond to the absorption peaks are very important; they can be used to determine the suitable wavelength for the photochemical degradation of the substance of interest (Champagne et al., 2008).

$$UVT_\lambda = 10^{-A_\lambda} \qquad or \qquad A_\lambda = -\log UVT_\lambda$$

Eq. 4

The reaction quantum yield Φ_r is a measure for the overall efficiency of a photolytic process and is defined as the number of transformed moles divided by the total number of moles of photons absorbed by the system P at wavelength λ (Stefan, 2004):

$$\phi_r(\lambda) = \frac{total\ number\ of\ moles\ of\ P\ transformed}{total\ number\ of\ moles\ of\ photons\ of\ \lambda\ absorbed\ by\ P\ in\ the\ system}$$

Eq. 5

The quantum yield can also be defined in kinetic terms (e.g. rates of decay and light absorption by P in the system):

$$\phi_r(\lambda) = \frac{-\frac{d[P]}{dt} \quad (mol\ L^{-1}s^{-1})}{I_a(\lambda) \quad (mol\ L^{-1}s^{-1})}$$

Eq.6

For polychromatic light, Braun et al. (1991) have defined a *reaction quantum efficiency* as the ratio of the number of molecules of a product formed to the number of photons absorbed (N_a), in the spectral region used, during the reaction period.

$$\eta = \frac{\int_{\lambda_1}^{\lambda_2} \phi(\lambda) N_a(\lambda)\, d\lambda}{\int_{\lambda_1}^{\lambda_2} N_a(\lambda)\, d\lambda}$$

Eq. 7

In natural waters the reaction quantum yield for degradation of organic micropollutants are generally less than 0.01 due to the low concentrations of micropollutants and the presence of other species that can inhibit the chain reactions (scavengers). Quantum yields for photolysis of atrazine (254 nm) for instance is 0.05 (Balci et al., 2009) while reaction quantum yield for nitrite from photolysis of nitrate (200-300 nm) is 0.1 (Goldstein et al., 2007).

When a photon with light energy *hv* is absorbed by a molecule, the molecule becomes unstable and several reactions can occur. A molecule in its ground state A_0 absorbs a photon of light energy hv, which converts the molecule into its excited state A^*. Five paths are possible from A^* (Champagne et al., 2008):

- The excess energy can be transferred to another molecule by a process called *intersystem crossing*, forming excited molecule A'* (Eq. 8 A_0 merely serves as a sensitizer, important for indirect photolysis, which will be explained in more detail later.
- *Internal conversion* (heat) may cause a release of the absorbed energy. The excited molecule is reverted back to its ground state (Eq. 9)
- A* can re-release its photon, which also reverts the molecule back to its ground state and is called *fluorescence* (Eq. 10).
- *Quenching*, consists of a second molecule Q_0 (in its ground state) absorbing energy from the first molecule, which transforms Q_0 into its heated state Q^ (Eq. 11).
- The excited molecule can undergo several chemical transformations (Eq. 12)

$$A_0 \xrightarrow{hv} A^* \xrightarrow{intersystem\ crossing} A'^* \qquad \textit{Eq. 8}$$

$$A_0 \xrightarrow{hv} A^* \xrightarrow{internal\ conversion} A_0 \qquad \textit{Eq. 9}$$

$$A_0 \xrightarrow{hv} A^* \xrightarrow{fluorescence} A_0 + hv \qquad \textit{Eq. 10}$$

$$A_0 \xrightarrow{hv} A^* + Q_0 \xrightarrow{quenching} Q^{\wedge} + A_0 \qquad \textit{Eq. 11}$$

$$A_0 \xrightarrow{hv} A^* \xrightarrow{chemical\ transformations} ? \qquad \textit{Eq. 12}$$

The excited molecule A′* formed during intersystem crossing undergoes further reactions:

$$A'^* \xrightarrow{internal\ conversion} A'_0 \qquad \textit{Eq. 13}$$

$$A'^* \xrightarrow{phosphorescence} A'_0 + hv \qquad \textit{Eq. 14}$$

$$A'^* + Q_0 \xrightarrow{quenching} A'_0 + Q^{\wedge} \qquad \textit{Eq. 15}$$

$$A'^* \xrightarrow{chemical\ transformation} ? \qquad \textit{Eq. 16}$$

The chemical reactions initiated by the energy within the molecule are of utmost importance since they lead to the transformation and degradation of the substance of interest. The reactions include photooxidation, photoreduction, photoimomerization, photosubstitution, photoaddition, photofragmentation and photohydrolysis (Champagne et al., 2008).

The general expression of the rate of direct photolysis of a molecule A under monochromatic radiation λ is described with the following reaction (Stefan, 2004)

$$-\left(\frac{d[A]}{dt}\right)_\lambda = \phi_r(\lambda) \cdot I_A(\lambda) \qquad \textit{Eq. 17}$$

$\phi_r(\lambda)$ and $I_A(\lambda)$ are the reaction quantum yield and the rate of light absorption by A (mol $L^{-1}s^{-1}$) respectively. Because $I_A(\lambda)$ is a function of the fraction of light absorbed by A, equation 17 becomes:

$$\left(\frac{d[A]}{dt}\right)_\lambda = \phi_r \frac{N_0}{V} \cdot \frac{\varepsilon_{A\,(\lambda)[A]}}{\alpha(\lambda) + \varepsilon_A(\lambda)[A]} \left(1 - 10^{-[\alpha(\lambda)+\varepsilon_A(\lambda)[A]]l}\right) \qquad \textit{Eq.18}$$

Where
$N_0(\lambda)$ = incident photon flow (mol s^{-1})

5.4 Oxidation by hydroxyl radicals

5.4.1 Characterization of free radicals

A free radical is a molecule that has an unpaired electron which it needs to repair. By reacting with another molecule, the radical will obtain the missing electron. If the radical takes an electron from another molecule, the latter one becomes a radical as well, initiating a self-propagating chain reaction. It is also possible that the radical reacts with a second radical, which terminates the chain reaction and 'neutralizes' both radicals (Parsons, 2000).

$$A\cdot + B\!: \rightarrow A\!: + B\cdot \qquad \textit{Eq. 19}$$

$$B\cdot + C\!: \rightarrow B\!: + C\cdot \qquad \textit{Eq. 20}$$

$$A\cdot + B\cdot \rightarrow A\!:B \qquad \textit{Eq. 21}$$

A hydroxyl is a molecule consisting of one oxygen atom and one hydrogen atom, which are connected by a covalent bond. The neutral form is known as a hydroxyl radical (OH·) and the hydroxyl anion (OH^-) is called a hydroxide. Hydroxyl radicals have a very high oxidative potential of 2.8V (Alfano et al, 2000) and therefore short lived. Because hydroxyl radicals will react with almost all substances in the water (they react non-selectively) a large number of radicals are necessary to degrade an undesirable substance sufficiently (IJpelaar et al., 2007).

Reactions of hydroxyl radicals and organic compounds will form carbon-centered radicals (R· and R·-OH). When O_2 is present, the carbon-centered radicals can by transformed to organic peroxyl radicals (ROO·). All these radicals react further, leading eventually to the decomposition and mineralization of the organic compounds (Gao, 2008).

5.4.2 Formation of hydroxyl radicals

Several processes are capable of producing hydroxyl radicals, some of which are explained in this paragraph. A well-known example is the Fenton's reaction in which ferrous iron (II) is oxidized by hydrogen peroxide, forming ferric iron (III), a hydroxyl radical and a hydroxyl anion (Wadley and Waite, 2004):

$$Fe^{2+} + H_2O_2 \rightarrow Fe^{3+} + \cdot OH + OH^- \qquad \textit{Eq. 22}$$

Hydroxyl radicals can also be produced by UV-light dissociation of hydrogen peroxide, independently of the pH. When a H_2O_2 molecule absorbs UV-radiation at a wavelength < 300 nm (Alfano, 2000), it splits homiletically, forming two ·OH radicals:

$$H_2O_2 \overset{hv}{\rightarrow} 2\ \cdot OH \qquad \textit{Eq. 23}$$

Dissociation of nitrite (NO_2^-) and nitrate (NO_3^-) forms hydroxyl radicals as well (de Ridder, 2006):

$$NO_2^- \overset{hv}{\rightarrow} \cdot O^- + NO\cdot \qquad \textit{Eq. 24}$$

$$NO_3^- \overset{hv}{\rightarrow} \cdot O^- + NO_2\cdot \qquad \textit{Eq. 25}$$

$$\cdot O^- + H^+ \overset{hv}{\rightarrow} \cdot OH \qquad \textit{Eq. 26}$$

Formation of hydroxyl radicals from nitrite only takes place at wavelengths > 298 nm (Φ =0.015 – 0.08) and from nitrate at wavelengths <250 nm (Φ = 0.09-0.14) (De Ridder, 2006). The quantum yield Φ of radical formation from peroxide is equal to 1. However, when comparing the UV absorbance of peroxide and nitrate (see figure below), it becomes apparent that the total UV absorbance of nitrate at wavelengths <250 nm is considerably higher than the total UV absorbance of peroxide. Perhaps nitrate can provide a significant contribution to the formation of hydroxyl radicals, even though the quantum yield is 10 times lower. It can be concluded that hydroxyl formation from H_2O_2 is probably more effective at longer wavelengths due to less competition for UV light from nitrate.

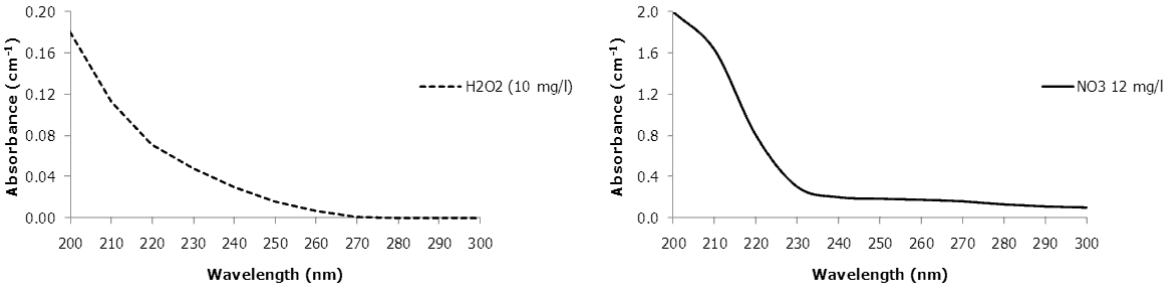

Figure 5.6: UV absorbance H_2O_2 (HWL, 2009) and NO_3^- (adapted from de Ridder, 2006)

Because UV absorbance by H_2O_2 is low, the concentration of H_2O_2 has to be rather high in order to generate a sufficiently high level of hydroxyl radicals in a solution containing strong photon absorbers (Tuhkanen, 2004). As a result, the concentration of peroxide in the effluent of water subjected to UV radiation will be high because only a fraction (approximately 10%) of the H_2O_2 is actually photolysed into hydroxyl radicals. Dunea intends to implement AOP before dune passage and because disinfectants such as hydrogen peroxide have adverse effects on biological activity, excess peroxide will have to be removed. Research has shown that activated carbon effectively degrades H_2O_2 into water and oxygen (Kruithof et al., 2002).

Under the influence of UV radiation, hydrogen peroxide is formed from ozone, followed by the same mechanism forming hydroxyl radicals in UV/H_2O_2 (de Ridder, 2006):

$$O_3 \xrightarrow{h\nu} O_2 + O(^1D) \qquad \textit{Eq. 27}$$

$$O_2 + O(^1D) + H_2O \rightarrow H_2O_2 \qquad \textit{Eq. 28}$$

$$H_2O_2 \xrightarrow{h\nu} 2 \cdot OH \qquad \textit{Eq. 29}$$

A disadvantage of advanced oxidation through UV/O_3 is the formation of bromate (BrO_3^-) from bromide (Br^-). Since bromate is suspected to be carcinogenic, this specific method of advanced oxidation is not widely used in drinking water production.

Titanium dioxide releases an electron under the influence of UV radiation. The electron is taken up by TiO_2 particles. At the surface of the TiO_2 particles that have released an electron, water is absorbed and converted to hydroxyl radicals (de Ridder, 2006):

$$TiO_2 \xrightarrow{h\nu} TiO_2(h^+) + TiO_2(e^-) \qquad \textit{Eq. 30}$$

$$TiO_2(h^+) + H_2O \rightarrow TiO_2 + H^+ + \cdot OH \qquad \textit{Eq. 31}$$

5.5 Advanced oxidation by UV/H_2O_2

5.5.1 Combined reaction

When UV radiation is combined with a dose of H_2O_2, the overall oxidative potential is significantly enhanced, even under ambient pressure and temperature. AOP through UV/H_2O_2 can degrade organic contaminants directly by photolysis or indirectly via oxidation with formed hydroxyl radicals. The following combined reaction occurs:

$$Substance + \cdot OH \xrightarrow{hv} degradation\ products + CO_2 + H_2O \qquad \textit{Eq. 32}$$

The degradation can be described in kinetic terms with the following reaction (Tuhkanen, 2004)

$$-\frac{d[C]}{dt} = I_0 \phi_C f_C \left(1 - \exp(-\mathrm{A_t})\right) + \mathrm{k_{OH,C}}\,[\cdot \mathrm{OH}][\mathrm{C}] \qquad \textit{Eq.33}$$

Where

I_0 = *incident flux of radiation*
ϕ_c = *quantum yield of C (fraction of absorbed radation resulting in photolysis)*
F_c = *ratio of light absorbed by C to the total absorbance of the solution times a factor 2.3*
A_t = *total absorbance of the solution*
$k_{OH,C}$ = *second-order reaction rate constant of hydroxyl radical with C*

If the wavelength is >254 nm, mostly hydroxyl radicals are responsible for initiating the oxidation reactions. However, degradation of certain compounds can also take place directly as a result of UV radiation, which improves the specific compound's potential to be oxidized by hydroxyl radicals (Tang, 2004). The formed hydroxyl radicals oxidize organic compounds primarily by *hydroxylation* (introduction of a hydroxyl group (-OH) into a compound or radical) or *hydrogen abstraction* (abstraction of a hydrogen atom from a compound) (Tang, 2004).

5.5.3 Chemical and photochemical reactions

The widely accepted photochemical and chemical reactions and their corresponding rate constants in AOP via UV/H_2O_2 are summarized below. The process is initiated by the formation of hydroxyl radicals from hydrogen peroxide when the applied wavelength is <300 nm (reaction 1). At longer wavelengths the molar absorption coefficient ε_{per} approaches zero and therefore inhibits the formation of hydroxyl radicals (see also figure 5.6 below). The UV absorbance by hydrogen peroxide is only 0.015 at 254 nm. Besides the initiation and degradation, propagation and termination reactions are relevant. Propagation reactions do not influence the total number of hydroxyl radicals, however termination and scavenging result in a decrease of the total number of available hydroxyl radicals.

It must be noted that once a free radical has been initiated, a series of simple degradation reactions occur. The reactions itself may be simple but a large number of reactions are likely to occur, creating a complex degradation mechanism which makes it very difficult to predict all the products of an oxidation reaction (Parsons et al., 2004).

Initiation

$$H_2O_2 \xrightarrow{k_1\ \ hv} 2 \cdot OH \qquad \textit{Eq. 34}$$

Hydroxyl radical propagation

$$H_2O_2 + \cdot OH \xrightarrow{k_2} HO_2 \cdot + H_2O \qquad \textit{Eq. 35}$$

$$H_2O_2 + HO_2 \cdot \xrightarrow{k3} \cdot OH + H_2O + O_2 \qquad \textit{Eq. 36}$$

Hydroxyl radical termination

$$2 \cdot OH \xrightarrow{k_4} H_2O_2 \qquad \textit{Eq. 37}$$

$$2\,HO_2 \cdot \xrightarrow{k_5} H_2O + O_2 \qquad \textit{Eq. 38}$$

$$\cdot OH + HO_2 \cdot \xrightarrow{k_6} H_2 + O_2 \qquad \textit{Eq. 39}$$

Degradation

$$OMP + \cdot OH \xrightarrow{k_7} degradtion\ product(s) + CO_2 + H_2O \qquad \textit{Eq. 40}$$

$$OMP \xrightarrow{k_8\ hv} degradation\ product(s) + CO_2 + H_2O \qquad \textit{Eq. 41}$$

Table 5.2: Rate constants radical reactions

Rate constant	$M^{-1}s^{-1}$	Source
k_1	0.5	Baxendale and Wilson (1957)
k_2	2.7×10^7	Buxton et al., 1988
k_3	3.0	Koppenol et al., 1978
k_4	5.5×10^9	Buxton et al., 1988
k_5	6.6×10^9	Schested et al., 1968
k_6	8.3×10^5	Bielski et al., 1985
k_7	System and compound dependent	
k_8	System and compound dependent	

5.5.4 Scavenging and corresponding rate constants

Hydroxyl radicals react non-selective, and are therefore subject to *scavenging* which inhibits the degradation efficiency of the targeted substances. Substances present in surface waters such as carbonate, bicarbonate, nitrite, nitrate, sulphate, phosphate, chloride, NOM, and DOC will compete with the target OMPs for hydroxyl radicals (Boncz, 2002, de Ridder, 2006 and Ray et al., 2007). The collective term *water matrix* is used to indicate these parameters and others such as the pH, temperature and turbidity. As a result of the water matrix, fewer radicals are available for the degradation of the target OMPs and higher doses of H_2O_2 are required when the concentration of scavengers is higher. However, hydrogen peroxide itself is also a hydroxyl scavenger.

When comparing the reaction rate constants of ·OH scavengers, it can be concluded that the concentrations of nitrite/nitrate and organic material are preferably very low. Nitrate has a relatively slow scavenging rate constant ($5.0 * 10^5$ M^{-1} s^{-1}). However, when nitrate is subjected to UV radiation it is converted to nitrite, which has a fast rate constant ($1.0 * 10^{10}$ M^{-1} s^{-1}) (Buxton et al., 1988).

Organic material (DOC) will limit the formation of hydroxyl radicals by absorption of UV light (entire spectrum) and also acts as a scavenger by reacting directly with ·OH radicals. The rate constant of DOC scavenging is high (10,7 to 10^{10} M^{-1} s^{-1} depending on the composition) and can therefore have a large contribution to the total scavenging effect.

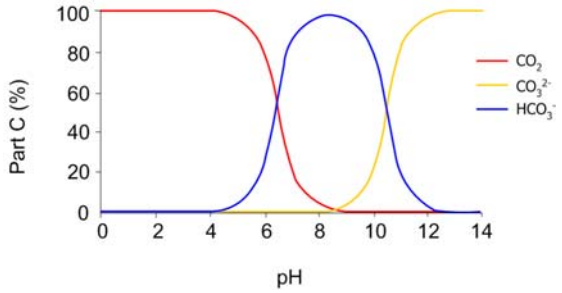

Figure 5.7: Calcium-carbonate equilibrium

Scavenging by either carbonate or bicarbonate is directly related to the pH of the water, as can be concluded from the calcium-carbonate equilibrium. The pH of the pre-treated Meuse water is approximately 8, so the concentrations of bicarbonate and carbonate will be ±100% and ±0% respectively.

According to Hoigné (1998) scavenging rate constants for phosphate, sulphate and chloride are generally very slow can be neglected. The following radical scavenging reactions and rate constants are relevant (Buxton et al., 1988):

$$HCO_3^- + \cdot OH \xrightarrow{k_9} HCO_3 \cdot + OH^- \qquad \textit{Eq. 42}$$

$$CO_3^{2-} + \cdot OH \xrightarrow{k_{10}} CO_3 \cdot + OH^- \qquad \textit{Eq. 43}$$

$$NO_3^- \xrightarrow{k_{11}} NO_2^- + O \qquad \textit{Eq. 44}$$

$$NO_2^- + \cdot OH \xrightarrow{k_{12}} NO_2 \cdot + OH^- \qquad \textit{Eq. 45}$$

$$H_2O_2 + \cdot OH \xrightarrow{k_{13}} H_2O + H^+ + O_2^- \cdot \qquad \textit{Eq. 46}$$

$$RH + \cdot OH \xrightarrow{k_{14}} R \cdot + H_2O \qquad \textit{Eq. 47}$$

Table 5.3: Rate constants scavenging reactions

Rate constant	$M^{-1}s^{-1}$
K_9	$8{,}5 * 10^6$
K_{10}	$3{,}9 * 10^8$
K_{11}	?
K_{12}	$1{,}0 * 10^{10}$
K_{13}	$2{,}7 * 10^7$
K_{14}	10^7 - 10^{10} M^{-1} s^{-1}

The scavenging effect of an individual species can be described with a simple second order reaction equation like equation 44:

$$\frac{dA}{dt} = -k\,[A][B] \qquad \textit{Eq. 48}$$

Where [A] is the is the concentration of hydroxyl radicals, [B] the concentration of the scavenging species and k the corresponding rate constants. The total amount of scavenging from the water matrix of the water used during the experiments can then be estimated with the following formula:

$$-\frac{d[\cdot OH]}{dt} = [\cdot OH] * (k_9 \cdot [DOC] + k_{12} \cdot [NO_2^-] + k_{13} \cdot [H_2O_2] + k_{14} \cdot [HCO_3^-] \qquad \textit{Eq. 49}$$

Where:

$$[NO_2^-] = initial\,[NO_2^-] + \phi(NO_2^-)_\lambda$$

5.5.5 Nitrite formation

Besides acting as a hydroxyl radical scavenger, nitrite has adverse effects on public health, like for instance methemoglobinemia (blue-baby syndrome) in infants younger then 6 months caused by decreased O_2 uptake of blood. Moreover, nitrite could be transformed into nitrosamines. The EC standard for nitrite concentration in drinking water is 0.1 mg/L. Nitrite is also capable of inducing methemoglobinemia in a wide range of species (among others cattle, sheep, dogs, chickens) and can

influence micro-organisms and their processes (Philips et al., 2002). Because artificial research and recovery forms the key element of drinking water production by Dunea Duin en Water, potential nitrite toxicity can be of interest. Literature review (Philips et al, 2002) shows that nitrite can inhibit ammonia oxidation activity, nitrite oxidation, denitrification, anoxic and aerobic phosphate removal, methanogenesis and cell growth. Nitrite levels associated with these negative influences are >42 mg/L N for inhibition of ammonia oxidation, >70 mg/L N for inhibition of cell growth for various Pseudomonas species, >100 mg/L N for nitrification activity.

Formation of nitrite during UV photolysis can be fully attributed to the irradiation and absorption of UV light by nitrate (IJpelaar et al, 2007).

Table 5.4: Nitrite yield at various wavelengths

λ (nm)	Φ(NO_2^-)
205	0.207
210	0.198
214	0.182
220	0.172
225	0.152
230	0.149
235	0.122
240	0.097
247	0.084
253.7	0.065
260	0.047
270	0.0197
300	0.0094

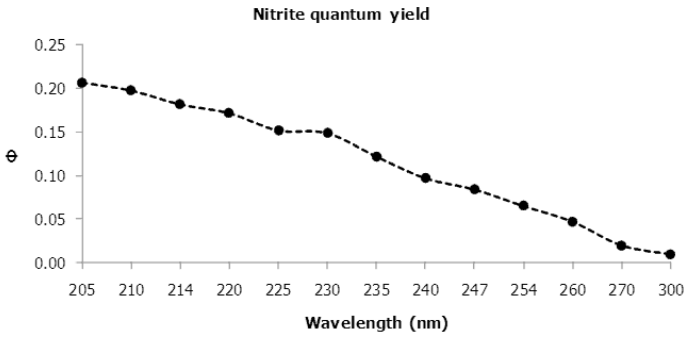

Figure 5.8: Nitrite quantum yields

Goldstein et al. (2007) have investigated the quantum yield Φ of nitrite from nitrate photolysis (using xenon vapour lamps) at wavelengths between 200-300 nm. The quantum yield is wavelength dependent and equal to 0.065 at 254 nm. Applying Braun's method of determining the quantum efficiency for polychromatic light (see equation 7), the quantum efficiency for nitrite formation from nitrate photolysis is estimated to be approximately 0.1. IJpelaar et al (2006) have found that nitrate absorbs UV radiation (using mercury vapour lamps) between 200 and 240 nm. The quantum yield for nitrite formed during nitrate photolysis was about 0.1. Nitrite yield at UV 254 nm was found to be less than 0.001.

Formation of nitrite in water (8,6 mg/L NO_3^-, UVT_{254} = 90%, UV dose unknown) treated with LP-UV was below 0.01 mg/L NO_2^-. Collimated beam experiments using water containing 14 mg/L NO_3^- (LP-UV dose 120 mJ/cm^2) showed a nitrite formation of 0.007 mg/L. Under MP-UV radiation (70 mJ/cm^2), nitrite concentrations up to 0.15 mg/L NO_2^- were found (see table 5.5 below).

Water company PWN found a significant increase in nitrite concentration (MP-UV dose of 600 mJ/cm^2, 6 ppm H_2O_2) from 15 µg/L in the influent (pre-treated water from Lake IJssel, 6-12 mg/L NO_3^-), to 100-300 µg/L in the AOP effluent (Martijn et al., 2007).

Table 5.5: Nitrite formation MP-UV, collimated beam (IJpelaar, et al. 2007)

Nitrate (mg/L NO_3^-)	DOC (mg/L C)	pH	UV dose (mJ/cm^2)	Nitrite (mg/L NO_2^-)
3.5	3	7.97	20	0.02
3.5	3	7.87	70	0.07
15	3	7.87	70	0.11
12.3	4.1	9.05	70	0.1
12.3	4.1	7.87	70	0.15
3.5	3	7.87	70	0.07
2.9	4.6	7.89	70	0.08

5.5.6 NOM, DOC and formation of AOC

Natural organic matter (NOM), a collective term for molecules containing a carbon atom, is formed from decaying organic material. NOM is usually measured as dissolved organic carbon (DOC).

Assimilable organic carbon (AOC), which is a food source for bacterial growth, is formed as a result from direct photolysis (≥100 mJ/cm^2) of DOC or trough a reaction of DOC with hydroxyl radicals (IJpelaar et al, 2007). Natural waters (containing NOM) show absorbance in the low wavelength region (200-230 nm). Consequently, AOC formation when applying LP lamps is significantly lower then when MP lamps are applied.

AOC in water may increase the heterotrophic plate counts (HPC) and can result in bio-films on surfaces like pipe walls. AOC levels <10 µg/L C indicate a limited growth potential (van der Kooij, 1992). In the Netherlands chlorination in the distribution net is not allowed which stresses the need for biologically stable water. Furthermore, increased biological growth may result in bioclogging: accumulation of microbial biomass in a porous medium which can lead to a reduction of pore space and is associated with decreased hydraulic conductivity of the medium (Tullner, 2009). AOC levels as low as 10 µg/L C were found to cause clogging of filter beds under experimental conditions modelling those for infiltration of pre-treated surface water in recharge wells (Hijnen et al., 1992). Observed head loss in filter beds resulting from filtration of water containing of 3.3 - 3.9 TOC (expressed in mg/L C) and 60 – 63 of AOC (µg/L C) were 25 kPa. It can be concluded that increased AOC levels will influence the biological activity in the dunes. Considering the fact that some organic micropollutants are biodegradable and can thus be removed during soil passage (Verstraeten et al, 2002; Seegers et al, 2007), one may also expect that increased biological activity can increase removal of organic micropollutants. However, predicting the nature of the effect of increased AOC levels to biodegradation of organic micropollutants during soil passage is beyond the scope of this research. This objective of this research is to compare the performance of low pressure and medium pressure ultraviolet lamps applied for advanced oxidation, which among other parameters is defined by the observed increase in assimilable organic carbon.

Observed increase of AOC levels in LP-effluent (influent consisted of pre-treated river water, DOC = 2-4 mg/L, UVT = 83-90%, AOC concentration unknown) were 6.6 µg/L, with an applied UV dose of 25 mJ/cm^2. In a laboratory-scale experiment with LP-UV (river water pre-treated with coagulation, sedimentation and rapid sand filtration) were insignificant up to a UV dose of 90 mJ/cm^2 (IJpelaar et al., 2007. MP-UV (90 mJ/cm^2) increased AOC levels from 7.5 µg/L in pre-treated river water (DOC 2 mg/L) to 15 µg/L in the effluent. Pilot scale research (MP-UV, 58 mJ/cm^2, 180 m^3/hr) using pre-treated surface water (DOC 2 mg/L, UV-T = 90%) resulted in AOC levels of 10 µg/L and 15 µg/L when the UV dose was increased to 95 mJ/cm^2. IJpelaar et al (2007) conclude that AOC formation in systems with LP lamps is lower then in systems with MP lamps. The authors also conclude that AOC formation is negligible with UV doses <90 mJ/cm^2, irrespective of the applied lamp type.

Maas et al. (2009) also investigated the formation of AOC during LP-UV disinfection, assuming the production AOC to be negligible. Their study has shown however that LP-UV (40 mJ/cm^2) elevates AOC concentrations by 50%. AOC concentrations increased from 11 µg/L to 16 µg/L after LP-UV radiation. Maas et al were the first to show a significant increase of AOC concentrations as a result of low dose LP-UV.

PWN Water Supply Company has observed AOC levels increasing from 5-33 µg/L to 100-150 µg/L after AOP with MP lamps. Biodegradation by the GAC filters reduced the AOC to 16-18 µg/L (Martijn et al., 2007). During research on the formation of AOC, performed by Greater Cincinnati Water Works (Ohio, USA), measured AOC levels were as high as 500 µg/L (IJpelaar et al., 2007). The influent used consisted of river-water pre-treated with rapid sand filtration and GAC, received a UV dose of 40 mJ/cm^2 (polychromatic irradiation). The raw water contained approximately 150 µg/L of AOC.

In order to keep the concentration of AOC as low as possible, post-treatment with GAC may be necessary. Dunea's primary motivation for implementing AOP before the dune passage was the objective to maintain low AOC concentrations in the distribution net.

5.5.7 Main performance indicators: degradation and EEO

The amount of conversion or degradation of a target substance can be expressed as a percentage, a relative reduction or as a log. In this report, the degradation is reported as a percentage reduction in the initial concentration:

$$-\frac{dC}{dt} = \frac{C_i - C_e}{C_i} * 100\%$$

Eq. 50

Performance comparison of achieved degradation based on variations in UV doses is difficult. The UV dose is a reactor specific characteristic and varies due to hydraulic influences and variations in the water quality. Therefore a parameter known as the electrical energy per order EEO (kWh/m^3) is used, defined as the electrical energy in kWh required to achieve 1 log degradation of a substance per unit of treated water (Bolton et al., 2003):

$$EEO = \frac{P}{Q \cdot \log\left(\frac{C_i}{C_e}\right)}$$

Eq. 651

Where:

P	=	*Power consumption reactor (kWh)*
Q	=	*Flow through the reactor (m^3/h)*
C_i	=	*Influent concentration specific compound*
C_e	=	*Effluent concentration specific compound*

5.6 Degradation mechanisms of model compounds

In paragraph 2.1 a list of organic micropollutants that pose a threat to drinking water production by Dunea was given. More then 40 substances were included on the list. Analysing the results from the weekly experiments in terms of degradation of all those substances would be a tremendous amount of work. Four model compounds (atrazine, bromacil, ibuprofen and NDMA) were selected for the weekly experiments because the proportional contribution of photolysis and oxidation to the total degradation is known or can be estimated.
Atrazine use has been banned since 2000 but the average concentration in the water abstracted from the Afgedamde Maas is 0.02 µg/L (Bertelkamp, 2009). Atrazine was selected because it is one of the most widely researched herbicides, yielding an abundance of reference materials. Also, atrazine can be degraded by photolysis under monochromatic and polychromatic radiations (Stefan, 2004) and via oxidation which makes it a good indicator for the overall performance of the AOP. Atrazine is also used as the main performance indicator in other AOP researches.
Concentrations of bromacil in the intake water are well below the detection limit of <0.05 µg/ (Bertelkamp, 2009). Polychromatic radiation can degrade bromacil, however it is not effective and oxidation is the primary mechanism. Bromacil cannot be photolyzed by monochromatic radiation (Acher et al., 1994). Ibuprofen is found in the intake water at an average concentration of 0.03 µg/L (Bertelkamp, 2009) and cannot be photolyzed using monochromatic irradiation. Photolysis of ibuprofen under polychromatic radiation is less effective then photolysis of bromacil. NDMA concentrations are below 1 ng/l (Bertelkamp, 2009) however NDMA is severely carcinogenic (Mitch et al., 2003) even at low concentrations. NDMA was selected because it can only degraded by photolysis; oxidation effects are negligible (Stefan et al., 2002 and Jobb et al., 1994). This paragraph describes the properties and degradation mechanisms of four compounds selected for experimental research.

Alkyl groups that characterize the model compounds are poorly removed using LP photolysis, dealkylation is a result of oxidation by hydroxyl radicals. LP-UV photolysis results in cleavage of C-Cl bond (dechlorination of atrazine), cleavage of the N-NO bond (NDMA). When MP-UV is applied, photolysis results in dechlorination, cleavage of N-NO bonds (NDMA), cleavage of the C-Br bond (bromacil), cleavage of the C-C bond (ibuprofen) and dealkylation. Dosing H_2O_2 enhances dealkylation dramatically. The mechanisms are further elaborated in the next subparagraphs.

5.6.1 Atrazine

Atrazine, 2-chloro-4-(ethylamine)-6-(isopropylamine)-s-triazine is a widely used herbicide which has become an environmental concern and consequently its use in the European Union was prohibited in 2005. Atrazine belongs to the chemical group of triazines, characterized by a heterocyclic ring structure, containing three nitrogen and three carbon atoms. The atrazine molecule ($C_8H_{14}ClN_5$) consists of a Cl atom, the s-triazine ring and its various alkyl groups, depicted in the figure below.

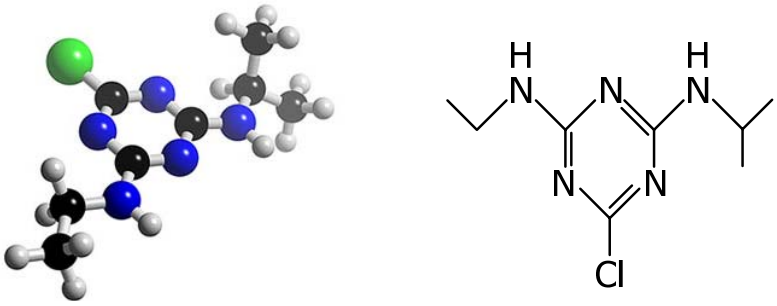

Figure 5.9: 3D model and chemical structure of an atrazine molecule

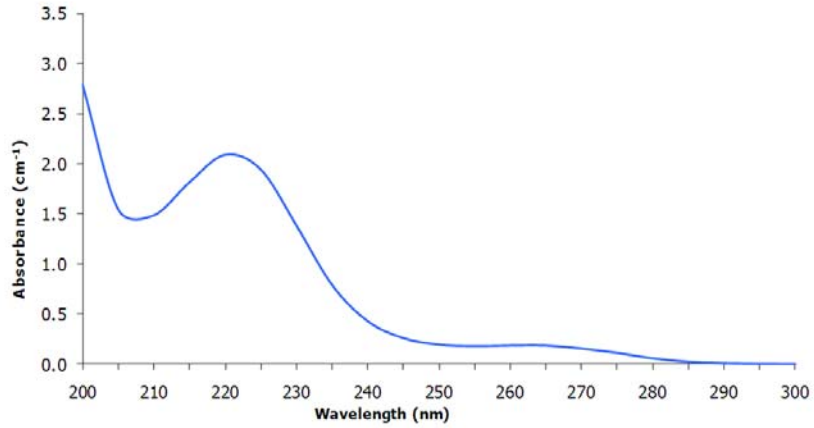

Figure 5.10: Absorbance spectrum atrazine, 10 µg/L in Mili-Q water (HWL, 2009)

Even though atrazine is no longer used, there are three reasons why atrazine was selected as a model compound. Firstly, the consequences of atrazine use have been researched around the world, creating an abundance reference material. Secondly, atrazine shows a strong absorption of UV radiation in the UVC range and can be photolyzed under monochromatic and polychromatic radiations (Stefan, 2004). Furthermore, Atrazine can also be oxidized by hydroxyl radicals. The latter two reasons make that atrazine can be used as an overall indicator for the performance of the AOP.

In a previous paragraph the difficulty to predict the exact degradation pathways and products was mentioned, due to the numerous possibilities. Literature review performed by Bertelkamp (2009) further substantiated this fact: different researches have found different degradation pathways for direct photolysis of atrazine. The authors seem to agree on the fact that *hydroxy-atrazine* or HATZ is the first degradation product formed after direct photolysis.

From the absorbance spectrum of atrazine can be concluded that direct photolysis of atrazine is more effective for MP lamps: the absorbance increases significantly at shorter wavelengths and at 254 nm a local minimum is present. Moreover, the absorbance is highest at 200 nm, 220 nm and a small peak can be distinguished at 265 nm. Comparison to literature yields the same conclusions.

Table 5.6: Atrazine degradation products

Abbreviation	Name
ATZ	atrazine
HATZ	2-hydroxy-atrazine
DIAT	2-chloro-4-ethylamino-6-amino-*s*-triazine *or* de-isopropyl-atrazine
DEAT	2-chloro-4-isopropyl-6-amino-*s*-triazine *or* de-ethyl-atrazine
DEDIAT	2-chloro-4,6-diamino-*s*-triazine
DEDIHAT	2-hydroxy-4,6-diamino-*s*-triazine
ADE	2,4-dihydroxy-6-amino-s-triazine
CYA	2,4,6-trihydroxy-s-triazine or cyanuric acid
OHDEA	2-hydroxy-4-ethylamino-6-amino-s-triazine
OHDIA	Hydroxydesisopropylatrazine or
AOHE	2-chloro-4-acetamino-6-isopropylamino-s-triazine
AOHI1	2-chloro-4-ethylmino-6-(1-methyl-1-ethanol)amino-s-triazine
AOHI2	2-chloro-4-ethylmino-6-(2-propanol)amino-s-triazine
OHOHIDEA	2-hydroxy-4-ethylamino-6-(1-methyl-1-ethanol)amino-s-triazine
OHOEDIA	2-hydroxy-4-ethylmino-6-(2-propanol)amino-s-triazine

5.7.1.1 Main degradation mechanisms atrazine using LP lamps

Direct photolysis of atrazine at monochromatic irradiation (λ=254 nm) yields decomposition of atrazine into hydroxyatrazine (HATZ) via fast de-chlorination trough homolytic cleavage of the C-Cl bond followed by an electron transfer from the carbon to the chlorine radical processed by the carbocation reaction with water (Bianchi et al, 2006) or the heterolytic cleavage of the excited state atrazine molecule (Héquet et al., 2001). Hydroxyatrazine appeared to be quite stable towards UV light at 254 nm. The next step can consist of de-alkylation, however the reaction very is slow; the amount of formed de-alkylated products is limited, so the main degradation mechanism of atrazine by LP lamps is de-chlorination. Efficient de-alkylation can only be achieved by reaction with ·OH radicals, which are less effective for de-chlorinating. The degradation pathway and (intermediate) reaction products are depicted in figure 5.11.

When atrazine reacts with hydroxyl radicals, DIAT (2-chloro-4-ethylamino-6-amino-s-triazine or de-isopropyl-atrazine) is formed by loss of the isopropyl group, followed by the formation of DEDIAT (2-chloro-4,6-diamino-s-triazine or de-ethyl-de-isopropyl-atrazine) (loss of the ethyl group). It is also possible that the ethyl group is lost first and the isopropyl group secondly. Both pathways yield the same intermediate product DEDIAT. De-alkylation is followed by partial de-chlorination, forming 2,4-dihydroxy-6-amino-s-triazine (ADE) and eventually 2,4,6-trihydroxy-s-triazine or cyanuric acid (S. Jain et al., 2009, Bianchi et al., 2006). It must be noted that the lost ethyl groups contribute to the total amount of AOC.

5.6.1.2 Main degradation mechanisms using MP lamps

Direct photolysis of atrazine at polychromatic irradiation (λ=200 – 600 nm) primarily yields hydroxyatrazine (HAT). It is also possible that de-chlorination is followed by de-alkylation, yielding OHDEA and OHDIA, but the observed concentrations were lower (Héquet et al., 2006). OHDEA and OHDIA eventually loose their ethyl and isopropyl groups respectively, forming A,4-dihydroxy-6-amino-s-triazine (ADE) when all alkyl groups are lost. The final formed product is 2,4,6-trihydroxy-s-triazine (cyanuric acid). It is also possible that de-alkylation precedes the de-chlorination, forming OHDEA and OHDIA via a series of likely intermediate products, depicted in pathway 2, options a, b and c (figure 5.12).

Degradation pathways of atrazine via hydroxyl radicals for MP lamps are more or less similar to the path described for the LP lamps. Héquet et al found several additional intermediate products before the formation of 2,4-dihydroxy-6-amino-s-triazine (ADE), depicted in figure 5.13. The final formed product is cyanuric acid.

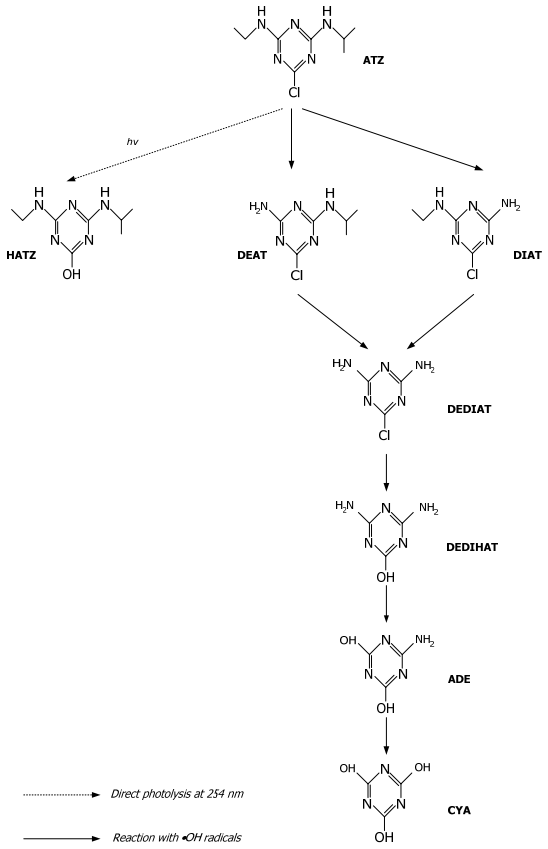

Figure 5.11: Summary degradation pathways atrazine, LP lamps

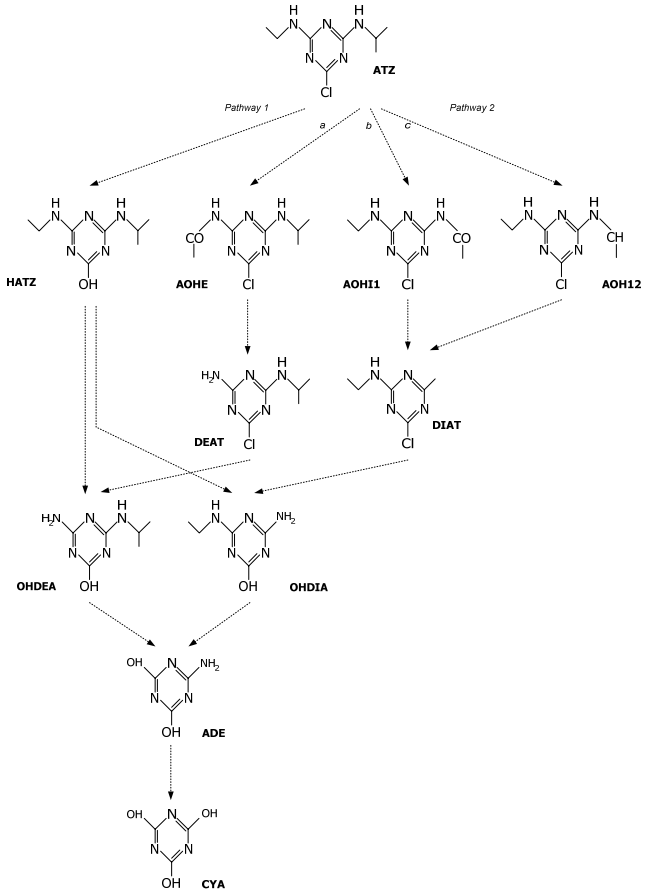

Figure 5.12: Photolysis pathways atrazine, MP lamps

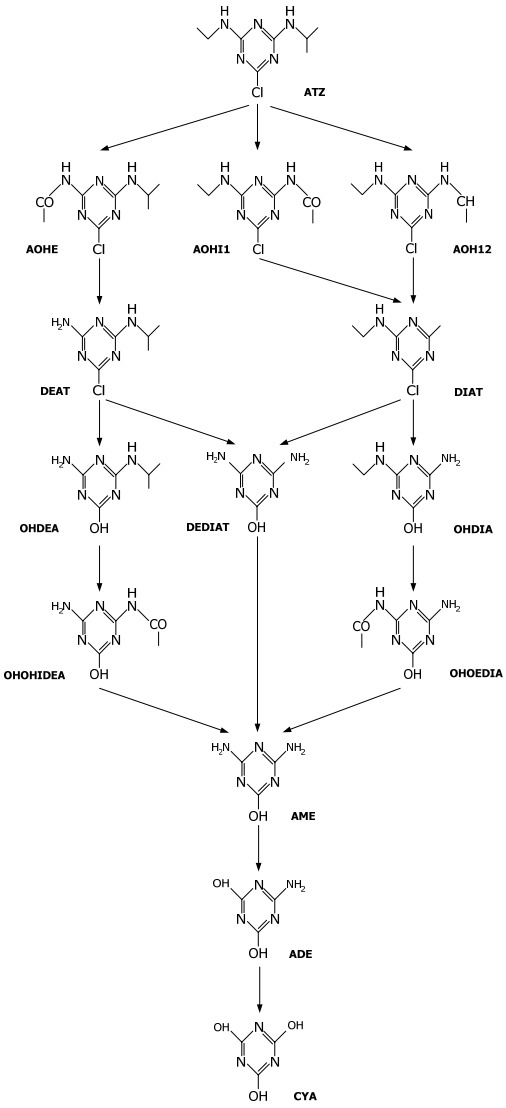

Figure 5.13: Oxidation pathways atrazine, MP lamps

5.6.2 Bromacil

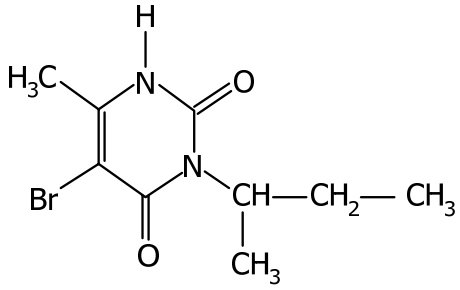

Figure 5.14: Bromacil chemical structure

Bromacil (5-bromo-3-sec-butyl-6-methyluracil) is a uracil herbicide, generally applied for weed control. The bromacil molecule ($C_9H_{13}BrN_2O_2$) consists of a Br-atom, two double oxygen bonds and two alkyl groups. Bromacil absorption shows a local minimum around 254 nm, indicating a low capacity of photolysis at 254. The absorbance spectrum of bromacil shows a broad peak around 275 nm. Moreover, the absorbance increases at wavelengths shorter then 240 nm.

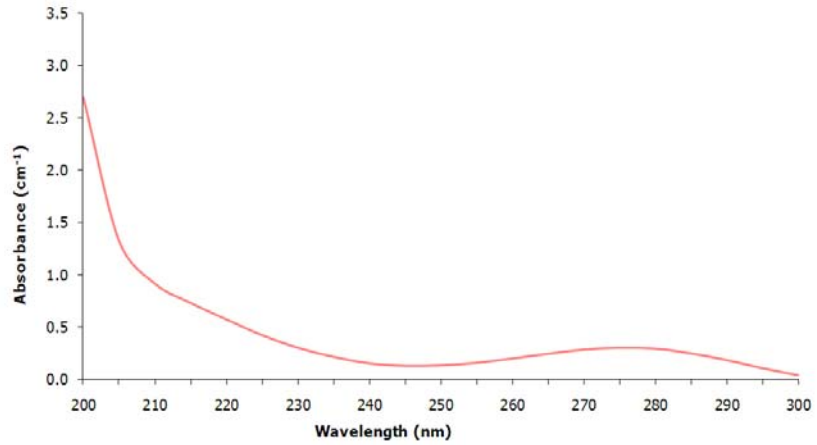

Figure 5.15: Absorbance spectrum Bromacil, 10 µg/L in Mili-Q water (HWL, 2009)

5.6.2.1 Main degradation mechanisms bromacil for LP lamps

Acher et al. (1994) conclude that photolysis of bromacil at 254 nm is not effective; after long exposure times, two degradation products were found, debromobromacil and dibromobromacil radical dimer. The dibromobromacil radical dimer was formed from a hemolytic cleavage of the C-Br bond, forming C• and Br• as well. However, the recovered yields were very low (5%). Photolysis by LP lamps can thus considered negligible. Dosing of hydrogen peroxide had a positive effect in terms of reaction times, yielding the same degradation products.

5.6.2.1 Main degradation mechanisms bromacil for MP lamps

Unfortunately very little information on the degradation pathways of bromacil was found. Moilanen et al. (1974) analysed degradation pathways under solar radiation (400-700 nm) which is also emitted by MP-UV lamps. Loss of the alkyl groups only occurred after extended radiation times.

When comparing the bromacil molecule structure to the molecule structure of atrazine and its degradation pathways, one can conclude that reaction of bromacil with hydroxyl radicals will result in removal of the alkyl groups. UV radiation will probably weak or break up the double N-NO bonds, a mechanism responsible for degrading NDMA (described in paragraph 5.7.4). Subsequently, radicals are formed that are responsible for further degradation mechanism.

5.6.3 Ibuprofen

Ibuprofen ($C_{13}H_{18}O_2$) is Non-Steroidal Anti-Inflammatory Drug, sold without prescription. The ibuprofen molecule consists of a double oxygen bond, several alkyl groups and an OH-group.
The absorbance spectrum shows that ibuprofen absorbs UV light primarily at wavelengths shorter then 240 nm. A peak can be distinguished around 225 nm. Moreover the absorbance is high at 200 nm. Looking more closely at the absorbance spectrum at wavelengths >240 nm yields the identification of a very small peak around 265 nm. The emission spectrum of the applied MP lams show a peak at 265 nm, indicating that photolysis of ibuprofen can occur at 265 nm.

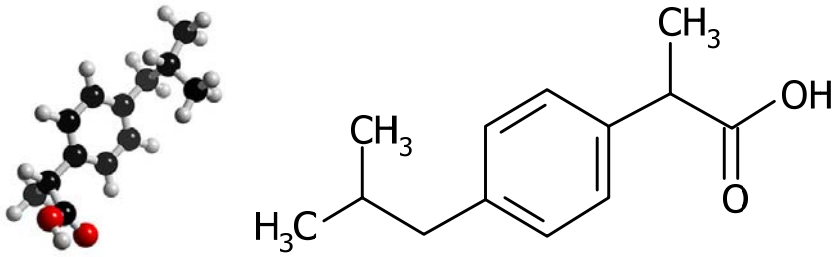

Figure 5.16: 3D model and chemical structure of an ibuprofen molecule

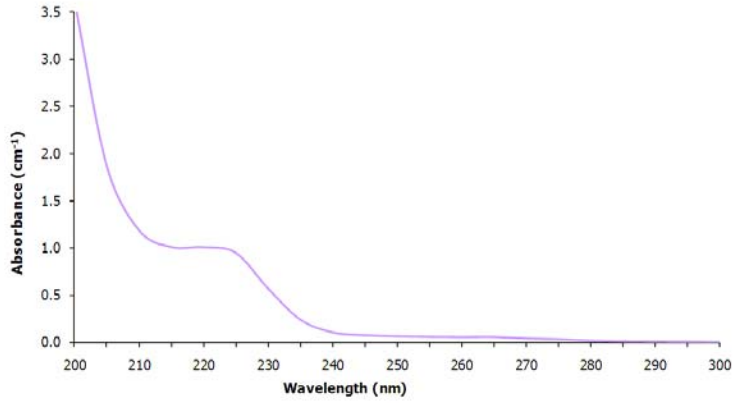

Figure 5.17: Absorbance spectrum Ibuprofen, 10 µg/L in Mili-Q water (HWL, 2009)

5.6.3.1 Main degradation mechanisms ibuprofen for LP lamps

Photolysis of ibuprofen at 254 nm is inefficient: application of extremely high UV doses (1271 mJ/cm^2) only degraded 27% of the initial concentration of ibuprofen. At a UV dose of 40 mJ/cm^2, typically applied for disinfection purposes, no conversion of ibuprofen was detected (Yuan et al., 2009).
Dosing just a small volume of H_2O_2 (0,29 and 1 mM), applying a UV dose of 40 mJ/cm^2 resulted in 25 and 40% conversion of ibuprofen respectively. The pathways were not reported. Ibuprofen concentrations were below the detection limit with a UV dose of 509 mJ/cm^2 and a peroxide dose of 0,29 mM (Yuan et al., 2009).

5.6.3.2 Main degradation mechanisms ibuprofen for MP lamps

From the UV absorbance spectra of ibuprofen can be concluded that direct photolysis by MP lamps is expected to be low, but should be higher than direct photolysis by LP lamps. Ibuprofen shows a poor UV absorbance at wavelengths >240 nm. First order photolysis rate constants found for ibuprofen are low: <0.1 (min^{-1}) *10^2 (Packer et al., 2003).
During experiments performed with UVA-visible light (315-800 nm) and UVB light (280-400) using humic water, degradation of ibuprofen was observed. The degradation of ibuprofen should be attributed to the formation of radicals from other compounds that are present such as CDOM or other pharmaceuticals. Natural chromophores in dissolved organic material (CDOM) act as a photosensitizer toward indirect phototransformations of pharmaceuticals in natural waters (Peuravuori et al., 2009). The main degradation mechanism for ibuprofen is the cleavage of the C-C bond to the carboxy group, producing a benzyl radical through decarboxylation. Packer et al. (2003) conclude that degradation of ibuprofen should be attributed to oxidation, but also suggests that photo generated radicals other

then hydroxyl radicals are involved. This latter conclusion seems reasonable taking the degradation pathways found for NDMA destruction (see next paragraph) into account.

5.6.4 NDMA

NDMA (N-Nitrosodimethylamine) is a carcinogenic industrial by-product, belonging to the chemical group of nitrosamines. The NDMA ($C_2H_6N_2O$) molecule consists of a double oxygen bond and two methyl groups, depicted in figure 5.18 below.

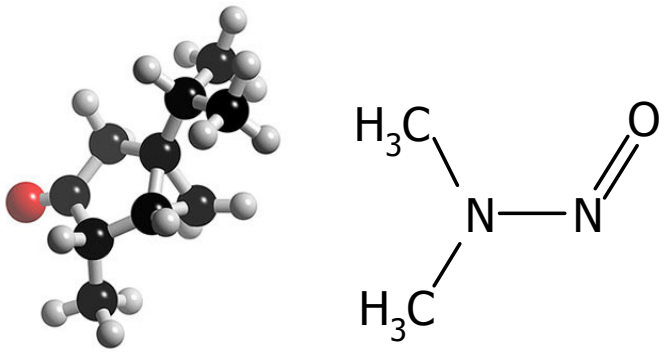

Figure 5.18: 3D model and chemical structure of NDMA

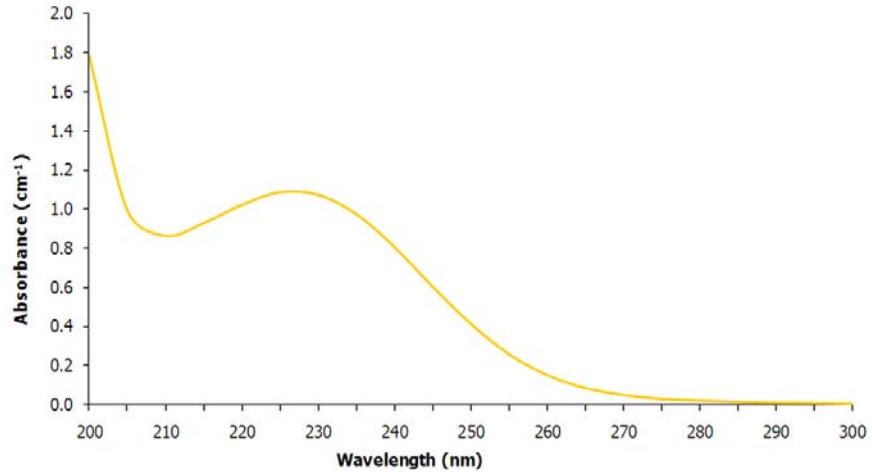

Figure 5.19: Absorbance spectrum NDMA, 10 µg/L in Mili-Q water (HWL 2009)

The photodegradation rate (poly- and monochromatic irradiation) of NDMA is not enhanced in the presence of H_2O_2 (Stefan et al., 2002 and Jobb et al., 1994). In order words, NDMA cannot be oxidized with hydroxyl radicals, only direct photolysis is effective.

5.6.4.1 Main degradation pathways NDMA

Photochemistry of N-nitrosamines has been studied intensively during the 1960s and 1970s and subsequently much is known about the degradation pathways of NDMA (at 254 nm). Irradiation causes excitation of the NDMA molecule (π → π*), followed by three possible reaction pathways (see figure 5.23)

The first pathway is the homolytic cleavage of the N-NO bond, producing nitric oxide (•NO) and the aminium radical ($\bullet NH^+$), reacting further to form N-methylidenemethylamine and nitroxyl (HNO) resulting from the detachment of the hydrogen atom from the aminium radical. The intermediate product N-methylidenem-ethylamine is hydrolysed into methylamine (MA) and formaldehyde.

The second pathway is the heterolytic cleavage of the N-NO bond, producing dimethylamine (DMA) and nitrite. Lee et al. (2005) also found a significant production of nitrate and formate as photolysis products of NDMA. Final yields of nitrate and formate after complete photolytic degradation of NDMA at a pH of 7.0 were 30 and 10% respectively.

Lee et al suggest a third pathway (O_2 saturation, pH=7.0): reaction of the excited NDMA molecule with dissolved oxygen or oxidation of NDMA into N-Methylidenemethylamine, NO radical and superoxide radical. The latter two can eventually form nitrate. A multitude of reactions can occur,

depending on the pH conditions. In figure 5.23 the three pathways of NDMA photolysis and the subsequent reactions are summarized.

When NMDA is irradiated with UV light (using an MP lamp), the N-NO bond is broken consequently generating radicals that are responsible for the further degradation (Stefan and Bolton, 2002). Degradation products found during photolysis (polychromatic UV spectrum) are DMA, nitrite, MA and formic acid (FA), which contributes to the total amount of formed AOC. It can be concluded that photolysis mechanisms involved in NDMA conversion are similar for both MP and LP lamps.

Table 5.7: NDMA degradation products

Abbreviation	Name	Formula
DMA	Dimethylamine	$(CH_3)_2NH$
MA	Methylamine	CH_3NH_2
HNO	nitroxyl	
N-MD	N-methylidenemethylamine or Methylaminomethyl radical	$CH_2=N^+HCH_3$
AMR	Aminium radical	$\bullet NH^+$
NOR	NO radical	$\bullet NO$
SR	Superoxide radical or Hydroperoxyl	$O_2\bullet$
PN	Peroxynitrate	$ONOO^-$
NMF	N-methylformamide	CH_3NHCHO
FA	Formic acid	CH_2O_2
FH	Formaldehyde or methanal	CH_2O
FM	Formate or methaonate	$HCOO^-$

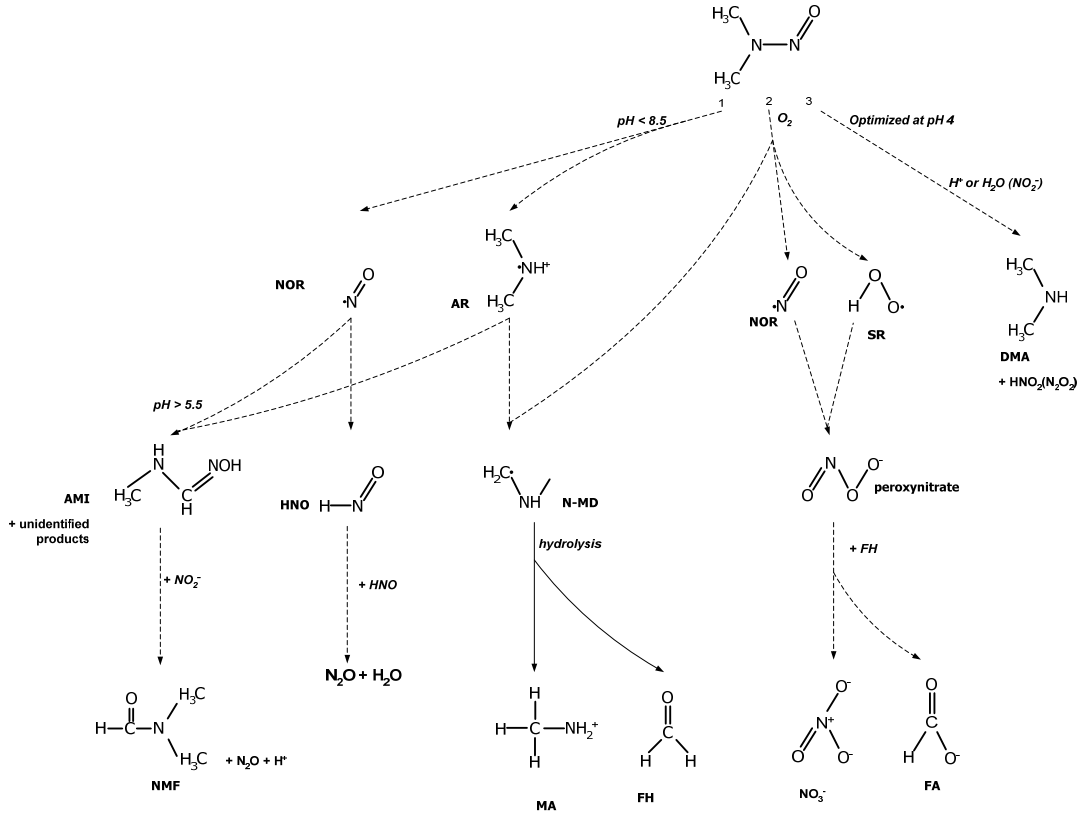

Figure 5.20: Degradation pathways for NDMA (photolysis), both lamp types

Table 5.8: Yields and rate constants model compounds

	Φ_{254}	$\Phi_{200\text{-}300}$	K_{OH} ($M^{-1}s^{-1}$)	K_{OH} s^{-1}
Atrazine	0.048	?	$2.54\pm0.22 * 10^9$ (Balci et al., 2009)	
Bromacil	-	?		0.23 min^{-1} [OH] Hapeman et al (1997)
Ibuprofen	-	?	$6.67 * 10^9$ (Yuan et al., 2009)	
NDMA	0.314±0.016 Lee et al (2005)	?	95±5 (Wink et al., 1991)	

6. Experimental research

6.1 Introduction

The experimental research is performed at Dunea's pre-treatment location in Bergambacht. With the UV/H_2O_2 pilot plant AOP experiments have been performed. Furthermore, the degradation of excess peroxide during transport and outflow in the dune area has been simulated.
This chapter describes the used materials and applied methods, the equipment and the set-up of the pilot plant/ simulation peroxide degradation, the measuring program and performed analysis. In chapter 7 the results are presented and discussed followed by the conclusions that can be drawn based on the performed experiments.

6.2 Materials and methods

6.2.1 Materials

Two reactors are used during the experiments: a reactor obtained from Berson UV techniek (Nuenen, the Netherlands) equipped with 4 medium pressure mercury vapour ultraviolet lamps (total installed power P =4.4 kW) and a reactor supplied by Wedeco (Herford, Germany) equipped with two low pressure mercury vapour ultraviolet lamps (total installed power P = 1.32 kW). The reactors are equipped with a sensor that measures the UV intensity at 254 nm which is reported in W/m^2 (LP reactor) and as a percentage of the minimum intensity expected at the end of life of the lamps (MP reactor). The maximum UV dose in the MP-reactor is approximately 850 mJ/cm^2 and the maximum UV dose in the LP-reactor is approximately 1140 mJ/cm^2. The UV doses are estimates based on the information given by the suppliers and at the time of writing have not been confirmed by Computational Fluid Dynamics (CFD) modelling yet. Both reactors receive a feed flow of 5 m^3/hr, spiked with selected model compounds and hydrogen peroxide.

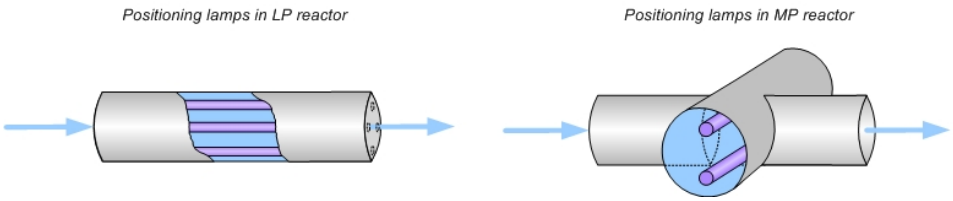

Figure 6.1: UV chambers reactors

The influent used for the experiments consists of river water pre-treated by coagulation, microstraining and dual media rapid sand filtration and is abstracted directly form the full-scale treatment plant. Because composition of the river water shows seasonal variations, experiments were performed weekly during a seven month period in order to assess the overall sensitivity of the AOP to seasonal variations.
10 L Mili-Q water solutions containing 100 mg of atrazine, bromacil and NDMA and 10 L Mili-Q water solutions containing 200 mg of ibuprofen were obtained from HWL. Both solutions were dosed into a reservoir and diluted further with regular tap water, yielding concentrations of 1 ppm atrazine, bromacil and NDMA and 2 ppm ibuprofen. The influent water was spiked continuously with the solution to obtain a concentration of 10 µg/L of atrazine, bromacil and NDMA and 20 µg/L of ibuprofen in both reactors. A hydrogen peroxide solution (10%) was purchased from Quaron (Zwijndrecht, the Netherlands). The hydrogen peroxide was dosed inline, obtaining a concentration of 0, 5 or 10 ppm H_2O_2 in both reactors. Static mixers are installed to ensure a homogenous mixture in the reactors.

6.2.2 Methods

The experimental research took place between March and October 2009. A typical standard experiment has a duration of 1.5 hours and was performed at least once a week. Each reactor is de-aerated before starting the experiment. The Erlenmeyer flasks used to collect the samples are rinsed 3 times with the specific sample water before taking a sample. During each experiment, the conditions and settings are monitored and recorded. When a UV setting is changed, it takes 15 minutes for the

reactor to become steady and when the H_2O_2 dose is adjusted, it takes approximately 4-5 minutes to reach a steady-state condition, so samples are taken after 6 minutes. In order to prevent unnecessary spills of the model compounds, the spike pump is switch off when UV settings are changed. The start-up time of the spike pump is approximately 4-5 minutes.
Since many samples are taken and many changes in settings are required, combined with continues monitoring of the conditions, the experiments are always performed by two persons.

Table 6.1: Standard experimental settings

Setting number	UV Ballast (%)	UV dose (mJ/cm^2) LP	UV dose (mJ/cm^2) MP	Dose H_2O_2 (ppm)	Model compounds (all settings)
1	100	1140	850	10	10 µg/L Atrazine 10 µg/L Bromacil 20 µg/L Ibuprofen 10 µg/L NDMA
2				5	
3				0	
4	80	1000	590	10	
5				5	
6				0	
7	60	630	380	10	
8				5	
9				0	

Note: at the time of writing, the UV dose distributions in the reactors have not been confirmed by CFD modelling yet. The doses given here are an estimate based on the information given by the suppliers.

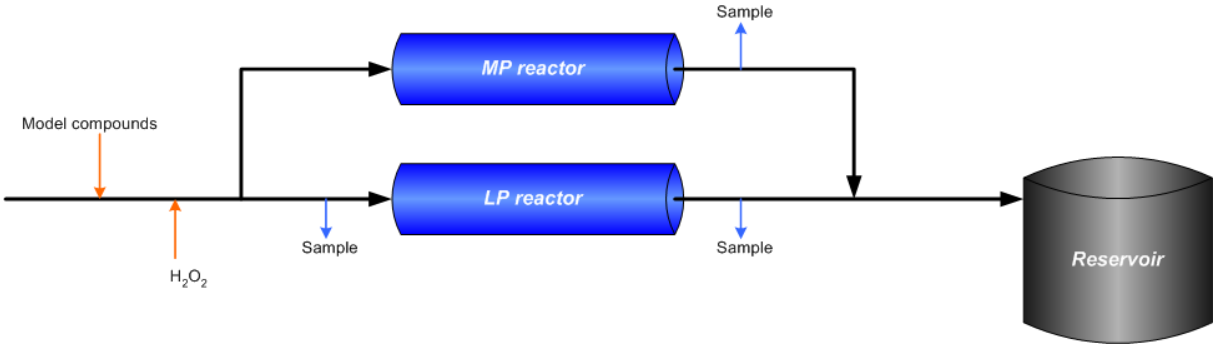

Figure 6.2: Overview experimental set-up

Because only a fraction of the dosed peroxide is used to form hydroxyl radicals, the concentration of hydrogen peroxide in the effluent is significant. When implemented in the full-scale treatment, the water is transported to the dune areas (10u < T 20u) when it is infiltrated. The dunes have a nature reserve status so infiltrating water containing high concentrations of H_2O_2 is not allowed. It is expected that reaction of peroxide with the biofilm on the walls of the transport pipe will become negligible after a certain period. Therefore it is relevant to analyse if and to what extend the water itself is capable of converting the residual peroxide. Effluent of the AOP is transferred to 2 L polyethylene bottles, prohibiting the penetration of light. The bottles are stored in a crate suspended in the supernatant water level above the dual media filters in the full-scale treatment plant to guarantee a constant and representative water temperature. Samples are taken and residual peroxide concentrations are determined via spectrophotometry at 420 nm, using $TiOSO_4$ as the reagent.
After discharge into infiltration ponds, the water passes slowly trough the soil. In the upper layers of the water column sunlight can still penetrate and possibly degrade peroxide, which is simulated by filling a house hold swimming pool (D=3 m) with 2 m^3 AOP effluent. In order to simulate the mixing effect of outflow from the transport pipes and wind, a small pump (Q = 200 l/h, H=0.5 m) Degradation of residual peroxide is monitored over a three day period.

Samples from the pilot-plant experiments are taken at the indicated sample points (see figure 6.2) and transferred to 40 ml glass flasks and stored in a cooler. Samples are also taken for the analysis of the water matrix (nitrite, ammonium, DOC, pH, bicarbonate, UVT) and AOC. All samples are collected within 2 days and transported to HWL for analysis.

Figure 6.3: Used sample containers for model compounds (left) and water matrix (right)

Table 6.2: Measured parameters

Category	Parameter	Unit
Model compounds	Atrazine	µg/L
	Bromacil	µg/L
	Ibuprofen	µg/L
	NDMA	µg/L
Water matrix	DOC	mg/L C
	AOC	µg/L C
	NO_2^-	mg/L NO_2
	NO_3^-	mg/L NO_3^-
	NH_4^+	mg/L NH_4^+
	HCO_3^{2-}	mg/L HCO_3^{2-}
	CO_3^-	mg/L CO_3^-
	pH	-
	UV-T	% at 254 nm
	Temperature	°C

The UV transmission of the water was measured at 1 nm intervals using a spectrophotometer and values measured at 254 nm were reported.
Bicarbonate concentrations are determined via titration of hypochloric acid (0.1 n increments) using the indicator methyl orange.
Nitrate concentrations were determined with continuous flow analysis (Skalar San^{++}). Nitrate is reduced to nitrite using metallic cadmium. A phosphoric acid reagent solution is added and the nitrite that was initially present and the nitrite resulting from the reduction of nitrate will diazotise sulphanilamide in the acid solution to diazonium salt which is then coupled with N-s-naphtyl)ethylenediamine, forming a red coloured complex. The extinction measured at 540 nm is a measure for the amount nitrate and nitrite that was already present. Subtracting the concentration of nitrite yields the nitrate level (NEN-EN-ISO 13395, 1997).
Concentrations of ammonium and nitrite have been determined with an automated discrete photometric analyser (Aquakem). The spectrometric extinction measured at 660 nm of a blue compound formed by a reaction of ammonium with salicylate and hypochlorite ions in the presence of sodium nitroprusside, is a measure for the level of ammonium (NEN 6604, 2007). Nitrite concentrations are determined using the same method described above (Vos, 2009).
Dissolved organic carbon (DOC) concentrations are determined with Non-Perguable Organic Carbon Analysis (Shimadzu TOC-V_{CPH}). A sample is acidified to a pH of 2-3 with hypochloric acid and the inorganic carbon is eliminated with a spurge gas (O_2). The remaining TC is measured to determine total organic carbon, and the result is generally referred to as TOC.
The sample is introduced in the TC combustion tube, filled with an oxidation catalyst and heated to 680 °C, burning the sample and converting the TC components to carbon dioxide. A carrier gas (flow rate of 150 ml/min) carries the combustion products to an electronic dehumidifier, cooling and dehydrating the gas. The sample combustion products are passed through a halogen scrubber, removing chlorine and other halogens. Finally, the carrier gas delivers the sample combustion products to the cell of a non-dispersive infrared (NDIR) gas analyser, where the carbon dioxide is

detected. The NDIR outputs an analog detection signal that forms a peak, which is proportional to the TC concentration of the sample. With a calibration curve expressing the relationship between the peak area and the TC concentration, the total concentration of DOC can be determined.
Analysis of the model compounds was performed using an Ultra Performance Liquid Chromatograph (UPLC, waters Acquity) equipped with a quaternary pump, combined with a Quattro Xevo triple quadrupole Mass Selective Detector (Waters Micromass). A sample of 15 µL was injected on a UPLC BEH C18 column (5 cm, particle size 1.7 µm, internal diameter 2.1 mm, Waters Acquity) with a flow rate of 0.45 ml/min. The eluens consisted of a mixture of two solvents: A (0.1% formic acid in water) and B (Methanol). Limits of detection were determined by analysis of nine drinking water samples spiked with 0.05 µg/L atrazine and bromacil and 5 µg/L ibuprofen. Recoveries were 0.063±0.003 µg/L atrazin, 0.058±0.004 µg/L bromacil, 4.0±0,6 µg/L ibuprofen. The limit of detection of NDMA was determined using a unspiked process water sample containing about 1.5 µg/L NDMA. Limits of detection, determined as 3*standard deviation from these results, were calculated to be 0.008 µg/L for atrazine, 0.013 µg/L for bromacil, 0.61 µg/L for NDMA and 1.8 µg/L for ibuprofen (Hooijveld, 2009).

7. Results experimental research

This chapter describes the results of the experimental research, which has generated larges volumes of data which can be found in annexes B, C, D, G and H.

7.1 Quality influent water

Pre-treated river water is used as influent, the quality of which shows seasonal variations. The temperature for instance can vary from approximately 0 °C during winter times to almost 25 °C during the summer. The temperature has been measured and recorded for every performed experiment. Seasonal variations can also be noticed for the UVT, concentrations of DOC, bicarbonate, nitrite and nitrate. DOC concentrations are highest during the spring (4 mg/L) and gradually decrease to 3 mg/L in September. From September onwards DOC concentrations rise again. Nitrate concentrations are highest during winter and spring (near 17 mg/L NO_3^-) and lowest in summer periods (8.6 mg/L NO_3^-). Concentrations of nitrite are generally well below the detection limit of 0.007 mg/L NO_2^-.

7.2 Observed system performance

Samples of the influent and effluent concentrations are taken for every setting. During a typical experiment, the UV ballast of the reactors is varied from 100 to 80 to 60% which corresponds to an UV dose of 850, 590 and 380 mJ/cm^2 respectively for the LP reactor and 400, 277 and 180 mJ/cm^2 respectively for the MP reactor. An experiment performed on July 9th 2009 is used as an example.

The measured concentrations of model compounds are plotted in figures 7.1 and 7.2 below. The degradation of each model compound at the various settings (1 to 9) has been determined from the measured concentrations and plotted (figure 7.3). It can be concluded from those plots that the degradation of NDMA is relatively insensitive to the peroxide setting. The opposite holds for ibuprofen and bromacil: the lines show a steep downwards trend corresponding with decreasing peroxide concentrations. Degradation of atrazine is influenced by both the UV setting and the peroxide setting. The observed degradation behaviour of the model compounds shows the same characteristics for both reactors.

The EEO of each model compound for the various settings is calculated based on the measured concentrations and are plotted in figure 7.4 below. The EEO of the LP reactor is generally lower then the EEO of the MP reactor. For both reactors the EEO for bromacil and ibuprofen at the settings with 0 mg/L peroxide is considerably higher then at 5 or 10 mg/L peroxide. This means that ibuprofen and bromacil are difficult to degradate just by photolysis at 254 nm. Furthermore, the EEO of the LP reactor for ibuprofen and bromacil at the settings 0 mg/L is considerably higher then the EEO the corresponding EEO of the MP reactor.

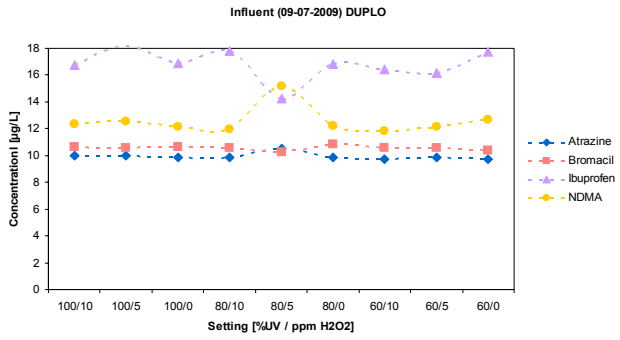

Figure 7.1: Measured influent concentrations (09-07-2009)

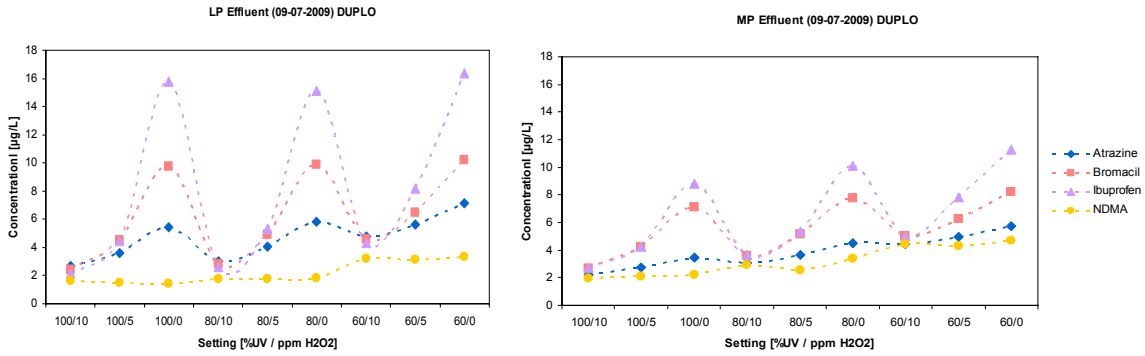

Figure 7.2: Measured effluent concentrations (09-07-2009)

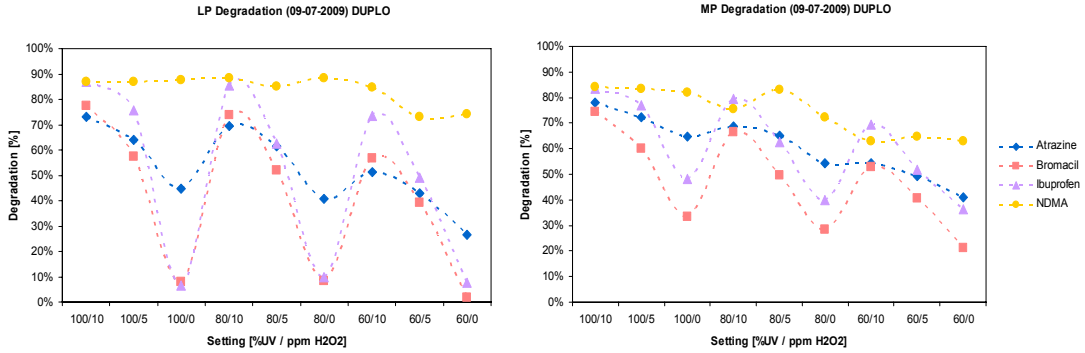

Figure 7.3: Calculated degradation (09-07-2009)

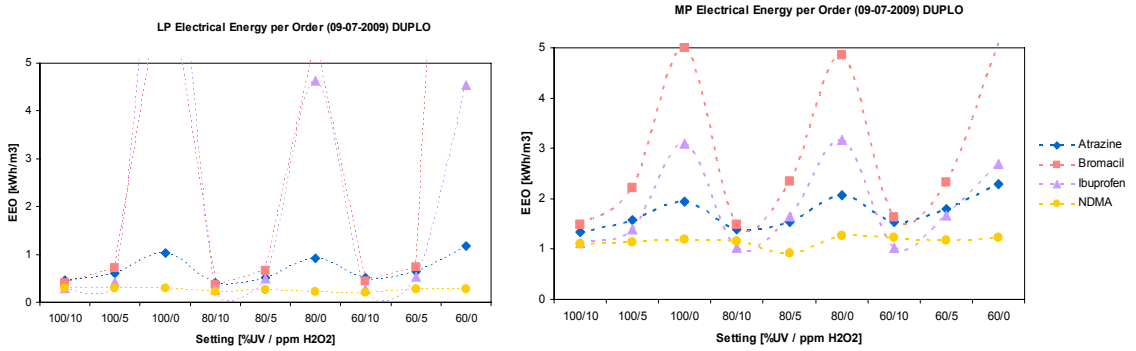

Figure 7.4: Calculated EEO (09-07-2009)

Both reactors are equipped with a sensor that measures the UV intensity at 254 nm, expressed in W/m^2 (LP) as a percentage (MP) of the dose expected at the end of life of the lamps. Higher values for UV intensity correspond with higher degradation levels. In order words, if the water quality is better (e.g. lower concentration of UV absorbing species) the UV intensity is increased which results in higher degradation of the model compounds (see figure below).

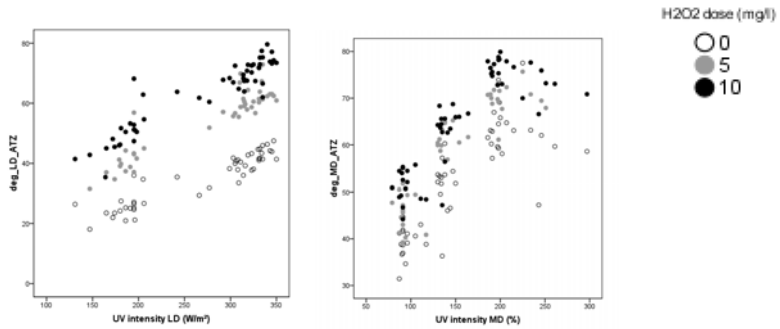

Figure 7.5: UV intensity vs. degradation of atrazine

7.3 Degradation of model compounds

7.3.1 Calculated degradation

The key performance indicator is the degradation of the model compounds, defined as the reduction in concentration (Eq. 64):

$$-\frac{dC}{dt} = \frac{C_i - C_e}{C_i} * 100\%$$

Eq. 64

The degradation of the four model compounds by both reactors, calculated every combination of UV and H_2O_2 for all of the performed experiments have been plotted in graphs that can be found in annex D.

7.3.2 Outliers

Close inspection of UPLC measurements at specific settings via SPSS interval diagrams and trend graphs constructed with Excel, yielded multiple outliers. For each outlier it was determined whether the value should be attributed to influences of the process performance or to poor measuring results. When it was absolutely clear that the occurrence of the outlier can be fully attributed to poor measuring results, the measured value has been disregarded (see annex E for elaboration). Fortunately enough data remained for statistical analysis (see annex F) and qualitative performance comparison.

7.3.3 Mean degradation levels

Mean degradation levels have been determined for the individual compounds at the specific combinations of UV and peroxide doses (see table 7.1 and figure 7.6). Using a least squares methods, fit lines are drawn between the mean degradation levels (all fit lines have an R^2>0.95) observed at varied UV doses (see figure 7.6). When comparing the degradation by the LP reactor to the degradation by the MP reactor, the first thing to note is the fact that the performances in terms of degradation are very comparable; the LP reactor's performance is not much inferior to the performance of the MP, except for the settings with 0 mg/L peroxide, which is due to the absence of peroxide and thus no oxidation via hydroxyl radicals occurs. Since the MP lamps emit polychromatic light (coinciding with the absorbance spectra of the model compounds) and LP lamps monochromatic light (254 nm), the photolytic capacity of MP lamps is much higher than that of the LP lamp.

Table 7.1: Mean degradation and 95% confidence intervals

	UV dose LP	10 ppm H_2O_2			5 ppm H_2O_2			0 ppm H_2O_2		
	mJ/cm²	**mean**	95% conf. int.		**mean**	95% conf. int.		**mean**	95% conf. int.	
ATZ	630	**47.8**	35.4	54.7	**39.3**	37.3	41.4	**24.7**	23	26.4
	1000	**67.1**	65.2	69.0	**56.7**	54.4	59.0	**37.7**	35.5	39.8
	1140	**72.4**	70.3	74.5	**61.8**	59.4	64.2	**42.3**	40.6	44.0
BRO	630	**49.9**	45.9	53.9	**32.5**	28.7	36.4	**4.7**	2.3	7.2
	1000	**69.3**	66.2	72.4	**47.4**	43.8	51.1	**6.9**	4.0	9.8
	1140	**72.7**	69.3	76.1	**54.2**	49.4	58.4	**6.5**	4.6	8.5
IBU	630	**60.1**	53.4	66.7	**45.2**	39.9	66.7	**4.8**	1.96	7.6
	1000	**75.6**	65.9	85.4	**61.5**	55.4	67.6	**8.7**	3.6	13.7
	1140	**78.2**	73.5	82.9	**65.2**	59.1	71.2	**11.2**	7.5	14.8
NDMA	630	**74.3**	70.5	78.1	**76.4**	71.9	81.0	**74.4**	70.9	78.0
	1000	**87.9**	69.5	93.3	**89.2**	84.3	94.4	**90.5**	88.1	92.9
	1140	**90.8**	89.3	92.4	**91.7**	90.1	93.4	**91.8**	90.6	92.9

	UV dose MP	10 ppm H_2O_2			5 ppm H_2O_2			0 ppm H_2O_2		
	mJ/cm²	**mean**	95% conf. int.		**mean**	mJ/cm²		**mean**	95% conf. int.	
ATZ	380	**52.1**	49.8	52.8	**46.8**	45.1	48.6	**39.9**	38.2	41.6
	590	**65.6**	64.4	66.7	**60.8**	59.0	62.6	**52.1**	50.4	53.9
	850	**75.6**	74.2	77.1	**70.8**	69.5	72.0	**63.0**	60.9	65.1
BRO	380	**48.5**	46.4	50.6	**36.4**	33.3	39.4	**19.7**	15.7	23.8
	590	**60.4**	58.5	62.3	**48.0**	44.8	51.2	**24.5**	26.6	27.4
	850	**70.1**	67.4	72.6	**56.8**	54.0	59.7	**32.8**	27.6	37.9
IBU	380	**58.1**	51.6	64.6	**49.3**	44.6	54.0	**28.5**	23.3	33.7
	590	**67.7**	59.2	76.3	**62.9**	58.8	67.1	**32.9**	25.6	40.2
	850	**74.6**	69.3	80.0	**67.1**	61.2	73.1	**40.5**	34.4	46.5
NDMA	380	**65.2**	62.6	67.8	**68.2**	64.1	72.4	**65.8**	62.1	69.5
	590	**77.6**	75.7	79.6	**77.4**	74.5	80.6	**76.6**	73.9	79.2
	850	**87.6**	85.6	89.5	**86.6**	81.3	89.0	**84.5**	82.1	87.7

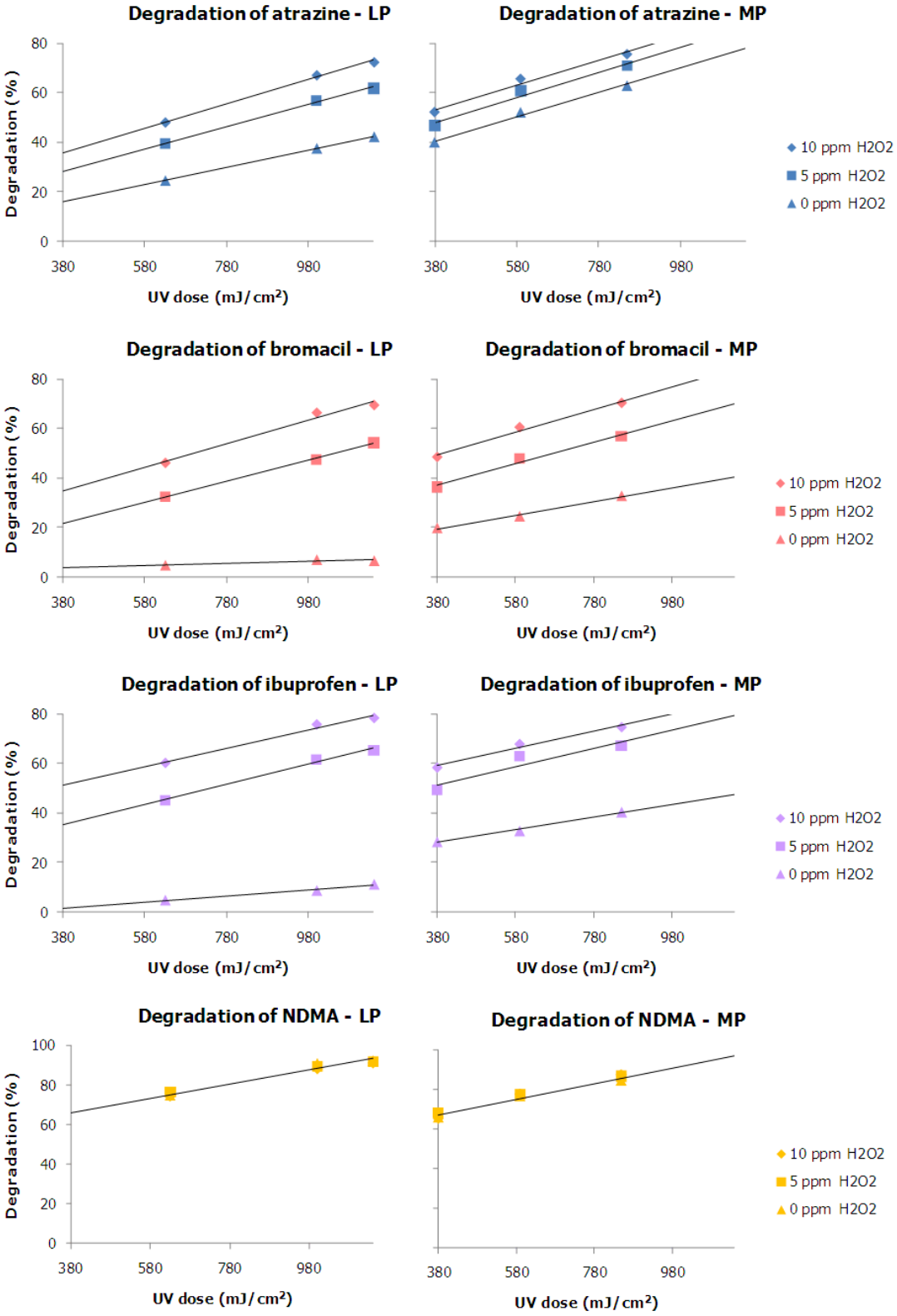

Figure 7.6: Mean degradation model compounds

Note: At the time of writing this report, the dose distribution in the reactors has not been modelled by CFD yet. The doses given here are an estimate based on information given by the suppliers.

7.3.4 Conclusions regarding achieved degradation levels

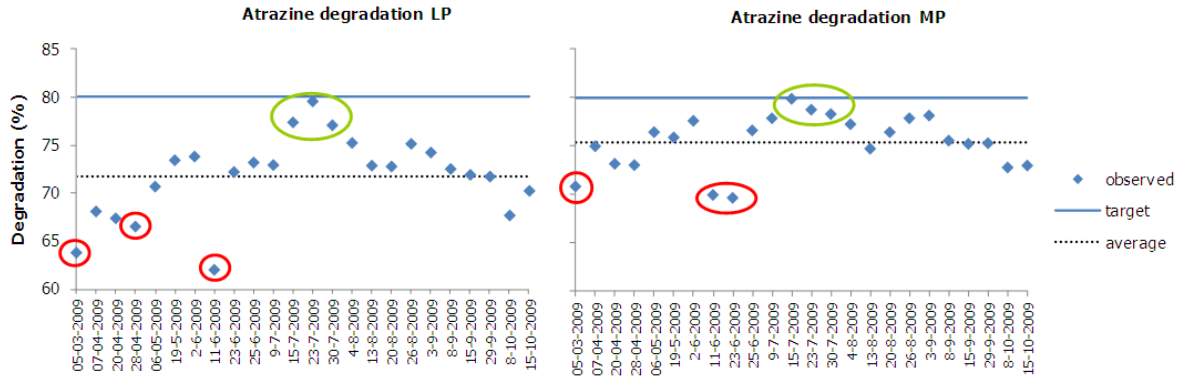

Figure 7.7: Atrazine degradation using LP lamps (1140 mJ/cm^2) and MP lamps (850 mJ/cm^2), 10 ppm H_2O_2

Achieved degradation of atrazine is considered to be the main performance indicator and should at least be ≥80%. Unfortunately that level is not reached yet: the average degradation of atrazine by the LP reactor (setting 1: 1140 mJ/cm^2, 10 ppm H_2O_2) is 72% and 75% degradation is reached with the MP reactor (setting 1: 850 mJ/cm^2, 10 ppm H_2O_2). However, the average degradation level of atrazine may not reach 80%, this level has been achieved by the LP reactor on July 23rd and by the MP reactor on July 15th.
Atrazine degradation levels using LP lamps are lower than when MP lamps are used (max UV, 10 ppm H_2O_2), however for degradation of bromacil, ibuprofen and NDMA the opposite is true: degradation levels reached using LP lamps are actually a bit higher than the degradation levels reached using MP lamps (see figure below).

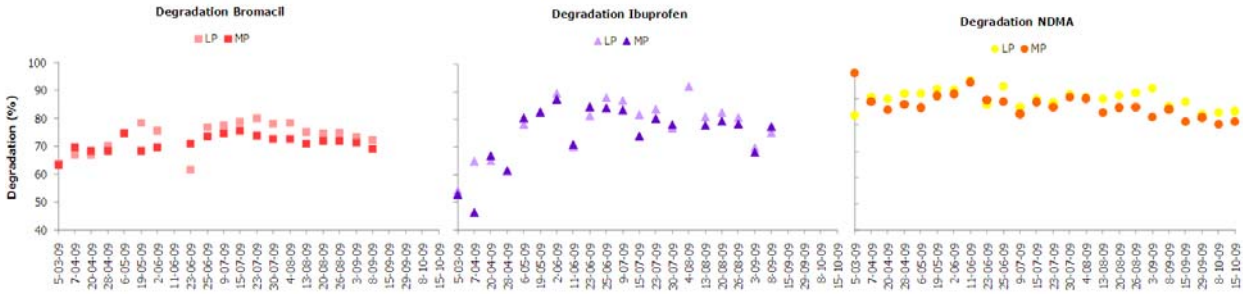

Figure 7.8: Degradation Bromacil, ibuprofen and NDMA using LP lamps (1140 mJ/cm^2) and MP lamps (850 mJ/cm^2), 10 ppm H_2O_2

From the table below can be concluded that both reactors performed best during the second half of July 2009, reaching atrazine degradation levels near 80%. The degradation levels of the other compounds on these dates can be found in table 7.2.
Degradation of bromacil by the LP reactor was also superior on these dates, degradation levels of ibuprofen (max 92%) and NDMA (max 97%) were good but not superior. The same holds for the MP reactor: degradation levels of bromacil were superior on the dates with the highest atrazine degradation but observed degradation of ibuprofen (max 88%) and NDMA (max 100%) was not maximal.

Table 7.2: Top 3 best performance (Atrazine degradation, max UV dose, 10 ppm H_2O_2)

	Degradation LP (%)					Degradation MP (%)			
Date	ATZ	BRO	IBU	NDMA	Date	ATZ	BRO	IBU	NDMA
23-07	80	80	84	87	15-07	80	76	74	89
15-07	77,4	79	82	90	23-07	79	74	81	87
30-07	77,1	78	77	92	30-07	78	73	78	91

March 5th and June 11th are the dates corresponding with the poorest degradation of atrazine by the LP and MP reactors. On these dates degradation levels of the other compounds achieved by the LP

reactor were also relatively poor, except for NDMA: almost complete degradation occurred on June 11th. The performance of the MP reactor in terms of degradation of ibuprofen and NDMA on June 11th was not poor; in fact it was actually very good. On March 5th the degradation ibuprofen was poor, NDMA was complete degraded and bromacil degradation was near the average.

Table 7.3: Top 3 poorest performance (Atrazine degradation, max UV dose, 10 ppm H_2O_2)

	Degradation LP (%)					Degradation MP (%)			
Date	**ATZ**	**BRO**	**IBU**	**NDMA**	**Date**	**ATZ**	**BRO**	**IBU**	**NDMA**
11-06	62	53	70	97	23-06	69,7	71	85	90
5-03	64	64	54	84	11-06	70	51	81	96
28-04	67	70	-	92	5-03	71	63	53	100

On July 23rd the UVT of the water was water 83% while the average UVT is 78%, which can account for the good performance of the LP reactor in terms of atrazine degradation. The quality of the influent water has not been determined on July 23rd, but is expected to be comparable to the quality determined on July 15th, explaining the good performance of the MP reactor on both dates. The UVT on July 23rd was however not as high as on July 15th. Perhaps measuring inaccuracies are responsible for the discrepancy.
The differences in best and poorest performances are due to the differences in the quality of the influent water. Concentrations of nitrate, DOC and bicarbonate are much lower on July 15th than on March 5th

Table 7.4: Differences in water quality

		Water quality best performance		**Water quality poorest performance**	
		15-07	23-07	5-03	11-06
UVT	%	77.1	83 [b]	74	77.5
NO_3^-	mg/L	8.65 [a]		15.94 [b]	11.10
NO_2^-	mg/L	<0.007		<0.007	<0.007
DOC	mg/l C	3.36		4.00 [b]	3.65
pH		7.78 [a]		7.98 [b]	8.01
HCO_3^-	mg/L	137 [a]		151	151
Temp.	°C	21.4 [b]		5.3 [a]	18.3

[a] *equal to lowest observed value*
[b] *equal to highest observed value*

An experiment performed with pre-treated river water that received an extra treatment step by Granular Activated Carbon (GAC) filtration decreased concentrations of DOC and nitrate to 0.23 mg/L C and 5 mg/L NO_3^- respectively and increased the UVT to 98%, which resulted in a atrazine degradations of >88% (LP) and 94% (MP). This particular experiment (September 10th, 2009) is part of current research regarding increased UVT and its influence on the AOP, using GAC, Ion Exchange and Ultra- and Nano-filtration. When comparing the average degradation levels to the observed degradation on September 10th, it becomes apparent that the degradation of all model compounds is significantly enhanced if the influent water quality is improved.
A more detailed conclusion and comparison to degradation levels found in full-scale applications and other pilot-scale research can be found in paragraph 7.8

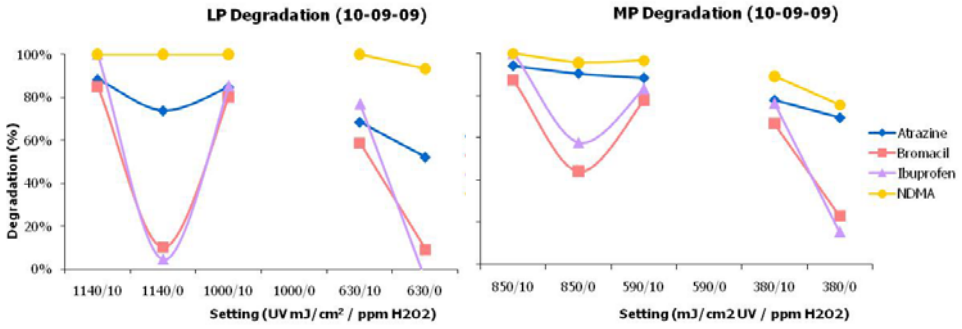

Figure 7.9: Degradation levels achieved with UVT of 98%

7.4 Degradation mechanisms

7.4.1 Correlations UV ballast, peroxide dose and degradation

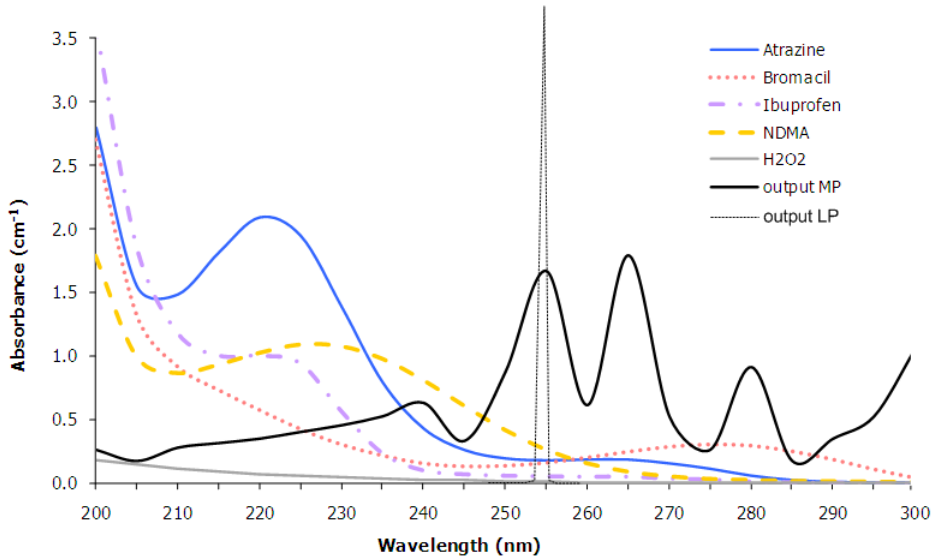

Figure 7.10: Absorption spectra model compounds, peroxide (HWL, 2009) and emission spectra lamps
Absorbance model compounds and H_2O_2 measured in Mili-Q water (conc. Atrazine/Bromacil/NDMA = 10 µg/L, conc. Ibuprofen = 20 µg/L and conc. H_2O_2 = 10 mg/L)
Note: emission spectra lamps do not reflect the true scale

In this paragraph a statistical analysis of the experimental results is performed in order to identity the underlying degradation mechanisms. For every model compound and lamp type the correlations between the degradation and dosages of UV and peroxide are determined and compared to results found in literature. Correlation statistics can be used to get a general understanding of the response of the model compounds to either the UV intensity (measured at 254 nm in both reactors) or the dose of hydrogen peroxide. Correlation is an indicator for the strength and the direction of a linear dependency between two variables and varies from –1.0 to 1.0 (see annex F for an elaboration).

Overall, the correlations between UV intensity (holding the effect of peroxide dose constant) and the degradation of the model compounds by the LP reactor are higher than those of the MP reactor. For the correlations between the H_2O_2 dose (holding the effect of UV intensity constant) and the degradation of model compounds, the relations show a similar characteristic: correlations between the degradation of model compounds by the LP reactor and the peroxide dose are larger then those of the MP reactor. Oxidation is the dominant degradation mechanism for the LP reactor. Another observation is the fact that no significant correlations exist between the peroxide dose and the degradation of NDMA (both reactor types): NDMA cannot be degraded via oxidation, only photolysis is effective. This is in line with results found in literature.

Table 7.5: Correlations intensity – degradation

Control variables	*UV intensity (W/m² or %)*	*Degradation Atrazine (%)*		*Degradation Bromacil (%)*		*Degradation Ibuprofen (%)*		*Degradation NDMA (%)*	
		LP	MP	LP	MP	LP	MP	LP	MP
H_2O_2 dose (mg/L)	Correlation	**.905**	**.812**	**.633**	**.646**	**.529**	**.284**	**.833**	**.821**
	Sig (2-tailed)	.000	.000	.000	.000	.000	.004	.000	.000
	df	99	99	99	99	99	99	99	99

Table 7.6: Correlation H_2O_2 dose – degradation

Control variables	*H_2O_2 dose (mg/L)*	*Degradation Atrazine (%)*		*Degradation Bromacil (%)*		*Degradation Ibuprofen (%)*		*Degradation NDMA (%)*	
		LP	MP	LP	MP	LP	MP	LP	MP
UV intensity LP (W/m²)	Correlation	**.937**	**.832**	**.945**	**.919**	**.900**	**.814**	**-.153**	**.010**
	Sig (2-tailed)	.000	.000	.000	.000	.000	.000	.128	.924
UV intensity MP (%)	df	98	98	98	98	98	98	98	98

7.4.2 Quantification degradation mechanisms

The degradation can be described in kinetic terms with Eq. 33:

$$-\frac{d[C]}{dt} = I_0 \phi_C f_C \left(1 - \exp(-\mathrm{A_t})\right) + \mathrm{k_{OH,C}} [\cdot \mathrm{OH}][\mathrm{C}]$$

Because the exact utilization of peroxide during a specific experiment is unknown (utilization has been determined on just a few occasions), the exact concentration of hydroxyl radicals is unknown as well. Also the reaction quantum yields at the incident flux rate I_0 (polychromatic irradiation) of the model compounds have not been determined during the experiments. Deriving the individual contribution of the mechanisms from the kinetic equation is therefore not possible. In order to define the proportion of each mechanism to the total degradation of a model compound, multiple regression analysis is performed for the degradation of individual compounds. These models are only valid for predicting and quantifying the degradation of atrazine, bromacil and ibuprofen by the LP reactor for the conditions under which the experiments were conducted (e.g. water matrix, reactor type, and flow patterns).

A total of eight regression models of the following form are estimated:

$$Y_i = c + B_1 X_1 + B_2 X_2$$

Where

Y_i = *predicted degradation of a specific model compound by the reactor*
C = *constant*
B_1 = *coefficient for effect of UV intensity*
X_1 = *value of UV intensity*
B_2 = *coefficient for effect of peroxide dose*
X_2 = *peroxide dose (0, 5 or 10 ppm)*

The total amount of explained variance is calculated, represented by R^2, which is a measure for the model fit. For the individual coefficients the amount of unique explained variance is determined.
The unique explained variance of UV intensity and peroxide dose in atrazine degradation using LP lamps are 0.37 and 0.53 respectively. Together these variables explain 0.90 of the variance in the

predicted degradation of atrazine. The relative contribution of each variable to the total amount of uniquely explained variance is considered to be to be equal to the proportional contribution to the degradation of a model compound. Consequently, the contribution of the UV intensity to the degradation of atrazine is then equal to:

$$Deg\ (ATZ|UVI) = \frac{VAR\left(\frac{d(ATZ)}{dt},\ UVI\right)}{VAR\left(\frac{d(ATZ)}{dt},\ UVI\right) + VAR\left(\frac{d(ATZ)}{dt},\ H_2O_2\right)}$$

$$= \frac{0.37}{0.37 + 0{,}53} = 0.41$$

The fit of the model for predicting atrazine degradation by the LP reactor is 0.92, which means that this model can predict atrazine degradation fairly accurate. Fit of the models for predicting degradation of bromacil, ibuprofen and NDMA by the LP reactor are 0.90, 0.81 and 0.68 respectively. The poor fit of the NDMA model does however not pose a problem: the models were constructed in order to quantify the effects of both variables (UV and peroxide dose) to the degradation. From the literature and the results of the experiments can be concluded that NDMA is not degraded by advanced oxidation, only photolysis is effective. Consequently it does not make sense to identify the effect of hydrogen peroxide. It must be noted however that due to the poor model fit, this particular model cannot be used for estimating the degradation of NDMA.
In tables 7.7 and 7.8 the quantification of the degradation mechanisms are depicted. In annex F an elaboration of the used regression methods and the constructed models can be found. Comparing the determined degradation mechanisms (LP) to the observed average degradation resulting from photolysis (table 7.9) shows that they correspond well.

Table 7.7: Determined degradation mechanisms LP reactor

	Atrazine	***Bromacil***	***Ibuprofen***	***NDMA***
H_2O_2 dose	59%	92%	91%	0%
UV dose	41%	8%	9%	100%

Table 7.8: Determined degradation mechanisms MP reactor

	Atrazine	***Bromacil***	***Ibuprofen***	***NDMA***
H_2O_2 dose	23%	85%	95%	0%
UV dose	77%	15%	5%	100%

Table 7.9: Observed degradation resulting from photolysis

	Atrazine	***Bromacil***	***Ibuprofen***	***NDMA***
LP	24-42%	4.7-6.5%	4.8-11.2%	74-91%
MP	40-63%	20-33%	29-41%	67-85%

The fit of the models for atrazine, bromacil, ibuprofen and NDMA degradation using MP lamps are low: 0.75, 0.78, 0.54 and 0.68 respectively. Moreover, the determined contribution of UV (see table 7.7) to the degradation of bromacil and ibuprofen were 15 and 5% respectively, while the average minimum degradation observed resulting from photolysis were 20-33% and 29-41% respectively, depending on the energy input of the reactor. The poor fit of the model could be the result of the spread in measured values. However, the amount of spreading in measured degradation values is similar if not smaller than the amount of spreading in measured degradation using LP lamps (see table 7.1). It is suspected that the UV intensity of the MP reactor, which is measured only at 254 nm, cannot be used for constructing a valid model that can quantify the effects to the degradation, because degradation occurs over the entire spectrum. The UV intensity signals incorporate the effect of the watermatrix; the value is lower if the quality of the water matrix is poorer (e.g. higher concentrations of species that absorb at 254 nm). From the emission spectrum of the MP lamps four peaks can be distinguished: at 240, 255, 265 and at 280 nm. If the UV intensity was monitored at the emission peaks, than perhaps those values can be used as the variables representing total UV intensity over the entire range.

7.5 EEO required for degradation of selected model compounds

7.5.1 Calculated means EEO

The energy consumption required to achieve 1 log degradation in the concentration of a specific compound per unit of treated water, the EEO, is determined using the following equation:

$$EEO = \frac{P}{Q \cdot \log\left(\frac{C_i}{C_e}\right)}$$

Eq. 51

The values for the EEO (determined for the maximum power input of the reactors, e.g. P_{LP} = 1.32 kW and P_{MP} = 4.44 kW and Q = 5 m^3/hr) can be found in figure 7.11 below. Dosing hydrogen peroxide reduces the required energy input considerably for both lamp types. The EEO for degradation of model compounds using LP lamps is equal to around 1/3 of the EEO using MP lamps, except in the absence of hydrogen peroxide.

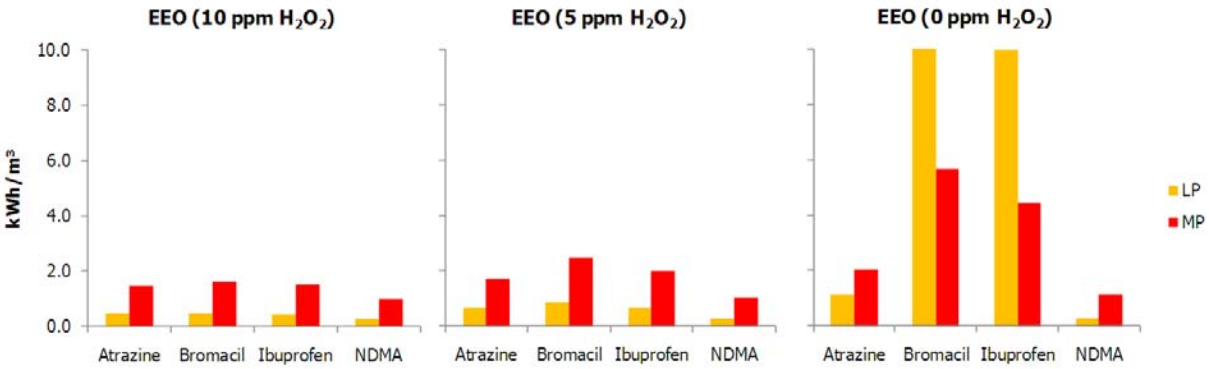

Figure 7.11: EEO for degradation of model compounds (1140 mJ/cm^2 LP, 850 mJ/cm^2 MP)

7.5.2 Conclusions regarding EEO

The EEO of the LP reactor is considerably lower than the EEO of the MP reactor. This applies for all the model compounds, except for ibuprofen and bromacil in the absence of hydrogen peroxide which is perfectly in line with the expectation: ibuprofen and bromacil cannot be degraded photolytically with monochromatic UV irradiation at 254 nm. The energy requirement of the MP reactor is 2 to 5 times higher then the energy requirement of the LP reactor, depending on the dosed amount of peroxide.
Determined EEO values for atrazine degradation are 0.48 kWh/m^3 (LP) and 1.45 kWh/m^3 (MP).

7.6 Interim conclusions

Applying advanced oxidation in the presence of 10 ppm H_2O_2 to pre-treated Meuse water results in 72% degradation of atrazine using LP lamps (1140 mJ/m^2) and 75% atrazine degradation MP lamps (850 mJ/cm^2). The corresponding values for the EEO are 0.48 and 1.45 kWh/m^3 respectively.
These results in terms of achieved degradation levels and corresponding energy requirements are compared to results found in other pilot-scale research and the full-scale implementation of AOP by PWN.

Results found in other AOP applications
Greater Cincinnati Water Works (GCWW) has performed a year long UV/H_2O_2-study with LP and MP lamps and is planning to implement UV/H_2O_2 for disinfection and conversion of organic micropollutants at the end of the treatment scheme. The UV doses of the reactor were set to target 80% atrazine degradation at a peroxide dose of 10 ppm. At this target level average observed ibuprofen degradations were 82% (LP) and 87% (MP). The UV transmission of the water was 84-95% (Metz et al., 2009). The energy requirements are unknown.

Experiments performed with Berlin tap water using LP lamps (135 W, UV dose unknown) resulted in 90% degradation of atrazine (9 µg/L) at peroxide doses of 8-17 mg/L (Müller et al, 2001). The applied flow-rates (60 an 80 L/h) resulted in long residence times ranging from 1.25 to 2.7 minutes and thus higher UV doses. Those long residence times, the fact that drinking water was used as influent (high UVT) and the high peroxide doses are responsible for this high level of conversion. The energy consumption at a flow of 90 L/h (17 ppm H_2O_2) was high, resulting in an EEO of 1.67 kWh/m^3.

PWN Water Supply Company achieved 70% atrazine degradation in their pilot-scale research. MP-UV radiation (1000 mJ/cm^2) in the presence of 8 mg/L H_2O_2 yielded an EEO of 1 kWh/m^3. Atrazine degradation was increased to 80% by addition of 13 mg/L peroxide. Bromacil degradation amounted to 42% and was increased to 80% with a peroxide dose of 15 mg/L. At PWN's full scale plant, 80% degradation of atrazine is achieved (MP-UV 540 mJ/cm^2, 6 ppm H_2O_2) with a required energy input of 0.56 kWh/m^3 (Martijn et al, 2007). The water source of PWN consists of pre-treated water from Lake IJssel, which has an average UVT of 82% (Kramer, 2002).

Conclusions
Comparing the results found in this particular pilot research to the results founds in other pilot research project, yields the conclusion that the performance of both the LP and MP reactor in terms of degradation and EEO is already good. The achieved atrazine degradation is near the target level of 80%. From the results can be concluded that even a small improvement of the UV transmission (lower concentrations of absorbing species) yields the desired atrazine degradation. This will also result in lower EEO values.

The objective of this research is to compare the performance of low pressure UV lamps to the performance of medium pressure UV lamps. It can be concluded that the application of LP lamps for advanced oxidation is an attractive option since the degradation levels of the model compounds are similar to those of the MP reactor while at the energy consumption of the LP reactor is considerably lower. The quality of the influent water yielding the best degradation of atrazine was better than the quality of the water resulting in the poorest performances. In the next paragraphs the performances in terms of by-product formation and sensitivity towards water quality parameters will be elaborated, which will together with the achieved degradation and energy prestations yield a final judgment about the performances of both lamp types.

7.7 Composition and influence water matrix

7.7.1 Average quality influent water (composition water matrix)

The influent used for the experiments consists of river water pre-treated by coagulation, microstraining and dual media rapid sand filtration. From samples taken during the experimental period, the average composition has been determined (see table 7.10 below). In annex B graphs of the measuring data can be found. The quality of the water matrix is described by a multitude of parameters such as the UV transmission, nitrogen compounds, pH, temperature and dissolved organic matter, collectively called the water matrix.

The water matrix negatively influences direct photolysis of a target compound via absorption of ultraviolet light. As a result the UV transmission is reduced. Moreover, absorption of ultraviolet light results in reduced photolysis of hydrogen peroxide and thus a reduced formation of hydroxyl radicals. If the concentration of scavenging species in the water matrix (DOC, bicarbonate, nitrite/nitrate) is higher, scavenging for hydroxyl radicals is increased, resulting in a lower availability of hydroxyl radicals for advanced oxidation of the target compounds.

Table 7.10: Quality influent water (pre-treated water from river Meuse)

Parameter	Unit	Minimum	Maximum	Mean
Temperature	°C	5.3	23.7	18.7
UV transmission at 254 nm	%	43.42	82.71	78
pH		7.70	8.07	7.9
Bicarbonate	mg/L HCO_3^-	133	174	147
Ammonium	mg/L NH_4^+	0.00	0.04	0.01
Nitrite	mg/L NO_2^-	0.0006	0.1603	0.0197

Nitrate	mg/L NO_3^-	8.6	15.9	11.4
DOC	mg/L C	2.97	4.01	3.48
AOC	µg/L C			13

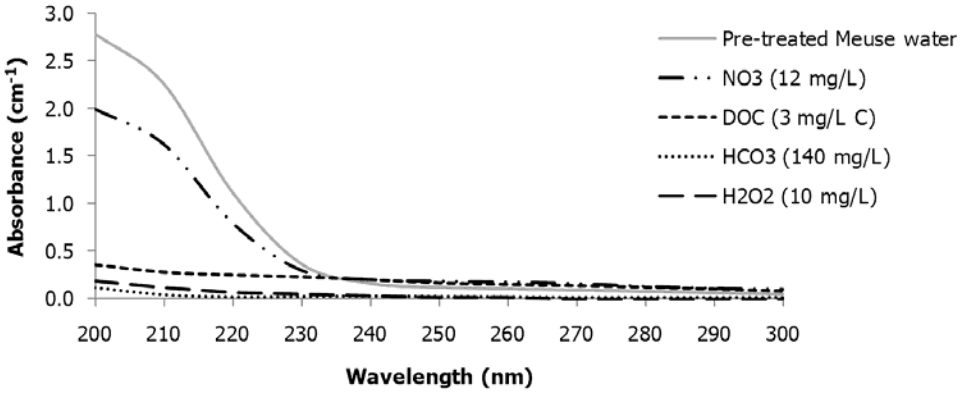

Figure 7.12: UV absorbance nitrate, DOC and bicarbonate (adapted from the Ridder, 2006), peroxide and pre-treated Meuse water (HWL, 2009)

The figure above portrays the UV absorbance of the used influent (absorbance scan from sample taken March 18th 2009). The influent absorbs primarily at wavelengths shorter then 240 nm; at 254 nm the absorbance is 0.105 which corresponds with a UVT of 78%. For wavelengths shorter then 235 nm, nitrate is a larger absorber then DOC. UV absorbance of bicarbonate and peroxide are relatively low over the entire spectrum. At 254 nm, the absorbance of DOC and nitrate are 0.15 and 0.1 respectively and the absorbances of bicarbonate (0.015) and peroxide (0.011) are low.
The UV absorbance of the pre-treated Meuse water shows characteristics of the absorbance spectrum of nitrate, indicating that competition for UV light between the model compounds and nitrate will be high.

7.7.2 Quantification of scavenging

The total amount of scavenging from the water used during the experiments can be estimated with the following formula:

$$-\frac{d[\cdot OH]}{dt} = [\cdot OH] * (k_9 \cdot [DOC] + k_{12} \cdot [NO_2^-] + k_{13} \cdot [H_2O_2] + k_{14} \cdot [HCO_3^-]) \qquad Eq.52$$

Where:

$$[NO_2^-] \quad = initial\,[NO_2^-] + \phi(NO_2^-)_\lambda$$

Assuming nitrite yield from nitrate photolysis at 254 nm (average of 11.4 mg/L NO_3^-) to be 0.001 the nitrite concentration is 0,001*[0,184] = [0.0002]. Nitrite yield from nitrate photolysis between 200 to 300 nm is 0.1, which yields a total nitrite concentration in the MP reactor of [0.018] mmol/L.

Table 7.11: Scavenging effects

Species	mg/L	mM	k (M^{-1} s^{-1})	S (s^{-1}) [·OH]
DOC	3.48	0.290	$1* 10^7$	$2.90 *10^6$
HCO_3^-	147	2.409	$8.5 * 10^6$	$2.05 *10^7$
H_2O_2	10	0.294	$2.7 * 10^7$	$7.94 *10^5$
H_2O_2	5	0.147		$3.97 *10^6$
Initial NO_2^-	0.00	0.000	$1* 10^{10}$	
LP NO_2^-	0.00	0.000	$1* 10^{10}$	$1.84 *10^6$
MP NO_2^-	0.845	0.018	$1* 10^{10}$	$1.84 *10^8$

The total scavenging rate in the LP reactor at a H_2O_2 dose of 5 ppm is calculated as followed:

$$S\,(5\ ppm\ H_2O_2)_{LP} = [\cdot OH] * (\,(1 \cdot 10^7) \cdot [0.290] + \,(1 \cdot 10^{10}) \cdot [0.0002] + \,(2{,}7 \cdot 10^7) \cdot [0.147] + \,(8.5 \cdot 10^6) \cdot [2.409])$$

$$= 2.92 \cdot 10^7\ s^{-1}\,[\cdot OH]$$

The same method has been applied for determining the total scavenging rate for the LP reactor at 10 ppm H_2O_2 and for the MP reactor at 5 and 10 ppm H_2O_2. Because the formation of nitrite at 254 nm is negligible, the total scavenging effect using LP lamps is lower than when MP lamps are used. However, since peroxide absorbance as 254 nm is low, less hydroxyl radicals are formed and scavenging can still have a significant influence.

Table 7.12: Total scavenging effects

	5 ppm H_2O_2 $s^{-1}[\cdot OH]$	**10 ppm H_2O_2** $s^{-1}[\cdot OH]$
LP	$2.92 \cdot 10^7$	$3.32 \cdot 10^7$
MP	$2.11 \cdot 10^8$	$2.15 \cdot 10^8$

7.7.3 UV transmission

The UV transmission measured at 254 nm decreases with increasing concentrations of absorbing species in the influent water, inhibiting direct photolysis of the model compounds and hydrogen peroxide. Consequently the performance of the reactors increases with increasing UV transmission, as was shown in paragraph 7.3.4: the best performance in terms of atrazine degradation for both reactor types was achieved when the UVT was maximal (see also figure below).
During the experiment performed on September 3rd 2009, the UVT of the water was 50%. Concentrations of nitrate (9.7 mg/L) and DOC (3.0 mg/L C) were low while concentrations of nitrite (0.084 mg/L NO_2^-) and ammonium (0.043 NH_4^+) where relatively high compared to the average values. Based on the value for the UVT it is expected to observe minimal degradation of model compounds, however both reactors performed very well; degradation of all model compounds was well above the average degradation levels.

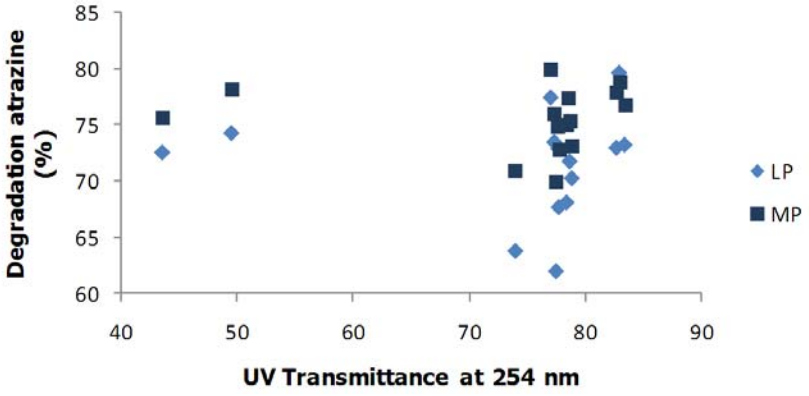

Figure 7.13: UV transmission vs. degradation Atrazine, 10 ppm H_2O_2, 1140 mJ/cm² (LP), 850 mJ/cm² (MP)

Unfortunately correlations between the UVT of the influent and the degradation of model compounds by the LP reactor are small and non significant, except for ibuprofen. No reasonable explanation other than measuring inaccuracies can be formulated. Significant correlations are found between the UVT and the degradation of bromacil and ibuprofen by the MP reactor. Because atrazine degradation was optimal when the UVT was maximal, it is surprising that the correlation between UVT and atrazine degradation was not significant.

Table 7.13: Correlations UVT - degradation

Control variables	*UVT influent*	*Degradation Atrazine (%)*		*Degradation Bromacil (%)*		*Degradation Ibuprofen (%)*		*Degradation NDMA (%)*	
		LP	MP	LP	MP	LP	MP	LP	MP
H_2O_2 dose	Correlation	**.217**	**.192**	**.210**	**.303**	**.352**	**.427**	**.132**	**-.187**
	Sig.	.130	.182	.144	.032	.012	.002	.361	.194
	df	48	48	48	48	48	48	48	48

7.7.4 Water temperature

The intensity of LP lamps is temperature dependent (Stefan, 2004); efficiency can decrease up to 30% near temperatures of 0° C (Kramer, 2002) Because the surface temperature of a low pressure lamp is relatively low, the influence of water temperature is significant. The optimal water temperature is around 20°C and variations above or below result in lower UV output by low pressure lamps. At temperatures below 5° C, UV output becomes unpredictable and low pressure lamps can fail to start. Medium pressure lamps have higher surface temperatures and are not influenced by the water temperature (Berson UV, 2009).

The lowest and highest observed water temperatures were 5.3 °C (March 5th, 2009) and 23.7 °C (August 8th, 2009) respectively. Unfortunately just one experiment has been performed with water temperatures below 10 °C. During the best performance the water temperature was 21.4 °C. However, during the experiment performed on June 11th the water temperature was high (18.3 °C) while the performance of both reactors was poor. Since the performance of MP lamps is not influenced by the temperature of the water, the observed relation should probably be attributed to other influences than the water temperature.

The influence of the water temperature on the degradation of the model compounds by the LP reactor has been explored by requesting SPSS to perform a partial correlation analysis between the water temperature and the observed degradation, holding the effects of UV intensity and hydrogen peroxide constant. Including other control parameters (e.g. DOC, nitrate, bicarbonate) was not possible, SPSS could not determine correlation statistics because the *degrees of freedom* (number of observations minus number of estimated parameters, relevance is elaborated in annex F) approached zero.
Selecting only the cases where the temperature was above 20°C yielded small, positive but non-significant correlations. In other words, water temperatures above 20°C do not exert a negative influence on the degradation. Selecting only the cases where the temperature was lower than 20 °C yielded positive significant correlations between the water temperature and degradation of ibuprofen (0.46) and NDMA (0.32). Apparently higher water temperatures up to 20°C have a positive effect to the degradation of ibuprofen and NDMA. When all cases were selected only ibuprofen degradation seems to be influenced positively by higher water temperatures.

Table 7.14: Correlations between water temperature and degradation LP, controlled for effect of UV intensity and H_2O_2 dose

		Atrazine	**Bromacil**	**Ibuprofen**	**NDMA**
All cases selected	Cor	**-.01**	**.108**	**.330**	**.082**
	Sig.	.46	.136	.000	.203
Temp < 20°C	Cor	**-.24**	**-.03**	**.46**	**.32**
	Sig.	.091	.438	.004	.036
Temp > 20°C	Cor	**.141**	**.143**	**.116**	**-.095**
	Sig.	.116	.113	.163	.211

Although it seems that increasing temperatures are associated with higher degradation levels using LP lamps, no conclusions regarding the influence of water temperature can be drawn yet. Moreover, the same trend can be distinguished for the MP reactor. Because MP lamps are not sensitive to variations in water temperatures, the relation is probably false. More data is required in order to relate the observed trend to the influence of the water temperature.

7.7.5 DOC

The average concentration of DOC in the pre-treated Meuse water is 3.48 mg/L

7.7.5.1 Observed DOC removal

Observed average decreases in DOC concentrations using LP lamps were 196-99-82 µg/L C at 10, 5 and 0 ppm H_2O_2 addition respectively. When MP lamps are used these values are 237-120-105 µg/L C. The observed DOC conversion is largest at 10 ppm H_2O_2 addition, regardless of the lamp type, confirming the fact that dissolved organic material acts as a hydroxyl radical scavenger. A significant amount of DOC conversion occurs when no peroxide is added. This can be a result of direct photolysis of the organic material or through reaction with radicals that are formed from compounds that are already present in the water. DOC conversion is considerably higher using MP lamps compared to using LP lamps.

Table 7.15: Average conversion of DOC

H_2O_2 dose (ppm)	**DOC (mg/L C)**			**DOC (µg/L C)**	
	Influent	***Effluent LP***	***Effluent MP***	***ΔDOC_{LP}***	***ΔDOC_{MP}***
10	3.48	3.226	3.186	196	237
5	3.48	3.250	3.229	99	120
0	3.48	3.308	3.274	82	105

7.7.5.2 Effect of DOC on degradation

MP reactor

From the literature was concluded that higher concentrations of DOC in the influent water have a negative influence on the degradation of model compounds by the MP reactor. A slightly negative trend in degradations with increasing DOC concentrations can be distinguished in figure 7.15.

The influence higher concentrations of DOC have on the degradation has been assessed by analysing the partial correlations. Unfortunately, most correlations between the degradation of the model compounds by the MP reactor (controlled for the effect of UV intensity and peroxide dose) are negative but not significant. The non significance (for atrazine, bromacil and ibuprofen) is perhaps explained by the fact that the number of observations is small (<50); including the necessary control variables resulted in low df values. It is also possible that the correlations are not significant because the value for UV intensity already incorporates the effect of increased DOC concentrations.

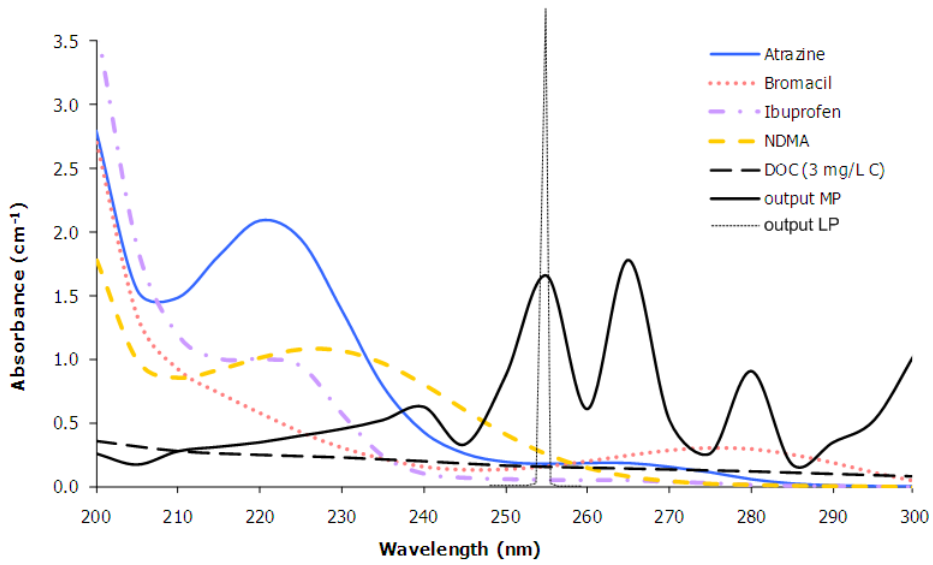

Figure 7.14: Absorbance DOC vs. absorbance model compounds
Absorption spectra model compounds (HWL, 2009), emission spectra lamps (Berson, Wedeco), DOC (adapted from de Ridder, 2006). Note: emission spectra lamps do not reflect the true scale

NDMA absorbs UV light over the whole spectrum. DOC absorbance is relatively constant between 200 to 300 nm. What is particularly of relevance is the fact that UV absorbance by NDMA between 235-260nm is much higher then the absorbance by the other model compounds and DOC; the MP output spectrum shows high peaks in this part of the spectrum. Consequently NDMA degradation is relatively independent of DOC concentrations, which is confirmed by the fact that the correlation was small and not significant. Also, NDMA is actually fully degraded when the DOC concentration was maximal.

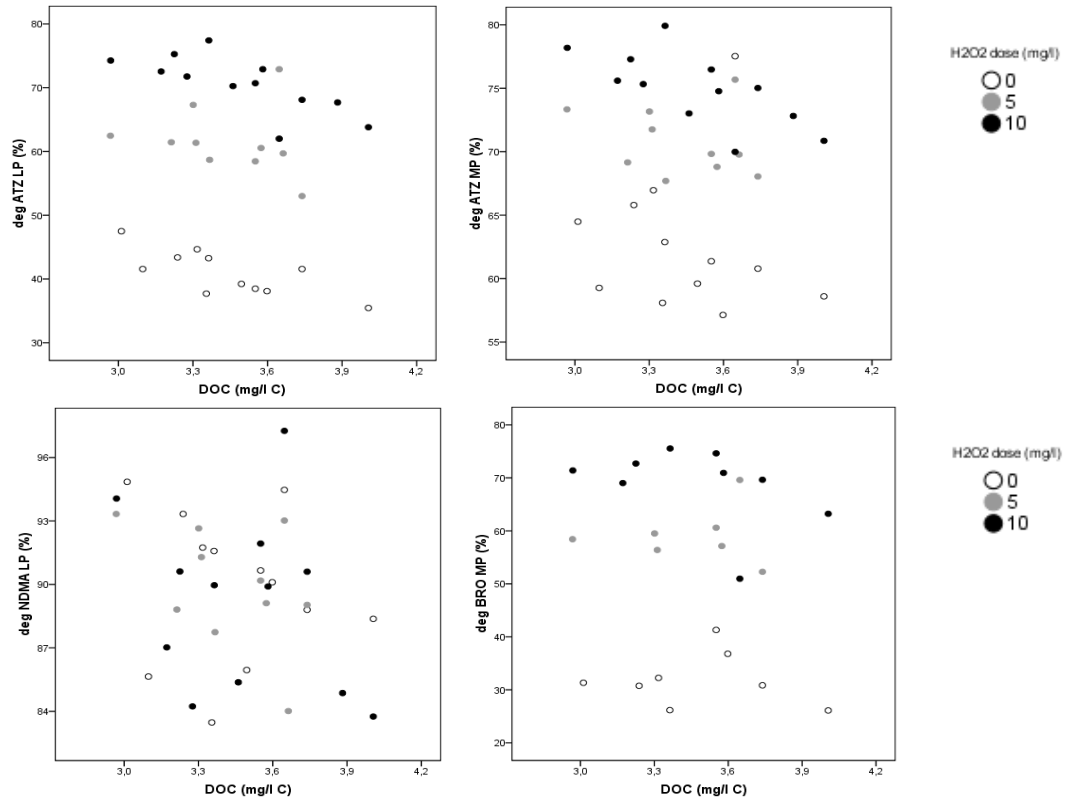

Figure 7.15: DOC concentration vs. degradation

UV absorbance by atrazine is almost equal to the UV absorbance of DOC at wavelengths >250 nm which means that the competition for UV light in this part of the spectrum is high. In paragraph 7.3 it was observed that during the poorest degradation of atrazine, the concentration of DOC was the highest (4 mg/L C). Also the correlation between DOC concentration in the influent and atrazine degradation by the MP reactor is significant; it can be concluded that DOC does in fact have a negative impact on the performance of the MP reactor because the UV transmission is reduced.
The bromacil absorbance spectrum shows a broad, low peak between 265-295 nm, overlapping with three emission peaks of the MP lamps. Bromacil is capable of absorbing more UV light in this part of the spectrum then DOC and the other model compounds do. However, bromacil (and ibuprofen) are more easily degraded by advanced oxidation than photolysis. This could perhaps also explain why correlations between degradation of bromacil/ibuprofen and DOC concentrations are small and non significant: apparently the DOC concentrations do not inhibit the formation of hydroxyl radicals, even though UV absorbance by peroxide is lower than UV absorbance by DOC (see figure 7.12).

LP reactor
At 254 nm the UV absorbance of DOC (0.15), atrazine (0.17) and bromacil (0.16) are approximately equal. Taking into account that during the poorest performance in terms of atrazine degradation, the DOC concentration of the influent water was 4 mg/L C, it is expected to find negative correlations between DOC concentrations and the degradation of atrazine. However, most of correlations found were positive and also not significant which yields the conclusion that DOC concentrations do not exert a large influence the performance of advanced oxidation of the LP reactor. Approximately 100 µg/L ≅ 0.008 mmol/l of DOC is converted extra when the peroxide dose is 10 ppm. Scavenging effects are lower than the scavenging effects of DOC in the MP reactor. The UV absorbance of NDMA at 254 nm (0.26) is higher then the UV absorbance of DOC. The found correlation is not significant, which is in line with the expectation.

Considering all of the above, formulating a statement on the influence of DOC on the performance of the reactors is difficult. The individual influence of DOC to the degradation cannot be quantified. Addressing it purely from a statistical point of view yields the conclusion that DOC does not have any influence because the correlations are not significant. Because the number of observations is relatively small (N<50), the effect of DOC on the degradation would have to very large in order to find significant correlations. Another problem is the fact UV intensity incorporates the combined effect of the water matrix, including DOC. Using the UV intensity as a control variable is therefore a bit problematic. Defining the individual water matrix parameters as control variables was also not possible because SPSS was then not able to determine the correlation statistics.

Table 7.16: Correlations DOC influent – degradation

Control variables	*DOC influent*	*Degradation Atrazine (%)*		*Degradation Bromacil (%)*		*Degradation Ibuprofen (%)*		*Degradation NDMA (%)*	
		LP	MP	LP	MP	LP	MP	LP	MP
H_2O_2 dose UV-I LP UV-I MP	Correlation	**.280**	**-.415**	**.091**	**-.206**	**-.045**	**-.180**	**.057**	**.073**
	Sig.	.066	.003	.524	.156	.756	.215	.691	.616
	df	49	47	49	47	49	47	49	47

Note: including more control variables reduced the number of df to such a low level that SPSS was not able to determine correlation statistics.

7.7.6 Alkalinity and bicarbonate

In paragraph 5.5.4 was concluded that the used influent water does not contain carbonate: the pH of the water is around 8 (calcium-carbonate equilibrium). This is relevant because the scavenging rate of carbonate (3.9 * 10^8 $M^{-1}s^{-1}$) is higher then the scavenging rate of bicarbonate (8.5 * 10^6 $M^{-1}s^{-1}$). The value of the pH itself was relatively constant during the experimental period and no effects to the degradation could be distinguished.

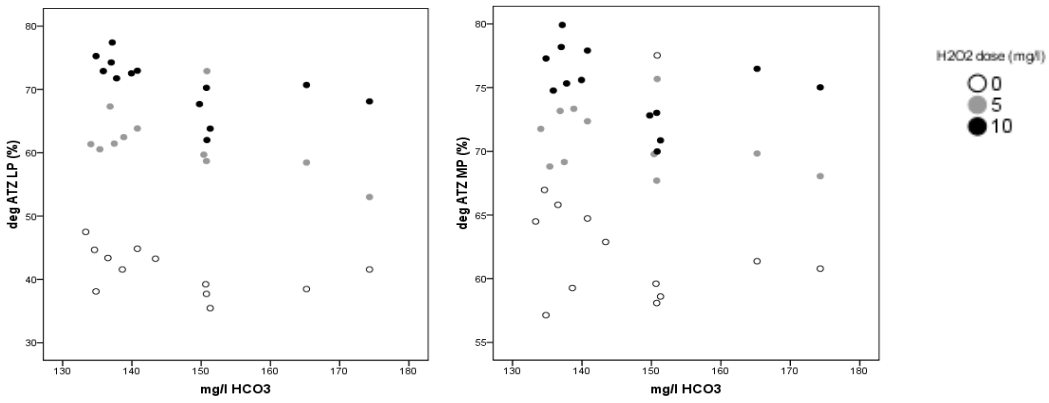

Figure 7.16: Bicarbonate vs. degradation

The average bicarbonate concentration during the experiments was 147 mg/L HCO_3^-. From the figure below can be concluded that the competition for UV light between bicarbonate and the model compounds is small: the UV absorbance of bicarbonate is considerably lower than the UV absorbance of the model compounds over the entire spectrum. Because scavenging of bicarbonate and competition for UV light is negligible, bicarbonate has a negligible influence on the degradation of model compounds by both reactors. Consequently, no significant correlations were found (data not shown). Also the scatter plots above do not portray a strong trend between concentrations of bicarbonate and degradation of model compounds.

Considering the above it is concluded that direct photolysis and advanced oxidation of the model compounds are independent of bicarbonate concentrations, regardless of the applied lamp types.

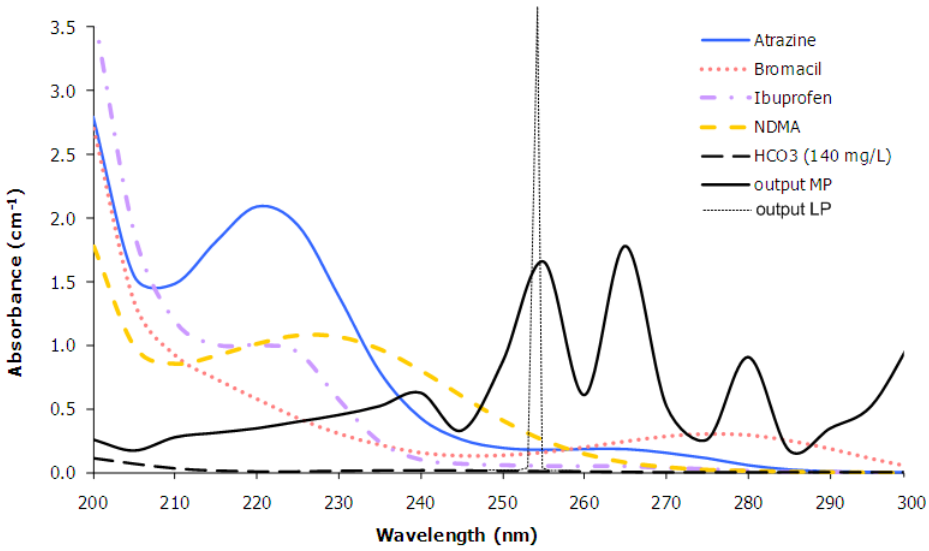

Figure 7.17: Absorbance bicarbonate vs. absorbance model compounds
Absorption spectra model compounds (HWL, 2009), emission spectra lamps (Berson, Wedeco), bicarbonate (adapted from de Ridder, 2006). Note: emission spectra lamps do not reflect the true scale

7.7.7 Nitrate

The average nitrate concentration of the pre-treated river water during the experiments was 11.4 mg/L. Degradation levels of atrazine and bromacil (both reactor types) were highest when the nitrate concentration was minimal (8.65 mg/L) and the opposite is true when the nitrate concentration was maximal (15.94 mg/L). The same characteristics are true for degradation of ibuprofen.

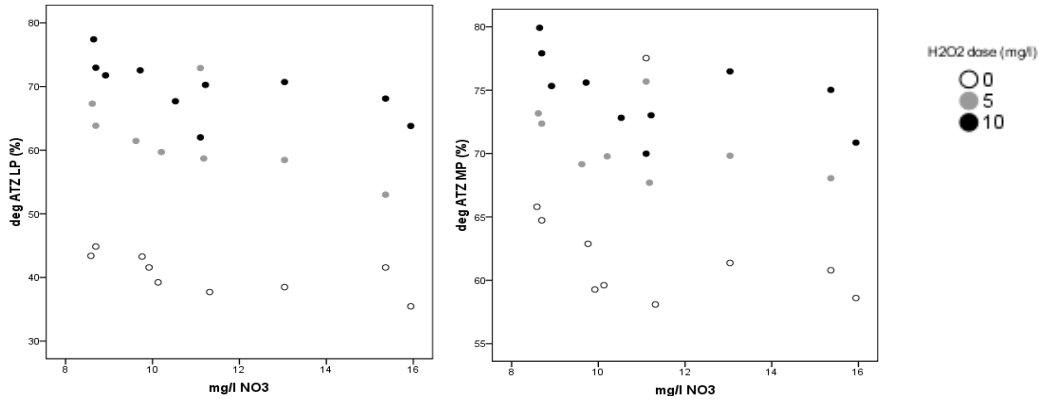

Figure 7.18: Influence nitrate on degradation

Nitrate absorbs more UV light then bicarbonate and DOC do, especially between 200-250 nm (see figure 7.12). Consequently the influence of higher nitrate concentrations to the degradation of model compounds is stronger than for the influence of DOC and bicarbonate, resulting in totally significant correlations (MP reactor), explained below.

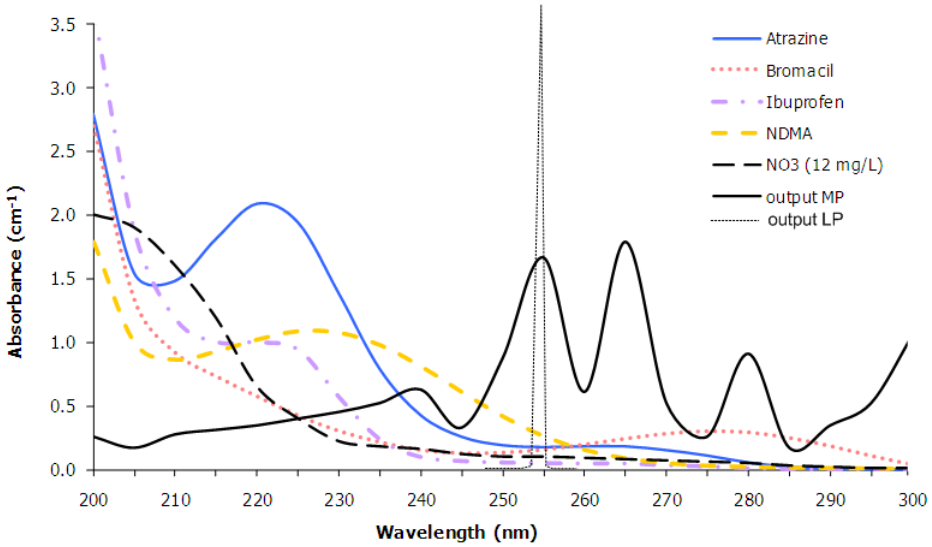

Figure 7.19: Absorbance of nitrate vs. absorbance of model compounds
Absorption spectra model compounds (HWL, 2009), emission spectra lamps (Berson, Wedeco), bicarbonate (adapted from de Ridder, 2006). Note: emission spectra lamps do not reflect the true scale

MP reactor
Photolysis (polychromatic irradiation) of ibuprofen is inhibited when nitrate concentrations are increased. At wavelengths >240 nm, UV absorbance of ibuprofen and nitrate are more or less equal. Between 200-205 nm and 215-240 nm are the only regions where UV absorbance of ibuprofen is larger then UV absorbance of nitrate. Since the emission spectrum of the MP lamps shows high peaks between 240 and 300 nm, it is no surprise to find a strong, negative correlation between nitrate concentrations and degradation of ibuprofen. Moreover, higher concentrations of nitrate result in higher concentrations of nitrite, increasing the amount of hydroxyl radical scavenging. Less hydroxyl radicals are then available for oxidation of ibuprofen. Degradation of bromacil is also negatively influenced by higher concentrations of nitrate. The bromacil absorbance spectrum shows a broad, low peak between 265-295 nm, overlapping with three emission peaks of the MP lamps. Bromacil absorbs more UV light in this part of the spectrum then nitrate does, but since bromacil is primarily degraded by oxidation the negative correlation between nitrate concentration and bromacil degradation, should be attributed to increased scavenging effects. NDMA absorbs UV light over the whole spectrum and between 215-265nm the absorbance is higher than the absorbance of nitrate. Because the MP output spectrum shows three peaks in this part of the spectrum, no significant correlation exist between degradation of NDMA and concentration of nitrate. The influence of nitrate on the photolysis of NDMA (polychromatic radiation) is small.
Although the UV absorbance of atrazine is higher than the UV absorbance of nitrate in most parts of the spectrum, from 250 nm onwards the absorbances are comparable. Since the highest emission peaks of the MP lamps overlap with this part of the spectrum, nitrate will compete with atrazine for UV light. Because it is suspected that photolysis contributes more to the total degradation of atrazine then oxidation does, it is no surprise to found strong significant negative correlation
(-.9) between nitrate concentrations and atrazine degradation.

LP reactor
At 254 nm, the UV absorbance of nitrate (0.1) is slightly lower than the UV absorbance of atrazine (0.17) and bromacil (0.16) and 2.5 times lower than the absorbance by NDMA (0.26). From the scatter plot in figure 7.18, the absorbance spectra and the experimental results regarding the best versus poorest performance can be concluded that the influence of nitrate to photolysis of NDMA is small. In fact, the correlation between concentration of nitrate in the influent and degradation of NDMA by the LP reactor is small and more importantly, not significant. Atrazine degradation is also influenced negatively by higher concentrations of nitrate, although the correlation is just above the significance level. The same is true for degradation of ibuprofen. Because the correlations between degradation of atrazine, ibuprofen and concentration of nitrate are small and not significant, it is suspected that advanced oxidation by the LP reactor is less sensitive to higher concentrations of nitrate than advanced oxidation by the MP reactor. Advanced oxidation is the dominant mechanism for atrazine degradation by the LP reactor (59%), explaining why the correlation found was not

significant. Radical formation is thus not influenced too much by higher nitrate concentrations. At 254 nm the yield of NDMA photolysis (0.3) is considerably lower than the yield of hydroxyl radicals from photolysis of H_2O_2 (1). Apparently enough radicals can be formed for oxidation of atrazine, bromacil and ibuprofen while NDMA can still be photolyzed. Moreover, photolysis of nitrate at 254 nm does not result in increased concentrations of nitrite (yield is less then 0.001). Scavenging of hydroxyl radicals by nitrite is negligible which is again confirmed by the fact that no significant correlations were found between nitrate concentrations and degradation of atrazine, bromacil and ibuprofen.

Table 7.17: Correlations nitrate influent - degradation

Control variables	*NO_3^- influent*	*Degradation Atrazine (%)*		*Degradation Bromacil (%)*		*Degradation Ibuprofen (%)*		*Degradation NDMA (%)*	
		LP	MP	LP	MP	LP	MP	LP	MP
H_2O_2 dose UV-I LP U-I MP	Correlation	**.333**	**-.899**	**.065**	**-.756**	**-.318**	**-.757**	**.092**	**-.273**
	Sig.	.058	.000	.718	.000	.071	.000	.611	.112
	df	31	33	31	33	31	33	31	33

Considering all of the above, it is concluded that increased nitrate concentrations have a relatively small, perhaps negligible effect on the formation of hydroxyl radicals at 254 nm. Moreover, increased nitrate concentrations do not increase scavenging from nitrite because nitrite formation is negligible. Direct photolysis of NDMA is marginally influenced by higher nitrate concentrations but this does influence atrazine degradation. It is suspected that the performance of the LP reactor is less sensitive to nitrate concentrations then the performance of the MP reactor.

The influence of nitrate concentration on direct photolysis (polychromatic irradiation) depends on the characteristics of the targeted compound. If a compound absorbs UV light at wavelengths >250 nm, photolysis is influenced less by nitrate: UV absorbance of nitrate at >250 nm is very small and the MP lamps emit more energy at that part of the spectrum than at shorter wavelengths (200-240 nm). Furthermore, photolysis of nitrate forms nitrite, increasing the amount of radical scavenging. It can be concluded that photolysis and advanced oxidation using polychromatic irradiation are both influenced negatively by increased concentrations of nitrate in the influent.

7.9.8 Seasonal influence

Relating the individual effect of a water matrix parameter to the observed contribution is not simple because the parameters are related to each other. For example; during the experiments higher concentrations of DOC were associated occasionally with higher concentrations of nitrate and both have a negative effect on the performance of the AOP due to a decreased UV transmission of the water.

Multiple regression analysis can correct for the effect of correlated parameters. However, if the correlations between the parameters are too high (>.3), the problem of multicollinearity yields unreliable results (Hair et al, 2006). One could state that multiple regression analysis cannot be applied if the independent variables (predictors) represent the same concept and thus are strongly related to each other. From the table below can be concluded that many water matrix parameters have large correlations with multiple other water matrix parameters , sometimes r can be as large as .8 (nitrate and bicarbonate). Moreover, seasonal variations of nitrate and bicarbonate follow the same characteristic. Concentrations of DOC and nitrate are both high in March and November, while between April and October lower concentrations of nitrate are associated with higher concentrations of DOC.

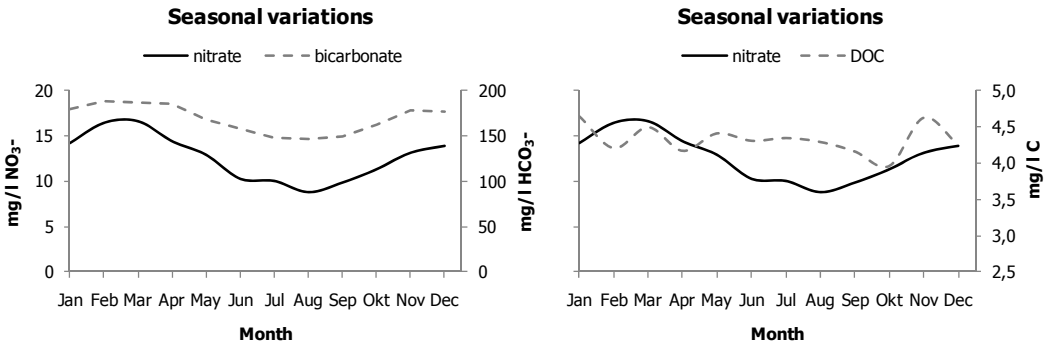

Figure 7.20: Seasonal variations nitrate, bicarbonate and DOC

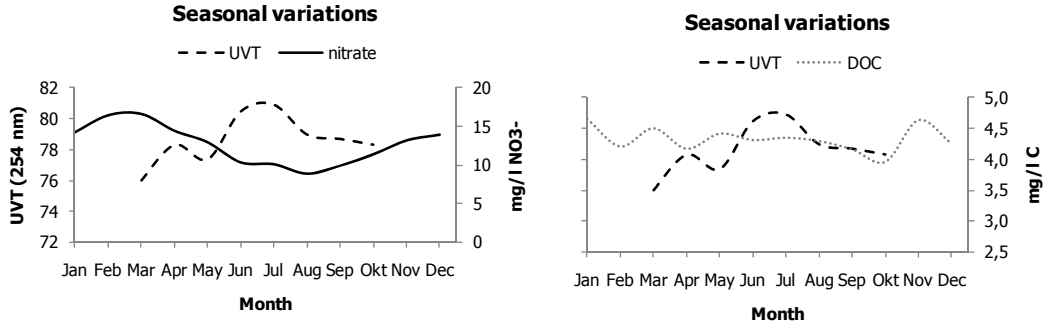

Figure 7.21: Seasonal variations nitrate, DOC and UVT

Table 7.18: Correlations water matrix parameters

		Temp.	UVT	HCO_3^-	NO_3^-	DOC	pH
Temp.	°C			-.691	-.960	-.677	-.412
UVT	%					.450	
HCO_3^-	mg/L	-.691			.789	.450	.686
NO_3^-	mg/L	-.960		.789		.793	.615
DOC	mg/L	-.677	.450	.580	.793		
pH	-	-.412		.686	.615		

Note: only significant correlations are included in the table

Table 7.19: Water matrix, monthly averages

	Temp.	UVT[a]	DOC[b]	HCO_3^-	NO_3^{-c}	NO_2^-
	°C	% (254 nm)	mg/L C	mg/L	mg/L	mg/L
January	6.0		4.75	180	14.2	0.025
February	4.9		4.37	189	16.4	0.007
March	7.5	76.0	4.61	188	16.6	0.005
April	11.8	78.3	4.37	185	14.4	0.002
May	16.5	77.4	4.62	169	12.9	0.001
June	19.4	80.5	4.72	158	10.3	0.001
July	20.5	80.9	4.61	148	10.1	0.002
August	20.7	79.0	4.62	147	8.9	0.002
September	17.9	78.7	4.36	150	9.9	0.002
October	13.7	78.3	4.17	163	11.3	0.003
November	9.4		4.85	178	13.1	0.007
December	5.3		4.32	177	13.9	0.015

a) no trend information available, monthly averages determined from experimental data
b) not monitored at Bergambacht, monthly averages determined from monitoring results intake point Brakel
c) not monitored at Bergambacht, monthly averages determined from monitoring results influent dune area Meijendel

In order to estimate the influence of seasonal variations, monthly averages of relevant parameters have been determined from monitoring data (HWL, 2007-2009). These monthly averages are compared to the average monthly degradation of the model compounds by both reactors.

Although the observed concentration of DOC was maximal in March when performances were poorest, plotting the average monthly concentrations of DOC and nitrate against the average monthly degradation of atrazine (see figures below) shows that nitrate must have a larger influence: during the summer period DOC concentrations are high while the performance of both reactors is optimal. Concentrations of DOC decrease in September and October while the performance of the reactors is not improved.
The average monthly degradation of atrazine increases with decreasing nitrate concentrations (see figure 7.22): the best performances are achieved during the summer period when nitrate concentrations are lowest. Moreover, the UVT of the water during the summer period is >80%. Comparing the average monthly concentrations of DOC and nitrate to the monthly average value of the UVT in relation to the achieved degradation of atrazine, yields the conclusion that nitrate has a larger influence on the UVT than DOC does. Nitrate is the water matrix parameter with the largest influence on the performance of the reactors because nitrate absorbs more UV light then bicarbonate and DOC do, especially between 200-250 nm. Moreover, the characteristic of the UV absorbance by the influent is similar to the characteristic of the UV absorbance by nitrate. Consequently the influence of higher nitrate concentrations on the degradation of model compounds is stronger than the influence of DOC and bicarbonate.

From the seasonal variations in nitrate the following can be concluded:
Between December and March the performance of both reactors will be poor because nitrate concentrations are maximal (14-17 mg/L NO_3^-), resulting in lower UV transmission of the water. Nitrate concentrations decrease from 14 mg/L NO_3^- in April to a minimum of 8.9 mg/L NO_3^- in August. During the summer period the performance will be optimal. In September the concentrations of nitrate start to increase, resulting in lower UVT transmissions and thus poorer performances of both reactors.

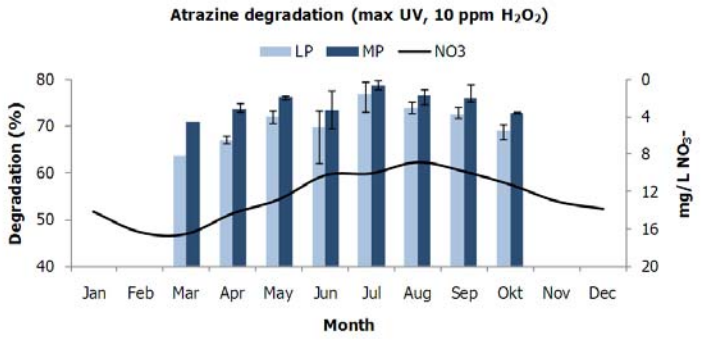

Figure 7.22: Influence of seasonal variations in nitrate concentrations

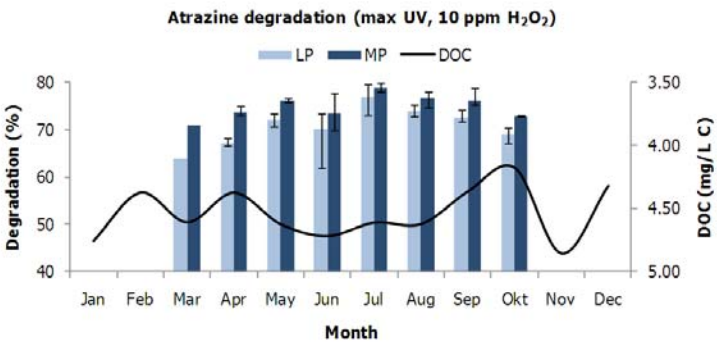

Figure 7.23: Influence of seasonal variations in DOC concentrations

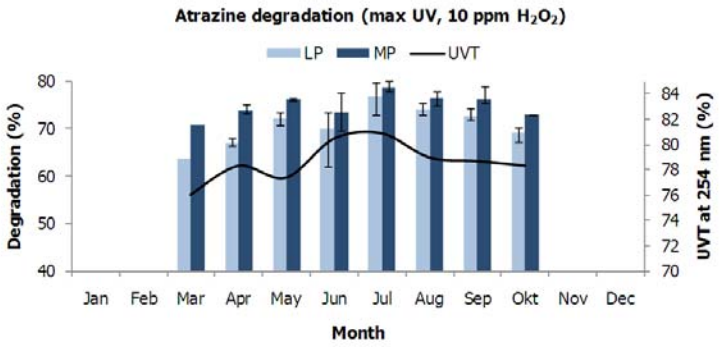

Figure 7.24: Influence of seasonal variations in UV transmission

7.7.9 Conclusions regarding influence water matrix

The best performance in terms of degradation of model compounds is achieved in the second half of July 2009 when the water quality of the pre-treated Meuse water was optimal: high UVT (>80%), low concentrations of nitrate (8.65 mg/L NO_3^-), DOC (3.36 mg/L C) and bicarbonate (137 mg/L HCO_3^-) and high temperature of the influent water (21.4 °C). The poorest performances are achieved on March 5th and June 11th when the quality of the pre-treated Meuse water was poor: UVT of 74 and 77.5%, high concentrations of nitrate (15.94 and 11.1 mg/L NO_3^-), DOC (4.0 and 3.65 mg/L C) and bicarbonate (151 mg/L HCO_3^-). The water temperatures were 5.3 and 18.3 °C respectively.

Higher concentrations of DOC have a small influence on the performance of the LP reactor. The dominant degradation mechanism in the LP reactor is oxidation by hydroxyl radicals, which does not seem to be influenced by higher DOC concentrations. Photolysis of atrazine is influenced by higher concentrations of DOC because the UV absorbance of DOC (0.15) and atrazine (0.17) are almost equal. However, atrazine degradation by the LP reactor results primarily from advanced oxidation (59%), explaining why the weak, negative correlation (-.28) between DOC concentrations and atrazine degradation is non significant (sig. = .066). Because the UV absorbance of NDMA at 254 nm (0.26) is higher then the UV absorbance of DOC, photolysis of NDMA is marginally influenced, confirmed by the fact that no correlation exists between DOC concentrations and degradation of NDMA by the LP reactor. Increased concentrations of DOC have a negative influence on the performance of the MP reactor; atrazine degradation is significantly reduced with increased DOC concentrations. The UV absorbances of atrazine and DOC are similar at wavelengths >250 nm. Because the MP output spectrum shows three large emission peaks in this part of the spectrum, the competition for UV light between atrazine and DOC is large. The bromacil absorbance spectrum shows a broad, low peak between 265-295 nm and absorbing more UV light in this part of the spectrum then DOC and the other model compounds do. UV absorbance of ibuprofen is at wavelengths >240 nm is considerably lower than the UV absorbance of DOC. Weak, negative correlations were found between DOC concentration and the degradation of ibuprofen (-.18) and bromacil (-.21). The correlations were not significant, indicating that the degradation of both compounds (photolysis and advanced oxidation) is marginally influenced by larger concentrations of DOC. Photolysis of NDMA is not influenced by DOC concentrations because the UV absorbance of NDMA is much larger then the absorbance by DOC at wavelengths <260 nm. Moreover, NDMA was fully degraded at the maximal DOC concentration.

Although the concentration of bicarbonate was highest during the poorest performances, bicarbonate does not influence the degradation of model compounds: the UV absorbance of bicarbonate is considerably lower than the UV absorbance of the model compounds and other parameters over the entire spectrum. Scavenging of bicarbonate and competition for UV light is negligible; therefore bicarbonate has a negligible effect on the degradation of model compounds by both reactors. The value of the pH was relatively constant during the experimental period and no effects to the degradation could be distinguished.

Nitrate absorbs more UV light then bicarbonate and DOC do, especially between 200-250 nm. Consequently the influence of higher nitrate concentrations (e.g. lower UVT) to the degradation of model compounds is stronger then the influence of DOC and bicarbonate. Photolysis of atrazine,

bromacil and ibuprofen is inhibited by nitrate. Moreover, higher concentrations of nitrate result in higher concentrations of nitrite, increasing the amount of hydroxyl radical scavenging. Less hydroxyl radicals are then available for oxidation reactions. Although the UV absorbance of atrazine is higher then the UV absorbance of nitrate in most parts of the spectrum, from 250 nm onwards the absorbances are very comparable. Since the highest emission peaks of the MP lamps overlap with this part of the spectrum, nitrate will compete with atrazine for UV light. Because it is suspected that photolysis contributes more to the total degradation of atrazine then oxidation does, it is no surprise to found a very strong significant negative correlation (-0.9) between nitrate concentrations and atrazine degradation. NDMA absorbs UV light over the whole spectrum and between 215-265nm the absorbance is a lot higher than the absorbance of nitrate. Because the MP output spectrum shows three peaks in this part of the spectrum, nitrate has a marginal influence photolysis of NDMA.

At 254 nm, the UV absorbance of nitrate (0.1) is slightly lower then the UV absorbance of atrazine (0.17) and bromacil (0.16) and a factor 2.6 lower than the absorbance by NDMA: influence of nitrate to photolysis of NDMA is marginal and no correlations were found. Atrazine degradation is influenced negatively by higher concentrations of nitrate, although the correlation is just above the significance level. The most important differences between the influence of nitrate to the performance of the MP and the LP reactor is the fact that increased nitrate concentrations do not increase scavenging from nitrite because nitrite formation is negligible at 254 nm. However, from the relation between seasonal variations in performances and nitrate concentrations can be concluded that the performance of the LP reactor is equally sensitive to nitrate concentrations as the performance of the MP reactor, because nitrate has a strong influence on the UVT of the pre-treated Meuse water.

Seasonal variations of nitrate concentrations can be used to estimate the seasonal variations in performance of both reactors. Between December and March the performance will be poor because nitrate concentrations are maximal (14-17 mg/L NO_3^-). Nitrate concentrations decrease from 14 mg/L NO_3^- in April to a minimum of 8.9 mg/L NO_3^- in August. During the summer period the performance will be optimal. In September the concentrations of nitrate start to increase, resulting in poorer performance of both reactors.

7.8 Formation of by-products

7.8.1 AOC

AOC analysis is done with a bioassay which quantifies the concentration of bacterial cells that have grown on the available carbon in a water sample. Mostly *Pseudomonas fluorescens P-17* and *Spirillum sp. strain NOX* are used as test organisms. The bacteria are inoculated to a 600 ml water sample and incubated at 15°C for 10-14 days. During incubation microbacterial growth is measured with plating on nutrient agar. The average net growth is related to the growth of the test organisms on pure solutions of acetate (P-17) or oxalate (NOX) with pre-derived yield values. The final result is reported as acetate C-equivalents (Hammes, 2008).
Measurements of AOC have an inaccuracy of 24% (Luc Zandvliet, HWL) and are therefore performed in duplex. Moreover, the presence of disinfectants such as H_2O_2 has a negative influence on the reliability of the measurements since it will inhibit bacterial growth. Residual H_2O_2 is quenched by the addition of sodium thiosulphate.
Storage of AOC samples may increase the AOC levels up to 65% (Escobar et al., 2000) within a week. This was determined to be the result of fermentation of biodegradable organic matter (BOM) to AOC by a yeast, *Cryptococcus neoformans*. The P-17 bacteria in particular benefit from the fermentation products since it has a greater diversity in terms of ability to utilize a larger variety then carbon sources compared to NOX bacteria (Escobar et al, 2000), as a consequence AOC levels determined with P-17 were a lot higher then AOC levels determined with NOX strains. The results from the experiments show indeed that levels of AOC_{P-17} are larger then levels of AOC_{NOX}, however this is only true for effluent concentrations from experiments with a peroxide dose of 10 ppm. When no peroxide is dosed, AOC_{NOX} levels are higher then AOC_{P-17} levels (results can be found in annex H).

7.8.1.1 Influent AOC levels

AOC levels in the pre-treated river water (without H_2O_2 addition) are between 9.5 to 16.3 µg/L, with an average of 12.9 µg/L. Influent concentrations with 10 ppm H_2O_2 addition show large dispersion (0 – 24 µg/L) but half of the measured concentrations were around 0 µg/L, which is considered to be wrong. Influent concentrations with 5 ppm H_2O_2 addition were measured only twice and in both cases the results are reasonable (10.2 and 13 µg/L). It is concluded that AOC determination in samples taken from the influent water are unreliable in the presence of high peroxide concentrations. Based on the measured concentrations (0 and 5 ppm H_2O_2), it is concluded that the average AOC concentration in pre-treated river water is equal to 13 µg/L.

7.8.1.2 AOC formation in the presence of 10 ppm H_2O_2

Measured AOC levels in the effluent (10 ppm H_2O_2) of both the LP and MP reactor show a large dispersion which makes it difficult to make a conclusive statement about the amount of AOC formation. It was decided to exclude measured AOC values < 5 µg/L, since obviously something must have negatively influenced the biomass yield during inoculation of the samples. Average concentrations of AOC in the LP and MP effluent are 64 µg/L C and 71 µg/L C respectively. It is concluded that formation of AOC resulting form advanced oxidation (10 ppm H_2O_2) is similar for both lamp types.

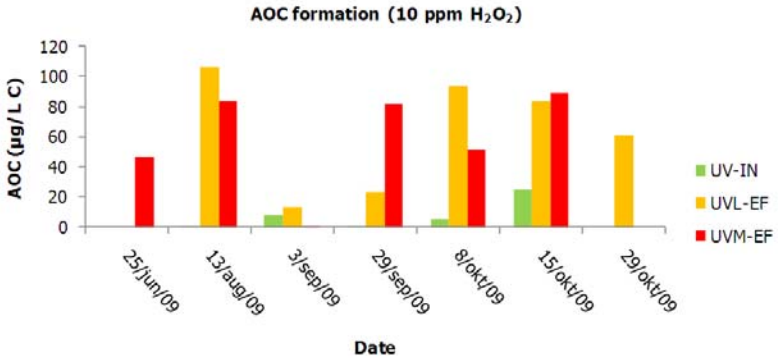

Figure 7.25: AOC formation using LP lamps (1140 mJ/cm^2) and MP lamps (850 mJ/cm^2), 10 ppm H_2O_2

7.8.1.3 AOC formation in the presence of 5 ppm H_2O_2

Effluent AOC levels applying advanced oxidation (5 ppm H_2O_2) were only determined twice resulted and in both cases resulted in higher AOC concentrations using LP lamps than using MP lamps: 81 and 47 µg/L and 65 and 40 µg/L respectively. This does not correspond well with results found in other research: LP-UV should result in lower AOC formation then MP-UV. However, since AOC concentrations were determined only twice, this could simply be a coincidence, more measurements are required for confirmation.

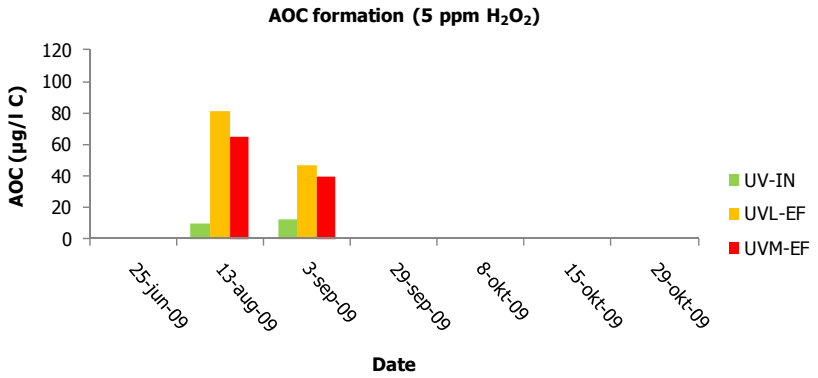

Figure 7.26: AOC formation using LP lamps (1140 mJ/cm^2) and MP lamps (850 mJ/cm^2), 5 ppm H_2O_2

7.8.1.4 AOC formation photolysis

AOC levels measured in the effluent (0 ppm H_2O_2) show a more constant pattern and are near 25 µg/L in the LP-effluent and 47 µg/L in the MP-effluent. It is concluded that AOC formation resulting from photolysis using LP lamps is twice as low as AOC formation using MP lamps.

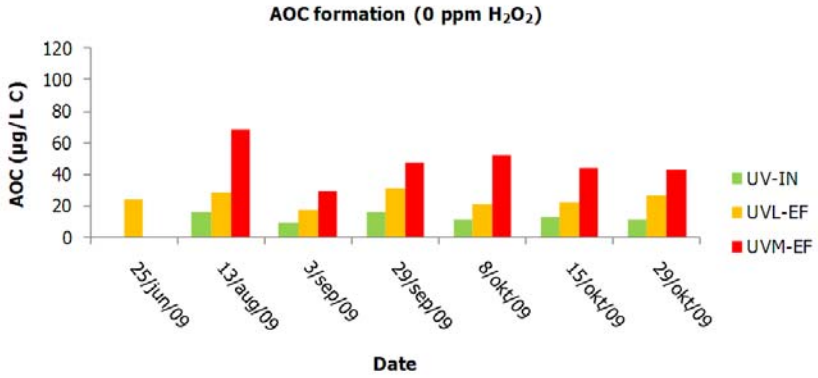

Figure 7.27: AOC formation using LP lamps (1100 mJ/cm^2) and MP lamps (850 mJ/cm^2), no H_2O_2 addition

7.8.1.5 Suspected origin AOC formation

The suspected origin of the formed AOC is analysed for photolysis using LP lamps, which converts on average 82 µg/L of DOC into degradation products such as AOC. Photolysis of atrazine using LP lamps primarily yields hydroxyatrazine, which is not qualified as a readily available carbon substrate for microbiological growth. Without the addition of peroxide, degradation levels of ibuprofen and bromacil under LP-UV were 11% and 6% respectively, which corresponds with a conversion of 2.2 µg/L of ibuprofen and 0.6 µg/L of bromacil. The types of degradation products are unknown.

Photolysis of NDMA can yield formic acid and formaldehyde, which contributes to the total amount of formed AOC. Observed average degradation for NDMA was 90.76%, which corresponds to a conversion of 9.08 µg/L NDMA into degradation products. Assuming that the yield of AOC from the converted compounds is 1 (i.e. all degradation products of ibuprofen, bromacil and NDMA are readily available carbon substrates), the AOC formation from degradation of the model compounds is estimated as follows:

$$AOC\ formation_{LP} = 0.11 * C_{IBU} + 0{,}06 * C_{BRO} + 0.91 * C_{NDMA}$$

$$= 2.2 + 0.6 + 9.08$$

$$= 11.88\ \mu g/l$$

Photolysis of atrazine, bromacil, ibuprofen and NDMA using MP lamps resulted in average degradation levels of 63, 33, 41 and 85% respectively. MP-UV photolysis of atrazine results in loss of the alkyl groups which increases AOC levels. Since the precise character of bromacil and ibuprofen degradation products are unknown, it is assumed that those increase the AOC levels as well. MP-UV photolysis of NDMA yields the same products as LP-UV photolysis. Again, it is assumed that the yield of AOC from converted compounds is 1, resulting in the following total estimate for AOC formation:

$$AOC\ formation_{MP} = 0.63 * C_{ATZ} + 0.41 * C_{IBU} + 033 * C_{BRO} + 0.85 * C_{NDMA}$$

$$= 6.3 + 8.2 + 3.3 + 8.5$$

$$= 26\ \mu g/L$$

Since the observed average AOC concentration resulting photolysis was near 25 µg/L (LP lamps) and 47 µg/L (MP lamps), it is concluded that the major contributor to the AOC levels in the effluent is the conversion of dissolved organic material rather then the lost alkyl groups of the model compounds.

7.8.1.6 Conclusions regarding AOC formation

The concentration of AOC in the influent water is approximately 13 µg/l C. AOC formation is significantly enhanced in the presence of H_2O_2 using LP lamps (1140 mJ/cm^2) and MP lamps (850 mJ/cm^2). Effluent AOC levels applying advanced oxidation (5 ppm H_2O_2) were determined twice and the observed AOC concentrations were higher using LP lamps than using MP lamps: 81 and 47 µg/L and 65 and 40 µg/L respectively. This does not correspond well with results found in other research: LP-UV should result in lower AOC formation then MP-UV (IJpelaar et al., 2006, 2007). However, the concentrations were determined only twice, this could simply be a coincidence; more measurements are required for confirmation. Increasing the peroxide dose to 10 ppm yields average AOC concentrations of 64 µg/L C (LP lamps)) and 71 µg/l C (MP lamps). Applying only direct photolysis yields AOC concentrations of 25 µg/L (LP lamps) and 47 µg/L (MP lamps).

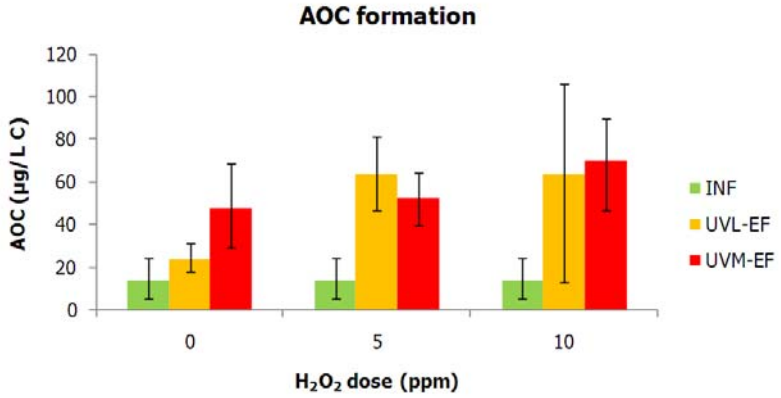

Figure 7.28: AOC formation using LP lamps (1140 mJ/cm^2) and MP lamps (850 mJ/cm^2)

From literature was concluded that UV fluencies <100 mJ/cm^2 did not result in significant AOC formation (IJpelaar et al, 2007) regardless of the applied lamp type. Recent research (van der Maas et al, 2009) showed that LP-UV resulted in a factor 1.5 increase in AOC concentrations (from 11 to 16 µg/L) at a fluency of 40 mJ/cm^2. Since the applied LP-UV dose in this research is a factor 20 higher, it is not surprising to find considerably higher AOC concentrations in the effluent. AOC formation is higher using MP lamps than using LP lamps except when 5 ppm H_2O_2 is dosed. However, only 2 measurements were performed for this latter experimental setting, so more measurements are required to confirm it.

PWN Water Supply Company has implemented UV/H_2O_2 in a full scale drinking water plant for disinfection and degradation of organic micropollutants. The applied MP-UV dose of 600 mJ/cm^2 and

H_2O_2 dose of 6 ppm resulted in AOC levels of 100-150 µg/L C (influent levels 5-33 µg/L), which is considerably higher than levels found in this research: 46-89 µg/L (10 ppm H_2O_2, 850 mJ/cm^2) and 40-65 µg/L (5 ppm H_2O_2, 850 mJ/cm^2). DOC levels found in pre-treated Lake IJssel water are 2.5 mg/L (Martijn et al, 2007) while pre-treated Meuse water contains 3.5 mg/L of DOC.

From the results can be concluded that AOC formation is enhanced in the presence of peroxide, since more DOC can be oxidized. In general, the observed AOC formation by both reactors is relatively low and similar levels for both reactors are observed in the presence of hydrogen peroxide.

7.8.2 Nitrite and nitrate

7.8.2.1 Nitrite formation

During the experimental period nitrate concentrations varied from 8.5 mg/L to 16 mg/L NO_3^-.
Concentrations of nitrite measured in the influent are below the detection limit (<7 µg/L) and are increased dramatically using MP lamps. The concentration of nitrite observed in the effluent of the MP reactor varies from 0.44-0.68 mg/L NO_2^-, depending on the peroxide dose.

Results from collimated beam experiments performed by Sharpless et al (2003) show that H_2O_2 addition during polychromatic UV irradiation significantly increases the levels of formed nitrite compared to solutions without hydrogen peroxide. Nitrite production rate is increased when the hydrogen peroxide concentration is increased from 5 to 10 mg/L (Sharpless et al., 2003). However, nitrite concentrations observed in the MP effluent during the research were highest in the absence of hydrogen peroxe (0.61 mg/L). Dosing 5 and 10 ppm H_2O_2 yields nitrite concentrations of 0.56 and 0.48 mg/L NO_2^- respectively.

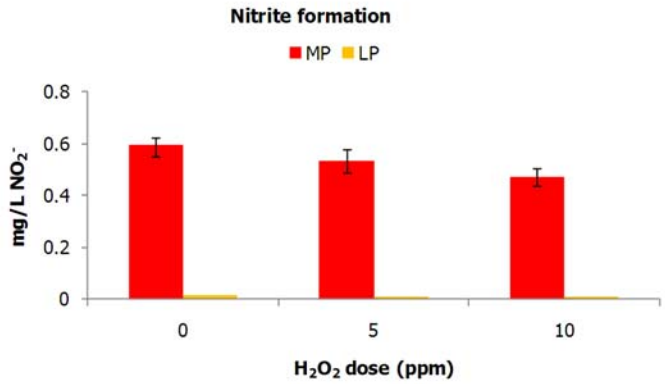

Figure 7.29: Nitrite formation resulting from AOP using LP lamps (1140 mJ/cm^2) and MP lamps (850 mJ/cm^2), N=7. Values portray means of observed concentrations, error bars represent minimum and maximum

PWN Water Supply Company has observed nitrite concentrations increase to 100-300 µg/ (average 160 µg/L) with a MP-UV dose of 600 mJ/cm^2 and 6 ppm H_2O_2. The nitrate concentrations in pre-treated IJssel Lake water show a slightly lower range (6-12 mg/L), than the observed nitrate concentrations during this research (8.5-12 mg/L). This latter fact combined with the higher applied UV dose can explain way higher nitrite levels found in this research are higher.

Observed nitrite formation applying LP-UV is generally well below 0.015 mg/L, regardless of the hydrogen peroxide doses and can be considered negligible, which is inline with results found in other experiments. On September 3 2009 however, nitrite concentrations in the LP effluent were 0.07 mg/L (10 ppm), 0.08 mg/L (5 ppm) and 0.1 mg/L (0 ppm). The quality of the pre-treated Meuse water on this particular date was poor, having an UVT of only 50% and nitrite concentration of around 0.08 mg/L. On this date nitrite concentrations are slightly reduced by LP-UV in the presence of hydrogen peroxide. It is concluded that a small part of the nitrite is oxidized by the hydroxyl radicals.

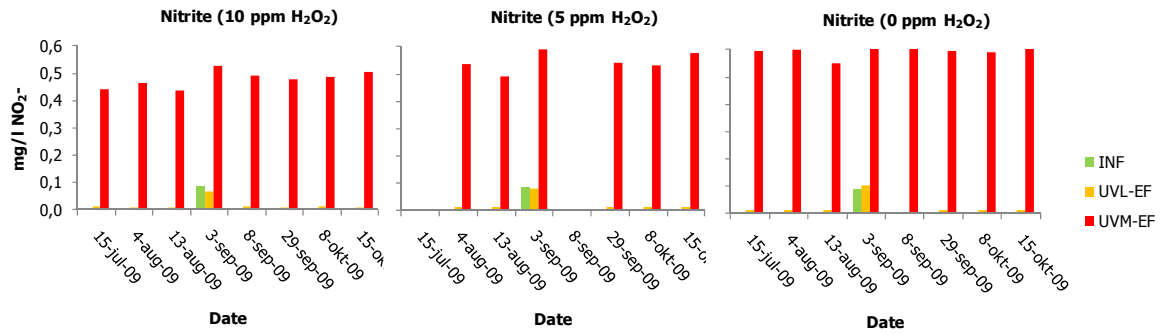

Figure 7.30: Measured concentrations of nitrite

7.8.2.2 Nitrate conversion and formation

Since nitrite formation is a result of nitrate photolysis, it is expected that effluent concentrations of nitrate are lower than the influent concentrations. From the measuring data the opposite can be concluded; nitrate concentrations in LP effluent are increased slightly on several occasions by 0.07-0.96 (average 0.3 mg/L NO_3^-). From the literature was concluded that photolysis of NDMA can yield increased nitrite and nitrate concentrations (yield factors unknown), which can account for the observed increment in nitrate. Applying the same reasoning as for AOC formation, one can conclude that nitrate formation by the LP reactor (average of 300 µg/L) should have an other origin than NDMA conversion, since the maximum NDMA conversion possible is 10 µg/L.

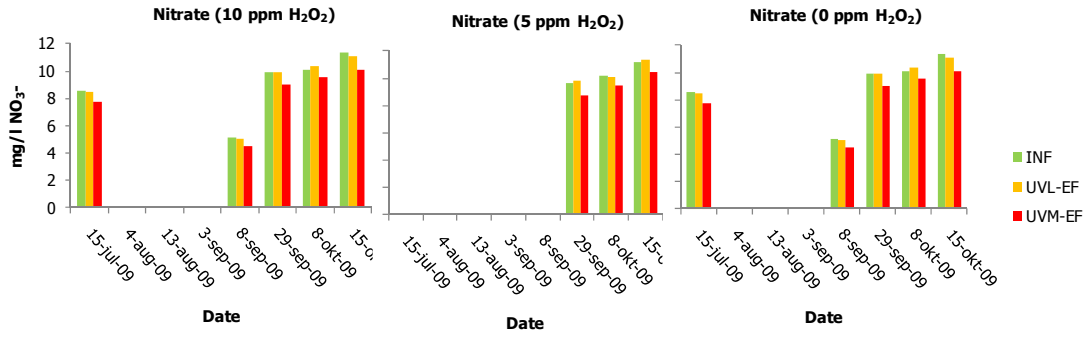

Figure 7.31: Nitrate concentrations

7.8.2.3 Estimation of radical scavenging

Nitrite yield from nitrate photolysis can be estimated as follows:

$$[NO_3^-]_{INF} * \phi = [NO_2^-]_{expected}$$

Formation of hydroxyl radicals is negligible in the absence of hydrogen peroxide. Therefore the actual quantum yield for nitrite can be estimated from the observed effluent $[NO_2^-]$ concentration in the absence of hydrogen peroxide:

$$\phi = \frac{[NO_2^-]_{ce}}{[NO_3^-]_{ci}}$$

Where
$[NO_2^-]_{ce}$ = observed concentration of nitrite in effluent, mmol/L
$[NO_3^-]_{ci}$ = observed concentration of nitrate in influent, mmol/L

The quantum yield determined from the results is 0.082 using MP lamps while the yield factor using LP lamps is only 0.002 (see table below).

Table 7.20: Nitrite yield factor

Exp. no.	$[NO_3^-]_{INF}$	$[NO_2^-]_{EF-MP}$	$\Phi_{200-300\ nm}$	$[NO_2^-]_{EF-LP}$	$\Phi_{254\ nm}$
15-jul-09	0.138	0.013	0.0933	0.000314	0.002269
4-aug-09	-	0.013	-	0.000286	-
13-aug-09	-	0.012	-	0.000328	-
8-sep-09	0.157	0.013	0.0848	0.000371	0.002358
29-sep-09	0.160	0.013	0.0811	0.000328	0.002053
8-okt-09	0.163	0.013	0.0786	0.000321	0.001967
15-okt-09	0.182	0.014	0.0742	0.000314	0.001721
mean	**0.160**	**0.013**	**0.0824**	**0.000323**	**0.002073**

From the literature was concluded that nitrite yield from nitrate photolysis is 0.1 (IJpelaar, 2006, Goldstein et al., 2007), which is close to the value 0.082 determined from the experimental results. Values for nitrite yield at 254 nm are <0.001 (IJpelaar, 2006) or 0.065 using not mercury but xenon lamps (Goldstein et al., 2007). The value determined from the experimental results is 0.0021.

Expected $[NO_2^-]$ concentrations using MP lamps are estimated with the date specific yields (see figure below) as follows:

$$[NO_2^-]_{expected(10\ ppm)} = [NO_3^-]_{INF\ (10\ ppm)} * \phi_{date}$$

The average $[NO_2^-]$ formation using MP lamps is estimated to be 0.012 mmol/L. The reduction in nitrite concentrations resulting from radical scavenging can then be estimated as follows:

$$[NO_2^-]_{scav(10\ ppm)} = [NO_2^-]_{expected\ (10\ ppm)} - [NO_2^-]_{UVM-EF\ (10\ ppm)}$$

When the peroxide dose is 10 ppm, approximately 0.0027 mmol/l of nitrite is oxidized and when the peroxide dose is 5 ppm 0.0010 mmol/l of nitrite is oxidized. It is concluded that higher doses peroxide result in lower concentrations of nitrite because more radicals are available for oxidizing nitrite.

Table 7.21: Radical scavenging nitrite

	5 ppm H_2O_2			10 ppm H_2O_2	
date	$[NO_3^-]_{inf}$	$[NO_2^-]_{UVM-EF}$	$[NO_2^-]_{scav}$	$[NO_2^-]_{UVM-EF}$	$[NO_2^-]_{scav}$
15-jul-09	0.14	-	-	0.010	0.0034
4-aug-09	-	0.012	-	0.010	-
13-aug-09	-	0.011	-	0.009	-
8-sep-09	0.16	-	-	0.011	0.0027
29-sep-09	0.16	0.012	0.0008	0.010	0.0026
8-okt-09	0.16	0.012	0.0014	0.011	0.0023
15-okt-09	0.18	0.013	0.0009	0.011	0.0026
AVE	**0.16**	**0.012**	**0.0010**	**0.010**	**0.0027**

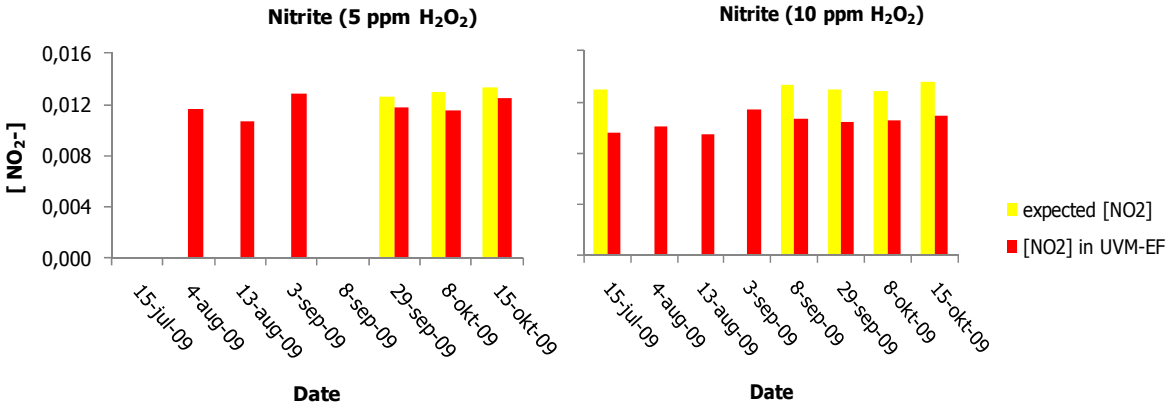

Figure 7.32: Expected nitrite concentrations (mmol/L) using MP lamps (850 mJ/cm^2)

7.8.3 Residual hydrogen peroxide

Effluent of both reactors was transferred to 2 L polyethylene bottles, prohibiting the penetration of light. The bottles are stored in the supernatant water level above the dual media filters in the full-scale treatment plant to guarantee a constant and representative water temperature. As can be seen from the graphs below, the residual peroxide concentrations in the effluent of the reactors are high: approximately 9.5 mg/L of the initial dose of 10 mg/L H_2O_2 and 4.2-4.8 mg/L of the initial dose of 5 mg/L is not utilized during AOP. The graphs below show that the residual peroxide does react with the water. However, repeating the experiment with bottles that are normally used for taking AOC samples (e.g. bottles that are free of organic material), yields a different conclusion: degradation of residual peroxide by the water matrix is negligible. This implies that somehow the samples collected and stored in PE-bottles have become contaminated. Perhaps the PE-bottles were not completely water-tight, resulting in intrusion of river water, causing the degradation of residual peroxide. It is also possible that a biofilm was present on the surface of the PE-bottles, because they have not been cleaned other then rinsing and shaking (4 times) with the sample water.

After discharge into infiltration ponds the water slowly passes through the soil. In the upper layers of the water column sunlight can still penetrate and possibly degrade peroxide, which is simulated by filling a house hold swimming pool with 2 m^3 AOP effluent. From the absorbance characteristic of peroxide can be concluded that peroxide can absorb solar light (>250 nm) resulting in photolysis of peroxide. However after a residence time of 80 hours, only 1.5 mg/L of residual H_2O_2 has been photolyzed.

It is concluded that degradation of residual peroxide by the water itself during transport and photolysis of residual peroxide in the infiltration ponds is negligible. Post treatment of the effluent by GAC filtration will be required for the removal of residual peroxide. PWN Water Supply Company has implemented GAC filtration for the quenching of residual peroxide, biodegradation of AOC and re-oxidation of nitrite into nitrate (Martijn et al., 2007).

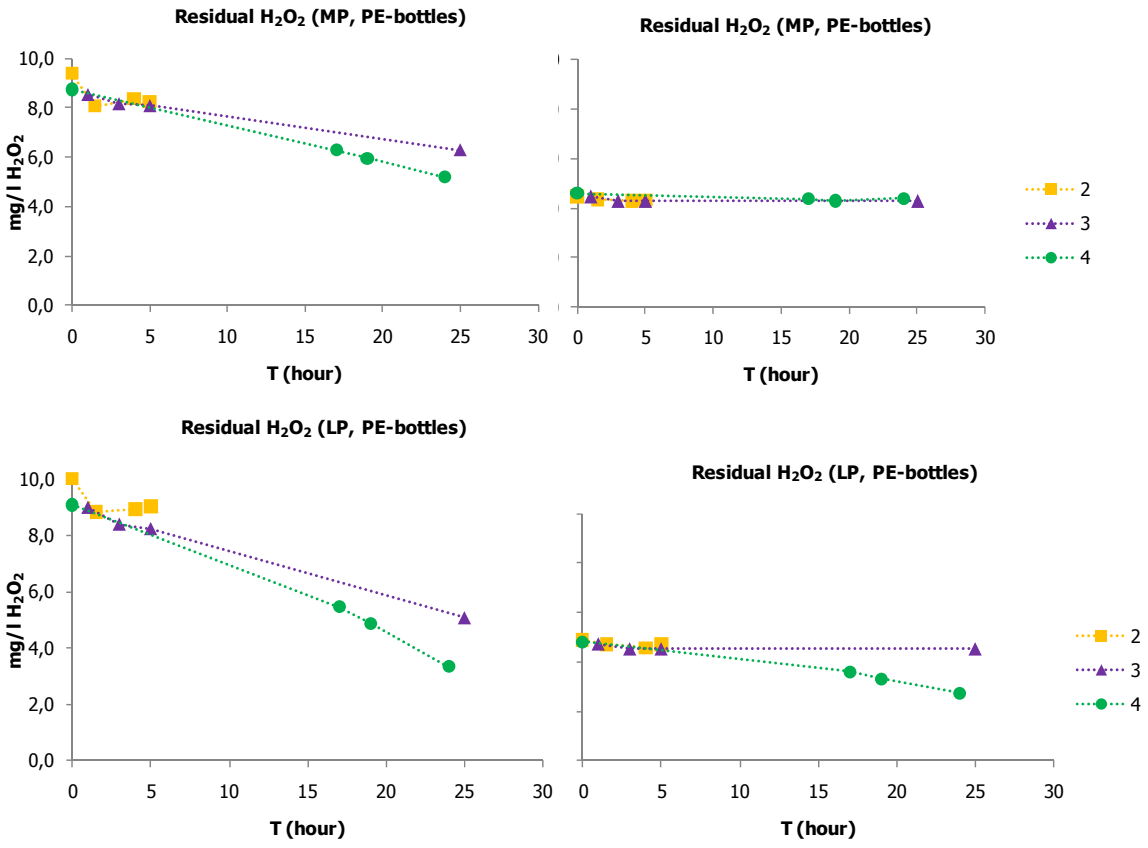

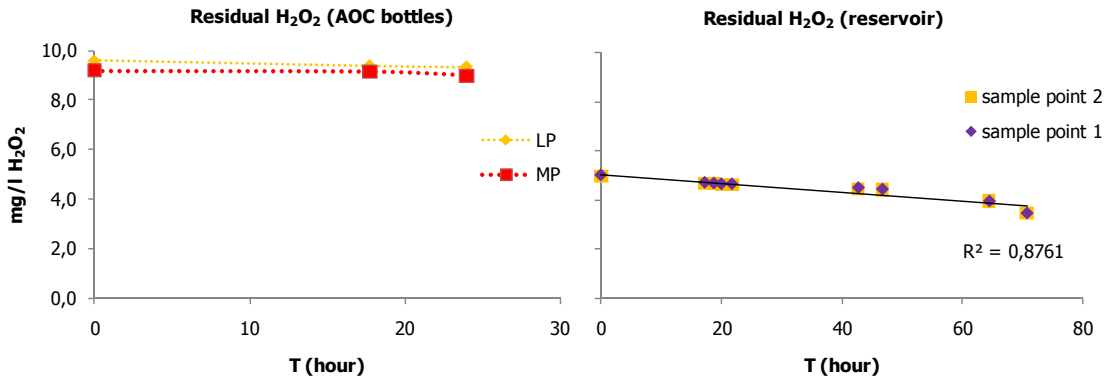

Figure 7.33: Degradation of residual hydrogen peroxide

8. Conclusions and recommendations

8.1 Conclusions

Dunea Duin en Water is performing research to extend the current multiple barrier treatment with advanced oxidation processes (AOP) via UV and hydrogen peroxide. AOP is an effective method for converting organic micropollutants found in Dunea's source - the river Meuse – into smaller, more biodegradable substances. Mostly medium pressure mercury vapour ultraviolet lamps are used that emit a broad spectrum of light, coinciding with the absorbance spectrum of many substances, which results in a high photolytic capacity. Low pressure mercury vapour lamps emit ultraviolet light at just one single wavelength (254 nm). Consequently, the direct photolysis of target substances is less effective and the yield of hydroxyl radicals is lower compared to MP lamps. However, LP lamps have advantages over MP lamps such as significantly lower energy consumption and fewer by products (e.g. AOC, nitrite) are formed. The objective of this research is formulated as follows:

Performance comparison of low pressure versus medium pressure mercury vapour lamps in advanced oxidation via UV/H_2O_2, by means of experimental research with a pilot scale set up.

In order to simulate the AOP, a pilot scale experimental set-up was built with a design flow of 5 m^3/h per reactor. Two reactors are used during the experiments: one reactor equipped with 4 medium pressure mercury vapour ultraviolet lamps (P_{total} = 4.4 kW) and another reactor equipped with two low pressure mercury vapour ultraviolet lamps (P_{total} = 1.32 kW). Atrazine, bromacil, ibuprofen and NDMA are dosed to the influent which is abstracted directly from the full-scale plant after pre-treatment by coagulation, microstraining and dual media rapid sand filtration. Hydrogen peroxide concentrations are varied (0, 5 and 10 ppm) and static mixers are installed to ensure homogenic water mixture and samples. The maximum UV dose in the MP-reactor is approximately 850 mJ/cm^2 and the maximum UV dose in the LP-reactor is approximately 1140 mJ/cm^2. The UV doses are estimates based on the information given by the suppliers which at the moment of writing have not yet been confirmed by CFD modelling. Experiments have been performed between March and October 2009, using different combinations of UV and peroxide doses.

Although reduction in concentration of the model compounds - atrazine in particular - is the key performance indicator, the degradation capacity should be judged in relation to the energy consumption, the formation of undesirable by- and degradation products and the overall sensitivity towards seasonal fluctuations.

Achieved degradation of atrazine should at least be 80%. Unfortunately that level is not reached yet: the average degradation levels of atrazine achieved at maximum UV and peroxide doses using LP and MP lamps are 72% and 75% respectively. However, the average degradation levels of atrazine may not reach 80%; this level has been achieved once by both reactors. During this particular experiment, the water quality of the pre-treated Meuse water was optimal: high UVT (>80%), low concentrations of nitrate (8.65 mg/L NO_3^-), DOC (3.36 mg/L C) and bicarbonate (137 mg/L HCO_3^-). The poorest performances occurred when the quality of the pre-treated Meuse water was poor: high concentrations of nitrate (16 mg/L NO_3^-), DOC (4 mg/L C) and bicarbonate (151 mg/L HCO_3^-). Observed degradation levels for bromacil, ibuprofen and NDMA using LP lamps (10 ppm H_2O_2) is slightly higher than using MP lamps.

Performance comparison of achieved degradation based on variations in UV doses is difficult. The UV dose is a reactor specific characteristic and varies due to hydraulic influences, refraction, reflection and variations in water quality. Therefore a parameter known as the electrical energy per order EEO (kWh/m^3) is used, defined as the electrical energy in kWh required for achieving 1 log degradation of a substance per unit of treated water. The EEO using LP lamps is considerably lower than the EEO using MP lamps. This applies for all model compounds, except for ibuprofen and bromacil in the absence of hydrogen because these substances cannot be degraded photolytically with monochromatic UV irradiation at 254 nm. Determined EEO values for atrazine degradation in the presence of 10 ppm H_2O_2 are 0.48 kWh/m^3 (LP lamps) and 1.45 kWh/m^3 (MP lamps).

From the results can be concluded that AOC formation is enhanced in the presence of peroxide, since more DOC can be oxidized. In general, the observed AOC formation is relatively low and similar levels for both lamp types (60-70 µg/L) are observed in the presence of 10 ppm H_2O_2. In the absence of hydrogen peroxide, AOC formation using MP lamps (47 µg/L) is twice as high as AOC formation using LP lamps (25 µg/L).

Observed nitrite concentrations using LP lamps is well below 0.015 mg/L, regardless of the hydrogen peroxide doses and can thus be considered negligible. Nitrite concentrations observed in the MP effluent during the research were highest in the absence of hydrogen peroxe (0.61 mg/L). Dosing 5 and 10 ppm H_2O_2 yields nitrite concentrations of 0.56 and 0.48 mg/L NO_2^- respectively.

Nitrate is the water matrix parameter with the largest influence on the performances of the reactors because nitrate absorbs considerably more UV light then other water matrix parameters, especially between 200-250 nm. Moreover, the characteristic of the UV absorbance by the influent is similar to the characteristic of the UV absorbance by nitrate. The influence of higher nitrate concentrations on the degradation of model compounds is stronger than the influence of other parameters such as bicarbonate and DOC. Seasonal variations of nitrate concentrations can be used to estimate the seasonal variations in performance of both reactors. Between December and March the performance will be poor because nitrate concentrations are maximal (14-17 mg/L NO_3^-), resulting in lower UV transmission. Nitrate concentrations decrease from 14 mg/L NO_3^- in April to a minimum of 8.9 mg/L NO_3^- in August. During the summer period the performance will be better because the UVT is higher. In September the concentrations of nitrate start to increase, resulting in poorer performance of both reactors.

In order to define the proportion of photolysis and advanced oxidation to the total degradation of a model compound by the LP reactor, multiple regression analysis is performed for the degradation of individual compounds. These models are only valid for predicting and quantifying the degradation of atrazine, bromacil and ibuprofen by the LP reactor for the conditions under which the experiments were conducted. It is concluded that degradation of atrazine, bromacil and ibuprofen result primarily from advanced oxidation: 59, 92 and 91% respectively. Degradation of NDMA can be fully attributed to photolysis using monochromatic irradiation (254 nm). Constructing models for quantifying the degradation mechanisms in the MP reactor was not successful.

Table 8.1: Summary performance comparison of LP vs. MP lamps

	Degradation model compounds (%)				**Energy performance**	**Formation of by-products**		
	ATZ	BRO	IBU	NDMA	EEO_{ATZ}	AOC (µg/L C)	mg/L NO_2^-	mg/L H_2O_2
LP lamps (1140 mJ/cm^2)	72	74	78	90	0.48	64 (23-106)	0.01-0.015	9.5
MP lamps (850 mJ/cm^2)	75	71	76	88	1.45	71 (51-90)	0.436-0.504	9.5

Considering all of the above it is concluded that the performance of low pressure mercury vapour lamps in terms of degradation of model compounds, energy performance and nitrite formation is superior to the performance of medium pressure mercury vapour lamps, when applied for advanced oxidation. Photolysis induced by monochromatic irradiation at 254 nm using high UV doses (>1000 mJ/cm^2) is only effective for degradation of NDMA. It is suspected that these high UV doses are responsible for the fact that the amount of AOC formed in the presence of 10 ppm H_2O_2 is similar to the amount of AOC formed when medium pressure lamps are applied. Both lamp types are equally sensitive to seasonal variations of nitrate concentrations in the pre-treated Meuse water. The levels of residual peroxide in the effluents are equal as well.

8.2 Further research

The results of the research show that advanced oxidation using low pressure mercury vapour lamps applying a peroxide dose of 10 pm and high UV doses (>1000 mJ/cm^2) is effective for degradation of atrazine, bromacil, ibuprofen and NDMA.

The target level of 80% atrazine degradation will be reached when the UVT of the influent water is increased from 75% to 83%. At the moment of writing, research towards improving the quality of the pre-treated Meuse water is already being performed.
In literature it is reported that low water temperatures have large, adverse effects on the performance of the low pressure lamps. At temperatures below 5° C, UV output becomes unpredictable and low pressure lamps can fail to start. The influence of the water temperature could not be determined from the results.
Because only a fraction of the dosed hydrogen peroxide is utilized during the AOP, residual concentrations of peroxide in the effluent are high. A few experiments have been performed in order to assess the amount of peroxide degradation during transport and outflow in the infiltration ponds. The results indicate that peroxide degradation is small and post-treatment of the effluent by GAC will be necessary.
Although the results show that advanced oxidation using low pressure lamps is a promising concept for degradation of four specific organic micropollutants, further research is required for confirmation. The selected model compounds are degraded adequately but during this research no experiments have been performed using a spike cocktail containing the OMPs that are threatening the drinking water production. This research also did not address the possible formation of toxic by-products during AOP. Ongoing industry consultation (BTO red.) between Dunea, KWR Watercycle Research Institute, HWL and other drinking water companies regarding the formation of genotoxic by-products should yield more information.

References

Acher, A.J. et al
Comparison of Formation and Biodegradation of Bromacil Oxidation Products in Aqueous Solutions
In: J. Agric. Food Chem. 1994, no. 42, p 2040-2047

Alfano, O.M., Brandi, R.J. and Cassano, A.E.
Degradation kinetics of 2,4-D in water employing hydrogen peroxide and UV radiation
In: Chemical Engineering Journal, volume 82, p 209-218

Balci, B., Oturan, N. et al
Degradation of atrazine in aqueous medium by electrocatalytically generated hydroxyl radicals: A kinetic and mechanistic study
In: Water research, volume 43, p 1924-1934, 2009

Baxendale, J.H. and Willson, J.A.
Photolysis of hydrogen peroxide at high light intensities
Trans. Faraday Soc. 56, 6195-6203, 1957

Beerendonk, E. and Siegers, W.
Robuustheid zuiveringen DPW-bedrijven
Nieuwegein: KWR, 2006

Berson UV Technologies
Use of UV light for disinfection of water
Referenced on December 28th 2009 via:
http://www.bersonuv.com/index.php?id=ourbusiness

Bertelkamp, C.
Degradation mechanisms of atrazine, bromacil, ibuprofen and NDMA - A literature review on the chemical structure and degradation pathways in the UV/H_2O_2 process
MSc thesis report, TU Delft – Department of sanitary engineering, 2009

Bianchi, C.L., Pirola C., Ragaini, V. and Selli, E.
Mechanism and efficiency of atrazine degradation under combined oxidation processes
In: Applied Catalysis B: Environmental, volume 64, p 131-138, 2006

Bielski, H.J., Benon, H.J. et al
Reactivity of perhydroxyl/superoxide radicals in aqueous solution
J. Phys. Chem. Ref. Data 14-40, p-1041–1100, 1985

Bolton, J.R. et al
Figures-of-merit for the technical development and application of advanced oxidation technologies for both electric- and solar-driven systems (IUPAC technical report)
In: Pure Appl. Chem, volume 73, issue 4, p 209-216, 2003

Boncz, M.A.
Selective oxidation of organic compounds in wastewater by ozone based oxidation process
Wageningen: Universiteit Wageningen, PhD thesis, 2002

Braun et al,
Photochemical Technology
Chichester (UK): Wiley, 1991

Buxton G.V. et al,
Critical review of rate constants for reactions of hydrated electrons, hydrogen atoms and hydroxyl radicals in aqueous solution
Journal of Phys. Chem. Ref. Data, 17, p-513, 1988

Champagne, P., Tyagi, R.D. and Lo, I.
Natural Processes and Systems for Hazardous Waste Treatment
Reston (USA): American Society of Civil Engineers, 2008

Christophersen, A. G., Jun, H., Jørgensen, K., and Skibsted, L. H.
Photobleaching of astaxanthin and canthaxanthin: quantum-yields dependence of solvent, temperature, and wavelength of irradiation in relation to packageing and storage of carotenoid pigmented salmonoids
In: Zeitschrift fur Lebensmittel-Untersuchung-und-Forschung, volume 192, p 433-439

Cooperative Research Centre (CRC) for Water Quality and Treatment
Organic Micropollutants in Water: Outcomes from the Research Programs of the CRC for Water Quality and Treatment
Salisbury (Australia): CRC, 2007

Dekking et al,
KANSTAT – Probability and Statistics for the 21st Century
Delft: Delft University of Technology, 2004

Derks, J.G.
Reduced emission of organic micropollutants: A network analyses aimed at identifying preventative measures, part of Master of Science Thesis
MSc thesis report, Delft University of Technology – Department of Sanitary Engineering, 2010

Environmental Protection Agency (EPA)
Ultraviolet Disinfection Guidance Manual
Washington: EPA, 2003

Environmental Protection Agency (EPA)
Alternative Disinfectants and Oxidants guidance manual
Washington: EPA, 1999

Escobar, I.C. and Randall, A.A.
Sample storage impact on the assimilable organic carbon (AOC) bioassay
In: Water Resources, Volume 34, No.5, p 1680-1686

Gao, N., Deng, Y. and Zhao, G.
Ametryn degradation in the ultraviolet (UV) irradiation/hydrogen peroxide (H_2O_2) treatment
In: Journal of Hazardous Materials, volume 164, p 640-645, 2009

Goldstein, S. and Rabani J.
Mechanism of Nitrite Formation by Nitrate Photolysis in Aqueous Solutions: The Role of Peroxynitrite, Nitrogen Dioxide, and Hydroxyl Radical
In: J. AM. CHEM. SOC. Vol 129, p 10597-10601, 2007

European Parliament and the Council
Directive 2000/60/EC Water Framework Directive

Hair, J.F. et al
Multivariate Data Analsysis – sixth edition
Upper Addle River (NJ, USA): Pearson Prentice Hall, 2006

Hammes, F.
A comparison of AOC methods used by the different TECHNEAU partners
Techneau, 2008

Hapeman, C.J. et al
Mechanistic Investigations Concerning the Aqueous Ozonolysis of Bromacil
In: J. Agric. Food Chem. 45, 1006-1011, 1997

Héquet, V. Gonzalez C. and Le Cloirec,
Photochemical processes for atrazine degradation: methodological approach
In: Wat. Res. Vol. 35, No. 18, p 4253–4260, 2001

Hijnen, W.A.M. and van der Kooij, DI
The effect of low concentrations of assimilable organic carbon (AOC) in water on biological clogging of sand beds
In: Water Research, Vol. 26-7, pp. 963-972, 1992

Hoekstra, R., Boer, M., Smidt, R. et al
Gebiedsconvenanten in de Bommelerwaard – Boeren en tuinders leveren zuiver water aan de Afgedamde Maas
Utrecht: CLM Onderzoek en Advies BV, 2002

Hoigné, J.
Chemistry of Aqueous Ozone and Transformation of Pollutants by Ozonation and Advanced Oxidation Processes
In: The handbook of environmental chemistry, volume 5, p83-142, 1998

Hooijveld, A.
Analysis of atrazin, bromacil, ibuprofen and NDMA with UPLC-MS, HWL, 2009

IJpelaar, G., Harmsen, D., Sharpless, C.M., Linden, K.G. and Kruithof, J.C.
Fluence Monitoring in UV Disinfection Systems: Development of a Fluence Meter
London: IWA, 2006

IJpelaar, G., Harmsen, D., Krijnen, S. and Knol, T.
UV/H_2O_2-oxidatie mogelijk met middendruk- én lagedruklampen
Schiedam: Nijgh Periodieken BV, article in H_2O magazine, volume 40, issue 4, p 44-46, 2007-a

IJpelaar, G., Harmsen, D. and M. Heringa
UV disinfection and UV/H_2O_2 oxidation: by-product formation and control
TECHNEAU, 2007-b

Jain, S., Yamgar, R. and Jayaram, R.V.
Photolytic and photocatalytic degradation of atrazine in the presence of activated carbon
In: Chemical Engineering Journal 148 (2009) 342–347

Jobb, D.B., Hunsinger, R.B. et al
Ultraviolet degradation of N-nitrosodimethylamine (NDMA) in Ohsweken (Six Nations) water supply
In: Proceedings of the Annual AWWA Conference, Denver, 1994

Kooij, van der, D.
Assimilable Organic carbon as indicator of bacterial growth
In : J. Am. Water Works Assoc. volume 84, no 2, p 57-65, 1992

Koppenol, W.H., Butler, J. and van Leeuwen, J.W.L.
The Haber–Weiss cycle
Photochem.Photobiol. 28, p-655–660, 1978

Kramer, M.W.
Licht op water: ontwerp voor een UV/H_2O_2 installatie
MSc thesis, TU Delft, section of sanitary engineering, 2002

Kruihof, J.C., Kamp, P.C. and Belosevic
UV/H_2O_2-treatment: the ultimate solution for pesticide control and disinfection
In: Water Science and Technology: Water Supply, Volume 2, No.1, p 113-122, 2002

Lee, C. et al
UV Photolytic Mechanism of N-Nitrosodimethylamine in Water: Roles of Dissolved Oxygen and Solution pH
In: Environ. Sci. Technol, 39, p 9702-9709

Lekkerkerker-Teunissen, K., Verberk, J.Q.J.C., Jonge, H.G., Amy, G. and van Dijk, J.C.
Advanced oxidation and artificial recharge: a synergistic hybrid system for removal of organic micropollutants
Cincinnati: WQTC conference proceedings, 2008

Lekkerkerker-Teunissen, K.
Nieuwe uitdagingen voor de Nederlandse duinen
In: "Nieuw uitdagingen"- 61e vakantiecursus in Drinkwatervoorziening
Delft: Delft University of Technology – Dept. of Sanitary Engineering, 2009

Lenntech water treatment
Disinfectants – Hydrogen peroxide
Rotterdam: Lenntech, 2008
Referenced on June 1 2009 via:
http://www.lenntech.com/water-disinfection/disinfectants-hydrogen-peroxide.htm

Maas, P. van der, Bruins, J. and Woerdt, D. van der
Effect of Low Pressure UV on the Regrowth Potential of Drinking Water
Amsterdam: IUVA congress proceedings, 2009

Martijn, B.J., Kruithof, J.C and Rosenthal, L.P.M.
Design and implementation of UV/H_2O_2 treatment in a full scale drinking water treatment plant
Velserbroek: PWN, 2007

Medcalf &Eddy
Introduction to Process Analysis and Selection, p-259
In: Wastewater Engineering – Treatment and Reuse
New York: McGraw-Hill, 2003

Metz, D.H., Meyer, M., Kashinkunti, R. and Beerendonk, E.F.
Efficacy of Ultraviolet Advanced Oxidation in a Drinking Water Utility with Full-Scale Granular Activated Carbon Adsorption
Amsterdam: IUVA congress proceedings, 2009

Mitch, W.A., Sharp, J.O., Trussell, R.R., Valentine, R.L., Alvarez-Cohen, L. and Sedlak, D.L.,
N-Nitrosodimethylamine (NDMA) as a Drinking Water Contaminant: a Review.
In: Environmental Engineering Science, 2003. 20(5): p. 389-404.

Milieu- en Natuurplanbureau (MNP)
Realisatie milieudoelen – tussenrapport 2008
Bilthoven: MNP, 2008

Moel, P.J. de, J.Q.J.C. Verberk and Dijk, J.C. van
Drinkwater – principes en praktijk
Den Haag: Sdu, 2005

Moilanen, K.W. and Crosby, D.G.,
The photodecomposition of Bromacil
In: Archives of Environmental Contamination and Toxicology, 1974. 2(1): p. 3-8.

Müller, J.P. and Jekel, M.
Comparison of advanced oxidation processes in flow-through pilot plants
In: Water Science and Technology, Vol. 44 No 5, p-303-309, 2001

MWH
Water treatment: principles and design
London: Wiley, 2005

Packer, J. et al
Photochemical fate of pharmaceuticals in the environment:Naproxen, diclofenac, clofibric acid, and ibuprofen
In: Aquatic Sciences, issue 65, p 342–351, 2003

Parsons, A.F.
An Introduction to Free Radical Chemistry
London: Wiley, 2000

Peuravuori, J., and Pihlaja,K. ,
Phototransformations of selected pharmaceuticals under lowenergy UVA-vis and powerful UVB-UVA irradiations in aqueous solutions-the role of natural dissolved organic chromophoric material
In: Anal Bioanal Chem. 394: p 1621-1636, 2009

Philips, S., Haanbroek, H.J. and Verstraete, W.
Origin, causes and effects of increased nitrite concentrations in aquatic environments
In: Environmental Science & Bio/Technology volume 1: p 115–141, 2002.

Puijker, L.M., Steen, R.J.C.A., Houtman, C.J. and Oorthuizen, W.A.
Inventarisatie van bedreigingen voor de zuivering van Duinwaterbedrijf Zuid-Holland
Nieuwegein: Kiwa Water Research, 2008

Ray, M.B, Chen, J.P, Wang, L.K and Pehkonen, S.O.
Advanced oxidation processes
In: Handbook of Environmental Engineering, Volume 4: Advanced Physicochemical Treatment Processes
Totowa (NJ, USA): The Humana Press Inc., 2007

Ridder, D.J.
UV/H_2O_2 behandeling bij drinkwater bereiding – Onderzoek en ontwerp
MSc thesis report, TU Delft – Department of sanitary engineering, 2006

Scheffer, W.
Toenemend gebruik geneesmiddelen vraagt andere route urine dan via riolering
Zoetermeer: Uneto VNI 2007
In: Intech Klimaat & Sanitair, issue 5, p-50, 2007

Sandt, T. van der
Drie zuiveringsconcepten in een reactor
In: Technisch Weekblad, Volume 40, Issue 19th, 2009

Schested, K. et al
Rate constants of OH with HO2, O2−and H2O2+ from hydrogen peroxide formation in pulse-irradiated oxygenated water
In: J. Phys. Chem. 72, p- 626–631, 1968

Schriks, M., Heringa, M., Kooi, M.M.E., van der Voogt, P. and van de Wezel, A.P.
Toxicological relevance of emerging contaminants for drinking water Quality
In: Water Research (2009) doi: 10.1016/j.watres.2009.08.023

Segers, W.C.J. and Stuyfzand, P.J.
Vóórkomen en gedrag van emerging substances tijdens duinfiltratie
MSc thesis report, TU Delft – Department of sanitary engineering, 2007

Sharpless, C.M., Page, M.A. and Linden, K.G
Impact of hydrogen peroxide on nitrite formation during UV disinfection
In: Water Research, Vol. 37, p 4703-4736, 2003

Spartan Water Technologies (SWT)
UV Ozone Peroxide Advanced Oxidation
Referenced on July 28th, 2009 from:
http://www.spartanwatertreatment.com/advanced-oxidation-UV-peroxide-ozone.html

Speets, R.
Zuiver-Water in de Bommelerwaard – evaluatie
Voorburg: DZH, 2005

Stefan, M.I. and Bolton, J.R.
UV Direct Photolysis of N-Nitrosodimethylamine (NDMA): Kinetic and Product Study
In: Helvetica Chimica Acta, volume 85, p 1416-1426, 2002

Stefan, M.I.
UV photolysis: background
In: Advanced oxidation processes for water and wastewater treatment,
London: IWA publishing, 2004

Stevens, L., Lanning, J.A., Anderson, L.G., Jacoby, W.A. and Chornet, N.
Photocatalytic Oxidation of Organic Pollutants Associated with Indoor Air Quality
Colorado: University of Denver, Dept. of Chemistry, 1998

Tang, W.Z.
Physicochemical treatment of hazardous wastes
Boca Raton (US): CRC Press, 2004

Tuhkanen, T.A.
UV/H_2O_2 processes
In: Advanced oxidation processes for water and wastewater treatment,
London: IWA publishing, 2004

Tullner, M.
Comparison of bioclogging effects in saturated porous media within one- and two-dimensional flow systems
In: Ecological Engineering. doi: 10.1016/j.ecoleng.2008.12.037.

Verstraeten, I.M. et al
Changes in concentrations of triazine and acetamide herbicides by bank filtration, ozonization and chlorination in a public water supply
In: Journal of Hydrology, Vol. 266, pp. 190-208, 2002

Vlaar, L. and Leendertse P.C.
Evaluatie "Zuiver Water in de Bommelerwaard" – Maatregelen
Utrecht: CLM, 2007

Visser, A. and Wal, E. van der
Evaluatie 'Zuiver Water in de Bommelerwaard' – Monitoring: Analyse en interpretatie monitoringsgegevens
Culemborg: WSRL, 2007

Vocht, A. de
Basishandboek SPSS
Utrecht: Bijleveld Press, 2000

Vos, M.
Principles of NPOC (Non-Purgeable Organic Carbon) Analysis, HWL, 2009

Wadley, S. and Waite, T.D.
Fenton processes
In: Advanced Oxidation Processes for Water and Wastewater Treatment
London: IWA, 2004

Wink, D. A et al
Kinetic Investigation of Intermediates Formed during the Fenton Reagent Mediated Degradation of N-Nitrosodimethylamine: Evidence for an Oxidative Pathway Not Involving Hydroxyl Radical
In: Chem. Res. Toxicol. Issue 4, p 510-512, 1991

Yuan, F., Hu, C., Hu, X., Qu, J. and Yang, M.
Degradation of selected pharmaceuticals in aquaeous solution with UV and UV/H_2O
In: Water Research, volume 43 issue 6, p 1766-1774, 2009

ANNEX A: Applied UV dosages

The UV dosage in a UV reactor can be determined by multiplication of the UV intensity (mW/cm^2) and the residence time T (s) in the reactor:

$$UV\ dose_{LP} = Intensity\ (mW/cm^2) * Time\ (s) \qquad (mJ/cm^2)$$

The UV intensity is strongly dependent on the UV absorbance of the solution and hydraulic processes, reflection, refraction in the reactor. Both the LP and MP reactor are equipped with a sensor that measures the intensity at 254nm. For the LP the intensity is expressed in W/m^2 and the UV intensity of the MP is expressed as a percentage. The residence time T in the LP reactor can be estimated with the inner dimensions of the reactor (L = 1.325m, D = 0.215m) and the applied flow (5 m^3/hr):

$$T = \frac{L}{v} = \frac{L}{Q/A} = \frac{1{,}325\ (m)}{0{,}0014\ (\frac{m^3}{s}) \Big/ \frac{1}{4}\ \pi\ 0{,}215^2\ (m^2)} = 34.6\ s$$

At every performed experiment, the observed UV intensity was recorded and the average values can be found in figure A.1 below. From those average UV intensity values, the average UV dosages (mJ/cm^2) were determined. According to the supplier (ITT Wedeco), the average UV dose of the LP reactor at a UV ballast is approximately 1000 mJ/cm^2, which corresponds with the determined values. It must be noted that the difference in UV dose between 80 and 60% ballast (370 mJ/cm^2) is much larger then between 100 and 80% ballast (140 mJ/cm^2).

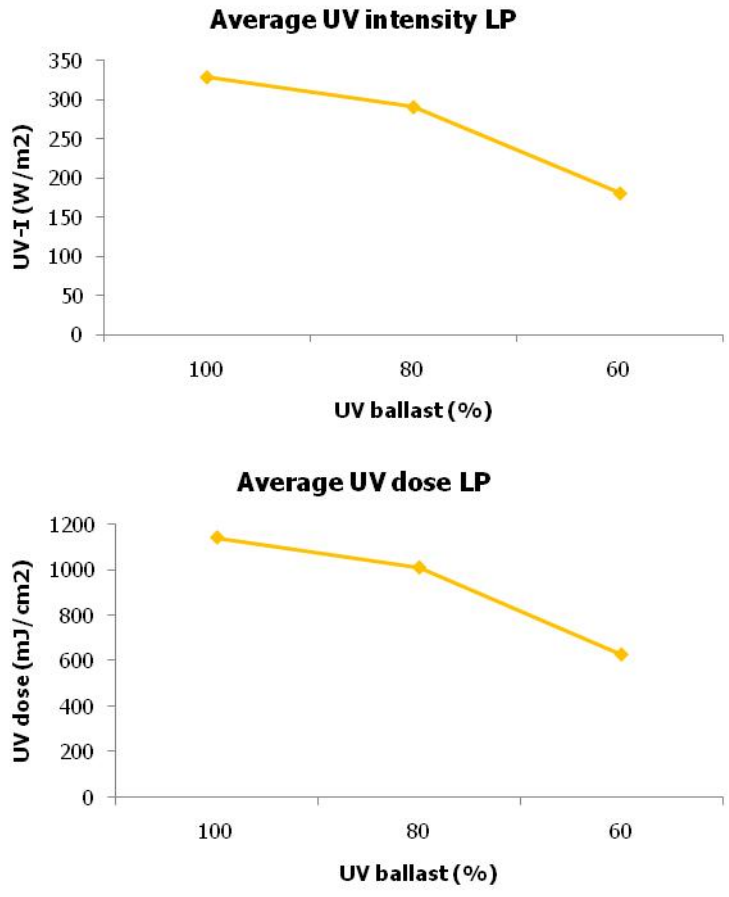

Figure A.1: UV intensity and dose (LP reactor)

The MP reactor reports the UV signal as a percentage. According to the supplier (Berson), the UV dose is 35-40 mJ/cm^2 (depending on the UVT of the water) for a design flow of 50 m^3/hr. The applied flow during the experiments is a factor 10 lower, hence the residence time, and thus the UV dose should approximately be 10 times higher (850 mJ/cm^2). The lamps are designed to emit 125% of the design dose at the end of life time. Furthermore, the design dose of 35-40 mJ/cm^2 is emitted at the minimum reactor ballast power to allow for higher doses when demanded. The relationship between UV ballast and UV dose is a linear one according to the supplier. The determined average of the measured UV intensities (%) confirm this assumption.
At 100% ballast power, the average UV intensity is 212% and at 60% UV ballast power the average UV intensity was calculated to be 95%. An UV dose of 850 mJ/cm^2 should more or less correspond to a measured UV intensity of 100%. Assuming the linearity between UV ballast, dose and intensity, the UV dosages were estimated as followed:

$$UV\ dose_{MP} = \frac{UVI_x\ \%}{100\ \%} * 400\ \ (mJ/cm^2)$$

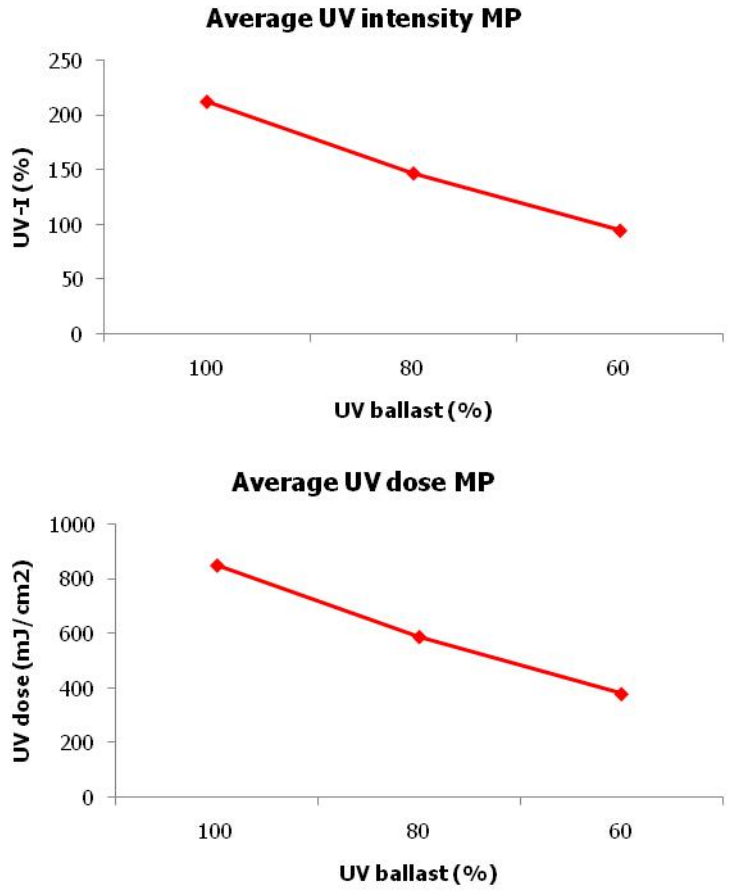

Figure A.2: UV intensity and dose (MP reactor)

ANNEX B: Water matrix influent

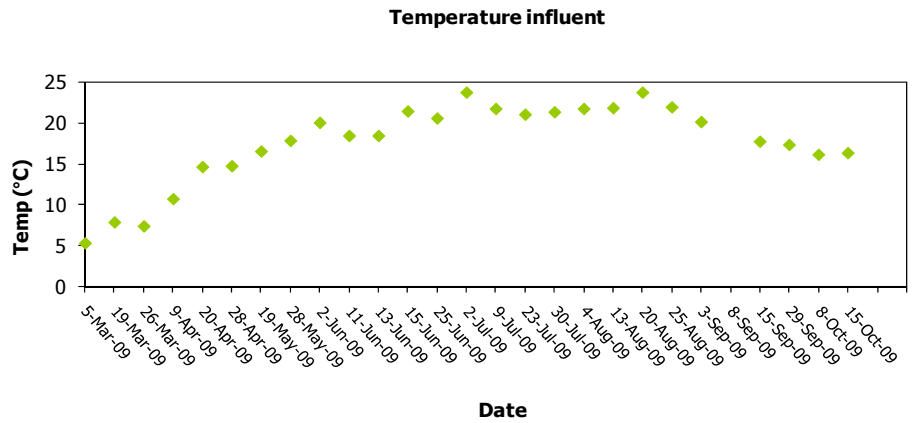

Figure B.1: Measured temperature of influent water

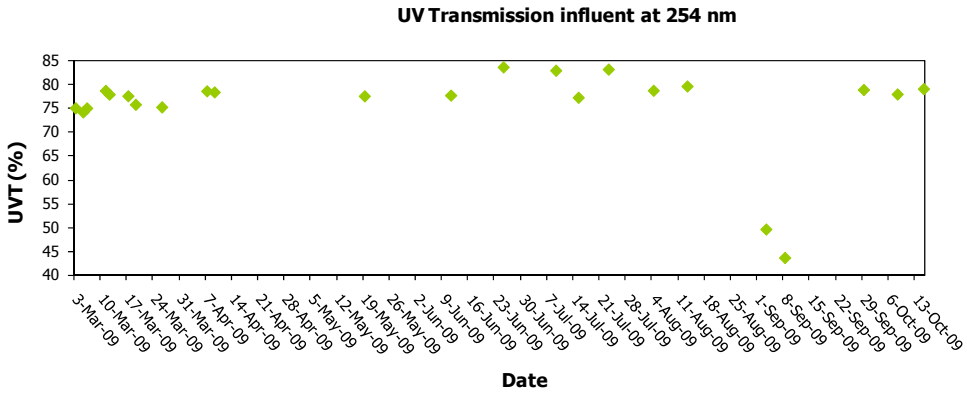

Figure C.2: Measured UVT (at 245 nm) influent

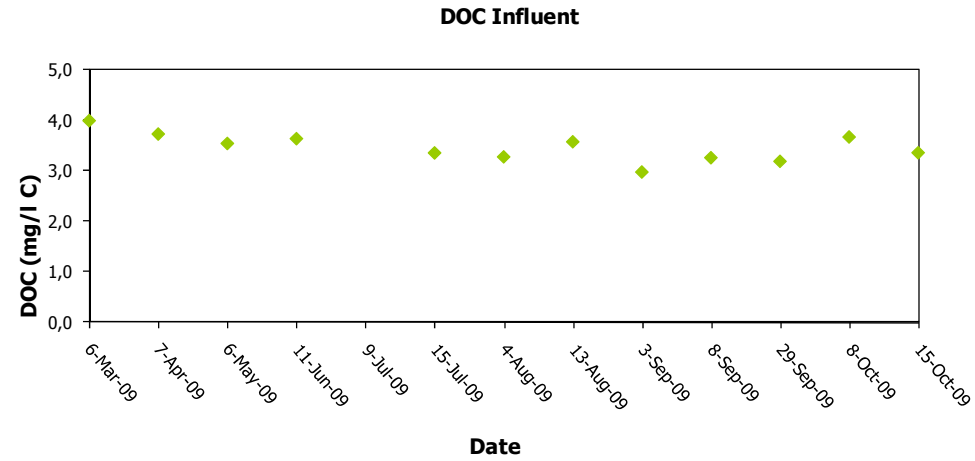

Figure B.3: Measured DOC concentrations influent

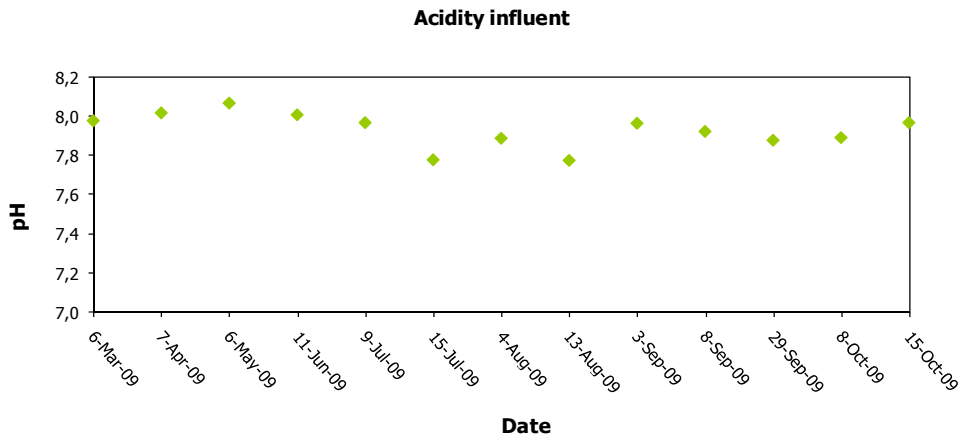

Figure C.4: Measured pH influent

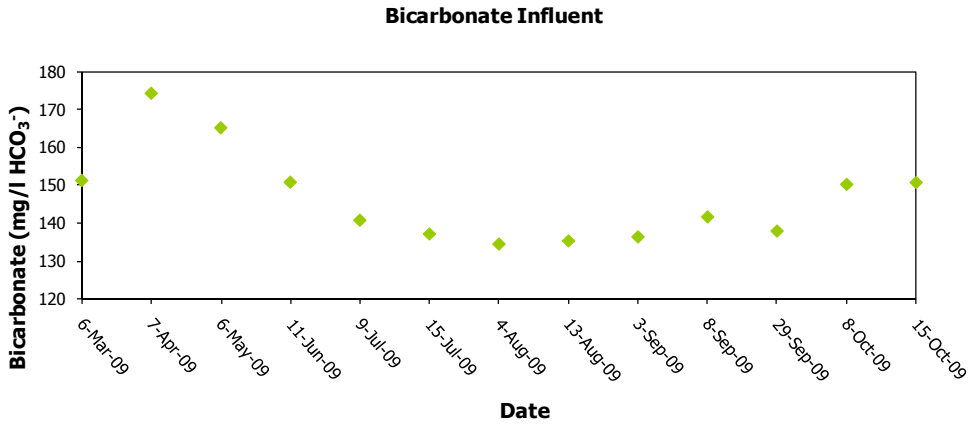

Figure B.5: Measured concentration bicarbonate influent

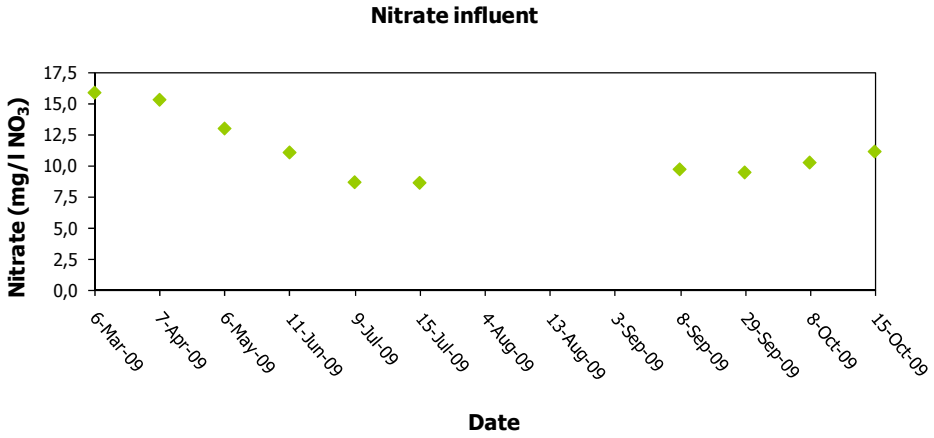

Figure C.6: Measured concentrations nitrate influent

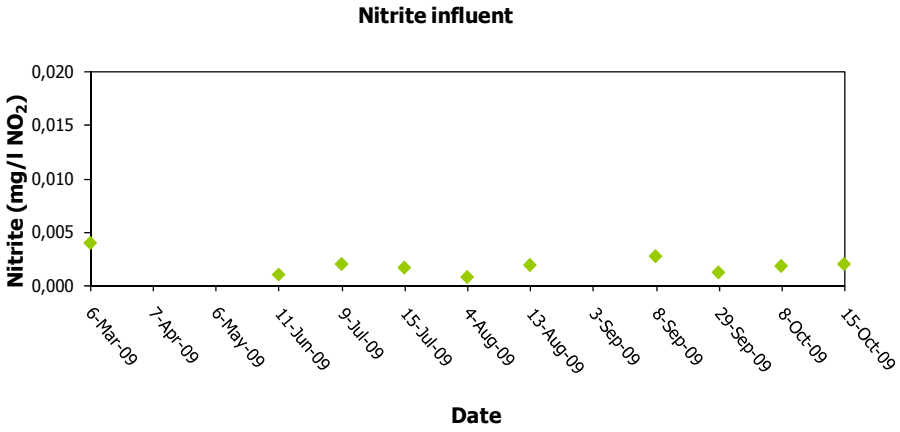

Figure B.7: Measured concentrations nitrite influent (detection limit = 0.007 mg/L)

ANNEX C: Measuring data UPLC

Table C.1: data UPLC

					UV intensity		Influent (µg/L)				Effluent LP (µg/L)				Effluent MP (µg/L)			
date	type	temp	UV	H2O2	LP (W/cm^2)	MP (%)	ATZ	BRO	IBU	NDMA	ATZ	BRO	IBU	NDMA	ATZ	BRO	IBU	NDMA
05-03-2009	100/10		100	10	242	297	10.76	11.26	15.31	10.95	3.89	4.07	7.02	1.78	3.14	4.14	7.19	0.00
05-03-2009	100/5		100	5							5.16	6.66	10.46	0.00	3.65	5.73	7.69	0.00
05-03-2009	100/0		100	0			10.68	11.42	14.73	10.93	6.89	10.88	13.17	1.27	4.42	8.44	10.82	0.50
05-03-2009	80/10		80	10	205	243	12.18	11.49	9.91	9.51	4.52	5.07	8.08	2.90	4.07	5.20	8.02	2.70
05-03-2009	80/5		80	5							5.67	6.97	10.66	0.00	4.60	6.64	9.17	0.00
05-03-2009	80/0	5,27	80	0			10.48	11.63	15.44	11.39	6.84	10.22	14.35	1.42	5.53	8.92	11.51	2.20
05-03-2009	60/10	5,27	60	10			10.68	11.44	14.47	10.69	6.25	6.75	9.38	4.84	5.64	6.46	8.60	4.93
05-03-2009	60/0		60	0	131	135	10.62	11.71	14.10	11.04	7.82	10.27	13.34	4.14	6.77	9.77	11.76	1.30
07-04-2009	100/10		100	10			9.91	12.51	14.42	11.08	3.16	4.12	5.06	1.04	2.48	3.80	7.73	1.24
07-04-2009	100/5		100	5			9.39	12.26	13.69	11.04	4.41	6.64	7.44	1.21	3.00	5.85	8.00	1.81
07-04-2009	100/0		100	0			9.62	12.58	13.45	11.06	5.62	11.73	12.15	1.24	3.77	8.70	10.83	2.04
07-04-2009	60/10		60	10			9.71	12.37	13.66	10.78	5.73	7.23	7.57	3.62	4.64	6.11	9.30	3.91
07-04-2009	60/5		60	5				12.68	13.45	10.73	6.44	9.42	9.59	4.03	5.05	7.42	9.79	3.84
07-04-2009	60/0		60	0			9.36	12.71	15.07	10.74	7.61	12.63	12.56	4.01	5.42	9.22	12.22	4.30
20-04-2009	100/10	14,60	100	10	327	251	9.74	10.63	12.44	10.78	3.18	3.49	4.34	1.08	2.61	3.37	4.10	1.52
20-04-2009	100/5	14,60	100	5	327	251	9.89	10.85	10.13	10.86	4.28	5.78	5.79	1.35	3.17	4.99	5.27	1.79
20-04-2009	80/10	14,60	80	10			9.93	10.46	11.62	10.70	3.91	4.11	5.22	1.73	3.53	4.38	5.93	2.40
20-04-2009	80/5	14,60	80	5			9.77	10.87	11.96	10.74	4.99	6.27	7.30	1.69	4.40	5.94	7.06	2.57
20-04-2009	60/10	14,60	60	10	164	111	9.52	10.46	10.86	10.39	6.15	7.36	8.25	3.75	4.89	5.56	7.21	3.92
20-04-2009	60/0	14,60	60	0	164	111	9.63	11.00	11.49	10.81	5.67	6.07	5.96	3.64	5.48	6.99	7.09	4.01
28-04-2009	100/10	14,70	100	10	335	261	9.32	8.22	16.21	10.82	3.12	2.47	0.00	0.86	2.51	2.60	6.21	1.31
28-04-2009	100/5		100	5	335	261	6.45	6.87	11.73	6.57	4.10	4.20	7.66	0.00	3.05	3.48	6.35	0.00
28-04-2009	100/0		100	0	335	261	9.55	9.55	14.28	11.01	5.59	8.11	13.76	1.12	3.85	6.10	10.08	0.00
28-04-2009	60/10		60	10	174	117	9.67	9.63	17.76	9.99	5.28	4.80	8.49	3.24	4.99	4.84	9.68	3.69
28-04-2009	60/5		60	5	174	117	9.41	9.63	16.73	8.13	6.14	6.06	10.31	0.20	5.57	6.38	9.49	2.03
28-04-2009	60/0	15,00	60	0	174	117	9.45	9.29	14.93	11.60	7.23	7.80	15.27	3.63	5.78	7.70	13.28	2.77
06-05-2009	100/10		100	10			10.28	10.60	13.76	10.54	3.01	2.68	2.99	0.85	2.42	2.69	2.65	1.40
06-05-2009	100/5		100	5			10.34	10.59	15.02	10.52	4.29	5.28	5.06	1.03	3.12	4.17	5.77	1.47
06-05-2009	100/0		100	0			9.61	10.85	15.21	10.27	5.91	10.19	11.40	0.96	3.71	6.37	8.25	1.58
06-05-2009	60/10		60	10			10.12	9.82	14.39	10.80	5.17	4.76	4.70	3.40	4.88	5.43	6.24	3.57
06-05-2009	60/5		60	5			10.17	10.96	15.97	10.39	6.36	6.65	7.33	3.06	5.35	6.32	7.34	3.70
06-05-2009	60/0		60	0			9.84	10.19	14.22	10.80	7.07	9.66	12.93	3.37	6.04	7.72	11.09	4.10
19-5-2009	100/10		100	10	350	246	10.27	9.35	16.49	12.02	2.73	2.03	2.79	0.74	2.47	2.95	2.84	1.07
19-5-2009	100/5	16,50	100	5			10.02	8.76	17.21	11.91	3.91	4.20	5.75	0.00	3.06	4.58	4.96	0.00
19-5-2009	100/0		100	0			10.03	9.05	16.36	12.87	5.88	9.06	13.59	1.11	3.81	7.31	9.27	0.00
19-5-2009	80/10		80	10			9.58	8.85	15.11	11.60	3.37	2.84	2.88	0.79	3.39	3.71	3.16	1.86
19-5-2009	80/5		80	5			10.16	9.06	15.93	11.90	4.52	5.07	6.86	1.01	4.15	5.11	6.52	0.00
19-5-2009	80/0		80	0	309		9.67	8.82	13.69	12.55	6.43	9.32	15.01	1.25	4.81	7.64	10.39	1.99
19-5-2009	60/10		60	10	180		9.77	8.56	16.30	12.14	5.25	4.91	5.99	2.12	4.80	5.07	5.71	2.65
19-5-2009	60/5		60	5			9.93	8.40	16.34	12.59	6.05	6.59	8.41	2.05	5.34	6.21	7.00	1.03
19-5-2009	60/0		60	0			9.88	8.91	15.69	10.86	7.49	9.91	16.08	2.23	6.14	8.44	11.64	2.14
2-6-2009	100/10		100	10			9.81	9.91	18.61	10.64	2.56	2.44	1.94	0.72	2.19	2.99	2.32	0.86
2-6-2009	100/5		100	5			9.75	10.10	17.86	11.22	3.61	4.69	4.11	0.60	2.85	4.77	5.69	0.81
2-6-2009	100/0	19,90	100	0	343	234	9.78	10.05	18.77	10.60	5.45	9.81	17.38	0.53	3.61	7.70	9.08	1.04
2-6-2009	80/10		80	10			9.79	10.70	18.37	9.53	2.86	2.79	2.88	0.73	3.26	3.97	4.86	1.51
2-6-2009	80/5		80	5			9.83	9.97	18.84	10.99	4.14	5.07	4.70	1.40	3.77	5.71	6.74	2.23
2-6-2009	80/0	20,00	80	0	318	164	9.64	9.99	18.05	10.89	2.97	2.78	2.10	0.68	3.36	4.15	4.19	1.55
2-6-2009	60/10		60	10			9.92	10.66	21.88	8.81	4.68	4.75	6.63	1.41	4.39	5.24	6.11	3.00
2-6-2009	60/5		60	5	195		9.98	10.56	20.13	9.34	5.66	6.76	8.93	1.71	5.05	6.68	10.40	3.29
2-6-2009	60/0	20,00	60	0	195	105	9.83	10.55	18.86	9.50	7.17	10.33	19.47	1.77	5.84	8.77	11.64	3.47
11-6-2009	100/10	19,50	100	10	335	225	9.87	9.57	17.42	11.44	3.75	4.51	5.19	0.31	2.96	4.69	5.04	0.42
11-6-2009	100/5		100	5			9.99	9.59	18.12	11.32	2.71	2.23	2.58	0.79	2.43	2.91	3.04	1.23
11-6-2009	100/0		100	0			9.90	9.51	17.06	11.78	2.52	2.42	2.03	0.65	2.22	2.95	2.44	0.82
11-6-2009	80/10		80	10	179	79	9.71	9.47	17.78	10.11	3.13	2.82	2.95	0.81	3.30	3.88	4.04	1.57
11-6-2009	80/5		80	5			10.00	9.55	17.64	11.46	4.29	5.09	6.18	1.13	3.95	5.44	6.00	1.06
11-6-2009	80/0	18,30	80	0	292	154	9.66	9.45	17.04	11.66	2.96	2.83	2.22	0.75	3.30	4.10	4.03	1.60
11-6-2009	60/10	18,40	60	10			9.76	9.57	17.29	10.73	5.27	4.92	6.04	2.25	4.79	5.01	6.02	2.80
11-6-2009	60/5		60	5			9.91	9.58	17.45	11.34	5.82	6.73	8.42	1.97	5.18	6.53	8.46	2.22
11-6-2009	60/0		60	0			9.89	9.79	17.68	9.81	4.62	4.83	6.13	1.37	4.36	4.84	5.98	3.24
23-6-2009	100/10		100	10			9.14	8.35	20.28	12.50	2.54	3.20	3.76	1.52	2.77	2.42	3.08	1.29
23-6-2009	100/5		100	5			9.32	8.68	20.52	12.00	3.97	5.27	6.20	1.11	3.04	4.33	5.95	1.90
23-6-2009	100/0		100	0			9.00	8.70	20.12	11.58	5.77	11.07	18.29	1.10	3.93	7.18	12.24	2.38
23-6-2009	80/10		80	10			9.19	9.17	19.81	12.43	3.38	3.40	3.88	1.21	3.49	3.90	5.12	2.53
23-6-2009	80/5		80	5			9.22	8.80	20.28	12.02	4.52	5.95	7.97	1.29	4.06	5.31	8.04	2.78
23-6-2009	80/0		80	0			9.13	9.01	19.96	12.31	6.26	10.99	18.64	1.35	4.79	7.53	12.68	2.81
23-6-2009	60/10		60	10			9.38	9.31	20.66	11.54	5.18	5.46	7.24	2.43	4.87	5.18	7.88	3.99
23-6-2009	60/5		60	5			9.30	9.53	19.57	11.38	6.17	7.78	10.69	2.29	5.14	5.73	10.37	4.75
23-6-2009	60/0		60	0			9.29	9.65	20.02	12.16	7.62	11.64	18.90	2.36	5.01	5.45	9.12	4.37
25-6-2009	100/10	20,40	100	10	345	215	9.56	10.26	15.35	13.16	2.56	2.37	1.84	0.68	2.23	2.70	2.39	1.46
25-6-2009	100/0		100	0			9.62	10.23	16.25	13.65	5.40	9.64	14.55	0.69	3.55	7.09	9.12	1.71
25-6-2009	80/10		80	10	314	150	9.47	10.05	15.20	13.82	3.00	2.70	2.79	1.19	3.23	3.77	3.94	2.33
25-6-2009	80/0		80	0			9.36	10.06	15.33	13.52	5.99	9.64	14.15	0.73	4.52	7.59	9.58	3.26
25-6-2009	60/10		60	10	196	96	9.57	10.10	16.10	13.22	4.68	4.47	5.02	3.10	4.59	4.95	5.68	4.49
25-6-2009	60/0		60	0			9.57	10.12	16.55	13.17	7.54	10.17	15.27	2.91	5.83	8.11	10.60	4.29
9-7-2009	100/10		100	10	332	207	10.00	10.66	16.74	12.33	2.71	2.42	2.18	1.61	2.21	2.70	2.74	1.94
9-7-2009	100/5		100	5			10.00	10.60	18.20	12.53	3.62	4.49	4.44	1.53	2.76	4.24	4.21	2.07
9-7-2009	100/0		100	0			9.87	10.62	16.88	12.19	5.44	9.76	15.76	1.42	3.48	7.08	8.77	2.21

9-7-2009	80/10		80	10	314	147	9.84	10.59	17.83	11.98	3.00	2.79	2.59	1.78	3.08	3.56	3.65	2.93
9-7-2009	80/5		80	5			10.54	10.26	14.26	15.17	4.06	4.94	5.32	1.76	3.66	5.15	5.34	2.55
9-7-2009	80/0		80	0	306		9.85	10.83	16.82	12.23	5.83	9.91	15.14	1.86	4.50	7.75	10.10	3.37
9-7-2009	60/10		60	10	195	96	9.72	10.59	16.42	11.84	4.75	4.57	4.35	3.19	4.43	5.01	5.05	4.40
9-7-2009	60/5		60	5			9.85	10.59	16.16	12.18	5.61	6.45	8.21	3.15	4.99	6.27	7.80	4.29
9-7-2009	60/0		60	0			9.69	10.39	17.74	12.70	7.12	10.21	16.37	3.36	5.71	8.19	11.28	4.72
15-7-2009	100/10	21,40	100	10	334	200	10.19	10.89	15.16	11.37	2.30	2.33	2.75	1.14	2.05	2.66	3.92	1.28
15-7-2009	100/5		100	5			10.46	11.21	18.85	11.82	3.42	4.43	4.66	0.87	2.81	4.54	4.41	1.39
15-7-2009	100/0		100	0			11.04	11.41	17.35	11.64	6.25	10.39	14.55	0.78	3.77	7.90	9.72	1.58
15-7-2009	80/10		80	10		130	8.52	9.82	15.53	11.74	2.78	2.66	3.03	0.78	3.04	3.65	4.26	2.93
15-7-2009	80/5		80	5	315		9.70	10.54	13.01	11.02	3.97	5.06	6.20	0.99	3.84	5.51	5.28	1.92
15-7-2009	80/0		80	0	308		10.79	11.27	16.62	11.32	6.70	10.81	16.98	0.67	5.01	8.38	12.07	1.93
15-7-2009	60/10		60	10		91	8.19	9.46	10.07	10.99	4.00	4.34	5.26	2.02	3.68	4.47	5.97	3.56
15-7-2009	60/5		60	5			8.82	10.12	12.84	10.62	5.54	6.60	9.56	2.53	5.02	6.54	8.62	3.16
15-7-2009	60/0		60	0			11.71	11.81	18.55	11.15	8.16	11.08	16.61	2.74	6.50	9.13	12.16	3.52
23-7-2009	100/10	21,00	100	10	340	198	10.01	10.77	14.45	11.15	2.04	2.17	2.34	1.27	2.12	2.80	2.81	1.48
23-7-2009	100/5		100	5			9.97	11.25	14.36	11.21	3.75	4.98	5.84	0.99	3.88	7.85	8.12	1.71
23-7-2009	100/0		100	0			11.04	11.94	15.57	11.68	5.92	10.73	12.65	0.96	2.88	4.62	5.00	1.58
23-7-2009	80/10		80	10	310	138	11.89	11.85	14.17	11.38	6.64	10.75	15.25	1.37	5.18	8.47	9.58	2.55
23-7-2009	80/5		80	5			7.79	9.77	12.52	10.99	2.58	2.71	3.40	1.14	2.75	3.66	3.75	2.22
23-7-2009	80/0		80	0			10.20	11.15	14.92	10.50	3.92	5.09	6.08	1.26	4.05	5.71	5.19	2.16
23-7-2009	60/10		60	10	191	91	9.22	10.76	15.18	10.98	4.31	4.57	4.41	2.69	4.13	5.02	6.00	4.08
23-7-2009	60/5		60	5			10.01	11.04	15.68	11.09	6.13	7.09	7.95	3.37	5.29	6.80	6.93	3.67
23-7-2009	60/0		60	0			10.62	11.52	16.34	11.51	7.96	11.06	13.88	2.73	6.51	8.92	9.93	4.34
30-7-2009	100/10	21,30	100	10	345	199	10.07	13.30	11.37	10.17	2.30	2.91	2.63	0.84	2.18	3.64	2.47	0.96
30-7-2009	100/5		100	5			10.49	14.48	13.24	10.75	3.88	6.20	4.79	0.58	2.98	6.09	3.67	1.47
30-7-2009	100/0		100	0	335		11.65	15.19	14.79	10.96	6.30	13.34	12.80	0.60	3.60	7.52	8.06	1.08
30-7-2009	80/10		80	10	318	138	9.13	12.70	12.68	10.40	2.97	3.43	2.45	0.90	3.14	5.15	4.39	2.68
30-7-2009	80/5		80	5	311		10.66	13.58	15.22	10.04	4.39	6.87	4.32	0.56	3.74	7.06	4.76	2.38
30-7-2009	80/0		80	0			11.78	15.20	16.43	11.01	7.01	12.80	13.67	0.16	5.46	10.96	11.14	2.61
30-7-2009	60/10		60	10	198	91	9.42	13.57	12.76	11.09	4.67	6.08	4.32	1.67	4.48	6.37	4.19	3.85
30-7-2009	60/5		60	5			9.43	11.11	12.68	7.71	5.51	8.42	8.24	2.30	4.55	6.63	5.46	2.07
30-7-2009	60/0		60	0	195		11.91	13.08	14.26	6.05	8.97	11.38	15.72	0.59	6.58	9.36	9.11	1.18
4-8-2009	100/10	21,70	100	10			10.01	11.20	16.83	11.11	2.48	2.40	1.34	1.04	2.27	3.06	0.00	1.09
4-8-2009	100/5		100	5			10.08	11.05	15.01	11.64	3.89	4.94	3.98	1.01	2.85	4.82	4.48	1.62
4-8-2009	100/0		100	0			11.64	12.47	15.29	11.29	6.44	11.70	12.66	0.93	3.85	8.45	9.00	2.33
4-8-2009	80/10		80	10			8.81	9.49	13.39	11.57	3.18	3.16	1.37	1.52	3.28	4.24	4.91	2.77
4-8-2009	80/5		80	5			10.69	12.02	15.10	11.86	4.21	5.49	4.86	1.11	3.93	5.92	5.16	3.07
4-8-2009	80/0		80	0			11.24	12.41	16.70	11.57	6.61	11.38	15.97	1.08	4.81	8.70	8.85	2.96
4-8-2009	60/10		60	10			9.60	11.18	13.27	11.46	5.05	4.77	5.95	2.83				
4-8-2009	60/5		60	5			9.48	10.62	13.55	11.31	5.97	7.08	9.35	3.10	5.16	6.94	6.44	4.17
4-8-2009	60/0		60	0			11.08	12.11	20.64	10.60	8.29	11.90	21.96	2.66	6.44	9.64	11.56	4.82
13-8-2009	100/10	21,80	100	10	325	191	10.70	11.70	13.20	9.90	2.90	2.90	2.50	1.00	2.70	3.40	2.90	1.50
13-8-2009	100/5		100	5			10.90	11.90	13.60	10.10	4.30	5.40	4.90	1.10	3.40	5.10	4.00	1.40
13-8-2009	100/0		100	0			10.50	12.50	12.90	10.10	6.50	11.30	14.40	1.00	4.50	7.90	9.40	1.80
13-8-2009	80/10		80	10	195	133	11.00	12.00	12.10	9.90	3.50	3.40	2.10	1.30	4.00	4.40	3.10	2.30
13-8-2009	80/5		80	5			10.90	11.80	14.70	10.00	4.70	6.00	4.70	1.30	4.50	5.50	5.40	2.40
13-8-2009	80/0		80	0			11.10	12.20	11.10	10.20	7.10	11.20	13.40	1.20	5.60	8.80	10.50	2.70
13-8-2009	60/10		60	10			10.70	12.20	14.70	9.80	5.30	5.20	5.70	2.40	5.70	5.70	4.50	3.20
13-8-2009	60/5		60	5	186	91	10.70	11.60	12.20	9.90	6.70	7.50	6.80	2.80	6.50	7.40	9.80	3.30
13-8-2009	60/0		60	0			11.10	12.00	12.40	10.10	8.30	11.60	13.20	2.70	7.00	9.50	12.70	3.70
20-8-2009	100/10	23,70	100	10		189	11.03	11.52	17.61	11.45	3.00	2.93	3.06	1.00	2.60	3.21	3.60	1.53
20-8-2009	100/5		100	5	319		11.29	11.68	14.11	10.91	4.02	5.24	6.17	1.00	3.30	4.91	5.45	1.79
20-8-2009	100/0		100	0			10.87	11.47	15.02	10.52	6.22	10.69	14.88	0.86	4.01	7.73	10.09	1.94
20-8-2009	80/10		80	10			11.20	11.41	16.30	10.84	6.62	10.71	17.33	1.33	3.54	4.23	4.63	2.16
20-8-2009	80/5		80	5	311	132	10.99	11.38	16.78	11.14	3.31	3.15	0.00	0.90	4.26	5.91	5.58	2.47
20-8-2009	80/0		80	0			11.15	11.38	15.64	10.82	4.62	5.80	5.83	1.04	5.21	8.65	11.62	3.05
20-8-2009	60/10		60	10	206	87	11.02	11.47	19.10	10.66	5.00	4.92	5.27	2.24	5.03	5.47	7.21	3.56
20-8-2009	60/5		60	5			11.16	11.57	17.99	10.78	6.14	7.10	8.17	2.49	5.52	6.93	8.62	3.56
20-8-2009	60/0		60	0			10.70	11.36	17.66	10.95	7.85	10.78	17.33	2.37	6.29	9.14	14.10	4.24
26-8-2009	100/10		100	10	332	186	11.39	12.32	18.64	10.23	2.83	3.10	3.58	0.78	2.52	3.47	4.00	1.33
26-8-2009	100/5		100	5			10.62	12.31	15.77	10.56	4.11	5.80	5.82	0.85	3.11	5.18	5.04	1.27
26-8-2009	100/0		100	0			10.71	12.31	16.19	10.83	6.24	11.85	14.96	0.62	4.12	8.68	8.50	1.63
26-8-2009	80/10		80	10			11.30	13.50	14.88	11.60	3.11	3.35	3.05	1.13				
26-8-2009	80/5		80	5			10.43	12.00	17.37	10.31	4.52	6.17	6.91	0.89	4.18	6.19	5.59	2.28
26-8-2009	80/0		80	0	305	130	10.75	12.27	16.38	10.66	6.46	11.45	12.92	1.08	5.16	9.12	10.50	2.39
26-8-2009	60/10		60	10			11.37	13.02	14.35	10.69	7.62	11.74	16.84	2.49	6.34	9.71	11.98	4.00
26-8-2009	60/5		60	5	186	91	10.59	12.23	17.10	10.70	5.90	7.54	7.31	2.35	5.71	7.74	8.03	3.20
26-8-2009	60/0		60	0			10.85	12.40	15.54	10.43	8.58	12.13	14.40	2.55	6.34	10.12	10.85	3.58
3-9-2009	100/10	20,10	100	10			10.21	11.65	15.25	10.09	2.63	3.11	4.61	0.60	2.23	3.33	4.84	1.70
3-9-2009	100/5		100	5	347	198	10.02	11.93	19.12	9.58	3.76	5.58	8.08	0.64	2.67	4.96	6.45	1.65
3-9-2009	100/0		100	0			10.22	11.75	15.76	8.20	5.37	10.87	15.27	0.42	3.63	8.07	12.10	2.14
3-9-2009	80/10		80	10			10.39	11.86	21.67	9.01	3.01	3.20	4.67	1.30	3.26	4.19	6.54	2.39
3-9-2009	80/5		80	5			10.40	11.76	20.81	9.91	4.48	5.94	8.58	1.51	4.06	5.99	7.03	3.29
3-9-2009	80/0		80	0			10.88	12.10	20.00	9.10	6.33	11.03	18.57	0.83	4.87	8.75	12.74	2.70
3-9-2009	60/10		60	10			10.27	11.65	19.44	9.96	4.96	5.46	7.01	2.17	5.25	6.62	8.56	2.57
3-9-2009	60/5		60	5	181	87	10.07	11.62	15.80	10.51	6.06	7.47	10.38	2.63	5.91	8.60	9.53	3.08
3-9-2009	60/0		60	0			10.30	11.55	19.45	9.24	7.47	10.98	18.97	2.85	7.06	11.17	16.30	3.65
8-9-2009	100/10		100	10			11.49	11.62	17.90	11.08	3.16	3.20	4.43	1.44	2.80	3.60	4.01	1.55
8-9-2009	100/0		100	0			11.52	11.82	19.81	10.22	6.54	11.42	14.98	0.86	4.28	8.73	9.54	2.01
8-9-2009	80/10		80	10			11.08	11.62	19.79	11.03	3.50	3.58	5.25	1.52	3.82	4.85	5.34	2.52
8-9-2009	80/0		80	0			11.39	11.95	21.91	11.61	7.03	11.22	16.85	1.43	5.50	9.17	9.92	2.70
8-9-2009	60/10		60	10			11.20	11.38	19.78	11.40	5.81	6.16	7.37	3.05	5.16	6.10	6.67	3.87
8-9-2009	60/0		60	0			10.97	11.78	17.95	11.04	8.56	11.58	18.14	2.83	6.95	10.01	14.23	4.30
15-9-2009	100/10	17,70	100	10			11.23	14.44	15.48	10.30	3.15	3.63	3.21	1.14	2.78	4.02	3.84	1.92

15-9-2009	100/5		100	5	331	190	11.54	14.90	17.75	10.88	4.58	6.87	5.75	1.07	3.46	6.41	4.51	1.72
15-9-2009	100/0		100	0			11.02	15.27	15.17	11.21	6.50	13.29	15.47	1.06	4.39	9.80	10.64	2.25
15-9-2009	80/10		80	10	303	134	10.97	14.38	12.56	10.66	3.63	4.15	2.94	1.32	3.90	5.20	6.00	2.29
15-9-2009	80/5		80	5			11.27	14.32	13.95	10.53	4.99	7.23	6.56	1.17	4.52	7.46	7.04	2.62
15-9-2009	80/0		80	0			11.87	14.83	17.23	10.53	6.91	13.22	17.65	1.68	5.58	10.50	14.00	2.80
15-9-2009	60/10		60	10	165	89	10.66	13.91	20.19	10.34	5.86	7.08	7.53	2.97	5.41	6.69	7.37	3.74
15-9-2009	60/5		60	5			10.89	14.04	16.30	10.11	6.86	9.32	9.48	2.99	6.03	8.70	8.00	3.97
15-9-2009	60/0		60	0			11.00	14.27	19.87	10.45	8.42	13.49	17.43	2.90	6.73	11.26	11.58	4.27
29-9-2009	100/10	17,30	100	10	331	198	10.97	17.72	2.16	11.12	3.10	4.93	1.04	1.75	2.71	5.12	0.99	1.90
29-9-2009	100/5		100	5			11.24	17.94	1.93	10.76	4.33	8.31	1.22	1.20	3.47	7.98	1.17	2.03
29-9-2009	100/0		100	0			11.08	17.95	2.07	9.86	6.47	16.44	1.81	1.42	4.51	12.61	1.60	2.04
8-10-2009	100/10	16,10	100	10			10.39	11.89	2.92	9.46	3.36	3.87	2.21	1.43	2.82	3.72	2.26	1.86
8-10-2009	100/5		100	5			10.35	11.61	3.02	10.25	4.17	5.39	2.21	1.64	3.13	4.93	2.37	2.02
8-10-2009	100/0		100	0	316	197	9.98	11.27	3.07	9.82	6.06	9.82	2.93	1.38	4.03	7.37	2.65	3.05
8-10-2009	80/10		80	10	277	141	9.65	10.67	2.94	9.28	3.82	3.95	2.35	1.48	3.61	4.24	2.24	2.63
8-10-2009	80/5		80	5			9.69	11.11	3.05	9.59	4.66	5.91	2.45	2.01	4.18	5.67	2.54	3.11
8-10-2009	80/0		80	0			9.36	10.46	3.08	8.91	6.38	9.71	3.03	1.89	5.05	7.55	2.89	2.85
8-10-2009	60/10		60	10	147	94	10.04	10.66	2.95	9.01	5.74	6.00	2.45	3.85	4.95	5.29	2.57	4.46
8-10-2009	60/5		60	5			9.40	10.23	2.91	9.25	6.43	7.57	2.82	4.42	5.61	6.54	2.56	4.06
8-10-2009	60/0		60	0			9.47	10.49	3.28	9.64	7.76	9.76	3.09	4.52	6.19	8.22	2.58	4.15
15-10-2009	100/10	16,30	100	10			10.72	11.76	2.25	10.86	3.19	3.35	0.90	1.59	2.89	3.82	1.10	2.03
15-10-2009	100/5		100	5	323	202	10.76	11.85	2.26	11.47	4.44	5.97	1.32	1.41	3.47	5.52	1.03	1.70
15-10-2009	100/0		100	0			10.57	11.73	2.21	11.11	6.58	11.30	2.09	1.84	4.43	8.71	1.61	2.60
15-10-2009	80/10		80	10	266	144	10.77	11.87	2.18	11.30	4.12	4.54	1.07	2.09	3.94	4.88	1.20	2.86
15-10-2009	80/0		80	0			10.27	11.51	2.21	10.89	7.25	11.10	1.94	2.19	5.49	9.14	1.55	3.49
15-10-2009	60/10		60	10			10.63	11.54	2.18	11.01	6.37	6.90	1.27	4.33	5.36	6.18	1.31	3.81

ANNEX D: Graphs degradation

In this annex the determined degradation for atrazine, bromacil, ibuprofen and NDMA by the LP and the MP reactor are depicted for all experimental settings are depicted. In parenthesis of the title the settings are depicted: 100/10 for instance, refers to a setting with 100% ballast power of the reactor and a dose of 10 ppm H_2O_2.

Figure D.1: Atrazine degradation, full ballast power

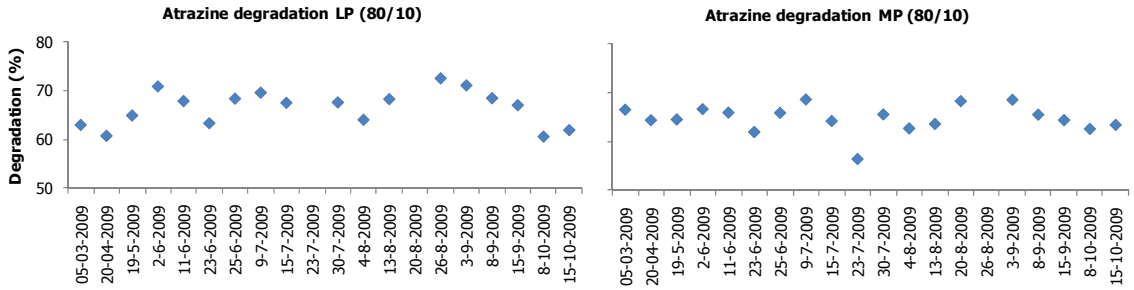

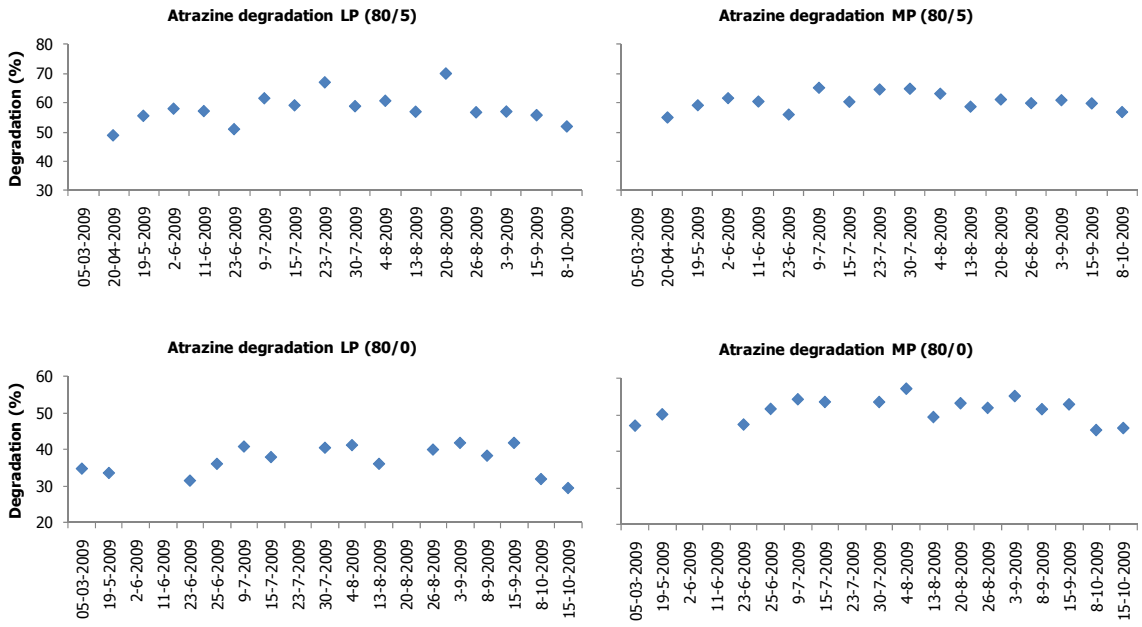

Figure D.2: Atrazine degradation, 80% ballast power

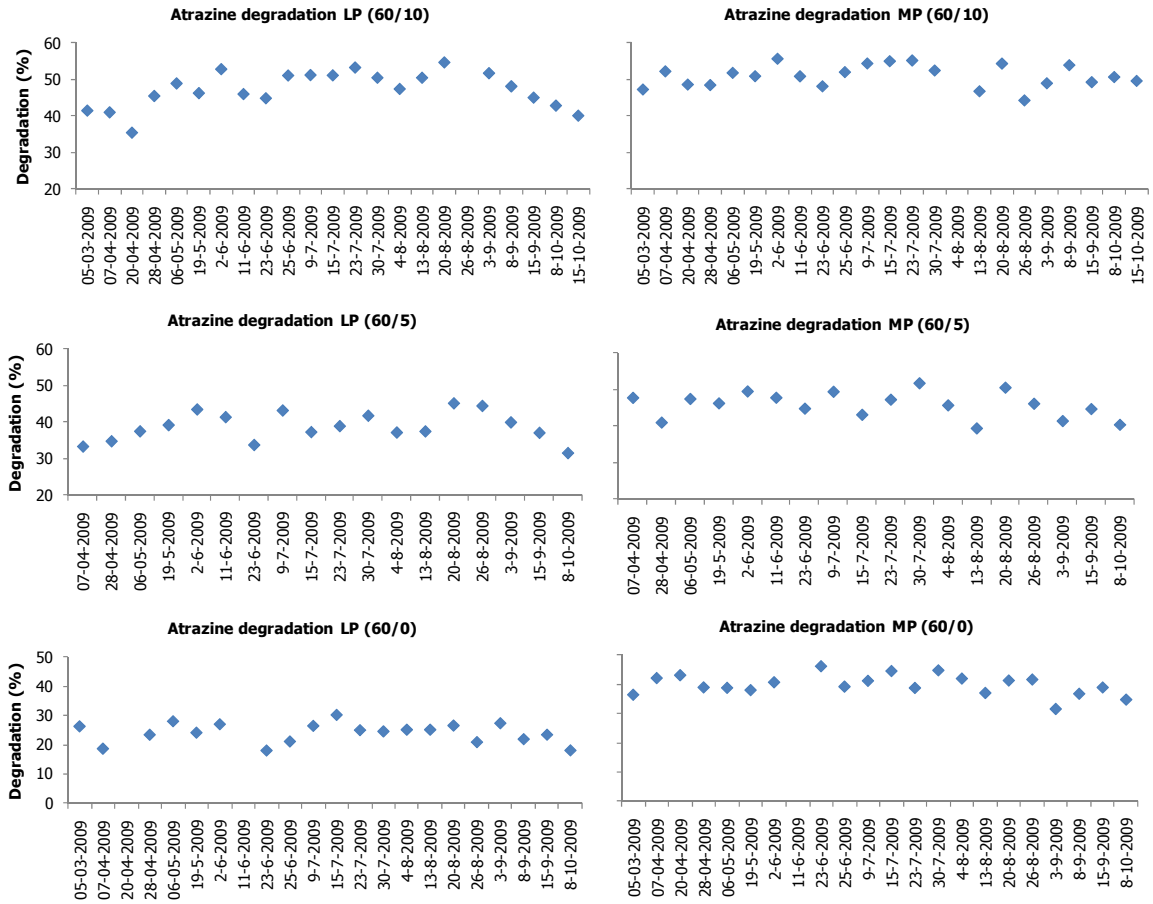

Figure D.3: Atrazine degradation, 60% ballast power

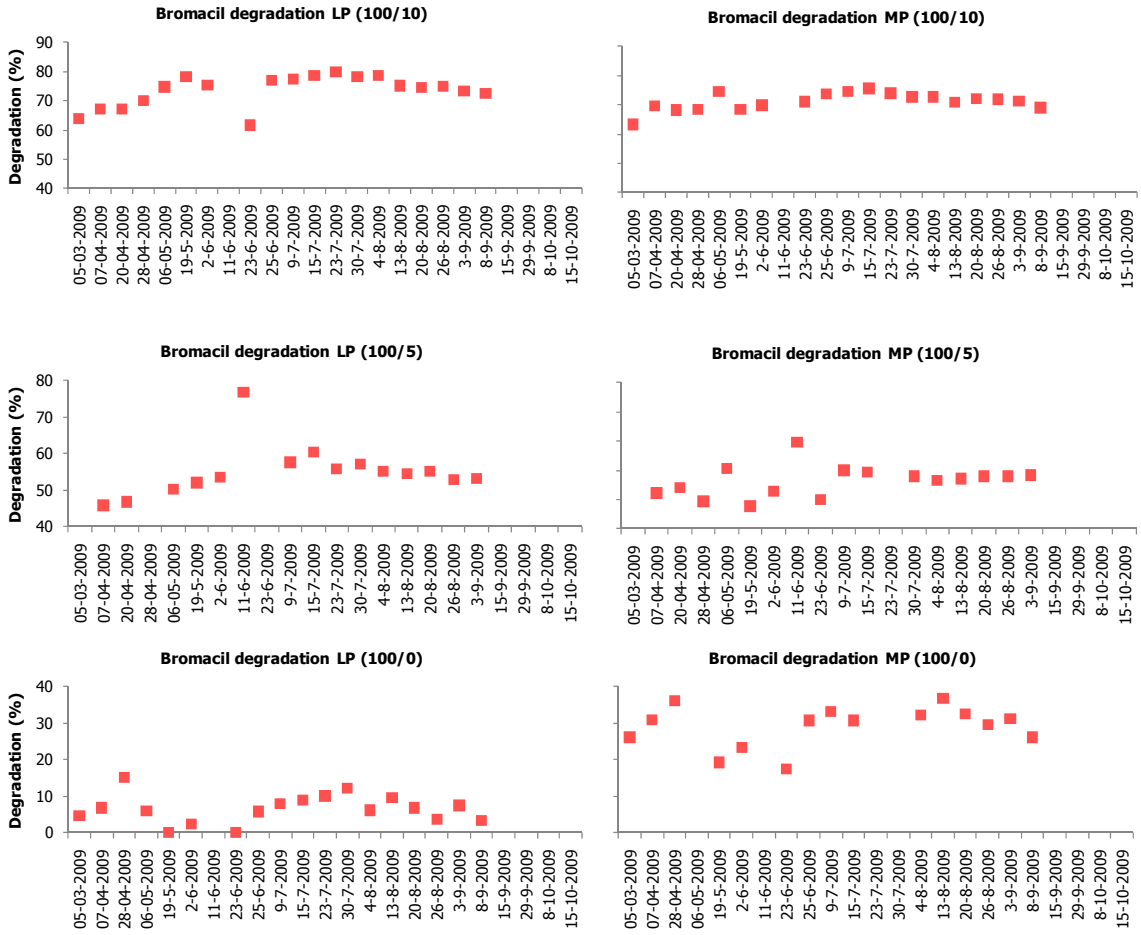

Figure D.4: Bromacil degradation, full ballast power

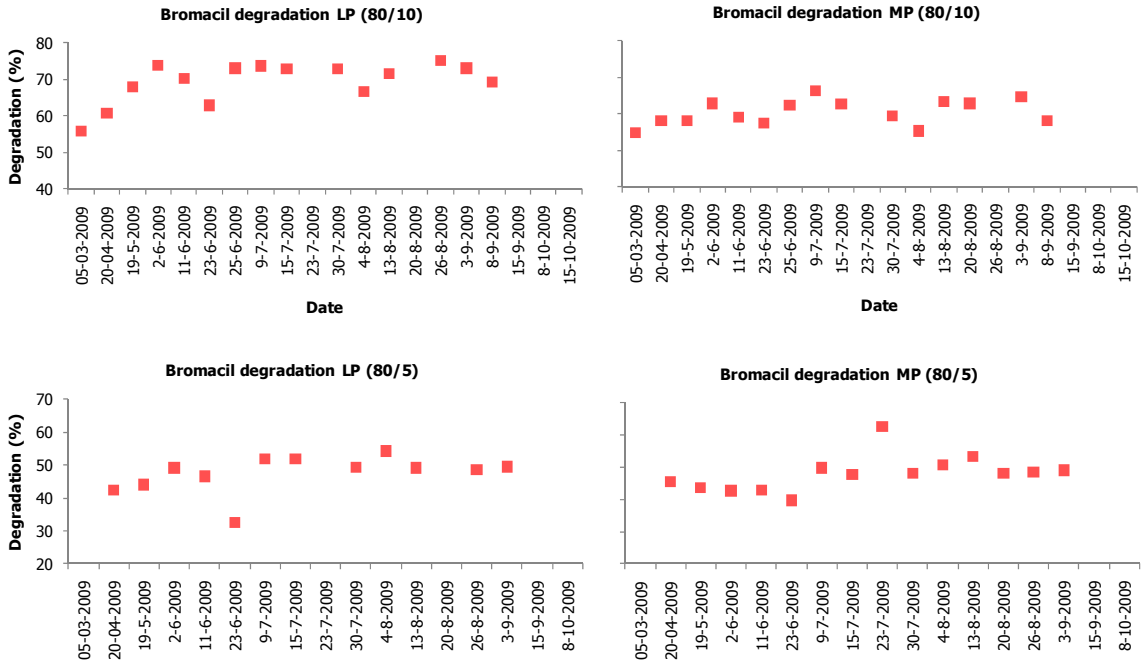

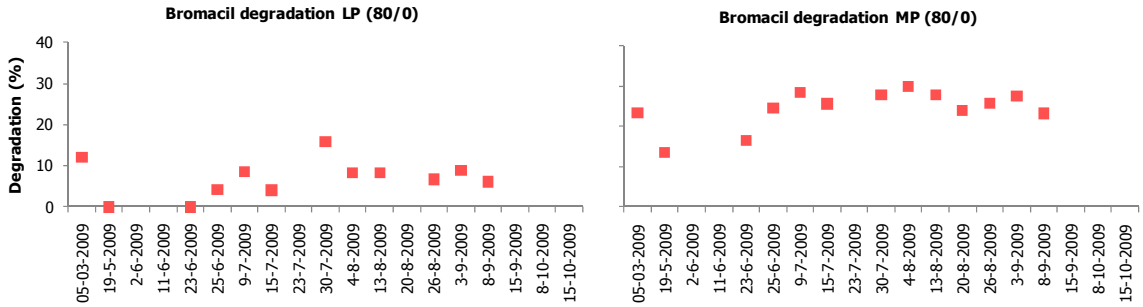

Figure D.5: Bromacil degradation, 80% ballast power

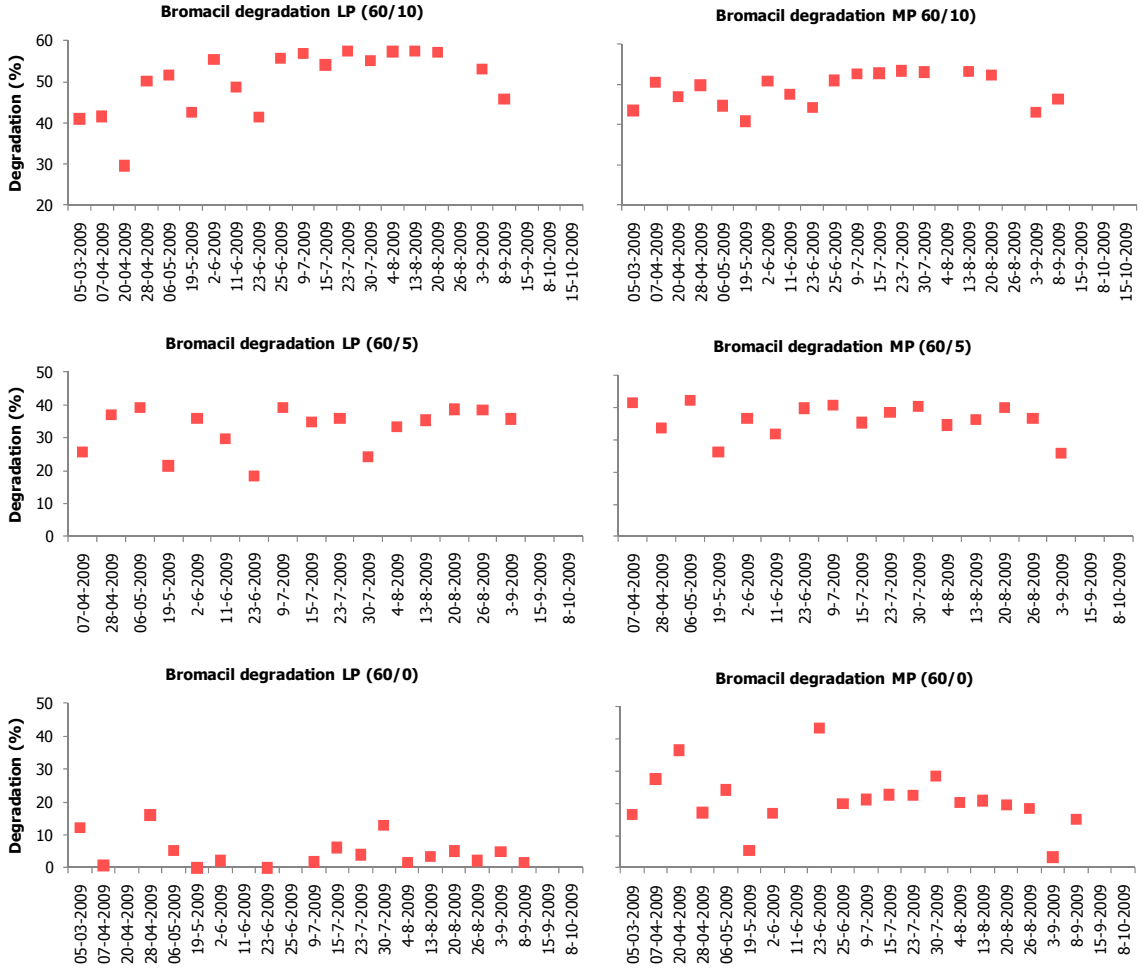

Figure D.6: Bromacil degradation, 60% ballast power

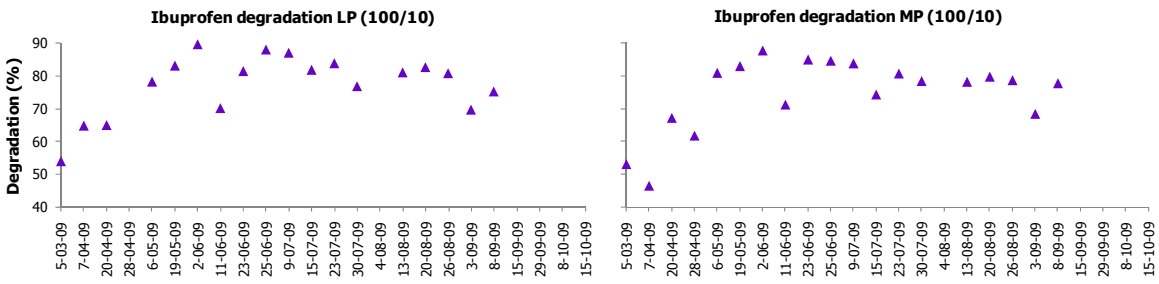

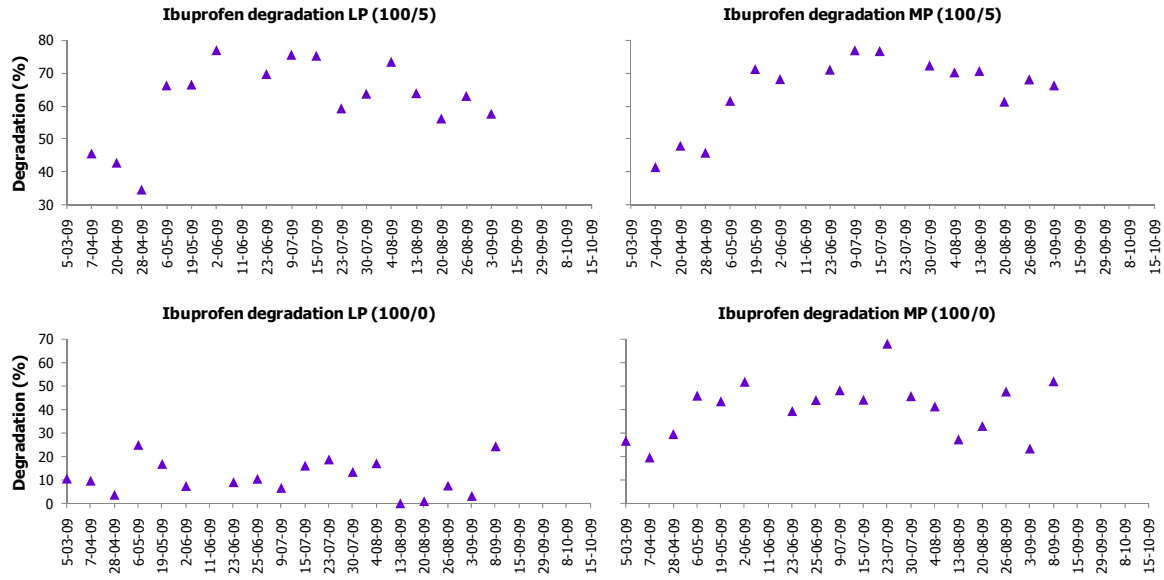

Figure D.7: Ibuprofen degradation, full ballast power

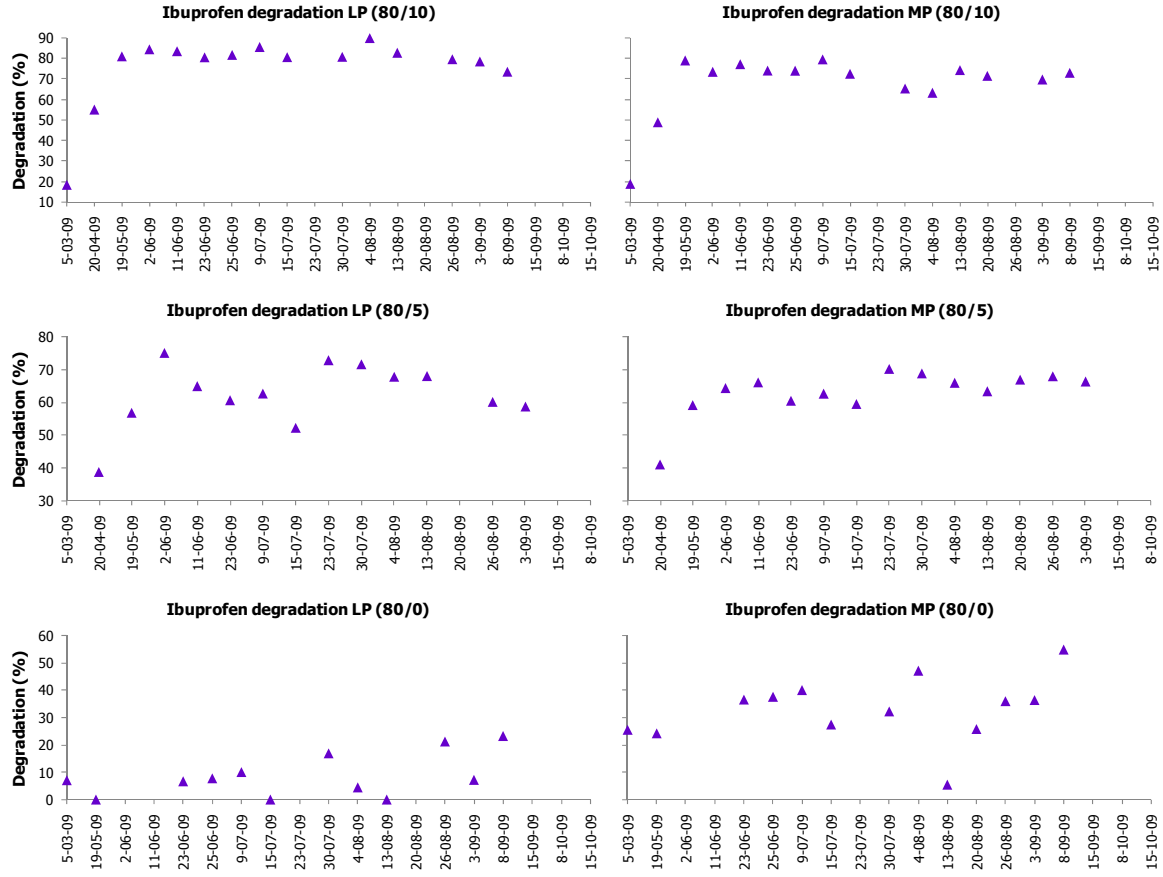

Figure D.8: Ibuprofen degradation, 80% ballast power

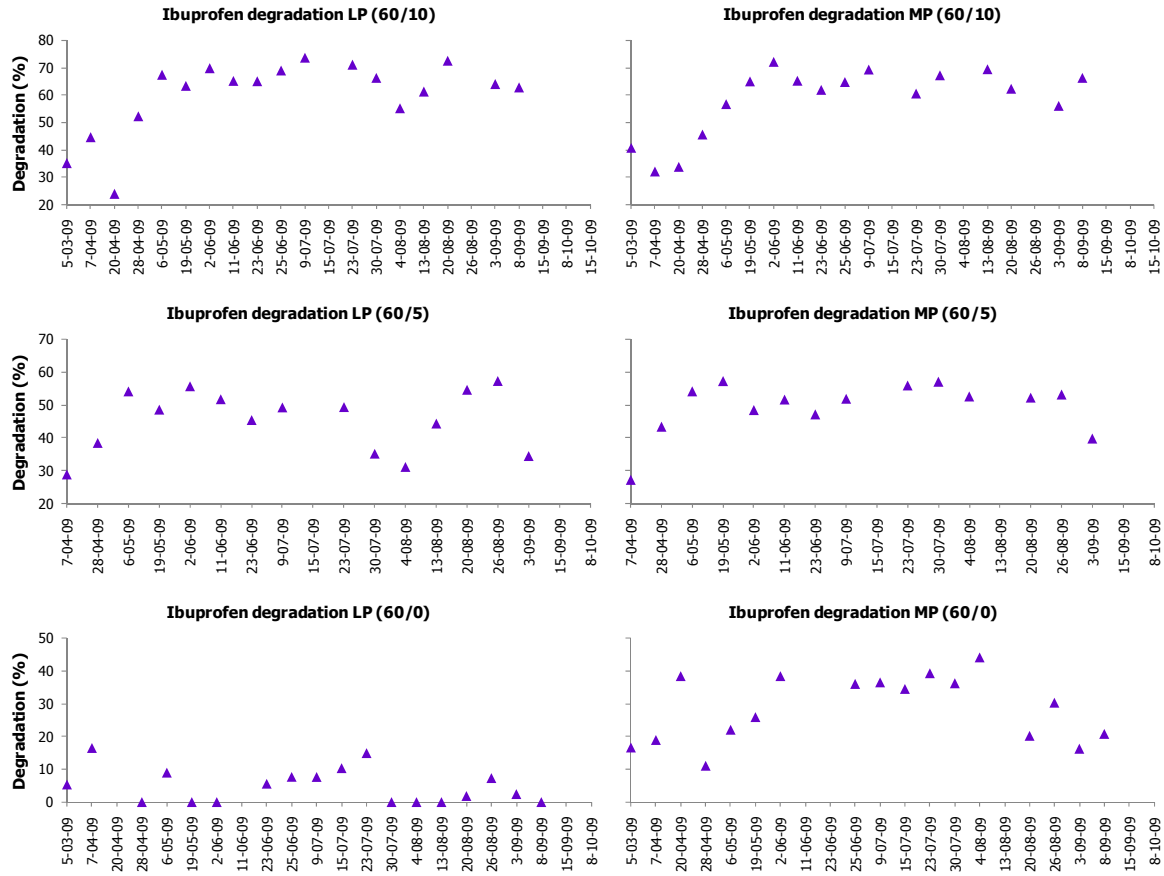

Figure D.9: Ibuprofen degradation, 60% ballast power

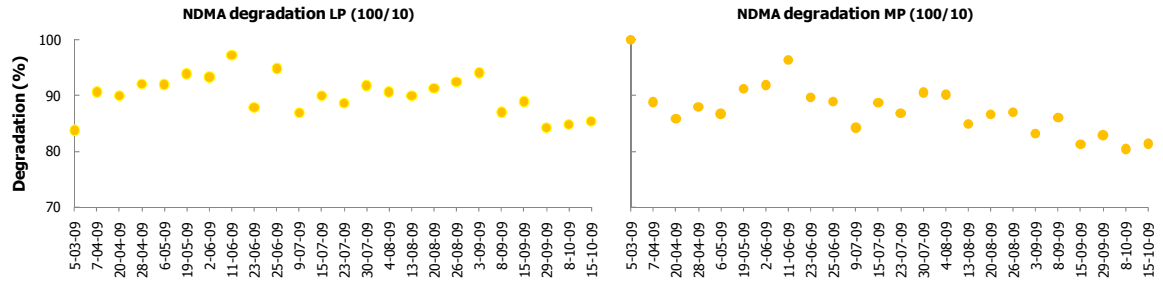

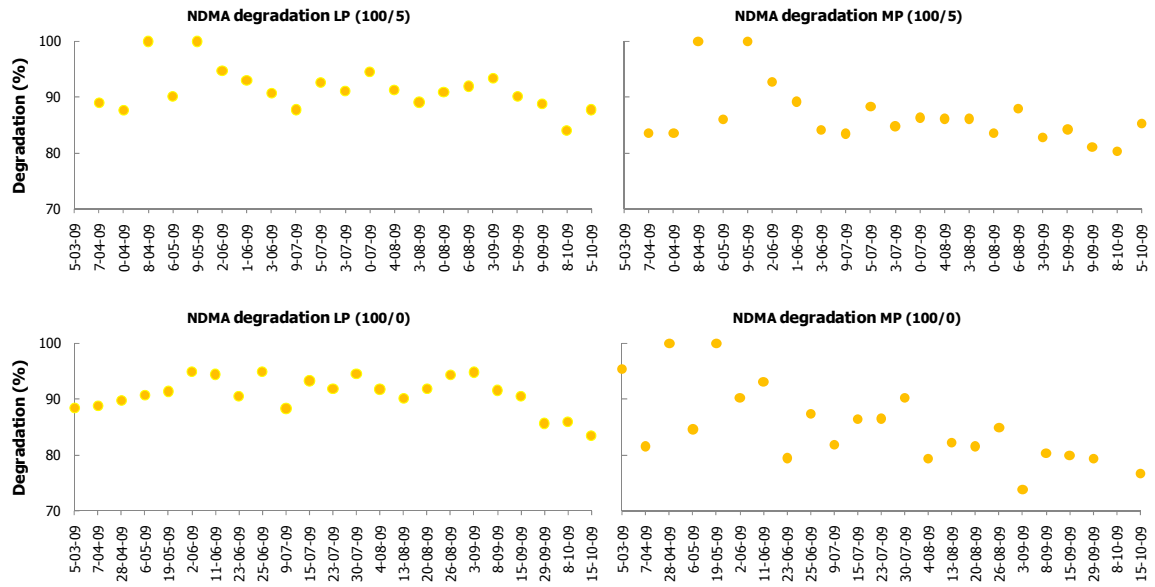

Figure D.10: NDMA degradation, full ballast power

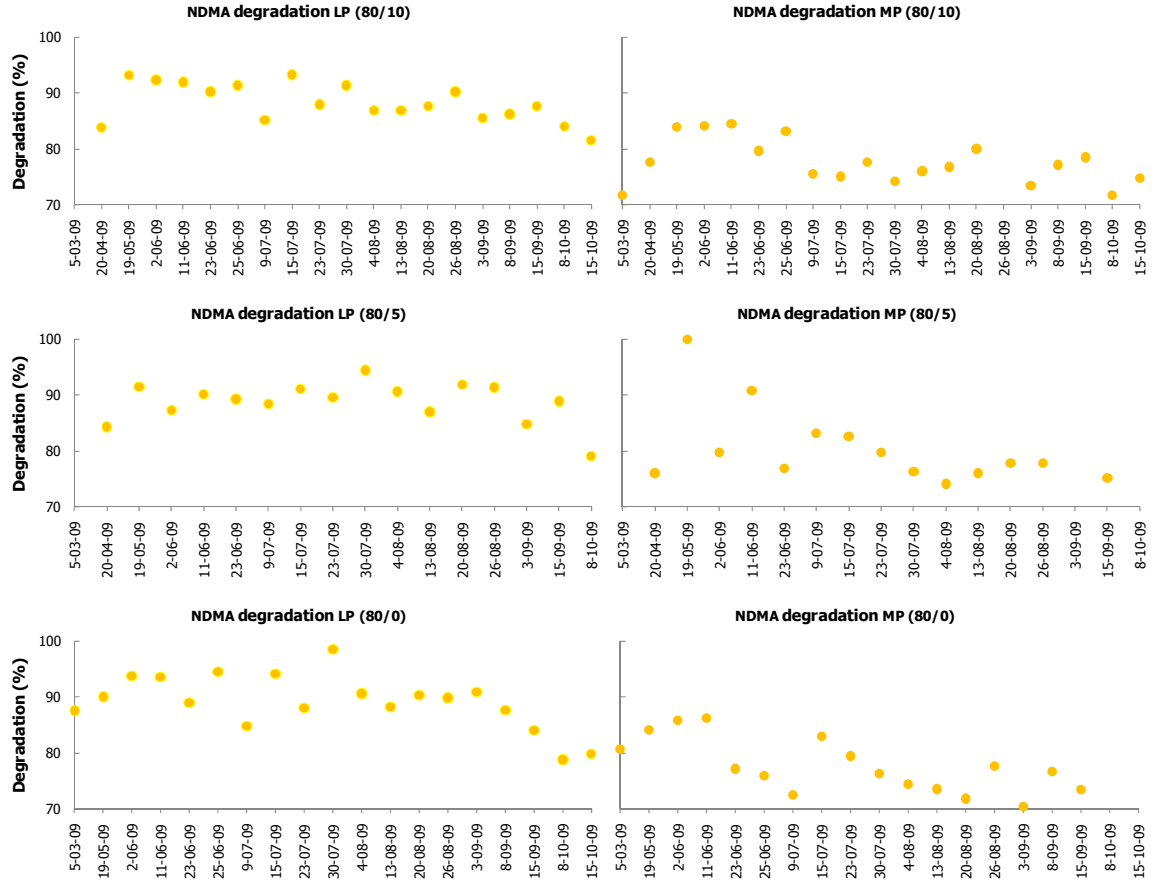

Figure D.11: NDMA degradation, 80% ballast power

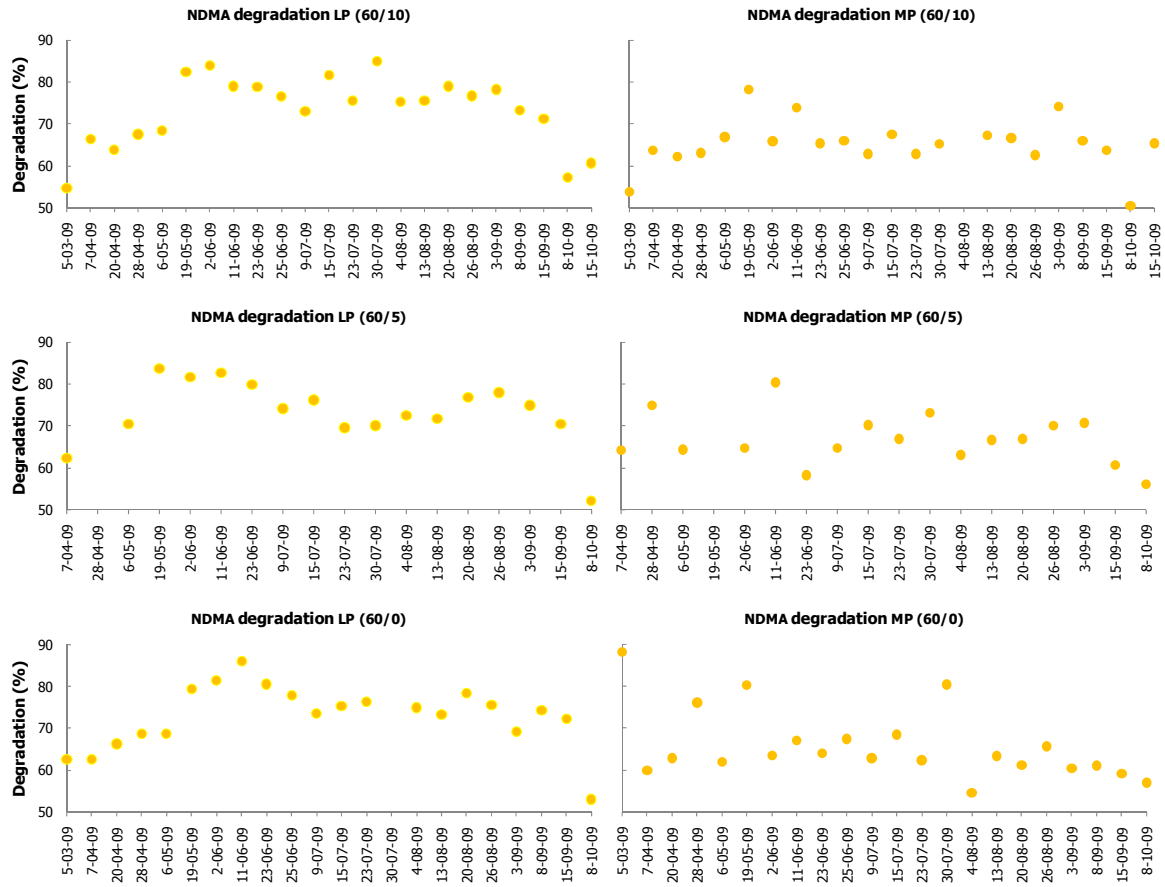

Figure D.12: NDMA degradation, 60% ballast power

ANNEX E: Outlier strategies

The concentrations of model compounds in the samples are determined by HWL via Ultra Performance Liquid Chromatography (UPLC) analysis, a method to separate, identify, and quantify compounds. Unfortunately the accuracy and thus the reliability of the measurements was poor due to a problem with the UPLC apparatus between June and August. On multiple occasions the measured effluent concentrations were higher than the measured influent concentrations. This problem occurred primarily with ibuprofen and bromacil at experimental settings with 0 ppm H_2O_2. HWL stated that ibuprofen is a difficult parameter to measure. Samples for the UPLC analysis have been stored in the freezer (at T = -20 °C) until the problems at HWL were solved. Fortunately freezing did not influence the concentrations of model compounds.

Between September 15th and October 15th, the reported results again deviated from normal results. The influent concentrations for ibuprofen were a factor 10 too low and the influent concentrations of Bromacil were a factor 1.5 – 2.0 too high. The effluent concentrations of both compounds were also not inline with the expectations. For atrazine and NDMA the concentrations seem to be correct. It was decided to disregard al measured concentrations of ibuprofen and bromacil between September 15th and October 15th

Closer inspection of all measurements at specific settings via SPSS interval diagrams and trend graphs constructed with Excel yielded multiple outliers. For each outlier it was determined whether the value should be attributed to influences of the process performance or to poor measuring results. When it was absolutely clear that the occurrence of the outlier can be fully attributed to poor measuring results, the measured value has been disregarded from the analysis. For instance, ibuprofen degradation using LP lamps at minimum UV ballast in the absence of hydrogen peroxide, cannot reach levels of 50 or 60% and are therefore disregarded. On several occasions effluent concentrations were higher then influent concentrations; the corresponding negative values for degradation have been replaced with 0. Fortunately enough data remained for statistical analysis. Measurements of atrazine on the other hand were very constant and no outliers could be discovered.

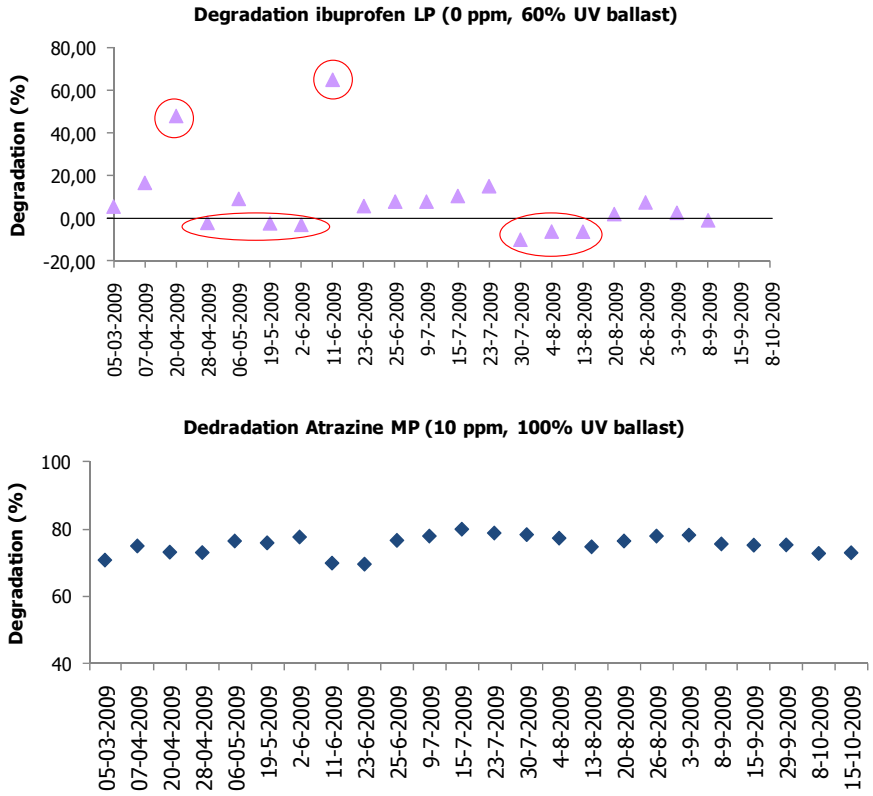

Figure E.1: Outliers, example

ANNEX F: Statistical analyses

Definitions

Definitions and equations adapted from Hair et al. (2006), Dekking et al. (2004) and de Vocht (2000)

Adjusted coefficient of determination (adjusted R^2)

Modified R^2 that takes into account the number of independent variables that are included in the regression equation and the size of the sample. Statistic can be used for comparison between equations with different numbers of independent variables, sample sizes or both.

Beta coefficient

Standardized regression coefficient, allowing direct comparison between the relative explanatory power of the independent variables.

Coefficient of determination (R^2)

Measure for the proportion of variance of the dependent variable Y that is explained by the independent variable X. The coefficient can vary from 0 (no variance explained) to 1 (all variance explained).

Collinearity / multicollinearity

Expression of a relationship between two (collinearity) or more (multicollinearity) independent variables. Two independent variables exhibit complete collinearity if their correlation coefficient is 1 and completely lack collinearity when their correlation coefficient is 0.

Multicollinearity occurs when a single independent variable X_1 is highly correlated (>0.3) with a set of other independent variables X.

Correlation coefficient (r)

Describes the strength and direction of a linear relation between any two metric variables X and Y, regardless of the individual measuring scales, expressed as a number between -1 and +1. The correlation is equal to the covariance divided by the product of the standard deviations of X and Y:

$$Cor\ (X,Y) = r = \frac{Cov(X,Y)}{std(X) \cdot std(Y)} = \frac{\sum(X - \bar{X}) \cdot (Y - \bar{Y}) \frac{1}{N}}{\sqrt{\left[\sum(X - \bar{X})^2 \frac{1}{N}\right] \cdot \left[\sum(Y - \bar{Y})^2 \frac{1}{N}\right]}}$$

Covariance

Measure that describes the linear relation between two variables X and Y. Covariance between a variable X with expected value $\bar{X}$ and Y with expected value $\bar{Y}$ is defined as:

$$Cov(X,Y) = \sum (X - \bar{X}) \cdot (Y - \bar{Y}) \frac{1}{N}$$

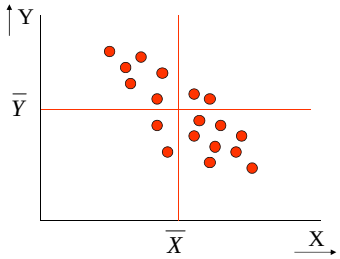

Figure F.1: Covariance

If the two variables are independent (no relation exists), the covariance is 0. A drawback of the measure covariance is that the strength depends on the measuring scale of the variables. A more appropriate measure to describe a linear relation between two variables is the correlation

Degrees of freedom (df)

Equal to the total number of observations minus the number of estimated parameters. Degrees of freedom provide a measure of how restricted the data are to reach a certain level of prediction. If the number of df is small, the resulting prediction may be less generalizable because all but a few observations were included in the prediction. A large df value indicates that the prediction is fairly robust with regard to being representative to the entire data set.

F-value and W-value
With the Levene's test on equality of variances, the test statistic W is determined and its significance is tested against F, where F is a quantile of the F test distribution. The Levene's test rejects the hypothesis that the variances are equal for all defined groups if:

$$W = \frac{(N-k)}{(k-1)} \cdot \frac{\sum_{i=1}^{k} N_i (Z_i - Z_{..})^2}{\sum_{i=1}^{k} \sum_{j=1}^{N_i} (Z_{ij} - Z_i)^2} > F(\alpha, k-1, N-k)$$

α = *level of significance = 0.05*
W = *result of the test;*
k = *number of different groups*
N = *total number of samples,*
N_i = *number of samples in the ith group,*
Y_{ij} = *value of the jth sample from the ith group,*
$\bar{Y}_i$ = *mean ith group*
Z_i = *mean of Z_{ij} for group i*
$Z_{..}$ = *mean of Z_{ij} for all values*
Z_{ij} = $Y_{ij} - \bar{Y}_i$

In the output generated by SPSS, the value of F is given and its level of significance. Small F-values with a significance >0.05 means that hypothesis 0 (equal variances) should not be rejected.

Homoscedasticity
The dependent variable Y has a constant variance for all values of the independent variable X. Can be tested with *Levene's test on equality of variances.*

Linearity
Linear models predict values that fall in a straight line by having a constant unit change of the dependent variable Y for a constant unit change of the independent variable X. In other words: the relation ship between X and Y is a linear one, the strength of which is expressed by the correlation.

(Multiple) regression analysis
Regression analysis can be used to describe a linear relation between a dependent variable Y and one or multiple independent variables X. The results can be used for predicting the value of Y or to explain the contribution of a specific variable X to the total amount of explained variance. The model is only valid when the following criteria are met:
- linearity
- homoscedasticity
- normality

Normality
Multiple regression analysis requires that the distribution of the observed values F(Y) is normal or Gaussian:

$$F(Y) = \phi\left(\frac{X - \bar{X}}{\sigma}\right)$$

If the sample size is large enough (>30) then the distribution is also considered to be normal.
The graph of the associated probability density function of a normal distribution is bell-shaped with a peak at the mean value. The F-test and t-test used in regression analysis require a normal distribution, otherwise the test results become unreliable.
In a graph such as the normal Q-Q plot the actual distribution is plotted against a 45 degree angled line. If the values deviate too much form the line, the distribution cannot be considered Gaussian. Furthermore, with Kolmogorov-Smirnov test, the normality of the distribution can be explored.

The probability density function of a random variable with a normal distribution is:

$$f(x) = \frac{1}{\sigma\sqrt{2\pi}}\, e^{-\frac{1}{2}\left(\frac{x-\mu}{\sigma}\right)^2}$$

And the corresponding distribution function is given by:

$$F(a) = \int_{-\infty}^{a} \frac{1}{\sigma\sqrt{2\pi}}\, e^{-\frac{1}{2}\left(\frac{x-\mu}{\sigma}\right)^2} dx$$

With the Kolmogorov-Smirnov test the Z-value is calculated and compared to a table of critical values of D, for a given sample size. For samples with a size n >35 for instance, the critical value at the 0.05 level of significance is

approximately $1.36/\sqrt{n}$. If the calculated Z is lower then the critical value, the null hypothesis (distribution is normal) cannot be rejected. The Z value is the largest absolute difference between the cumulative observed proportion and the cumulative proportion expected from a normal distribution:

$$Z_y = \sup|F(y) - F(a)|$$

The corresponding p-value (level of significance) is calculated. If p >0.05 then the distribution of the sample can be considered normal.

Part correlation
Measures the strength of the relationship between a dependent variable Y and a single independent variable X_i when the predictive effects of other independent variables in the regression model are removed. It portrays the unique predictive effect due to a single independent variable among a set of independent variables.

Partial correlation
Measures the strength of the relationship between a dependent variable Y and a single independent variable X_i when the predictive effects of other independent variables in the regression model are held constant. For example r(Y, X_2, X_1) measures the variation in Y associated with X_2 when the effect of X_1 on both X_2 and Y is held constant. Value is used in sequential variable selection methods of multiple regression model estimation (stepwise, enter etc.) to identify the independent variable with the greatest incremental predictive power beyond the independent variables that are already included in the regression model.

Residual (ε)
Predictions will seldom be perfect, and the error in the prediction of the sample data is called the residual. The error in the prediction should have a distribution with a mean of 0 and a constant and thus *homoscedastic* variance. Furthermore, the sum of all residuals should be 0 (just as much errors above the expected value as below), and when plotted against the values of the independent variable no systematic pattern should be distinguishable (variance is homoscedastic).

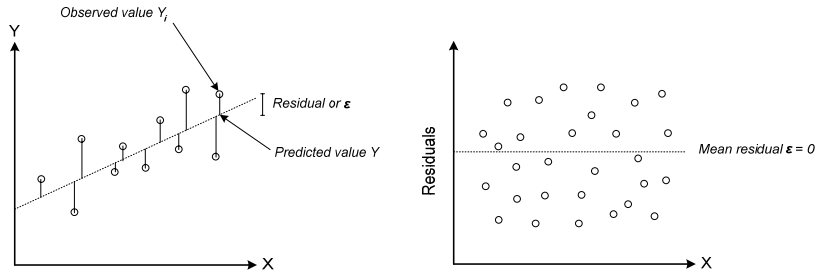

Figure F.2: Residuals

The residuals can be calculated with a simple least squares method. When performing a simple regression analysis with SPSS, one can select the option 'safe unstandardized residuals'. For every prediction of Y (photolytic degradation of atrazine for instance) based on X (UV intensity) the residuals are stored as a new variable.

Standard deviation
A measure describing the spread or variation in the distribution of a variable. The standard deviance is equal to the square root of the variance of a variable and has the same unit as the expected value or mean $\bar{X}$ of the specific value. It can be used to describe the accuracy of a calculated mean/average.

$$std\ (X) = \sqrt{Var(X)} = \sqrt{\sum (X - \bar{X})^2 \frac{1}{N}}$$

Variance
Variance is a measure that describes the spread in measured values, usually defined as the average squared deviation from the mean:

$$Var(X) = \sum (X - \bar{X})^2 \frac{1}{N}$$

Methods

SPSS 16.0 (short for Statistical Package for Social Sciences, version 16) is a spreadsheet based software package combining advanced mathematics and statistics. It is designed primarily for applications in social sciences but can also be used in other fields due to its readily available options for data analysis, data management and graphical functions.

Determination of individual contributions to degradation

In advanced oxidation via UV and H_2O_2, degradation of target compounds is achieved via two mechanisms: photolysis (degradation is strictly the result of UV radiation) and oxidation with hydroxyl radicals. Since the hydroxyl radicals are formed from photolysis of H_2O_2, it is a bit problematic to define the exact individual contribution of photolysis and oxidation to the observed degradation. If the degradation of a model compound can be predicted by a regression model consisting of two independent variables X_1 (photolysis: UV intensity) and X_2 (advanced oxidation: UV intensity and H_2O_2 dose) that are correlated and one dependent variable Y (degradation of the specific model compound), the part correlations of X_1 and X_2 with Y can be used to determine the specific amounts of explained variance in Y.

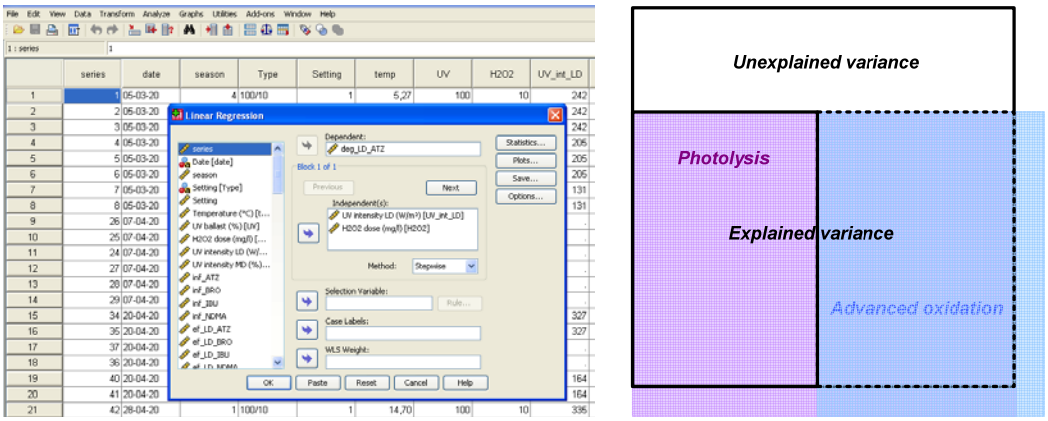

Figure F.3: Using Linear Regression in SPSS to estimate the amount of explained variance in degradation of atrazine

With linear regression an equation representing the linear relation between the dependent and independent variables is estimated. Using the stepwise method, the independent variable with the largest partial correlation is included in the model first. The model is finished when the significances of all excluded variables are >0.05. Only significant variables are included in the model.
The output of a regression analysis consists of three tables. The ***Model Summary*** and ***ANOVA*** present information about the fit of the model and the actual model regression coefficients can be found in the table called **Coefficients.** At the end of this chapter the meaning of the relevant results and their interpretation are elaborated.

The results of a regression model are valid if certain criteria are met. In paragraph below the results of the test concerning linearity, homoscedasticity and normality can be found. From these tests it can be concluded that the response of the observed degradation (all compounds, both reactors) to a change in UV intensity and peroxide dose is indeed linear. The variances in observed degradation as a result of advanced oxidation are homoscedastic (all compounds, both reactors). However, for MP- photolysis of atrazine and LP-photolysis of IBU and NDMA the variances are not constant. For now this violation of homoscedasticity is accepted but in a later model (one that includes the influence of the water matrix) this problem should be addressed.
Furthermore the observed values for the degradation of the model compounds all have a normal distribution for both reactor types.
Regression analysis can be applied and the results and conclusions can be found in paragraph 2.1.2.

Criteria for application regression analysis

Test for linearity
Linear regression analysis is only valid if the analysed relations are linear. With scatter plots the linearity is assessed and it can be concluded that the relations between UV intensity and the observed degradation are more or less linear. Perfect linear relationships will not be found since the degradation is influenced not only by the UV intensity but by several water quality parameters as well, which introduce extra variance from the mean. The relation between the H_2O_2 dose and the observed degradation is also nearly linear.

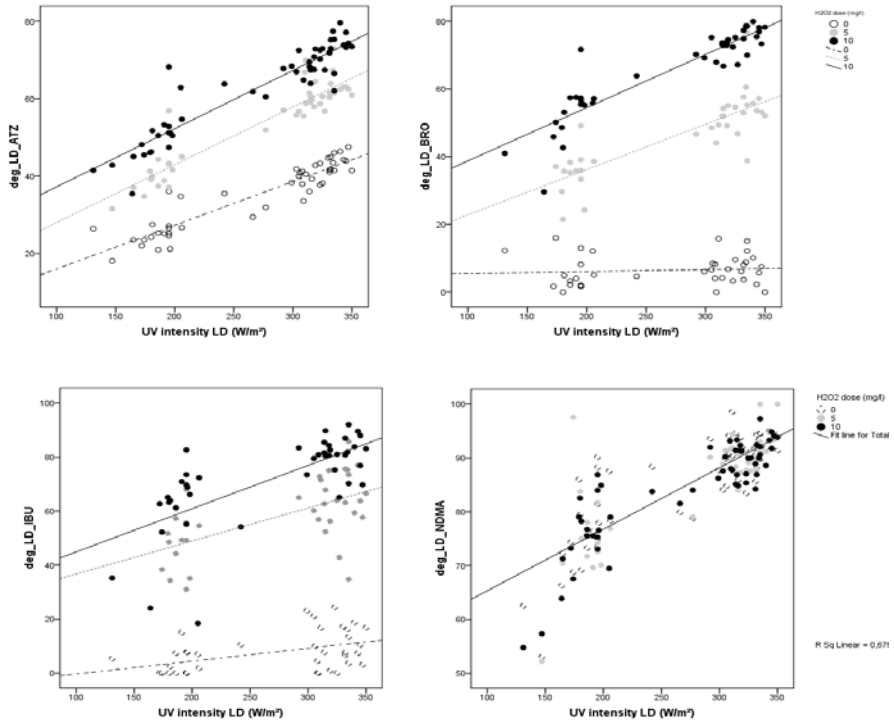

Figure F.4 Scatter plots degradation model compounds– UV/H_2O_2, LP reactor

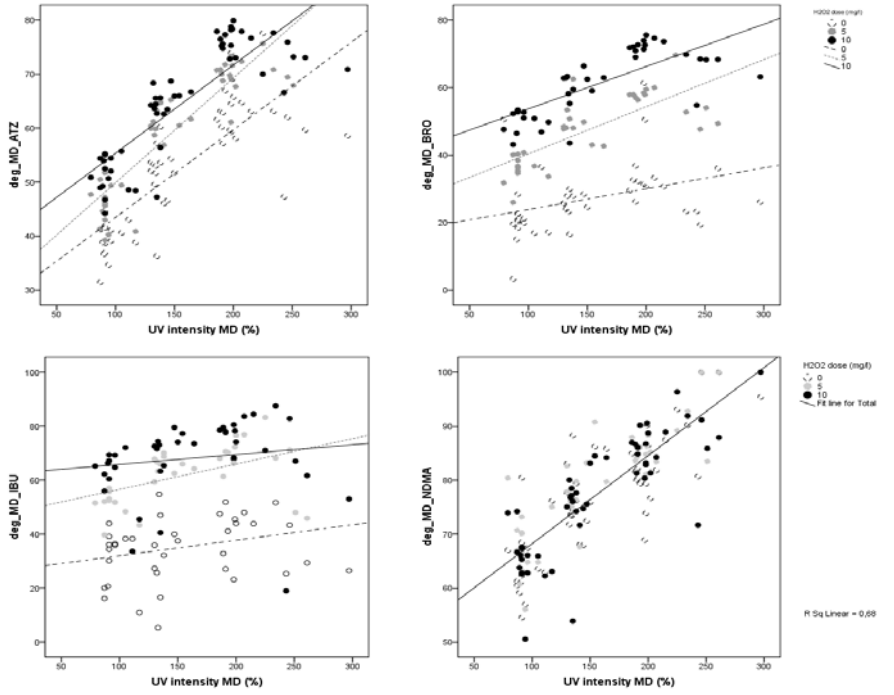

Figure F.5: Scatter plots degradation model compounds – UV/H_2O_2, MP reactor

Tests for homoscedasticity

The dependent variable Y (degradation of a specific model compound) should have a constant variance for all values of the independent variables X_1 (UV intensity LP in W/m^2) and X_2 (H_2O_2 dose) This can be tested via visual inspection of the residual plots and with *Levene's test on equality of variances.*

SPSS has no option that allows for direct computation of the Levene's test. However, using the independent samples t-test, defining two groups based on the UV intensity, yields the desired output.

The variances in the observed degradation for both groups should be equal in order to meet the criterion of homoscedasticity.

The equality of variances in atrazine degradation is analysed first. This poses a problem because the observed atrazine degradation can be attributed to photolysis and oxidation. A model predicting the photolytic degradation

of atrazine ($Y_{1,\ atz}$) will consist of one independent variable (X_1) and a model for predicting the degradation of atrazine as a result of advanced oxidation ($Y_{2,\ atz}$) consists of two independent variables (X_1 and X_2).
Firstly the variances in observed photolytic degradation (LP reactor) of atrazine are analysed. For that purpose the only the cases with a peroxide dose of 0 ppm are selected. The observed UV intensities have a mean of 268 W/m^2. This mean value is used as a cut-point for dividing the sample in two groups:

1. UV-I >268
2. UV-I <268

The group statistics show that the mean atrazine degradation for group 1 is 41% (std =3.67) and for group 2 this is 26% (std = 4.75). The F-value of the Levene's test is low (0.743) and not significant (sig = 0.393) meaning that the variances in observed photolytic degradation are equal for all levels of the independent variable X_1 (UV intensity). Furthermore, in the scatter plot of the residuals, no distinctive pattern can be distinguished. It can thus be concluded that atrazine photolysis by the LP reactor meats the criterion of homoscedasticity.

Group Statistics

			N	Mean	Std. Deviation	Std. Error Mean
deg_LD_ATZ	UV intensity LD (W/m²)	>= 268	28	41,1014	3,66751	,69309
		< 268	20	26,1590	4,75498	1,06325

Independent Samples Test

		Levene's Test for Equality of Variances		t-test for Equality of Means		
		F	Sig.	t	df	Sig. (2
deg_LD_ATZ	Equal variances assumed	,743	,393	12,294	46	,000
	Equal variances not assumed			11,773	34,229	,000

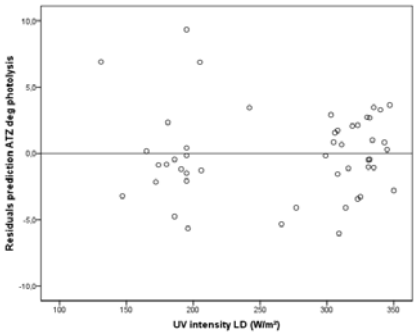

Figure F.6: Results Levene's test LP photolysis atrazine and scatter plot residuals

Secondly the variances in observed atrazine degradation resulting from advanced oxidation analysed. For that purpose all cases with a peroxide dose are selected. The specific peroxide dose is used to divide the sample in two groups:

1. 5 ppm H_2O_2
2. 10 ppm H_2O_2

The group statistics show that the mean atrazine degradation for group 1 is 53% (std =11.1) and for group 2 this is 62% (std = 11.4). The F-value of the Levene's test is low (0.204) and not significant (sig = 0.652) meaning that the variances in degradation are equal for all levels of the independent variable X_2 (peroxide dose). Furthermore, in the scatter plots of the residuals, no distinctive pattern can be distinguished. It can thus be concluded that advanced oxidation of atrazine by the LP reactor meets the criterion of homoscedasticty.

Table F.1: Results Levene's test advanced oxidation Atrazine, LP reactor

Group Statistics

			N	Mean	Std. Deviation	Std. Error Mean
deg_LD_ATZ	H2O2 dose (mg/l)	5	54	52,7759	11,08561	1,50856
		10	64	61,8516	11,67219	1,45902

Independent Samples Test

		Levene's Test for Equality of Variances		t-test for Equality of Means		
		F	Sig.	t	df	S
deg_LD_ATZ	Equal variances assumed	,204	,652	-4,305	116	,(
	Equal variances not assumed			-4,324	114,353	,(

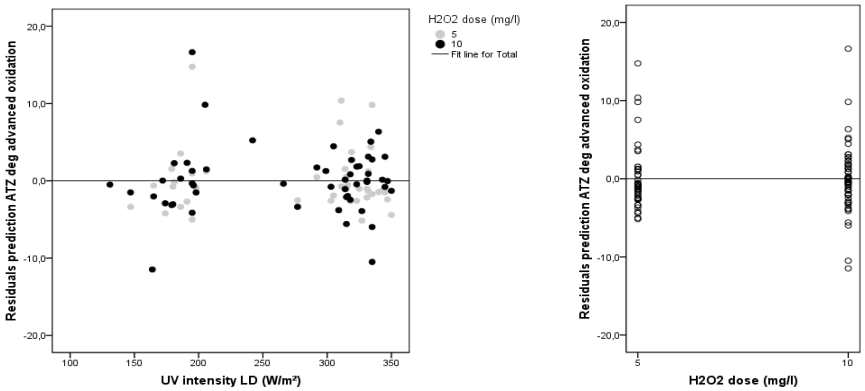

Figure F.7: Results Levene's test LP advanced oxidation of atrazine and scatter plots residuals

Thirdly the differences in variance in degradation between all cases (regardless of the applied mechanism) are compared. The groups are defined in such a way that the sample sizes are comparable, using the UV intensity as a cut point (309 for LP and 141 for MP). The same procedures have been followed for the degradation of bromacil, ibuprofen and NDMA by the LP reactor and for the degradation of all compounds by the MP reactor. The results of the tests for homoscedasticity can be found in the tables below.

Table F.2: Results tests for homoscedasticity of variances in observed degradation by LP reactor

Compound	Groups		N	Mean	Std.dev	Std. Error mean	F	sig	Homoscedasticity
Atrazine	Excl. peroxide	UV-I >268 UV-I <268	28 20	41.10 26.16	3.67 4.75	.69 1.06	.743	.393	+
	Excl. photolysis only	5 10	54 64	52.78 61.85	11.09 11.67	1.51 1.46	.204	.652	+
	All cases	UV-I >309 UV-I <309	73 72	59.59 42.13	12.61 13.54	1.48 1.60	.116	.734	+
Bromacil	Excl. peroxide	UV-I >268 UV-I <268	22 16	6.96 5.82	4.13 4.94	.88 1.24	1.193	.289	+
	Excl. photolysis only	5 10	45 53	44.30 63.97	11.53 12.30	1.72 1.69	.655	.420	+
	All cases	UV-I >309 UV-I <309	59 57	47.84 32.38	28.13 23.09	3.66 3.06	2.483	.118	+
Ibuprofen	Excl. peroxide	UV-I >268 UV-I <268	22 17	1.45 3.84	7.87 4.67	1.68 1.13	6.806	.013	-
	Excl. photolysis only	5 10	45 33	57.01 7.33	13.67 16.71	2.05 2.30	.471	.494	+
	All cases	UV-I >309 UV-I <309	60 58	55.27 37.28	3.87 28.29	3.99 3.71	.248	.619	+
NDMA	Excl. peroxide	UV-I >268 UV-I <268	33 22	9.67 76.25	4.18 9.09	.73 1.94	9.768	.003	-
	Excl. photolysis only	5 10	55 67	85.16 83.47	9.60 9.61	1.29 1.17	.000	.990	+
	All cases	UV-I >309 UV-I <309	80 76	9.99 78.47	3.47 9.61	.39 1.10	47.14	.000	-

Table F.3: Results tests for homoscedasticity of variances in observed degradation by MP reactor

Compound	Groups		N	Mean	Std.dev	Std. Error mean	F	sig	Homoscedasticity
Atrazine	Excl. peroxide	UV-I >154 UV-I <154	21 31	62.77 45.10	6.20 7.52	1.30 1.37	3.823	.056	-
	Excl. photolysis only	5 10	54 65	59 64	1.77 1.77	1.40 1.33	.000	.990	+
	All cases	UV-I >141 UV-I <141	74 73	67.63 5.18	7.97 8.94	.93 1.05	1.362	.245	+
Bromacil	Excl. peroxide	UV-I >154 UV-I <154	16 25	31.71 23.48	1.41 8.30	2.60 1.70	.257	.615	+
	Excl. photolysis only	5 10	46 52	46.84 6.30	9.95 1.15	1.47 1.41	.370	.545	+
	All cases	UV-I >141 UV-I <141	55 62	52.6 38.4	17.28 14.89	2.33 1.89	1.942	.166	+
Ibuprofen	Excl. peroxide	UV-I >154 UV-I <154	16 23	4.58 31.45	12.24 11.96	3.06 2.49	.023	.881	+
	Excl. photolysis only	5 10	44 51	59.64 67.09	11.62 14.52	1.75 2.03	.581	.448	+
	All cases	UV-I >141 UV-I <141	55 57	6.5 49.22	18.62 18.03	2.54 2.40	.239	.626	+
NDMA	Excl. peroxide	UV-I >154 UV-I <154	23 31	84.82 69.42	7.69 8.21	1.60 1.48	.645	.426	+
	Excl. photolysis only	5 10	55 65	78.33 77.10	1.52 1.63	1.42 1.32	.058	.809	+
	All cases	UV-I >141 UV-I <141	77 74	84.5 69.6	7.46 7.85	.85 .92	2.817	.095	+

Test for normality

SPSS has a built-in function to compare the sample distribution to the normal distribution: *Kolmogorov-Smirnov test.* The tests have been performed separately for photolysis and for advanced oxidation (see the output in the tables below). It can be concluded that the observed values for the degradation of the model compounds all have a normal distribution for both reactor types, except for the degradation of NDMA by the LP reactor. However, as was stated previously, in order to meet the normality criteria the variable should have a normal distribution or the sample size should be larger then 30. Fortunately the sample sizes of NDMA degradation by the LP reactor are large enough for the distribution to be considered normal.

Table F.4: Results Kolmogorov-Smirnov test photolysis LP

One-Sample Kolmogorov-Smirnov Test

		deg_LD_ATZ	deg_LD_BRO	deg_LD_IBU	deg_LD_NDMA
N		57	47	48	64
Normal Parameters[a]	Mean	34,3579	5,9577	8,2138	84,4875
	Std. Deviation	8,57084	4,40224	7,22970	9,77973
Most Extreme Differences	Absolute	,143	,088	,130	,185
	Positive	,105	,084	,130	,126
	Negative	-,143	-,088	-,128	-,185
Kolmogorov-Smirnov Z		1,082	,603	,899	1,483
Asymp. Sig. (2-tailed)		,192	,860	,394	,025

a. Test distribution is Normal.

Table F.5: Results Kolmogorov-Smirnov test advanced oxidation LP

One-Sample Kolmogorov-Smirnov Test

		deg_LD_ATZ	deg_LD_BRO	deg_LD_IBU	deg_LD_NDMA
N		118	98	98	122
Normal Parameters[a]	Mean	57,6983	54,9802	64,2171	84,2338
	Std. Deviation	12,23303	15,41319	16,74150	9,60292
Most Extreme Differences	Absolute	,093	,096	,087	,157
	Positive	,063	,075	,053	,102
	Negative	-,093	-,096	-,087	-,157
Kolmogorov-Smirnov Z		1,010	,949	,857	1,738
Asymp. Sig. (2-tailed)		,259	,329	,455	,005

a. Test distribution is Normal.

Table F.6: Results Kolmogorov-Smirnov test photolysis MP

One-Sample Kolmogorov-Smirnov Test

		deg_MD_ATZ	deg_MD_BRO	deg_MD_IBU	deg_MD_NDMA
N		61	51	48	64
Normal Parameters[a]	Mean	51,9238	26,6325	34,1796	75,7309
	Std. Deviation	10,80061	10,52486	12,34122	10,75299
Most Extreme Differences	Absolute	,098	,112	,097	,085
	Positive	,098	,112	,064	,080
	Negative	-,080	-,088	-,097	-,085
Kolmogorov-Smirnov Z		,768	,797	,675	,676
Asymp. Sig. (2-tailed)		,596	,548	,752	,750

a. Test distribution is Normal.

Table F.7: Results Kolmogorov-Smirnov test advanced oxidation MP

One-Sample Kolmogorov-Smirnov Test

		deg_MD_ATZ	deg_MD_BRO	deg_MD_IBU	deg_MD_NDMA
N		119	98	95	120
Normal Parameters[a]	Mean	61,7838	53,9789	63,6414	77,6630
	Std. Deviation	11,00378	12,06977	13,69936	10,55418
Most Extreme Differences	Absolute	,087	,076	,100	,096
	Positive	,087	,050	,051	,096
	Negative	-,084	-,076	-,100	-,088
Kolmogorov-Smirnov Z		,947	,749	,970	1,049
Asymp. Sig. (2-tailed)		,331	,629	,304	,221

a. Test distribution is Normal.

Results

A total of eight regression models of the following form are estimated:

$$Y_i = c + B_1X_1 + B_2X_2$$

Where

Y_i	*= predicted degradation of a specific model compound by the reactor*
C	*= constant*
B_1	*= coefficient for effect of UV intensity*
X_1	*= value of UV intensity*
B_2	*= coefficient for effect of peroxide dose*
X_2	*= peroxide dose (0, 5 or 10 ppm)*

The output of a regression analysis consists of four tables. ***Variables entered/removed*** reports what variables were included/excluded in the sequential model estimations. The ***Model Summary*** and ***ANOVA*** present information about the fit of the model and the actual model regression coefficients can be found in the table called **Coefficients.** The model for atrazine degradation by the LP reactor is used to explain and interpret the regression output tables.

Model Summary

The coefficient *R* (multiple correlation coefficient) portrays the correlation of Y with all with all predictors (C, X_1 and X_2). The direction of the relation cannot be deducted from the multiple R but from the regression coefficients in the coefficients table.

R square (R^2, coefficient of determination) is the total amount of variance in Y that is explained by the predictors that are included in the model. In the case of atrazine degradation by the LP reactor, 91.6% of the variance in the prediction of Y_i is explained by photolysis and oxidation. Larger R^2 values mean a better model fit: if R^2 =1 the model fit is perfect and when R^2=0 no linear relation exists.

The model fit of (small) samples is usually a bit over estimated. Therefore the *Adjusted R Square* (R^2 corrected for the number of cases N and the number of independent variables k in the model) is determined:

$$Adjusted\ R^2 = R^2 - \frac{k(1-r^2)}{N-k-1}$$

The difference between R^2 and adjusted R^2 for the estimation of atrazine degradation (LP) is very small (0.1%) , indicating that the model fit was already accurate.

The *change statistics* report the change in explained variance after the addition of new variables. Including UV intensity explained 0,370 more variance (sig = 0.000).

The last parameter in the model summary is the *Standard Error of the Estimate* which is the standard deviance of the residuals.

ANOVA

Abbreviation for analysis of variances. The total variance in the dependent variable Y (degradation of atrazine) is split in two components: *Regression* (explained variance) and *Residuals* (unexplained variance). The term df refers to degrees of freedom and is equal to the number of independent variables. For the residuals the df is equal to N – k -1 (number of cases minus number of independent variables minus 1).

The *total sum of squares* is the total amount of variation in Y and can be used to determine the amount of explained variance in the prediction of atrazine degradation:

$$explained\ Var(Y) = \frac{explained\ varation\ (Regression)}{total\ variation\ (tot.sum\ of\ squares)} = \frac{32527}{1365035517} = 0.916 = R^2$$

The *Means Square* is equal to the sum of squares divided by the degrees of freedom. With the F-test it can be determined if the model is significant. The F-value is determined as follows:

$$F = \frac{Mean\ square\ Regression}{Mean\ square\ Residual} = \frac{5976}{18} = 331$$

The null-hypothesis (correlation coefficient does not differ from 0) is rejected at the 99.99% level of confidence (Sig= 0,000). It can be concluded that the model is significant, has a very high model fit and the results can be used to estimate the effect of photolysis and advanced oxidation in the degradation of atrazine by the LP reactor.

Coefficients

The actual parameters of the regression model are reported in the Coefficients table, together with the corresponding standard errors. The *unstandardized B coefficients* are the parameters of the regression equation

that predict the actual value of atrazine degradation (prediction) and the *standardized coefficients Beta* express the relative (standardized) influence of the model parameters.
Because UV intensity and peroxide dose have different measuring scales, comparing the B coefficients to each other is difficult. Comparison is possible with the Beta coefficients that are calculated from the standardized variables:

$$Beta = B \cdot \frac{Std.dev\ (X)}{Std.dev\ (Y)}$$

In this case H_2O_2 dose has the largest absolute Beta value (0.730) and thus the largest relative contribution to the degradation of atrazine.
The direction of the relation is positive: higher UV intensities and higher peroxide dosages result in higher degradation of atrazine. The value of the intercept (Constant) is -0.842 and is not significant. B_1 is 2.74 and B_2 is 0.139 and both parameters are significant. Both t-values (B/Std. Error) differ significantly from 0 in contrast to the constant (sig = 0.611).

The actual observed degradation of atrazine on July 9th 2009 (UV-I = 332 W/m^2, 10 ppm H_2O_2, c_i = 10.003 µg/L and c_e = 2.705 µg/L) was 72.96 %. Using the regression model for estimating the degradation yields the following:

$$\begin{aligned} Y_i &= B_1X_1 + B_2X_2 \\ &= 2.74 \cdot H_2O_2\ dose + 0.139 \cdot UV\ intensity \\ &= 2.74 \cdot 10 + 0.139 \cdot 332 \\ &= 72.71\ \% \end{aligned}$$

The prediction of the degradation as a result of advanced oxidation is very accurate. On the same date the observed degradation at a UV-I of 332 W/m^2 and no peroxide, the model predicts 45.1% degradation while the observed degradation was 44.9%. At a UV-I of 195 W/m^2 and no peroxide the model predicts 26.3% degradation and the observed atrazine degradation was 26.6%. Simply filling in 0 for peroxide dose does yield accurate predictions for photolysis. It can be concluded that this model can also be used to predict the photolytic degradation of atrazine. If used for predicting degradation, the model is only valid for predicting the degradation of the atrazine for the conditions under which the experiments were conducted (e.g. water matrix, reactor type, flow patterns)
However, the purpose of the regression model was to estimate the individual contribution of photolysis and advanced oxidation given the average water matrix and a certain amount of observed degradation of atrazine In the coefficients table the part correlations are given (equal to the Beta coefficients) which portray the unique predictive effect from the variables UV intensity and peroxide dose. The following reasoning is applied in determining the contribution of UV intensity to degradation of atrazine:

$$\begin{aligned} part\ correlation &= \sqrt{unique\ amount\ explained\ variance} \\ part\ cor\ (Y_{LP,ATZ}, UV_I) &= \sqrt{unique\ amount\ of\ variance\ in\ Y_{LP,ATZ}\ explained\ by\ UV_I} \\ &= \sqrt{Var_u(Y_{LP,ATZ}, UV_I)} = 0.608 \\ contribution\ to\ degradation &= \frac{Var_u(Y_{LP,ATZ}, UV_I)}{Var_u(Y_{LP,ATZ}, UV_I) + Var_u(Y_{LP,ATZ}, H_2O_2)} \\ &= \frac{[part\ cor\ (Y_{LP,ATZ},\ UV_i)]^2}{[part\ cor\ (Y_{LP,ATZ},\ UV_i)]^2 + [part\ cor\ (Y_{LP,ATZ},\ H_2O_2)]^2} \\ &= \frac{0.608^2}{0.608^2 + 730^2} = \frac{0.370}{0.903} = 0.41 \end{aligned}$$

For any amount of observed degradation in atrazine, 41% is the result of photolysis and 51% of the degradation results from advanced oxidation. The same procedure has been applied for the degradation of bromacil, ibuprofen and NDMA and for the degradations of the model compounds by the MP reactor.

Table F.8: Output regression analysis degradation Atrazine, LP

Variables Entered/Removed[a]

Model		Variables Entered	Variables Removed	Method
Model	1	H2O2 dose (mg/l)	.	Stepwise (Criteria: Probability-of-F-to-enter <= ,050, Probability-of-F-to-remove >= ,100).
	2	UV intensity LD (W/m²)	.	Stepwise (Criteria: Probability-of-F-to-enter <= ,050, Probability-of-F-to-remove >= ,100).

a. Dependent Variable: deg_LD_ATZ

Model Summary

Model		R	R Square	Adjusted R Square	Std. Error of the Estimate	Change Statistics				
						R Square Change	F Change	df1	df2	Sig. F Change
Model	1	,739[a]	,546	,543	10,62090	,546	171,858	1	143	,000
	2	,957[b]	,916	,915	4,58904	,370	623,977	1	142	,000

a. Predictors: (Constant), H2O2 dose (mg/l)

b. Predictors: (Constant), H2O2 dose (mg/l), UV intensity LD (W/m²)

ANOVA[c]

Model			Sum of Squares	df	Mean Square	F	Sig.
Model	1	Regression	19386,177	1	19386,177	171,858	,000[a]
		Residual	16130,901	143	112,804		
		Total	35517,078	144			
	2	Regression	32526,664	2	16263,332	772,266	,000[b]
		Residual	2990,413	142	21,059		
		Total	35517,078	144			

a. Predictors: (Constant), H2O2 dose (mg/l)

b. Predictors: (Constant), H2O2 dose (mg/l), UV intensity LD (W/m²)

c. Dependent Variable: deg_LD_ATZ

Coefficients[a]

Model			Unstandardized Coefficients		Standardized Coefficients	t	Sig.	Correlations		
			B	Std. Error	Beta			Zero-order	Partial	Part
Model	1	(Constant)	36,575	1,405		26,024	,000			
		H2O2 dose (mg/l)	2,773	,212	,739	13,109	,000	,739	,739	,739
	2	(Constant)	-,824	1,616		-,510	,611			
		H2O2 dose (mg/l)	2,740	,091	,730	29,970	,000	,739	,929	,730
		UV intensity LD (W/m²)	,139	,006	,608	24,980	,000	,619	,903	,608

a. Dependent Variable: deg_LD_ATZ

Table F.9: Regression constants LP

	ATZ		BRO		IBU		NDMA	
Parameter	B	sig	B	sig	B	sig	B	sig
C	-.824	.611	-18.125	.000	-18.438	.001	53.889	.000
UV	.139	.000	.103	.000	.119	.000	.114	.000
H_2O_2	2.740	.000	5.832	.000	6.348	.000	-	-

Table F.10: Regression constants MP

	ATZ		BRO		IBU		NDMA	
Parameter	B	sig	B	sig	B	sig	B	sig
C	26.651	.000	12.237	.000	29.375	.000	51.910	.000
UV	.170	.000	.105	.000	.0573	.000	.163	.000
H_2O_2	1.191	.000	3.326	.000	3.248	.000	-	-

Conclusions

The fit of the model for predicting atrazine degradation by the LP reactor is 0.92, which means that this model can predict atrazine degradation fairly accurate. Fit of the models for predicting degradation of bromacil, ibuprofen and NDMA by the LP reactor are 0.90, 0.81 and 0.68 respectively. The poor fit of the NDMA model does however not pose a problem: the models were constructed in order to quantify the effects of both variables (UV and peroxide dose) to the degradation. From the literature (4) (5) and the results of the experiments can be concluded that NDMA is not degraded by advanced oxidation, only photolysis is effective. Consequently it does not make sense to identify the effect of hydrogen peroxide. It must be noted however that due to the poor model fit, this particular model cannot be used for estimating the degradation of NDMA.

Table F.11: Individual contributions of degradation mechanisms, LP

		ATZ	BRO	IBU	NDMA
Adjusted R^2		0.915	0.9	0.812	0.677
Part correlations	UV	0.608	0.268	0.267	0.824
	H_2O_2	0.730	0.911	0.86	
Unique explained variance	UV	0.370	0.072	0.071	0.679
	H_2O_2	0.533	0.830	0.740	
	Σ	0.903	0.902	0.811	0.679
Contribution to degradation	***UV***	***0.41***	***0.08***	***0.09***	***1.00***
	H_2O_2	***0.59***	***0.92***	***0.91***	***0.00***

Because the UV intensity of the MP reactor is measured only at 254 nm, this variable cannot be used for constructing a valid model that can quantify the effects of photolysis and advanced oxidation under polychromatic radiation. Consequently, fit of the models for atrazine, bromacil, ibuprofen and NDMA degradation are low: 0.75, 0.78, 0.54 and 0.68 respectively. Moreover, the determined contribution of UV intensity to the degradation of bromacil and ibuprofen were 15 and 5% respectively, while the average minimum degradation observed resulting from photolysis were 20-30% and 30-40% respectively, depending on the energy input of the reactor.

Table F.12: Individual contributions of degradation mechanisms, MP

		ATZ	BRO	IBU	NDMA
Adjusted R^2		0.741	0.777	0.538	0.678
Part correlations	UV	0.750	0.341	0.168	0.825
	H_2O_2	0.413	0.798	0.712	
Unique explained variance	UV	0.563	0.116	0.028	0.681
	H_2O_2	0.171	0.637	0.507	
	Σ	0.733	0.753	0.535	0.681
Contribution to degradation	***UV***	***0.77***	***0.15***	***0.05***	***1.00***
	H_2O_2	***0.23***	***0.85***	***0.95***	***0.00***

ANNEX G: Water matrix effluent

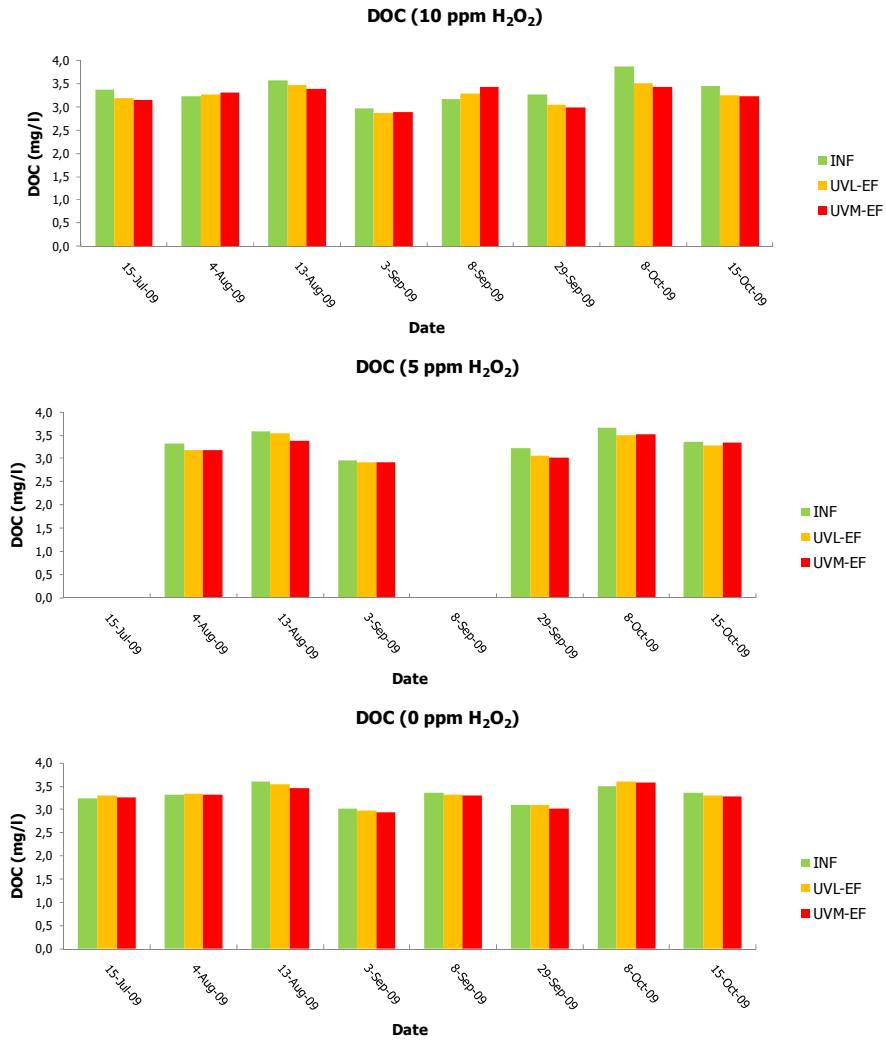

Figure G.1: Concentrations of DOC, influent and effluent

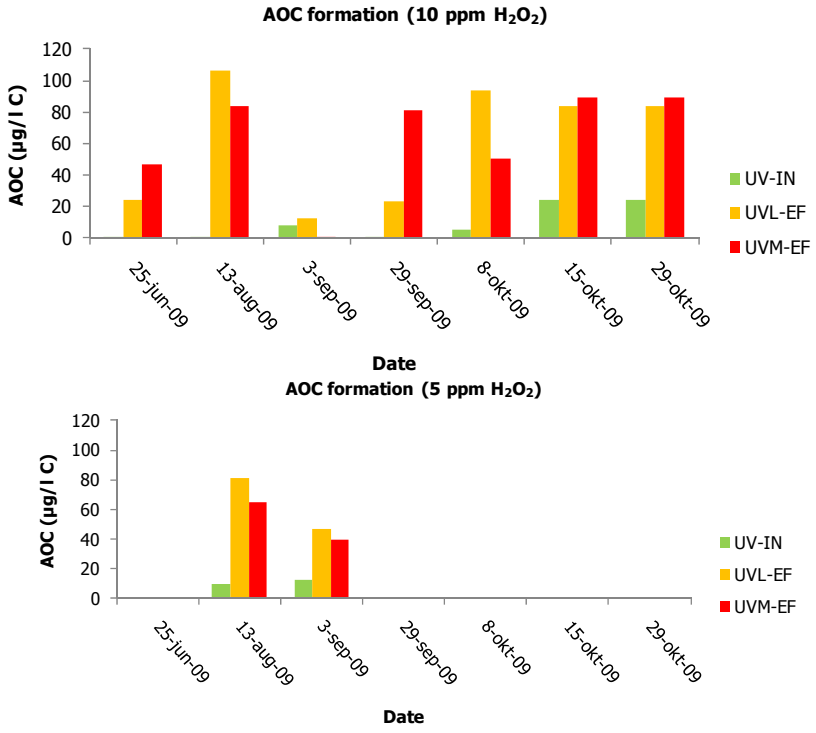

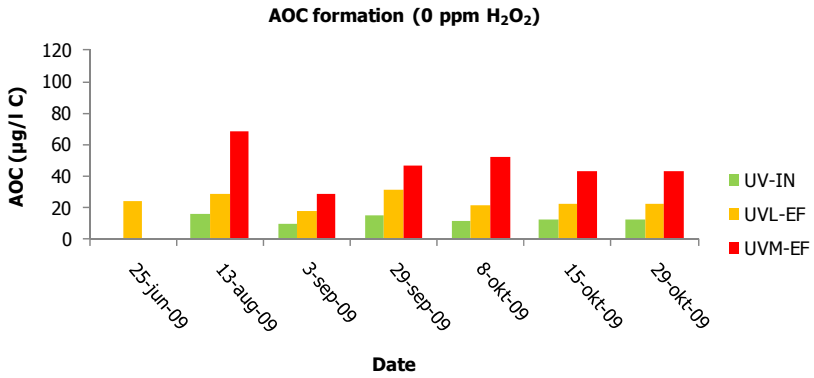

Figure G.2: Concentrations of AOC, influent and effluent

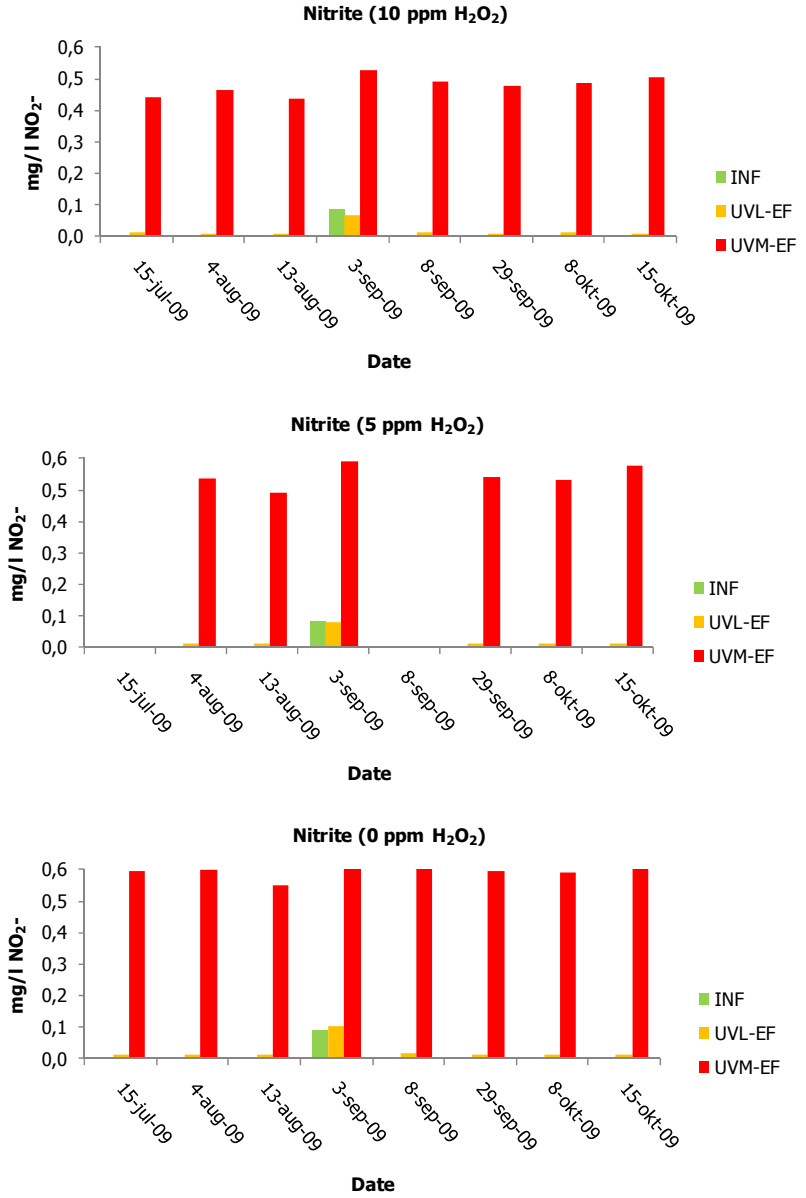

Figure G.3: Concentrations of nitrite, influent and effluent

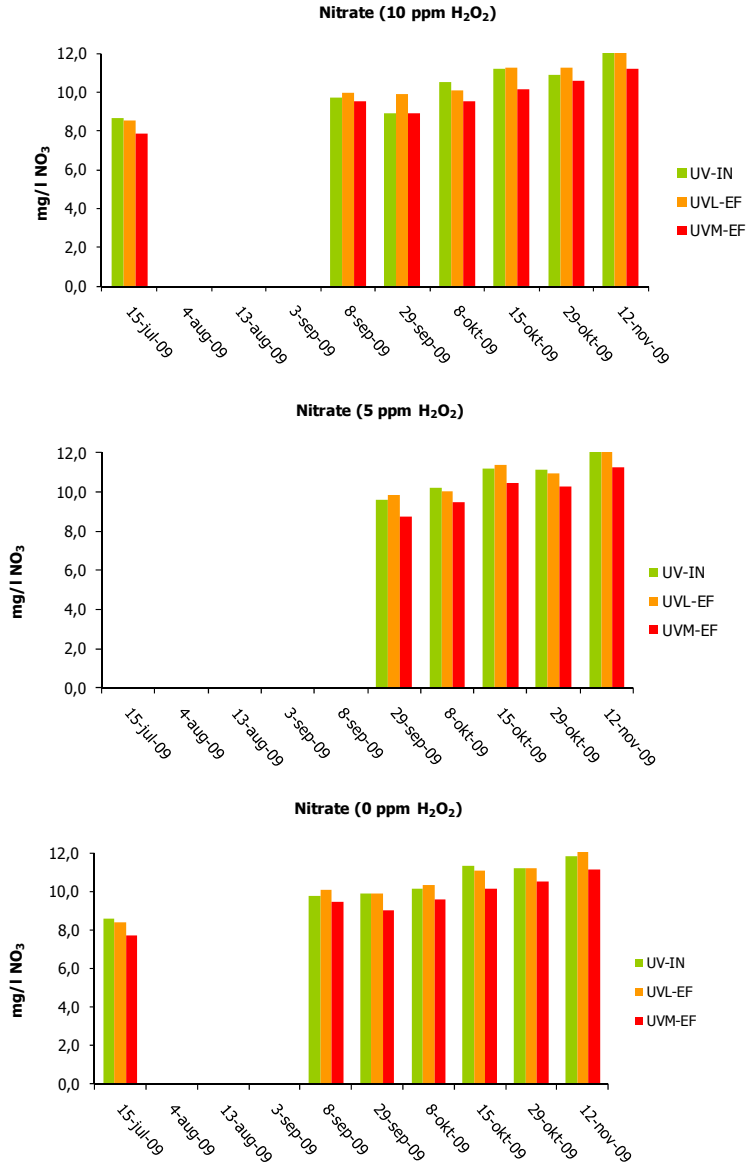

Figure G.4: Concentrations of nitrate, influent and effluent

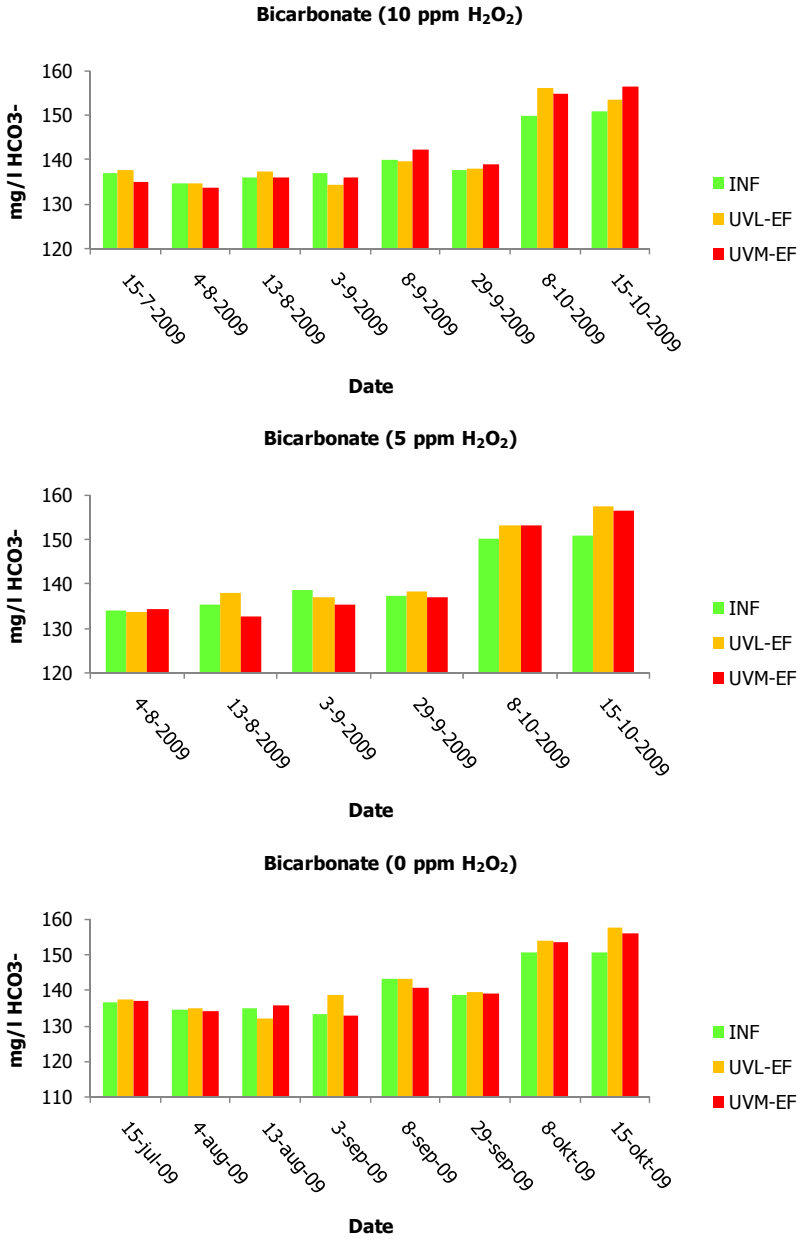

Figure G.5: Concentrations of bicarbonate, influent and effluent

ANNEX H: Measuring data AOC

Table H.1: data AOC

date	H_2O_2 ppm	sample	AOC-NOX (µg/L C) total	sample 1	sample 2	AOC-P17 (µg/L C) total	sample 1	sample 2	AOC (µg/L C)
25-jun	10	INF	0.01	0.01	0.01	0.06	0.06	0.06	**0**
25-jun	10	UVL-EF	0.01	0.01	0.01	0.05	0.04	0.06	**0**
25-jun	10	UVM-EF	37.305	37.28	37.33	9.355	9.51	9.2	**47**
25-jun	0	UVL-EF	15.5	13.28	17.72	8.66	9.12	8.2	**24**
25-jun	0	UVM-EF	0.01	0.01	0.01	0.06	0.05	0.07	**0**
13-aug	10	INF	0.025	0.02	0.03	0.08	0.01	0.15	**0**
13-aug	10	UVL-EF	27.725	42.56	12.89	78.215	99.84	56.59	**106**
13-aug	10	UVM-EF	31.5	25.22	37.78	52.195	53.82	50.57	**84**
13-aug	5	INF	6.885	6.44	7.33	3.35	3.53	3.17	**10**
13-aug	5	UVL-EF	51.945	53.89	50	29.025	28.29	29.76	**81**
13-aug	5	UVM-EF	35.275	41.11	29.44	29.51	28.78	30.24	**65**
13-aug	0	INF	11.695	11.17	12.22	4.56	5.43	3.69	**16**
13-aug	0	UVL-EF	18.835	18.67	19	9.755	9.59	9.92	**29**
13-aug	0	UVM-EF	48.61	49.44	47.78	19.84	26.67	13.01	**68**
3-sep	10	INF	5.47	3.72	7.22	2.51	1.69	3.33	**8**
3-sep	10	UVL-EF	10.22	7.5	12.94	2.735	3.84	1.63	**13**
3-sep	10	UVM-EF	0.01	0.01	0.01	0.01	0.01	0.01	**0**
3-sep	5	INF	10.22	7.5	12.94	2.735	3.84	1.63	**13**
3-sep	5	UVL-EF	21.89	24.28	19.5	25.285	29.11	21.46	**47**
3-sep	5	UVM-EF	20.11	20	20.22	19.43	18.86	20	**40**
3-sep	0	INF	6.28	6.5	6.06	3.18	3.3	3.06	**9**
3-sep	0	UVL-EF	12.75	13.44	12.06	5.18	4.7	5.66	**18**
3-sep	0	UVM-EF	21.67	22.56	20.78	7.515	7.97	7.06	**29**
29-sep	10	INF	0.015	0	0.03	0.01	0.01	0.01	**0**
29-sep	10	UVL-EF	0.01	0.01	0.01	23.095	46.18	0.01	**23**
29-sep	10	UVM-EF	18.385	20.44	16.33	63.09	44.23	81.95	**81**
29-sep	0	INF	11.25	11.17	11.33	4.245	4.91	3.58	**15**
29-sep	0	UVL-EF	9.435	8.46	10.41	22.165	24.5	19.83	**32**
29-sep	0	UVM-EF	30.47	33	27.94	16.67	14.8	18.54	**47**
8-okt	10	INF	4	8.83	0.02	1	1.27	0.29	**5**
8-okt	10	UVL-EF	65	70.56	59.44	28	27.97	28.94	**93**
8-okt	10	UVM-EF	28	27.83	28.44	23	19.35	26.02	**51**
8-okt	0	INF	8	7.94	8.06	4	5.74	1.85	**12**
8-okt	0	UVL-EF	15	15.5	14.83	6	7.14	5.58	**22**
8-okt	0	UVM-EF	38	43.33	31.89	15	13.01	16.1	**52**
15-okt	10	INF	13.92	13.67	14.17	10.58	11.71	9.45	**25**
15-okt	10	UVL-EF	28.53	36.56	20.5	55.445	28.78	82.11	**84**
15-okt	10	UVM-EF	27.25	30.17	24.33	62.275	85.04	39.51	**90**
15-okt	0	INF	8.86	8.89	8.83	3.895	4.91	2.88	**13**
15-okt	0	UVL-EF	15.86	15.33	16.39	6.31	8.08	4.54	**22**
15-okt	0	UVM-EF	30	32.22	27.78	13.5	14.8	12.2	**44**
29-okt	10	INF	-	-	-	-	-	-	
29-okt	10	UVL-EF	19	19.28	18.94	42	37.4	47.15	**61**
29-okt	10	UVM-EF	-	-	-	-	-	-	
29-okt	0	INF	9	6.78	10.5	3	2.94	2.98	**12**
29-okt	0	UVL-EF	21	16.06	26.83	5	5.72	4.5	**27**
29-okt	0	UVM-EF	35	32.5	38.44	8	7.48	7.85	**43**